Universidade Federal do Rio de Janeiro

Escola Politécnica & Escola de Química

Programa de Engenharia Ambiental

Igor Lapenda Wiesberg

CO$_2$ MANAGEMENT TECHNOLOGIES: ASSESSMENT THROUGH MODELING AND EXERGY ANALYSIS

Rio de Janeiro

2022

UFRJ

Igor Lapenda Wiesberg

CO$_2$ MANAGEMENT TECHNOLOGIES: ASSESSMENT THROUGH MODELING AND EXERGY ANALYSIS

Tese de Doutorado apresentada ao Programa de Engenharia Ambiental, Escola Politécnica & Escola de Química, da Universidade Federal do Rio de Janeiro, como parte dos requisitos necessários à obtenção do título de Doutor em Engenharia Ambiental.

Orientadores: José Luiz de Medeiros, DSc.
            Ofélia de Queiroz F. Araújo, PhD.

Rio de Janeiro
2022

UFRJ

CO₂ MANAGEMENT TECHNOLOGIES: ASSESSMENT THROUGH MODELING AND EXERGY ANALYSIS

Igor Lapenda Wiesberg
Orientadores: José Luiz de Medeiros, DSc.
Ofélia de Queiroz F. Araújo, PhD.

Tese de Doutorado apresentada ao Programa de Engenharia Ambiental, Escola Politécnica & Escola de Química, da Universidade Federal do Rio de Janeiro, como parte dos requisitos necessários à obtenção do título de Doutor em Engenharia Ambiental.

Aprovada pela banca:

_____
Prof. José Luiz de Medeiros, DSc, UFRJ (Orientador, Presidente)

_____
Prof. Ofélia de Queiroz Fernandes Araújo, PhD, UFRJ (Orientadora)

_____
Prof. Bettina Susanne Hoffmann, DSc, UFRJ

_____
Prof. Cláudia do Rosário Vaz Morgado, DSc, UFRJ

_____
Prof. Estevão Freire, DSc, UFRJ

_____
Prof. Fábio dos Santos Liporace, DSc, PETROBRAS

_____
Prof. Rita Maria de Brito Alves, DSc, USP

Rio de Janeiro
2022

RESUMO

WIESBERG, I. L. **Tecnologias de Gerenciamento de CO₂: Avaliação através de Modelagem e Análise Exergética.** Tese (Doutorado em Engenharia Ambiental), Programa de Engenharia Ambiental, Escola Politécnica & Escola de Química, Universidade Federal do Rio de Janeiro, 2022. Orientadores: José Luiz de Medeiros, Ofélia de Queiroz Fernandes Araújo.

A transição para uma economia de baixo carbono requer soluções tecnológicas para construir pontes para um futuro sustentável. Além da viabilidade econômica, as soluções devem ser capazes de mitigar as emissões de carbono e também buscar a maior eficiência na exploração dos recursos, atingindo alguns objetivos da Agenda 2030 para colaborar com o meio ambiente do planeta. Esta Tese de ecologia industrial avalia potenciais soluções tecnológicas para uma produção mais sustentável em termos técnicos, econômicos, ambientais e de conservação de exergia. São analisados processos químicos e bioquímicos comprometidos com a produção de energia fóssil, de bioenergia e de metanol de acordo com quatro Linhas de Pesquisa que correspondem diretamente aos quatro principais artigos publicados: A Linha#1 analisou tecno-economicamente uma nova rota de Captura e Utilização de Carbono alimentada com gás de combustão de usinas termoelétricas a carvão, adotando a fixação de carbono de microalgas seguida de gaseificação de biomassa de microalgas e finalizando com a síntese de metanol. A Linha#2 avaliou a conservação de exergia do abatimento de CO_2 do gás de combustão de termoelétricas a gás natural rico em CO_2 através de três rotas; nomeadamente, Captura Pós-Combustão e Armazenamento de Carbono; Captura e Utilização de Carbono via produção de metanol via hidrogenação de CO_2; e produção de metanol via birreforma de gás natural rico em CO_2. A Linha#3 estudou a Captura e Armazenamento de Carbono acopladas às unidades de cogeração de biorrefinaria de bioetanol de cana-de-açúcar por meio de modelos reduzidos para tomada de decisão em relação aos investimentos em ambas as unidades. Finalmente, a Linha#4 estudou a conservação de exergia e a otimização do condicionamento *offshore* de gás natural rico em CO_2 usando processamento inovador com separadores supersônicos. As simulações de processos com o portfólio AspenOne são utilizadas para obter balanços de massa/energia, necessários para avaliar os aspectos técnicos, econômicos, ambientais e exergéticos da sustentabilidade. Os principais resultados concretos desta Tese, no que diz respeito a soluções sustentáveis para o processamento de gás natural rico em CO_2, são: primeiramente, a hidrogenação direta do CO_2 capturado é evidenciada, em termos exergéticos, como a via mais sustentável para extração de energia simultaneamente com mitigação de carbono; em segundo lugar, os separadores supersônicos fornecem a maneira mais sustentável de realizar o condicionamento de gás natural rico em CO_2.

Palavras-chave: Captura de CO_2; geração de eletricidade; gás natural; análise exergética; utilização de CO_2, biorrefinaria.

ABSTRACT

WIESBERG, I. L. **CO₂ Management Technologies: Assessment through Modeling and Exergy Analysis.** DSc. Thesis (Doctorate in Environmental Engineering), Environmental Engineering Program, Escola Politécnica & Escola de Química, Federal University of Rio de Janeiro, 2022. Advisors: José Luiz de Medeiros, Ofélia de Queiroz Fernandes Araújo.

The transition to a low-carbon economy requires technological solutions to build bridges for a sustainable future. Besides economic feasibility, the solutions must be able to mitigate carbon emissions and also pursuit the highest efficiency in the exploration of the resources, achieving some goals of the Agenda 2030 to contribute to the environment of the planet. This Thesis on industrial ecology evaluates potential technological solutions for a more sustainable production on technical, economic, environmental and exergy conservation grounds. Chemical and biochemical processes committed to fossil-energy, bioenergy and methanol productions are analyzed according to four Research Lines that directly correspond to the main four published articles: Line#1 techno-economically analyzed a new Carbon Capture and Utilization route fed with flue-gas of coal-fired power plants adopting microalgae carbon fixation followed by microalgae biomass gasification and ending at methanol synthesis; Line#2 evaluated exergy conservation of CO_2 abatement from flue-gas of power plants firing CO_2-rich natural gas via three routes; namely, Post-Combustion Carbon Capture and Storage; Carbon Capture and Utilization via methanol production from CO_2 hydrogenation; and methanol production via CO_2-rich natural gas bi-reforming. Line#3 studied Carbon Capture and Storage coupled to cogeneration units of sugarcane-bioethanol biorefinery by means of surrogate models for decision making regarding investments on both units. Finally, Line#4 studied exergy conservation and optimization of offshore conditioning of CO_2-rich natural gas using innovative gas processing with supersonic separators. Process simulations with AspenOne portfolio are used to obtain mass/energy balances, needed to access the technical, economic, environmental and exergy quantitative aspects of sustainability. The main concrete results of this Thesis, regarding sustainable solutions for CO_2-rich natural gas processing, are: firstly, the direct hydrogenation of captured CO_2 is evinced on exergy grounds as the most sustainable route for energy extraction simultaneously with carbon abatement; secondly, supersonic separators provide the most sustainable way of performing CO_2-rich natural gas conditioning.

Keywords: CO_2 capture; power generation; natural gas; exergy analysis; CO_2 utilization; biorefinery.

CONTENTS

1. INTRODUCTION

It is well known and accepted that some climate change is taking place in the earth, including the global warming. The scientists claim that one of the main reasons is the emission of greenhouse gases (GHGs) in the atmosphere, as nitrous oxide (N_2O), methane (CH_4), and carbon dioxide (CO_2). Despite being 28 times less impactful than methane and 264 times than N_2O in a horizon time of 100 years (IPCC, 2014), CO_2 is the major contributor to this phenomena, accounting for about 60% of the global warming impacts (ALI et al., 2013). Therefore, to avoid possible adversities caused by an increase in the average earth temperature, an efficient framework for mitigating CO_2 emissions needs to be established.

The growing concern about the harmful aspects of climate change has led to agreements on ways to reduce and reverse the increasing concentration of anthropogenic carbon. One of the most important is the Paris agreement, established at the 21st conference of the Parties (COP 21) in 2015, and agreed by 195 countries, including Brazil. This agreement is intended to hold the increase in the average temperature of the world to well below 2°C, when compared to pre-industrial levels, and pursuing efforts to limit it to 1.5°C. It claims that this accomplishment would significantly decrease the climate change impacts. Such stringent climate targets demand carbon neutral or carbon-negative technologies, especially in large-scale source (De Cian & Massim, 2012). Fig. 1.1 depictures the historical evolution of CO_2eq emission, in terms of component and origin.
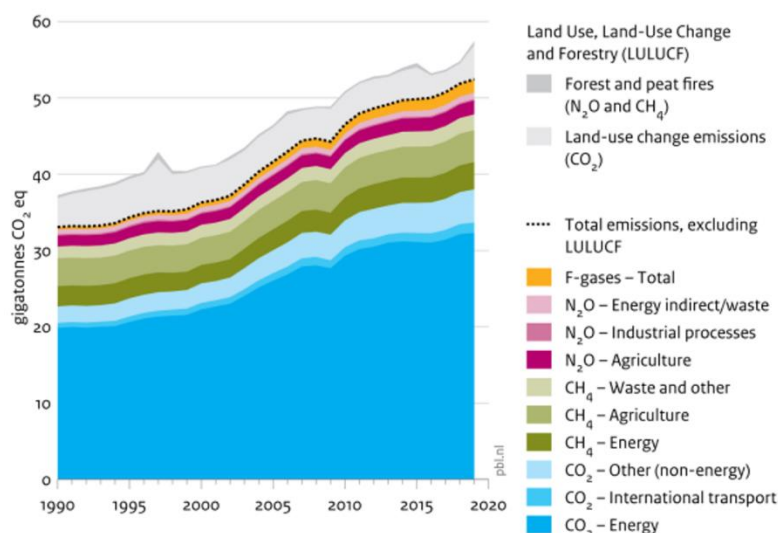
Fig. 1.1. Global emissions of greenhouse gases by component and origin (Olivier & Peters, 2020).

It is possible to be seen, from Fig. 1.1, that the main responsible for the CO_2eq emission is the energy sector, contributing for more than 30 gigatonnes of CO_2eq per year from CO_2 and a minor amount, of less than 5 gigatonnes of CO_2eq per year, from CH_4 emissions. Therefore, it is critical to implement ways for carbon mitigation in this sector to achieve the target of 1.5°C.

The world economy is widely dependent on fossil fuels for energy production, which upon combustion generates a flue gas, containing CO_2 as its main component. As shown in Fig. 1.2, some fossil fuels, as petroleum and natural gas (NG), are going to continue to increase considerable its consumption, albeit renewables are expected to become one of the main resource for primary energy. Reducing CO_2 emissions in a context of expanding energy demand, strongly supported by fossil fuels, is a big challenge. Efforts are being dedicated to the development of efficient technologies to produce energy in a sustainable way. However, there is currently no mature technology that mitigates carbon emissions without imposing a strong economic penalty to the emitting industry.

<table>
<tr><td>(a)</td><td>(b)</td></tr>
</table>
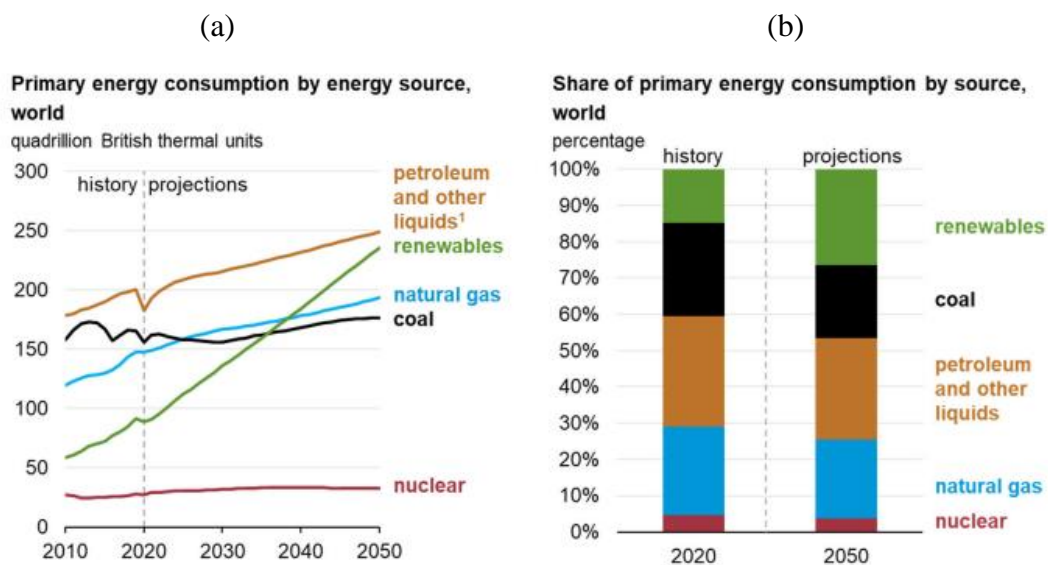
Fig. 1.2. Primary energy consumption by energy source by (a) absolute values and (b) share (EIA, 2021).

In the period from pre-industrial activities up to 2006-2015, the increase in global near-surface air temperature is estimated to be 0.97°C (±0.12°C) (IPCC, 2018). There is a remaining carbon budget, i.e., cumulative CO_2 emissions, of about 420 $GtCO_2$ for a two-thirds chance of limiting warming to 1.5°C or 580 $GtCO_2$ for an even chance (IPCC, 2018b).

This is equivalent to 10 years of current GHG emissions (Friedlingstein et al., 2021), showing that the time is short and actions need to be put into practice urgently.

To shed some light on how to address the agreement's target, the assessment of the impacts and mitigation pathways of climate change can be performed considering scenarios of the energy-economy-land system. Recently, the Shared Socio-economic Pathways (SSPs) was developed to represent five distinct storylines of this system: (SSP1) development under a green-growth paradigm; (SSP2) a middle-of-the-road development along historical patterns; (SSP3) a regionally heterogeneous development; (SSP4) a development that results in both geographical and social inequalities; and (SSP5) a development path that is dominated by high energy demand supplied by extensive fossil-fuel use (O'Neill et al., 2017).

Using six Integrated Assessment Models (IAM) to foresee the climate change based on human development and societal choices, some successful scenarios limiting the temperature increase in 1.5°C by the end of the century could be obtained (Rogelj et al., 2018). In SSP1, all six IAM have found a viable 1.5°C scenario, while no model found a viable scenario in SSP3. The models are allowed to temporarily overshoot the target, as can be seen in Fig. 1.3, requiring some Negative Emission Technology (NET) to draw CO_2 from the atmosphere and bring the global temperature back down.
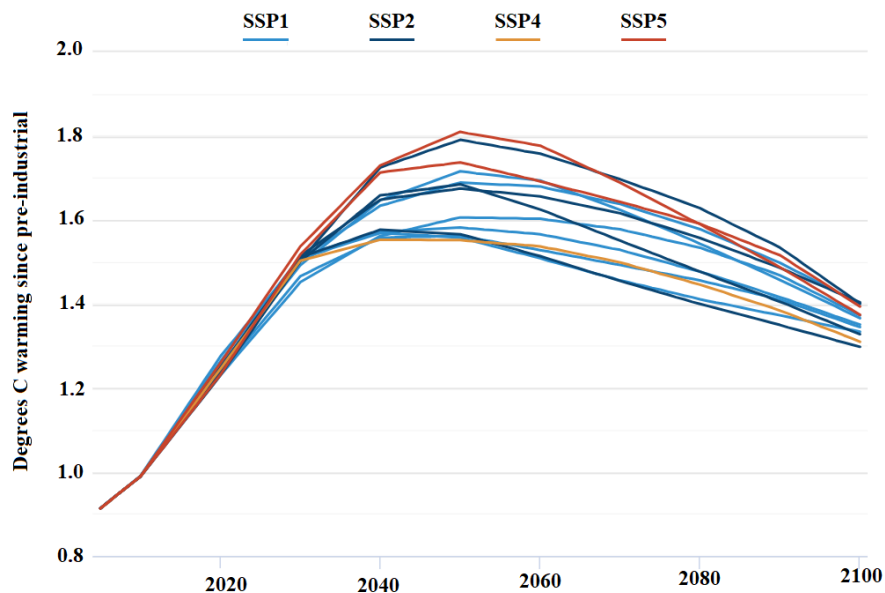
Fig. 1.3. Global mean temperature across the viable scenarios from Rogelj et al. (2018). (Source: Carbonbrief, 2018).

Therefore, Bioenergy with Carbon Capture and Storage (BECCS) plays an important role to achieve viable scenarios. The combination of Bioenergy production with Carbon Capture and Storage (CCS) technologies is required because the bioenergy adoption *per se* only achieves a carbon neutral emission, since the carbon absorbed during biomass growth will return to the atmosphere (Carminati et al., 2019). On the other hand, BECCS is considered a NET, since it can reduce the concentration of CO_2 in the atmosphere. In the simulations performed by Rogelj et al. (2018), from 150 to 1,200 $GtCO_2$ is removed from the atmosphere with this technology, with variations between the IAM and SSPs (Rogelj et al., 2017).

In the context of increasing natural gas (NG) and oil demand, concerns about the sustainability of the oil & gas exploitation industry in the future is reasonable. In fact, NG demand predictions shows a rise of 1.1% a year, until 2050, the biggest one among the fossil fuels (EIA, 2019). The main advantage of the NG expansion against the other fossil fuels is the lower CO_2 emission per energy production. About 50 kg of CO_2 are emitted per MMBtu generated, while more than 90 kg of CO_2 is emitted from coal and more than 72 kg of CO_2 from distillate fuel oil. The clean combustion of NG contributes to its increasing use for power generation (EIA, 2021).

To supply the increasing demand, the exploration and production of offshore oil-and-gas fields with high gas-to-oil ratio and high CO_2 content is increasing substantially, in spite of its lower methane content that imposes technological challenges for its utilization and conditioning. This is the case of the Brazilian pre-salt deep-water fields with CO_2 contents up to 79%mol with gas-to-oil ratios around 20,000 scf/bbl (Gaffney, Cline & Associates, 2010). The development of a more sustainable NG conditioning, adequate to a CO_2-rich condition, is required. In this sense, the most plausible destination of the CO_2 is the reinjection into the reservoir, for Enhanced Oil Recovery (EOR) purposes.

The uncommon conditions of high gas-to-oil ratio and CO_2 content of the associated NG of recent pre-salt exploitation imposes a challenge in its conditioning process, required prior to transportation and commercialization. In a recent past, the gas was fully burned in giant flares emitting indescribable amounts of CO_2 to the atmosphere, since there was total prioritization to oil production in offshore oil-and-gas enterprises (Araújo et al., 2017). As environmental law is more restrictive about CO_2 emissions, an upstream conditioning system for CO_2

removal is required. This results in an unusual high topside area and weight requirement in platforms for the pre-salt oil exploitation, stimulating the design of new FPSOs.

In chemical processes, the CO_2 captured from combustion gases is currently used as a renewable raw material to boost urea (NH_2CONH_2) production, by reacting it with NH_3. However, most of the CO_2 required is still provided by the reform of the NG in the hydrogen production stage, which is reacted with N_2 to produce NH_3 (Araújo et al., 2014). Currently, the greatest demand for CO_2 is in enhanced oil recovery (EOR), where it is used to increase oil productivity. It is estimated that for each ton of CO_2 injected, 2 to 3 barrels of oil are recovered. A large part of the CO_2 generated by anthropogenic activities is emitted into the atmosphere due to the lack of competitive technology capable of capturing and transforming the CO_2 into raw material. Therefore, it is still little used in the chemical industry (Hong, 2013).

Power plants are major stationary sources of CO_2 and environmental constraints demand technologies for its abatement. A potential solution is its capture from the flue gas to produce a pure stream of CO_2 and then converting it into products of commercial value, such as chemical commodities and polymers (Aresta, 2010). Carbon Capture and Utilization (CCU) to methanol has the potential to address relevant sustainability issues. Besides the mitigation, this technology can also be an economically feasible replacement of fossil raw materials for downstream products. For example, methanol can replace crude oil through Methanol-To-Olefins (MTO) route (Wang et al., 2015), through its use as vehicle fuel or in power production. It can even shift NG demand because it is the most common raw material for its production.

The driving force for the development of alternatives to methanol synthesis lies in the use of CO_2 as a raw material for the chemical industry. These alternatives have the potential to reduce industrial dependence on crude oil and NG. In addition, the low cost of NG, the traditional methanol feedstock, is cited as the driving force for expanding the methanol-based industry (Efenberger, 2014), a required step for a methanol economy in which methanol replaces fossil fuels as energy storage. The fossil fuel route is a required step for a sustainable methanol economy, which can be substituted, afterwards, for a renewable feedstock, as CO_2.

1.1. Carbon Mitigation Technologies

Carbon Capture and Storage (CCS) and Carbon Capture and Utilization (CCU) are the main technologies for carbon mitigation from stationary sources. In the former, a pure stream of CO_2 is obtained, with the process varying accordingly to the capture route (pre-combustion, pos combustion or oxyfuel). The purified CO_2 is then compressed to high pressures, up to 200 bar, where CO_2 is in its supercritical state. The CO_2 is then transported to the location of the geological reservoir and then disposed in it. Presently, CCS is the only CO_2 management chain that all the steps are ready to be put into operation at high scales (Araújo et al., 2014). In the latter, the captured CO_2 is used as raw material to produce an environmentally friendly product, as methanol, with the capacity of achieving two objectives of sustainable production: economically feasible displacement of fossil fuels and avoidance of GHG emissions (Wiesberg et al., 2016).

On the other hand, CCS only has some revenue when the CO_2 is used for EOR purposes, despite being capital and energy intensive. Therefore, a green premium in the cost of electricity (COE) is required, so that CCS can become feasible. Another possibility is the adoption of GHG emission taxation by governmental policies. In this way, the advantage of performing the investment is the avoidance of the taxation.

There are three main technologies for the capture step of a flue gas: (i) post-combustion; (ii) pre-combustion; (iii) oxyfuel. Fig. 1.4 shows the block flow diagram of the configurations. As can be seen, the post-combustion consists in separating N_2 from CO_2 after the combustion of the fuels with air in the boiler. The advantage of such configuration is the drop-in characteristic, since it can be attached in an operating plant, without any modifications. The post-combustion technology with the highest maturity is the chemical absorption using monoethanolamine, used in the NG industry for CO_2 removal at onshore processing. In its turn, the pre-combustion technology uses pure oxygen, produced in an Air Separation Unit (ASU), for the gasification of the fuel, producing a syngas. The syngas is then shifted to H_2 and CO_2, by means of the Water-Gas Shift reaction. The CO_2 capture unit, then, removes the CO_2 and the pure H_2 is used as the fuel, producing only water upon its combustion. Finally, the oxyfuel uses pure O_2 from an ASU, eliminating the presence of the N_2 in the flue gas, which contains almost pure CO_2.
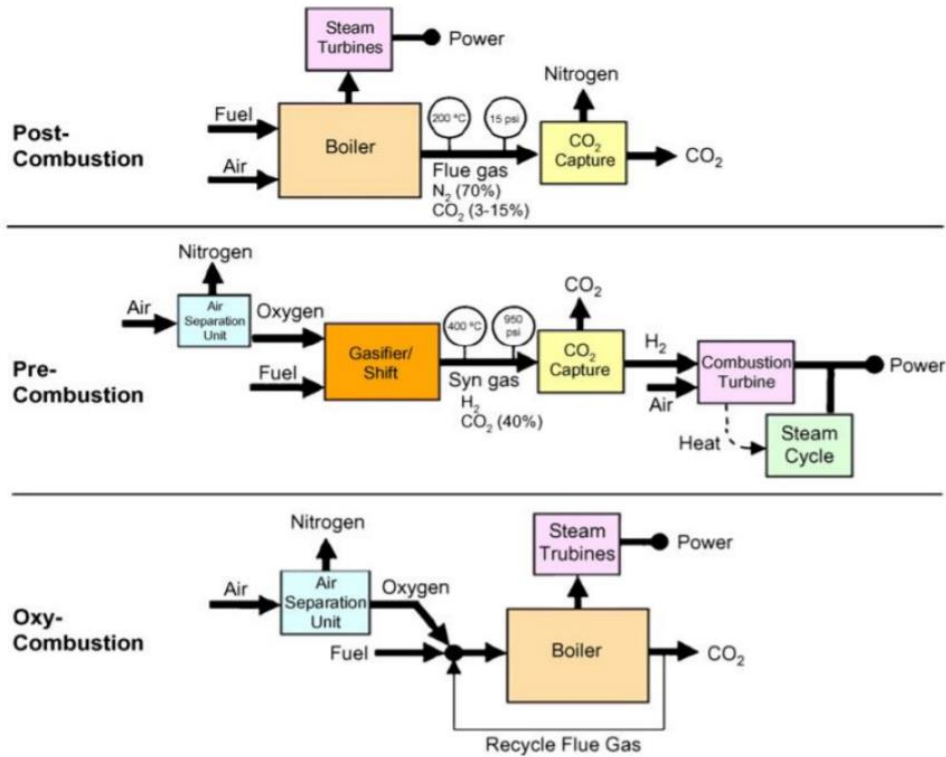
Fig. 1.4. Block flow diagram of the post-combustion, pre-combustion, and oxy-combustion configuration (Source: Wu et al., 2018).

Fig. 1.5 shows a possible BECCS configuration, where the flue gas of a cogeneration system, fueled by sugarcane bagasse, is captured with a post-combustion configuration.
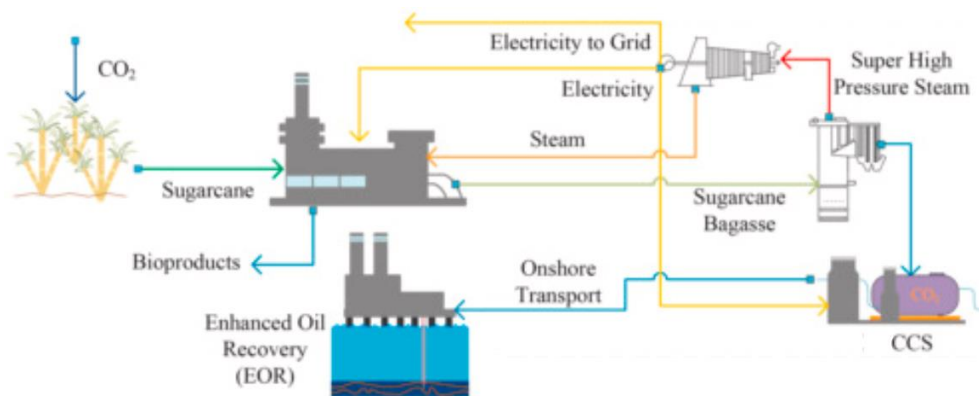
Fig. 1.5. Bioenergy production with Carbon Capture and Storage with post-combustion configuration (Source: Wiesberg et al., 2020).

In the context of CO_2 capture from NG, the Membrane Permeation (MP) is the most mature technology, where CO_2 permeates the membrane, while the hydrocarbons flow to the retentate outlet stream. However, supersonic separation technology is a novel and promising technology, with a low topside area requirement. In this technology, the Laval expansion

16

generates a deep temperature drop, condensing heavy species as a mist, the CO_2 in this case is directed to the walls by the centrifugal field and caught in the liquid collector. Other possible technologies are the Physical absorption and Chemical absorption. It is also possible to perform NG conditioning with a combination of them (Araújo et al., 2017).

1.2. Exergy Analysis

This Thesis uses the concept of Exergy Analysis for sustainability assessment, which is described in this section.

The First Law of Thermodynamics establishes, through Joule's experiments, that heat and work are two forms of energy transfer to/from a given system, and these forms of energy transfer contribute similarly to the content of internal energy of the system. However, in spite of establishing the principle of system energy conservation, the First Law does not provide information on the thermodynamic quality of these kinds of energy transfer. Through the First Law it is possible to carry out energy balances in open systems performing chemical and/or physical processing. This type of balance calculates the amount of energy that must be supplied or that is generated by the system. Again, it provides information neither on quality nor energy degradation information throughout the process.

The Second Law of Thermodynamics restricts processes by stating that no equipment can function in order to completely and cyclically transform heat into work, differing from one to another. With the concept of entropy, the Second Law further states that every process develops in the sense in which the entropy variation of the Universe is positive, being zero in reversible processes, in which they have theoretical maximum work achievable by a thermodynamic cycle. In this way, the quality of energy always degrades since all processes are irreversible, generating heat effects that cannot be integrally used as work if the process is reversed; for example, when work done on a system becomes pure heat through friction. This heat cannot be used to regenerate integrally the original expended work (i.e., the Universe has irreversibly changed).

Considering steady-state open systems, the exergy flowrate associated to a feed or a product stream of this system is a thermodynamic property based on the First and Second Laws that expresses the maximum rate of work that can be obtained by bringing this stream to full

equilibrium with a chosen Reference Environmental Reservoir (RER). Thus, exergy flowrate is a measure of the "thermodynamic distance" between the initial state of the stream to the RER state and therefore can be translated as a connection between environmental impacts associated to that stream and the laws of thermodynamics (BILGEN et al., 2015). The exergy rate entering or exiting a system has a power unit and is an extensive property because it depends on the flow of the analyzed stream. The higher its value, the greater the rate of work that can be produced from said stream.

Thus, unlike the entropy that always increases or remains constant in the Universe (therefore it is indestructible), exergy is always destroyed in irreversible processes (i.e., disappears), remaining constant only for reversible processes (therefore it is destructible). The maximum exergy content of the Universe and the minimum entropy content simultaneously occurred sometime after its creation, and since then the former has always decayed as it is continually destroyed by spontaneities, while the latter always grows as it is created by spontaneities (irreversibilities), according to the respective rates of exergy destruction and of entropy creation that can be shown to be directly proportional. Another useful comparison between them is that just as entropy is usually interpreted with the disorder of a system, exergy can be interpreted as its order (Rosen et al., 2008).

On the other hand, a similarity between exergy and entropy is that both are positive properties per unit of material: entropy due to the Third Law of Thermodynamics and exergy because any stream produces some power when brought to equilibrium with RER, unless it is the RER itself in which the exergy flowrate is naturally zero because it is already in equilibrium with RER. Due to these characteristics, the steady-state exergy balance can provide information about the rate of degradation of mechanical energy associated to a steady-state open system undergoing a process.

An example of the difference between exergy efficiency and thermodynamic yield (which should not be confused with thermodynamic efficiency) is a Carnot Machine that operates with hot source temperature equal to twice the cold source temperature. This cycle has a thermodynamic yield of 50%, even though it is perfectly ideal and there is no room for improvement (i.e., it provides the best yield of heat-work conversion). On the other hand, the exergy efficiency and the thermodynamic efficiency, however, are both equal to 100%,

evidencing that the process is absolutely reversible and ideal (Rosen et al., 2008). It is clear that exergy can better identify technological benefits than the energy. The assessment of exergy efficiency of processes is called an Exergy Analysis of Processes, while the assessment of thermodynamic efficiency of processes corresponds to Thermodynamic Analysis of Processes (Milão et al., 2021). Both Exergy and Thermodynamic Efficiencies of steady-state processes variate solidarily in the same direction and are virtually equivalent forms of measuring the efficiency and sustainability of processes, but their values are generally not the same. Then, what is the difference between them? The main difference is that Thermodynamic Analysis of Process is absolute; i.e., derives from the Second Law of Thermodynamics and does not require a RER, while RER has a critical role in Exergy Analysis and must be chosen very wisely as shown in this Thesis. An interesting idea, apparently self-contradictory, is to say that the RER is, at the same time, the strongest point and the Achilles Heel of Exergy Analysis of Processes.

Thus, Exergy Analysis is useful for improving the efficiency of using natural resources by locating, identifying and quantifying wastes and losses. Systems are better evaluated using Exergy Analysis or Thermodynamic Analysis than pure Energy Analysis because they provide clearer data, especially for (exergy or thermodynamic) efficiency improvement. The waste reduction, particularly from technologies that use energy from non-renewable sources, helps to improve sustainability (Ozbilen et al., 2012).

In addition, Exergy Analysis and Thermodynamic Analysis identify, better than Energy Analysis, the environmental and economic benefits of a technology. The reason is that exergy, sustainability and environmental impacts are closely related. When Exergy and Thermodynamic Efficiencies approach 100%, environmental impacts approach zero because all the raw material has been converted into a product, without emissions and losses. On the other hand, sustainability approaches zero for Exergy and Thermodynamic Efficiencies close to zero, since nothing is produced despite the resources consumed (Ozbilen et al., 2012). The ideal would be to obtain the greatest possible Exergy and Thermodynamic Efficiencies, with maximum sustainability and minimum environmental impact.

1.3. Literature Gaps

This section shows the literature gaps in the literature that this Thesis has explored to develop several original studies publicly published.

1.3.1. CO_2 utilization for methanol production

The CCU for methanol production can be achieved by different routes. One possibility is via biomass production by CO_2 consuming organisms, as microalgae, in a post-combustion configuration. Then, the biomass is gasified to produce syngas (mixture of carbon monoxide (CO), H_2 and a minor part of CO_2), which is converted to methanol in a conventional reaction unit and then purified. Most of the works in the literature about CO_2 bio-capture with microalgae reports experimental results for lab scale of a single equipment, generally the bioreactor. However, to be relevant, a sustainability analysis of a chemical conversion technology must go beyond simple evaluation of part of a process. The individual performance indexes, such as conversion and percentage of CO_2 captured, are often the only data evaluated, while the ideal would be to evaluate the process as a whole.

Although the study of microalgae-based technology for CCU is not new, the literature is rare in analyses comparing the return in the investment and the resulting cost of CO_2 avoided with respect to CCS. Therefore, use of Process Engineering System tools, as process simulators and economic evaluation software, is a lack in the literature. This Thesis explores this gap by simulating this CCU process and evaluating its economic performance, considering the best results of the experimental results available in the literature.

Other options for the methanol production from CO_2 are the bi-reforming of NG and the direct hydrogenation of the CO_2. In the bi-reforming of NG, the CO_2, steam, and the hydrocarbons are reacted in a single reactor to produce the syngas. The idea is that the addition of CO_2 reduces the amount of CH_4 required. Then, a conventional reaction step to convert the syngas to methanol is required. On the other hand, the direct hydrogenation requires only the reaction itself and the purification step. Due to the chemical stability of CO_2, the proposed routes require severe reactive conditions, which demand energy for compression and heating, adding capital, operational and environmental costs. The assessment of technical-economic and environmental aspects of the CCU to methanol is well documented in the literature.

However, there is a gap in the literature about the exergy performance of the CCU for methanol production, considering the entire chain from power plant generation of the flue-gas until CO_2 final conversion to methanol. Moreover, the comparison of this route with CCS and the simple emission to the atmosphere is also a lack. Both lacks are explored in this Thesis.

1.3.2. Bioenergy Production

The ethanol production from sugarcane has two points of CO_2 emission: (i) the off-gas as a result of the fermentation process, which contains only CO_2, eliminating the capture step of the BECCS, and (ii) a flue-gas stream from the Combined Heat and Power (CHP), as a result from sugarcane bagasse combustion in the boiler. The technical-economic assessment of the ethanol biorefinery with BECCS of both streams, individual and simultaneously, are well investigated in the literature. However, the developed models available in the literature are not user friendly and not flexible to changes in capacity. If another operating condition for the CHP unit is sought, all the projects must be remodeled to accommodate the new conditions, which can take some days to obtain the new results. In addition, few data are available in the literature about the investment of a standalone (BE)CCS or of a CHP.

This Thesis explores the use of surrogate models to mimic the behavior of the economic performance of the BECCS. Hence, it is used for immediate technical-economic analysis. Its advantage is its simplicity and the agility to obtain a new result for a new set of conditions. The original idea is to use the CHP/BECCS surrogate models together with similar models for other units (e.g., ethylene production from ethanol, bioethanol production, etc.), so that a simulator of the investment in a biorefinery can be developed.

1.3.3. CO_2-rich raw natural gas conditioning

The stages required for the conditioning of the CO_2-rich NG is: (i) Water Dew-Point Adjustment, to prevent hydrate formation, (ii) Hydrocarbon Dew-Point Adjustment (HDPA), consisting of heavy hydrocarbon removal, to satisfy market specifications of hydrocarbon contents, (iii) removal of CO_2, to increase gas heating value, reduce flowrate and avoid corrosion. The most mature configuration for the conditioning of this type of NG is water absorption with Triethylene Glycol (TEG) for water removal, expansion in a Joule-Thomson (JT) valve for HDPA and Membrane Permeation (MP) for CO_2 removal.

The main drawback of this conditioning configuration is the high loss of CH_4 in the MP, the high pressure drop in the permeate stream, containing the captured CO_2, requiring a powerful

compression system, the high pressure drop in the JT valve and the high footprint and weight of the equipment. A recent technology involves the utilization of Supersonic Separators (SS) for CO_2 removal and for HDPA. This technology is already proven to be technical (de Melo et al., 2019) and economically (Arinelli et al., 2017) favorable, when compared to the conventional one. However, the benefits of the SS technology are still not covered in the literature in terms of exergy efficiency to analyze its sustainability, which is explored in this Thesis. This analysis can be another proof that the conditioning process with SS units is more sustainable.

1.4. The Present Work

The main objective of this Thesis is to contribute for the sustainable development of the chemical and energy sector, producing a cleaner energy and combating the climate change and its impacts, thus fulfilling some goals of the United Nations 2030 agenda. This is accomplished by developing and analyzing new technologies, which has potential to be more sustainable than the conventional ones. The main scope of this Thesis is (bio)chemical processes directed to power plants and to CO_2-rich NG exploitation to mitigate CO_2 emissions and the sustainability is verified on technical, economic, environmental and exergy conservation grounds. The technological innovations are presented according to four research lines – Line#1, Line#2, Line#3 and Line#4 – with great contribution to the increase of the state-of-the-art knowledge through scientific publications:

Line#1 – Evaluates the sustainability of a new CCU from coal-fired power plant flue-gas via microalgae carbon capture, passing through microalgae biomass gasification, and reaching methanol production.

Line#2 – Evaluates the sustainability of the CCU for methanol production from power plant flue-gas, comparing it with the CCS technology.

Line#3 – Evaluates the sustainability of applying CCS to bioenergy production in sugarcane biorefineries.

Line#4 – Evaluates the sustainability of novel technologies for offshore CO_2-rich NG conditioning system with Supersonic Separators with EOR destination.

Despite associated to different sectors (bioenergy production, fossil-energy production, methanol production, and CO_2-rich NG processing), all the analyzed routes are possible

pathways to achieve a sustainable development. They are plausible solutions for mitigating CO_2 emissions from flue-gas, displacing fossil fuels or for increasing the performance of the current technologies.

1.4.1 Outline of Thesis structure

This Thesis is structured as a collection of published articles in international indexed journals (Chapters 2, 3, 4 and 5). They are inserted chapter-wise after formatting adjustments of the reference lists, figures, tables and equations, which were indexed according to the respective chapter. Each work belongs to a Research Line as shown in Table 1.1. One large appendix chapter shows all the scientific production related to this Thesis.

Table 1.1. Research Lines associated with each chapter.

Research Line	Chapters	Articles References
Line#1: Techno-Economic Analysis of CCU to methanol production via microalgae culture using flue-gas of coal-fired power plants	02	Wiesberg et al. (2017)
Line#2: Exergy Analysis of CCU to methanol production from CO_2-rich NG versus CCS	03	Wiesberg et al. (2019)
Line#3: Techno-Economic Analysis of Bioenergy production with CCS in sugarcane biorefinery	04	Wiesberg et al. (2021a)
Line#4: Exergy Analysis of Offshore CO_2-rich NG processing with supersonic separators	05	Wiesberg et al. (2021b)

A brief description of each chapter in this Thesis is presented in the following paragraphs.

Chapter 1 summarizes the themes related to this Thesis, contextualizing and discussing key aspects of the Research Lines and demonstrating the motivations, achievements and structure of the Thesis.

Chapter 2 evaluates the CCU for methanol and lipids production from coal-fired power plant flue-gas, by means of microalgae biofixation. The biomass is converted to methanol via its gasification, prior to conventional syngas conversion to methanol. The microalgae are chosen because of its high capacity to perform CO_2 fixation and greater lipid content. This CCU route is economically compared to the conventional CCS adopting the chemical absorption with amine as the CO_2 capture step. The sustainability is assessed by technical-economic and

environmental aspects. This chapter presents a full-length paper published in the Journal of Environmental Management (Wiesberg et al., 2017).

Chapter 3 evaluates the sustainability of two routes of CCU for methanol production: the direct CO_2 hydrogenation and the bi-reforming of NG. The capture step is performed with chemical absorption with MEA. The sustainability is assessed via Exergy Analysis over the power plant operation until the CO_2 destination. The CCU exergy performance is compared with the performances of the CCS and of the flue-gas emission.

Chapter 4 evaluates the sustainability of the BECCS of a CHP unit from sugarcane bagasse, assessed by technical-economic aspects. The carbon capture is performed by chemical absorption with MEA. A surrogate model is generated for each step, i.e., for the CHP and for the CCS.

Chapter 5 evaluates the sustainability of the SS technology for offshore CO_2-rich NG conditioning for WDPA, HDPA, and CO_2 removal via Exergy Analysis and compares it to conventional processes using TEG+JT+MP. Two innovative SS-based processing routes are analyzed. The first one is the use of SS for WDPA+HDPA, simultaneously, being the CO_2 removal performed by MP. The second one uses the same SS of the first configuration plus another one for CO_2 removal, in place of the MP.

Chapter 6 finally presents an overall conclusion of the results achieved in this Thesis.

Appendix A presents the productions gathered throughout this Thesis. Productions are organized in chronological order in which they were achieved.

Finally, **Appendix B** presents the Supplementary material of the Chapter 2.

1.5. References for Chapter 1

Araújo, O. Q. F.; de Medeiros, J. L., Alves, R.M.B., CO2 Utilization: A Process Systems Engineering Vision, In CO2 Sequestration and Valorization, edited by Claudia Rosario, Victor Pecanha. London: IntechOpen, 2014.

Araújo, O. Q. F.; Reis, A. C.; de Medeiros, J. L.; Nascimento, J. F.; Grava, W. M.; Musse, A. P. S. Comparative analysis of separation technologies for processing carbon dioxide rich natural gas in ultra-deepwater oil fields. Journal of Cleaner Production, 155, 12–22, 2017. https://doi.org/10.1016/j.jclepro.2016.06.073

ARESTA M., Carbon dioxide as chemical feedstock. Wiley-VCH: Weinheim, 2010.

Ali, E.; Alnashef, I.; Ajbar, A.; Mulyono, S.; Hizaddinm H.F.; Hadj-Kali, M.K. Determination of cost-effective operating condition for CO2 capturing using 1-butyl-3-methylimidazolium tetrafluoroborate ionic liquid. Korean Journal of Chemical Engineering, 30(11), 2068-2077, 2013.

Arinelli L. O.; Trotta T. A. F.; Teixeira, A. M.; De Medeiros, J. L.; Araújo O. Q. F. Offshore Processing of CO_2 Rich Natural Gas with Supersonic Separator versus Conventional Routes. Journal of Natural Gas Science and Engineering, 46, 199–221, 2017. https://doi.org/10.1016/j.jngse.2017.07.010

Carbonbrief. New scenarios show how the world could limit warming to 1.5C in 2100. 2018. Available at: <https://www.carbonbrief.org/new-scenarios-world-limit-warming-one-point-five-celsius-2100>. Accessed on 1st feb. 2022.

CARMINATI, H. B. et al. Bioenergy and full carbon dioxide sinking in sugarcane-biorefinery with post-combustion capture and storage: Techno-economic feasibility. Applied Energy, v. 254, p. 113633, 2019.

de Melo, D. C.; Arinelli, L. O.; de Medeiros, J. L.; Teixeira, A. M.; Brigagão, G. V.; Passarelli, F.; Grava, W. M.; Araújo, O. Q. F. Supersonic separator for cleaner offshore processing of supercritical fluid with ultra-high carbon dioxide content: economic and environmental evaluation. Journal of Cleaner Production, 234, 1385-1398, 2019. https://doi.org/10.1016/j.jclepro.2019.06.304

Efenberger, F. X. Vision: Technical Photosynthesis. in Methanol: The Basic Chemical and Energy Feedstock of the Future: Asinger's View Today. Bertau, M., Offermanns, H., Plass, L., Schmidt, F., Wernicke, H. J., Eds. , Chapter 3, 2014, pages 39-50.

EIA, 2019, World Energy Outlook 2019. U.S. Department of Energy.

EIA, 2020. International Energy Outlook 2021. https://www.eia.gov/outlooks/ieo/pdf/IEO2021_Narrative.pdf. Assessed on 21th jan. 2022.

EIA. Natural gas and the environment - U.S. Energy Information Administration (EIA), 2021. Available at: https://www.eia.gov/energyexplained/natural-gas/natural-gas-and-the-environment.php. Assessed on: 1st feb. 2022.

Friedlingstein, P., Jones, M.W., O'Sullivan, M. et al., 2021. Global Carbon Budget 2021. Earth System Science Data Discussions 1–191.

Gaffney, Cline & Associates: Review and Evaluation of Ten Selected Discoveries and Prospects in the Pre-salt Play of the Deepwater Santos Basin, Brazil, CG/JW/RLG/C1820.00/GCABA.1914 ANP 2010.

Hong, S. H., 2013, Catalytic Hydrogenation of Carbon Dioxide. Organic Chem Curr Res 2:e119.

IPCC. Climate change 2014: synthesis report. Contribution of Working Groups I, II and III to the Fifth Assessment Report of the Intergovernmental Panel on Climate Change. Core Writing Team, Pachauri, R. K.; Meyer, L. A. (eds.). IPCC, Geneva, Switzerland, 151 pp, 2014.

Milão RFD., Araujo OQF., de Medeiros J.L., Second Law analysis of large-scale sugarcane-ethanol biorefineries with alternative distillation schemes: Bioenergy carbon capture scenario. Renew Sustain Energy Rev 2021;135(110181). DOI: 10.1016/j.rser.2019.109251.

O'NEILL, B. C. et al. The roads ahead: Narratives for shared socioeconomic pathways describing world futures in the 21st century. Global Environmental Change, v. 42, p. 169–180, 1 jan. 2017.

OZBILEN, A.; DINCER, I.; ROSEN, M. Exergetic life cycle assessment of a hydrogen production process. International Journal of Hydrogen Energy, v. 37, n. 7, p. 5665-5675, 2012.

Rogelj, J., Popp, A., Calvin, K.V. *et al.* Scenarios towards limiting global mean temperature increase below 1.5 °C. *Nature Clim Change* **8,** 325–332 (2018). https://doi.org/10.1038/s41558-018-0091-3

ROSEN, M.; DINCER, I.; KANOGLU, M. Role of exergy in increasing efficiency and sustainability and reducing environmental impact. Energy Policy, v. 36, n. 1, p. 128-137, 2008.

United Nations. Paris Agreement. Article 2, p.3. 2015. Available at.: <https://unfccc.int/sites/default/files/english_paris_agreement.pdf. Accessed on Jan. 31th, 2022.

IPCC, 2018a, Framing and Context. In: Global Warming of 1.5°C. An IPCC Special Report on the impacts of global warming of 1.5°C above pre-industrial levels and related global greenhouse gas emission pathways, in the context of strengthening the global response to the threat of climate change, sustainable development, and efforts to eradicate poverty. Available at: https://www.ipcc.ch/site/assets/uploads/sites/2/2019/02/SR15_Chapter1_Low_Res.pdf Accessed on Jan. 31th, 2022.

IPCC, 2018b, Framing and Context. In: : Mitigation Pathways Compatible with 1.5°C in the Context of Sustainable Development. An IPCC Special Report on the impacts of global warming of 1.5°C above pre-industrial levels and related global greenhouse gas emission pathways, in the context of strengthening the global response to the threat of climate change,

sustainable development, and efforts to eradicate poverty. Available at: https://www.ipcc.ch/site/assets/uploads/sites/2/2019/02/SR15_Chapter2_Low_Res.pdf Accessed on Jan. 31th, 2022.

Wiesberg, I. L., Medeiros J.L., Alves, R.M.B., Coutinho, P.L.A., Araújo, O. F., Carbon dioxide management by chemical conversion to methanol: HYDROGENATION and BI-REFORMING. Energy Conversion and Management, Sustainable development of energy, water and environment systems for future energy technologies and concepts. v. 125, p. 320–335, Outubro 2016.

Wang, C., Xu, J., Qi, G., Gong, Y., Wang, W., PAN, G., Wang, Q., Feng, N., Liu, X., Deng, F., Methylbenzene hydrocarbon pool in methanol-to-olefins conversion over zeolite H-ZSM-5, J. Catal., Vol. 332, pp 127-137, 2015.

Wiesberg, I. L.; Brigagão, G. V.; de Medeiros, J. L.; Araújo, O. Q. F. Carbon dioxide utilization in a microalga-based biorefinery: efficiency of carbon removal and economic performance under carbon taxation. Journal of Environmental Management, 203, 988-988, 2017. https://doi.org/10.1016/j.jenvman.2017.03.005

Wiesberg, I.L., Brigagão, G.V., Araújo, O. de Q.F., de Medeiros, J.L., 2019. Carbon dioxide management via exergy-based sustainability assessment: Carbon Capture and Storage versus conversion to methanol. Renewable and Sustainable Energy Reviews 112, 720–732. https://doi.org/10.1016/j.rser.2019.06.032

Wiesberg, I.L., de Medeiros, J.L., Paes de Mello, R.V., Santos Maia, J.G.S., Bastos, J.B.V., Araújo, O. de Q.F., 2021. Bioenergy production from sugarcane bagasse with carbon capture and storage: Surrogate models for techno-economic decisions. Renewable and Sustainable Energy Reviews 150, 111486. https://doi.org/10.1016/j.rser.2021.111486

Wiesberg, I.L., Arinelli, L. de O., Araújo, O. de Q.F., de Medeiros, J.L., 2021b. Upgrading exergy utilization and sustainability via supersonic separators: Offshore processing of carbonated natural gas. Journal of Cleaner Production 310, 127524. https://doi.org/10.1016/j.jclepro.2021.127524

Wu, D., He, D., Yao, G., Jin, F., Recent Advances in Fixation and Hydrogenation of Carbon Dioxide. In: 2018 2ND International Conference on Advances in Energy, Environment and Chemical Science (AEECS 2018). Atlantis Press, mar. 2018.

2. CARBON DIOXIDE UTILIZATION IN A MICROALGA-BASED BIOREFINERY: EFFICIENCY OF CARBON REMOVAL AND ECONOMIC PERFORMANCE UNDER CARBON TAXATION.

This chapter corresponds to an article published in the Journal of Environmental Management.

Abstract

Coal-fired power plants are major stationary sources of carbon dioxide and environmental constraints demand technologies for abatement. Although Carbon Capture and Storage is the most mature route, it poses severe economic penalty to power generation. Alternatively, this penalty is potentially reduced by Carbon Capture and Utilization, which converts carbon dioxide to valuable products, monetizing it. This work evaluates a route consisting of carbon dioxide bio-capture by Chlorella pyrenoidosa and use of the resulting biomass as feedstock to a microalgae-based biorefinery; Carbon Capture and Storage route is evaluated as a reference technology. The integrated arrangement comprises: (a) carbon dioxide biocapture in a photobioreactor with biomass production, (b) oil extraction from part of the produced biomass, (b) gasification of remaining biomass to obtain bio-syngas, and (c) conversion of bio-syngas to methanol. Calculation of capital and operational expenditures are estimated based on mass and energy balances obtained by process simulation for both routes (Carbon Capture and Storage and the biorefinery). Capital expenditure for the biorefinery is higher by a factor of 6.7, while operational expenditure is lower by a factor of 0.45 and revenues occur only for this route, with a ratio revenue / operational expenditure of 1.6. The photobioreactor is responsible for one fifth of the biorefinery capital expenditure, with footprint of about 1000 ha, posing the most significant barrier for technical and economic feasibility of the proposed biorefinery. The Biorefinery and Carbon Capture and Storage routes show carbon dioxide capture efficiency of 73% and 48%, respectively, with capture cost of 139\$/t and 304\$/t. Additionally, the biorefinery has superior performance in all evaluated metrics of environmental impacts.

Keywords: Carbon capture and storage; carbon dioxide utilization; microalgae; biorefinery; biomass gasification; methanol synthesis.

Abbreviations

AP – Acidification Potential
ASU – Air Separation Unit
ATP – Aquatic Toxicity Potential
BAU – Business as Usual
BM – Biomass
BRY – Biorefinery
CAPEX – Capital Expenditure
CCS – Carbon Capture and Storage
CCU – Carbon Capture and Utilization
CCUS – Carbon Capture, Utilization and Storage
EOR – Enhanced Oil Recovery
GOX – Gaseous Oxygen
GSD – Greenhouse Solar Drying
GWP – Global Warming Potential
HE – HydroElectric power plant
HHV – Higher Heating Value
HTPE – Human Toxicity Potential by Exposure
HTPI – Human Toxicity Potential by Ingestion
IRR – Internal Rate of Return
LHV – Lower Heating Value
MARR – Minimum Acceptable Rate of Return
MEA – Monoethanolamine
MeOH – Methanol
MMUS$ – Millions of United States Dollars
NG – Natural Gas
NGCC – Natural Gas Combined Cycle
NPV – Net Present Value
ODP – Ozone Depletion Potential
OPEX – Operational Expenditure
PBR – Photobioreactor
PC-SAFT – Perturbed-Chain Statistical Association Fluid Theory
PCOP – Photochemical Oxidation Potential
PEA – Process Economic Analyzer
PEI – Potential Environment Impact
SRK – Soave-Redlich-Kwong
TTP – Terrestrial Toxicity Potential
UNIQUAC – Universal QuasiChemical
WAR – Waste Reduction Algorithm

2.1. Introduction

The world economy is heavily dependent on fossil fuels, generating massive emissions of carbon dioxide (CO_2). Coal fired power plants are among the major stationary sources of CO_2 emissions, where Carbon Capture and Storage (CCS) is the leading technology for CO_2

management. Besides recognized technical barriers – e.g., existence of geological sites (Cuéllar-Franca and Azapagic, 2015), CO_2 monitoring for leakage (Cheah et al., 2016) – the absence of revenues imposes relevant economic penalty to the CO_2 source processes due to the significant capital investment required.

Alternatively, utilization of CO_2 aims to add value to the captured CO_2 (Carbon Capture and Utilization, CCU), through its chemical conversion (Aresta, 2010). The ensemble of technologies for CO_2 management is referred to CCUS (i.e., CCS+CCU), spanning from storage to physical, chemical and biochemical utilization (e.g., Enhanced Oil Recovery – EOR, methanol production). It is worth noting that a few chemical syntheses employ CO_2 as feedstock at a commercial scale (e.g., urea) (Aresta, 2010), where most alternatives are at the earlier stages of technology readiness level (most of them are still at laboratory or bench scale). Conversion of CO_2 to methanol (MeOH) outstands as a promising alternative, accordingly to technical and economic studies evaluating capital and operational expenditures, and environmental performance. Kourkoumpas et al. (2016) investigated the methanol production based on CO_2 capture from lignite power plants, estimating MeOH production cost of 421€/t in case of a power plant owner investment. Pérez-Fortes et al. (2016) investigated the direct CO_2 hydrogenation, estimating an avoidance of 2 ton of CO_2 per ton of MeOH produced. Gong et al. (2016) analyzed a superior use of the usually emitted coke oven gas, claiming higher techno-economic performance when compared to other carbon to methanol routes.

In fact, EOR and CCS are presently the only CO_2 management chains that include steps ready to be put into operation at high scales: some separation technologies for CO_2 post-combustion capture, CO_2 compression and CO_2 transportation via pipelines (Araujo et al., 2014). Except for EOR, lack of large commercial scale application is mainly due to technological gaps. Technology changes in energy and transportation systems play a central role in response to climate changes, and most of these routes face technological challenges and economic barriers, requiring support to widespread use (Kypreos and Turton, 2011).

Based on a review of life cycle analyses, Cuéllar-Franca and Azapagic (2015) observed that the environmental benefit of CO_2 removal with CCS is accompanied by the increase of other environmental impacts (e.g., acidification and human toxicity), and recommend consideration of a wider range of impacts from CCS and CCU, rather than focusing exclusively on the GWP (Global Warming Potential).

Economic aspects are rarely present in the literature as comparison ground between CCS and CCU, and the relevance of the missing approach is magnified within the scenario of carbon taxation. There is a growing convergence of policy-makers and economists that stablishing a carbon price is the most effective way to reduce carbon footprint (Kypreos and Turton, 2011). Despite the purpose of increasing the marginal cost of greenhouse gas emissions (Pereira et al., 2016), most studies on carbon taxation conclude for recessive impact on households due to the increase in the prices of energy and energy-intensive goods (Dissou and Siddiqui, 2014).

However, from an engineering standpoint, carbon taxes have the potential of catalyzing the progress to technological maturity, when faced as a production cost to be avoided (or reduced) by abatement and destination route. Üçtug et al. (2014) evaluates installing a CCUS unit as a non-linear optimization problem where the objective is to maximize the net returns from pursuing an optimal mix of CCUS (with MeOH synthesis as example of utilization) and carbon trading, concluding for the dominance of carbon price and discount rate on the results. Carbon taxation was not considered by Üçtug et al. (2014) despite a conditioning scenario for investigating the potential of CCUS technologies being expansion of CO_2 taxes worldwide (Eberhard, 2014) (with Sweden having presently the highest tax - US\$150/t emitted CO_2).

In this context, carbon taxes parallel environmental taxes (Chiu et al., 2015) and can be approached as an operational cost (OPEX). Hence, reducing emissions (e.g., via CO_2 management technologies) decreases OPEX due to the minored incidence of carbon taxes. This is especially relevant with growth in proven natural gas reserves accompanied by the increase in fossil fuels (Zhang et al., 2017), which leads to coexistence of fossil based energy generation and carbon taxes, constituting a relevant driver for CCUS technologies.

In its early stage of technological readiness, microalgae have received intense research, due mainly to its high growth rates – microalgae have the capacity to fix carbon dioxide with efficiency 10 times higher than terrestrial plants – and superior lipid content (Skjanes et al., 2007). For instance, *Chlorella pyrenoidosa* has total lipid content in dry biomass of up to 51% (Liu et al., 2011). Goli et al. (2016) reviewed the literature for biological CO_2 fixation, with emphasis on microalgae, and recognize superiority of photobioreactors (PBR) facing raceways, although improvements in scale-up criteria are needed. Comparatively to raceways, PBR require higher capital expenditure, but can achieve much higher biomass and lipid productivities (Moheimani, 2016). If successfully developed, biofixation of CO_2 by

microalgae and utilization of the grown biomass in biorefineries may generate revenues that ultimately reduce the cost of mitigating CO_2 emissions from fossil fired power plants.

In this direction, the use of thermochemical processes (e.g., gasification) in biorefinery designs are attractive due to the flexibility to process a variety of biomass feedstock (Garcia et al., 2016), and yielding products with a wide range of large scale applications, e.g., synthesis gas, which is a common raw material to several mature technologies (e.g., MeOH and ammonia) replacing their original fossil source, as syngas is conventionally derived from natural gas reforming. It is noteworthy that the scale of emissions associated to a fossil fired power plant requires chemical commodities (e.g., ammonia) and energy products (e.g. MeOH) for leveling large scale production and CO_2 supply. Production of high added value functional biomolecules, although important for revenues, does not impact CO_2 inventory due to their limited demand, and an excess of supply would drastically reduce its sale price. In fact, the portfolio of energy products and the processing scale are the most important variables that must be considered to improve the profitability of biorefineries (Garcia et al., 2016). Hence, for a biorefinery focusing at CO_2 utilization, a single or few products, with long-term forecast of large demand, are recommended. High-added value biomolecules should be produced at small scale to increase revenue.

Chea et al. (2016) reviewed current advances in biological CO_2 capture and valorization, and concluded that the economic aspects must be considered to make the biofuel-driven biomass refinery more sustainable. Although the view of microalgae-based technology for CCU is not new, the literature is rare in analyses comparing CAPEX, OPEX and the resulting cost of CO_2 avoided with respect to CCS. Equally impacting to the context of the present work is the inclusion of CO_2 taxation into a process engineering analysis, a relevant and often neglected aspect. CO_2 captured as revenue (carbon credits) is rather the dominant approach in the literature (e.g., Üçtug et al., 2014) while policy-makers are moving to CO_2 as cost (taxation).

Although technological bottlenecks still prevent operation of microalgae mediated abatement of CO_2 emissions on a commercial scale, this work contributes with a process engineering approach to identify potential barriers, under carbon tax incidence, and quantitatively compares the biorefinery alternative to CCS. Specifically, the study presents economic feasibility and environmental analyses of the performance of capturing CO_2 by *Chlorella pyrenoidosa* and its chemical utilization to produce MeOH through biomass gasification, with co-production of microalga oil to provide additional revenue (biorefinery as a CCU

technology). The results from the microalga-based biorefinery are compared with the CCS option, under carbon tax incidence. Both analyses are performed considering that the evaluated alternatives are in Brazil, where carbon taxation, although foreseen, is not yet enforced. Moreover, process design decisions are defined to benefit the economic return of the operation (Davis et al., 2014), and to propose further improvements and optimization.

2.2 Methods

Two alternatives are proposed to abate CO_2 emission from a coal-fired power plant: a microalga-based biorefinery (BRY) route and the CCS route. The BRY route consists of biomass production (microalga cultivation and harvesting), oil extraction, biomass gasification and conversion to MeOH. The CCS route combines CO_2 capture by chemical absorption with amine and CO_2 compression for transportation and storage. To evaluate the feasibility of BRY and CCS, the process configuration for each route is defined and simulated in Aspen Hysys (AspenTech Inc.) for mass and energy balance calculation. Process simulation results are then used for equipment costing in Aspen PEA (AspenTech Inc.) and for inventory assessment to support economic and environmental analyses. Fig. 2.1 presents an overview of the applied methods, and Fig. 2.2 depicts the abridged scope of the economic and environmental analyses. The coal fired power plant is outside the boundaries of the study as it is not affected by design decisions adopted in the CCU or CCS alternatives.
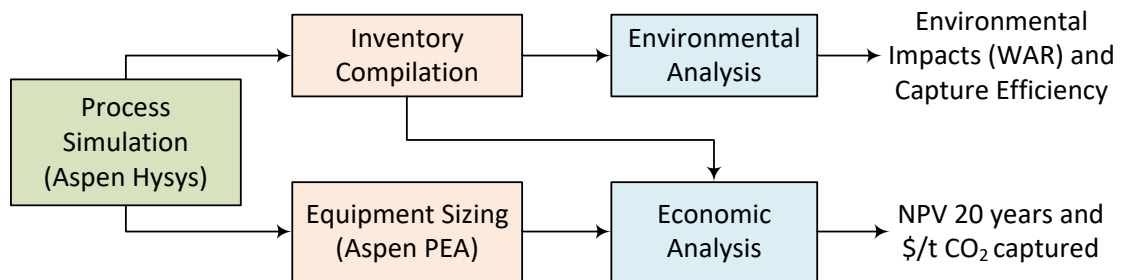
Fig. 2.1. **Comparative analysis of BRY and CCS: sequenced steps.**
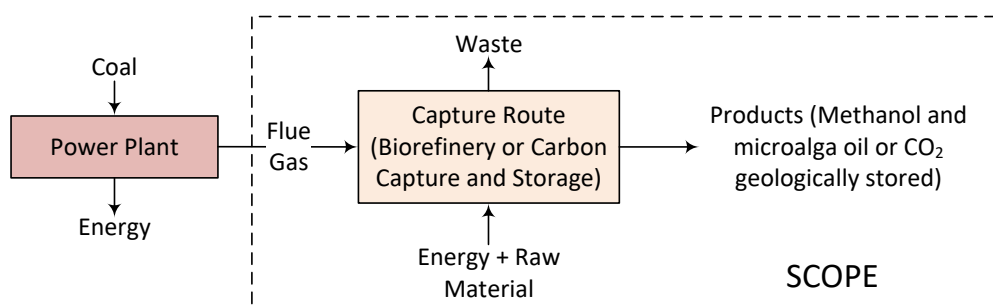
Fig. 2.2. **Scope of the environmental and economic analyses.**

The flows of products, waste, energy and raw materials of each technology are obtained by process simulation. Most of the unit operations (e.g., compression, absorption, solvent regeneration and distillation) are available in the Aspen Hysys library ("unit operation blocks"). However, to simulate the biomass production in the PBR of the BRY, a compositional approach is required. A stream of "pure" microalga is created by the combination of its components (the metabolic pools "lipids", "proteins" and "carbohydrates") in proportions to meet lipid profile and biomass composition obtained from the literature. "Carbohydrates" is represented as sucrose, "lipids" are simulated as a set of carboxylic acids and "proteins" as a pseudo-component with molecular formula $C_{10}H_{16}N_2O_8$. The volumetric flow entering the PBR is obtained from the amount of biomass that must be produced to yield a biomass concentration of 4 g/L, considering the stoichiometric ratio of CO_2 to biomass production in the photosynthesis reaction, given in Eq. 2.1. The PBR model also computes the amount of oxygen (O_2) produced and water (H_2O) consumed (Eq. 2.1). The last degree of freedom of the PBR unit is the dilution rate, which is adjusted to achieve a specified residual CO_2 in the medium, calculated by the CO_2 consumption efficiency of the PBR.

$$1CO_2 + 0.5bH_2O + c\,N + d\,P + e\,S \rightarrow CO_aH_bN_cP_dS_e + (1 + 0.25b - 0.5a)O_2$$
(2.1)
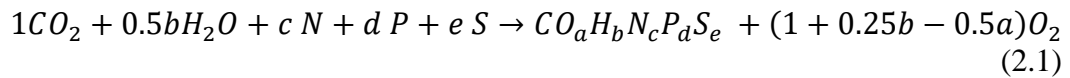
2.3. Process description

This section presents simplified Process Flow Diagram (PFD) of the evaluated processes, BRY and CCS. Detailed process flowsheets are provided in Appendix A of the Supplementary Material.

2.3.1. Biomass production, conversion to methanol and oil extraction (biorefinery)

Fig. 2.3 depicts the simplified PFD for the first area of the BRY route: biomass production and oil extraction (BRY-1), while Fig. 2.4 depicts the PFD of the biomass gasification and MeOH production (BRY-2).
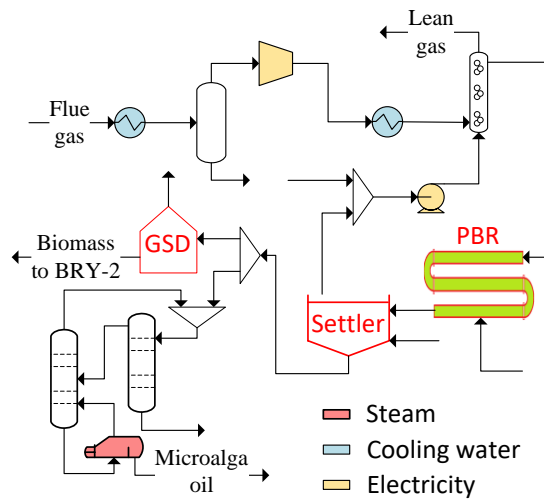
Fig. 2.3. **Process Flow Diagram of biomass production and oil extraction (BRY-1).**
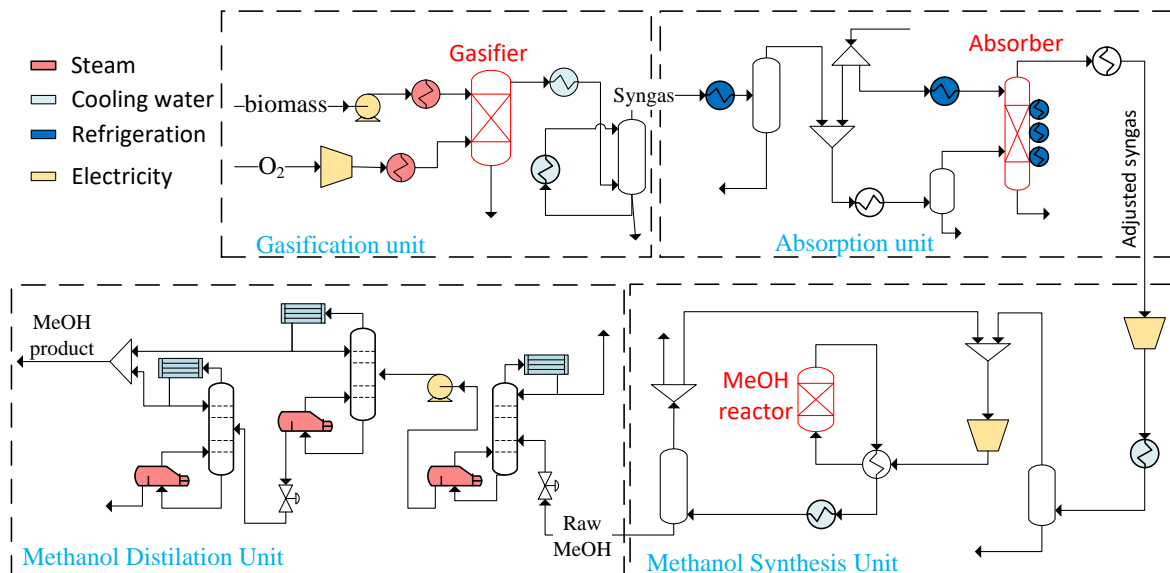
Fig. 2.4. **Process flow diagram for biomass gasification and MeOH production (BRY-2). Solvent regeneration, CO₂ liquefaction and cogeneration are omitted, although considered in the simulation and related analyses.**

Considering limitations in market demand for abrupt increase in the supply of microalgae oil, only 25% of the produced biomass is destined to oil extraction, while the remainder is sent to MeOH production. CO_2 from flue gas is absorbed into water in an air lift arrangement, which contacts the gas feed stream with the water recycle from the dewatering unit, allowing mass transport of CO_2 from the gas into the liquid phase. The carbonated water is fed, driven by gravity, to the PBR, consisting of horizontal transparent tubes in a vertical arrangement. The reactor effluent is sent to dewatering, which accounts for 20-30% of the overall biomass production cost (Molina Grima et al., 2003). Two unit operations are used for dewatering: a

gravity settler and a Green Solar Dryer (GSD), which requires energy for mixing and venting (Kurt et al., 2015).

In the second area of the biorefinery (BRY-2), dewatered biomass and residual biomass are directed to gasifier, producing syngas, which is then converted to MeOH. In the thermochemical conversion of biomass to syngas, low-purity gaseous oxygen (95%mol) supplied by an Air Separation Unit (ASU) is utilized as gasification agent (autothermal gasification). The syngas is sent to a Rectisol unit (methanol-based physical absorption) where CO_2 removal occurs to adjust the hydrogen/carbon (H/C) ratio in the syngas, resulting in a syngas stoichiometric number (S, given in Eq. 2.2) slightly above 2, as recommended for MeOH synthesis (Olah et al., 2009). The separated CO_2 is sent to liquefaction and exported at 100 bar as product.

$$S = (nH_2 - n\,CO_2)/(n\,CO + n\,CO_2) \hspace{3cm} (2.2)$$

where $n\,CO_2$, $n\,CO$ and $n\,H_2$ are the molar flow of carbon dioxide, carbon monoxide and hydrogen.

The MeOH production unit is based on the Lurgi process configuration for MeOH synthesis. The raw MeOH stream exiting the reactor is sent to the distillation section for purification. Significant amount of low pressure steam is required for process heating and is produced in the cogeneration unit, which is fueled by MeOH synthesis purge gas, besides steam generation by heat recovery in MeOH reactor and syngas cooling section.

2.3.2 Carbon Capture and Storage

The simplified PFD for the CCS route is presented in Fig. 2.5. The flue gas from the power plant is sent to the MEA (monoethanolamine) Capture Unit, where CO_2 is separated and the lean gas emitted to atmosphere. The CO_2 rich stream proceeds to compression (four stages) prior to transportation (not simulated) for geological storage.
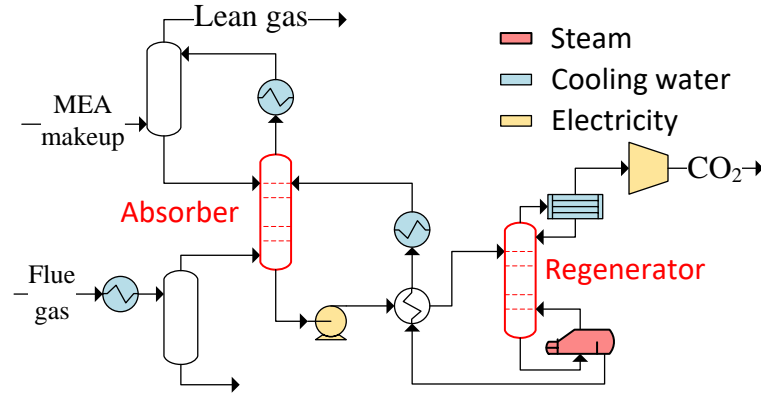
Fig. 2.5. **Process diagram for the CCS route.**

2.4. Environmental Analysis

The environmental performances of the investigated routes (BRY and CCS) are evaluated based on CO_2 footprint, considering the ratio of the sum of direct and indirect CO_2 generation to the total CO_2 feed for each process alternatives ($CO_{2\ produced}/CO_{2\ feed}$). To calculate the direct emissions, the CO_2 emitting potential of a process stream is evaluated by its complete combustion, while indirect emissions are calculated from the power demand of electricity and heat utility (low-pressure steam). The total avoided CO_2 in the MeOH production is compared with emerging chemical routes of CO_2 utilization, namely CO_2 hydrogenation and bi-reforming, through Eqs. 2.3 and 2.4 (Pérez-Fortes et al., 2016), where $CO_2(conventional)$ is the amount of CO_2 generated in the production of MeOH in a conventional technology, while $CO_2(generated)$ and $CO_2(consumed)$ refer to each emerging route.

$$CO_2(not\ produced) = CO_2(conventional) - CO_2(generated) \tag{2.3}$$
$$CO_2(avoided) = CO_2(not\ produced) + CO_2(consumed) \tag{2.4}$$

Additional environmental performance metrics are obtained with the Waste Reduction (WAR) Algorithm (Young and Cabezas, 1999). The method consists in the analysis of inlet and outlet material streams to evaluate the Potential Environment Impact (PEI) of the process, an unified score obtained by the weighted sum of eight impact categories: Global Warming Potential (GWP), Human Toxicity Potential by Exposure (HTPE), Human Toxicity Potential by Ingestion (HTPI), Ozone Depletion Potential (ODP), Photochemical Oxidation Potential (PCOP), Acidification Potential (AP), Aquatic Toxicity Potential (ATP), and Terrestrial Toxicity Potential (TTP). PEI results are not considered in the analysis, which is

focused on the individual categories to identify the nature of the environmental impacts generated by the process.

Fossil fuel consumption is also considered in the analysis, as it causes indirect impacts, while impacts from product streams are not considered. The functional unit of comparison between the two routes is one metric ton of net CO_2 captured, considering the capture efficiency. Impacts associated to thermal energy (low-pressure steam) and electricity (supplied by a coal power plant) demands are considered.

2.5. Economic Analysis

The economic feasibility analysis employs Aspen Process Economic Analyzer (Aspen PEA, AspenTech Inc.), a costing software that provides estimates of capital and operational expenditures (CAPEX and OPEX). Additionally, cash flow calculation is performed in a spreadsheet that is described in a previous work (Wiesberg et al., 2016), which also presents the parameters utilized in Aspen PEA.

Since the objective of the operation is to avoid CO_2 emissions with minimum cost, it is assumed that the Minimum Acceptable Rate of Return (MARR) is 0% for Net Present Value (NPV) calculation, which means that if the investment is reimbursed, and has achieved its goal. The capture cost of a certain cash flow is calculated by Eq. 2.5, where $CO_{2\,processed}$ is the gross captured gas. The cost is given in US$ per net metric ton of CO_2 captured.

Moreover, CO_2 taxation is considered and assumed to apply to both direct and indirect emissions. The cash flow difference between investing in the capture and paying CO_2 taxes is calculated by Eqs. 2.6-2.8. A negative NPV indicates that paying the taxes is more advantageous than avoiding taxation through CO_2 capture. It is worth noting that the capture cost is calculated using NPV obtained from Eq. 2.7 (the $Cash\,flow_{invested}$). Otherwise, NPV is calculated based on the difference cash flow (Eq. 2.6).

$$Capture\,Cost\,(US\$/t) = NPV/(CO_{2\,processed} * capture\,efficiency) \qquad (2.5)$$
$$Cash\,flow_{difference} = Cash\,flow_{invested} - Cash\,flow_{not\,invested} \qquad (2.6)$$
$$Cash\,flow_{invested} = Cash\,flow_{technology} - CO_2\,tax * (1 - capture\,efficiency) \quad (2.7)$$
$$Cash\,flow_{not\,invested} = CO_2\,tax \qquad (2.8)$$

Aspen PEA results refer to USA based plants in the first quarter of 2013. Hence, a nationalization factor is required to transfer results to the Brazilian context and a plant cost index is needed to update costs in time. Pipeline costs and CAPEX are given in US$ for a different reference year, and are also corrected by a cost index. The project lifetime is set to

20 years, except for the PBR (E6), which is set to 5 years (requiring replacement along process lifetime). Table 2.1 presents parameters and additional premises for the economic analysis. In the case of CCS, the cost of pipeline transportation of CO_2 is obtained from the literature, shown in Table 2.2.

Table 2.1. **Premises for the economic evaluation.**

Variable	Value
Nationalization Factor [1]	1.25 (Brazil/USA)
IC index [1]	2015Q4=136.0, 2013Q1=147.0, 2003=107.0
Component Price [2]	$NaNO_3$=320 US$/t, NaH_2PO_4=1000 US$/t, $FeCl_3$=350 US$/t
Product Prices	MeOH=400 $/t [3], Microalga oil=0.5 $/kg [4]
Utility Costs	Electricity=0.127US$/kWh[5], Natural gas=19.5 US$/MMBtu [6], Steam (6.9bar)=55.0$/t [7]
PBR price	0.197 MMUS$/ha [8]
Carbon Credit	0 US$/t
CO_2 taxation	50 US$/t [9]
O_2 production cost	31 US$/t [10]
O_2 production required power	158 kWh/t [11]
Project Lifetime	20 years [12]
PBR Lifetime	5 years
MARR	0 %

[1] INTRATEC, 2016. Useful indexes for the chemical industry. http://www.intratec.us/free-tools/other-relevant-indexes (accessed 28/5/2016)

[2] ALIBABA, Find Quality Manufacturers, Suppliers, Exporters, Importers, Buyers, Wholesalers, Products and Trade Leads from our award-winning International Trade Site. Import & Export on alibaba.com. http://alibaba.com (accessed 28/5/2016).

[3] ALICEWEB. Sistema de Análise das Informações de Comércio Exterior. http://aliceweb.desenvolvimento.gov.br/ (accessed10/28/2015).

[4] http://www.soleybio.com. (accessed 05/25/2016).

[5] FIRJAN: custo da energia elétrica para a indústria subirá 27% em 2015. www.firjan.org.br (accessed 11/02/2015).

[6] FIRJAN: Custo do gás para a indústria sobe 21,7% nos últimos quatro anos. www.firjan.org.br (accessed 11/02/2015).

[7] Turton et al. (2012).

[8] Huntley and Redalje (2007).

[9] Carbon taxation is not yet used in Brazil. A value is assumed, based on the study by Kishinami, R., Appy, B., Watanabe Jr., K., 2015. The economic and social impacts of a carbon tax in Brazil. Instituto Escolhas. Available at: www.escolhas.org.

[10] U.S. Department of Energy (US DOE), 2013. Appendix B: Carbon dioxide capture technology sheets. Advanced Carbon Dioxide Capture R&D Program: Technology Update, May 2013.

[11] Higginbotham et al. (2011).

[12] Start year: 2015.

Table 2.2. **Premises for pipeline transportation costs in CCS route.**

Variable	Value
Compression cost	12.58 $/t (electricity cost: 0.12 $/kWh) [1] (McCollum and Ogden, 2006)
Maintenance cost	3,100 $/km/year (source $_{2003}$), 4,259 $/km/year [2] (Wong, 2006)
CAPEX	20,989 $/in/km (source $_{2003}$), 28,835 $/in/km [2] (Wong, 2006)
Tube diameter	8 in
Pipeline length	300 km

[1] Inflation not considered. [2] IC corrected

2.6. Results and Discussion

Results of the economic and environmental analyses are presented in this section, including intermediate results (e.g., inventory compilation and the process simulation).

2.6.1. Process simulation results

The inventory of mass and energy resulted from process simulation can be found in the Supplementary Material, Appendix B. Table 2.3 shows the main simulation results and literature values for comparison, when applicable.

Table 2.3. **Process simulation results for biorefinery (BRY) and CCS.**

Item	Route	This work	Literature results
Chlorella high heating value	BRY	22.2 MJ/kg	22.6 (Duan et al., 2013)
Dilution rate	BRY	0.4046 m³/m³	0.384 (Chisti, 2007)

Item	Route	This work	Literature results
PBR area and cost	BRY	986 ha, 200 MMUS$	
GSD area and cost	BRY	60 ha, 150 MMUS$	
Microalga oil	BRY	2.9 t/h	
MeOH production	BRY	13.87 t/h	
Liquefied CO_2 production	BRY	31.8 t/h	
Stripper reboiler duty	CCS	4.36 GJ/tCO2captured.	4.56 (Feron, 2010)

It is worth noting that the area required for the PBR and GSD are excessively large, whose availability close to a power plant is unlikely to exist. A sensitivity analysis of PBR land area to the design parameter V/S (volume to projected surface ratio) and volumetric productivity ($kg\ m^{-3}\ d^{-1}$) shows that a targeted projected area of 50 ha (reduction by a factor of 20 from the base case) can only be achieved at volumetric productivity >3.0 $kg\ m^{-3}\ d^{-1}$ at V/S higher than 0.8 m³/m², as shown in Fig. 2.6. Despite the high cost of PBR compared to raceways (Gupta et al., 2015), productivity in a well-operated raceway can only attain an average annual dry biomass areal productivity of around 0.025 $kg\ m^{-2}\ d^{-1}$ at a typical culture depth of 0.25–0.30 m, limited by light irradiance profile (maximum concentration of ~0.5 g/L) (Chiste, 2016). Consequently, raceway volume productivity remains in the range 0.08-0.10 $kg\ m^{-3}\ d^{-1}$, demanding prohibitive projected area. Although PBR with volumetric productivity > 3.0 $kg\ m^{-3}d^{-1}$ remain unrealistic given the state of the art (Acién et al., 2012), much denser cultures than in raceways can be potentially reached (e.g., 2-8 g/L).
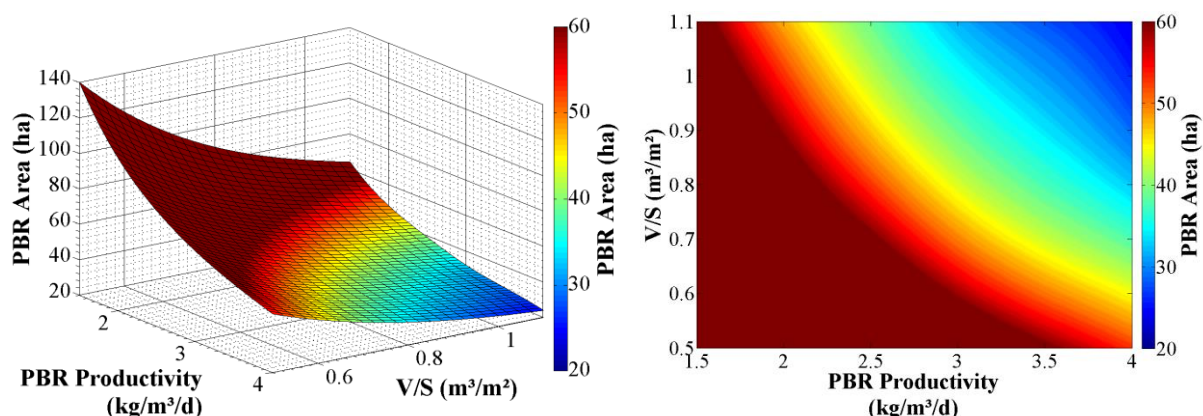
Fig. 2.6. **Sensitivity analysis of PBR area (ha) to PBR productivity and Volume:Surface ratio (V/S): 3D plot (Left); contour levels (right).**

2.6.2. Environmental analysis results

Fig. 2.7 presents CO_2 footprint for both routes, discriminating direct and indirect emissions (caused by electricity and heating demands). The emission factor for burning natural gas with LHV of 47.2 MJ/kg, based on the combustion reaction, is ~2.7 kg CO_2/kg. Two scenarios are analyzed for power supply: (a) steam generation by natural gas-fired boiler (NG) and electricity generation by Natural Gas Combined Cycle (NGCC), as a conventional fossil fuel based scenario, and (b) steam generation by biomass-fired boiler (BM) and electricity generation by hydroelectric power station (HE), as an alternative scenario with renewable energy sources. CO_2 generation from NGCC is set to 388 gCO_2/kWh (Mazzetti et al., 2014), while 14 gCO_2/kWh is set to the HE scenario (IPCC, 2011).
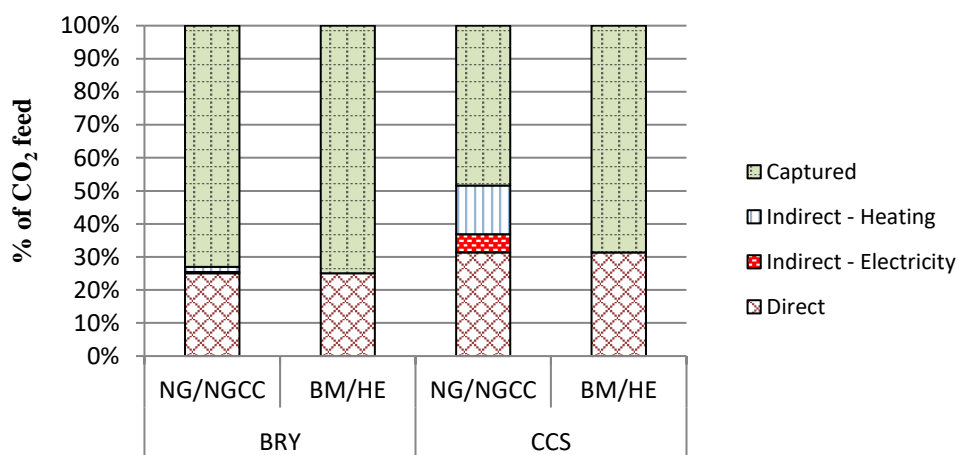
Fig. 2.7. **Direct and indirect CO_2 emission for biorefinery (BRY) and CCS. NG/NGCC: Natural Gas based processes for steam and electricity generation; BM/HE: Biomass-fired boiler for steam generation and hydroelectric power station for electricity supply.**

In the NG/NGCC scenario, BRY fixes 73% of the CO_2 from flue gas, while CCS is limited to 48%, mainly due to its high heating demand. Moving to the BM/HE scenario, since BRY is almost self-sufficient in terms of power demand, no significant improvements occur, while the CCS route efficiency increases to 69%. Nevertheless, displacement of NG use to produce syngas in the conventional MeOH synthesis route is a relevant factor to be considered. Table 2.4 shows the total CO_2 emission avoided by MeOH production in BRY, when compared with the average emission of a conventional MeOH plant in Europe, considered the Business as Usual scenario (BAU). The CO_2 avoided in the BRY is twice the amount avoided by the CO_2 hydrogenation process and six times the amount avoided by the bi-reforming process,

two promising routes for CO_2 mitigation. However, direct emissions are greater mainly because of biofixation inefficiencies.

Table 2.4. **Technology comparison for MeOH production with CO_2 mitigation.**

Metrics (Unit/t MeOH)	Unit	BRY [3]	Bi-reforming [4]	CO_2 Hydrogenation [5]	CO_2 Hydrogenation [6]	BAU [1]
Heating demand	MW	0.51	1.91	-	-	-
Electricity demand	MW	0.07	0.42	0.17	-	0.147
Direct CO_2 emissions	t CO_2	1.66	0.01	0.09	0.05	0.695
Indirect CO_2 emissions	t CO_2	0.13	0.40	0.14	0.16	0.073
CO_2 emissions	t CO_2	1.79	0.41	0.23	0.21	0.77
Inlet CO_2	t CO_2	5.08 [2]	0.28	1.46	1.43	0.00
CO_2 not produced	t CO_2	-1.03	0.36	0.54	0.56	0.00
CO_2 avoided	t CO_2	4.05	0.64	2.00	1.99	0.00

[1] Average of the existing MeOH synthesis plants in Europe for comparison, as in Pérez-Fortes et al. (2016).
[2] Considering that the inlet is 3/4 of the total CO_2 inlet, since 1/4 is sent to oil production.
[3] This work
[4] Wiesberg et al. (2016)
[5] Pérez-Fortes et al. (2016)
[6] Matzen et al. (2015)

Results of the environmental assessment for both routes are summarized in Fig. 2.8, where the impact of a given category is divided by the maximum absolute value among the two routes, so that it ranges from -1 (more environmentally benign) to 1 (more impactful). Moreover, a positive value indicates an increase of the impact on the environment while a negative value indicates CO_2 abatement. BRY outperforms in all categories, including Global Warming Potential (GWP), as expected from the CO_2 footprint analysis. The CCS shows more scores with values nearly zero, while BRY has more negative scores.

For both BRY and CCS, the categories with the greatest environmental impacts are Acidification Potential (AP) and Ozone Depletion Potential (ODP). However, it is worth noting that BRY, comparatively to CCS has nearly null impact in these categories and, most

importantly, has negative impact in the remaining six categories (i.e., BRY is beneficial to the environment). Cuéllar-Franca and Azapagic (2015) also observed that CO_2 removal with CCS is accompanied by increase of other environmental impacts (e.g., acidification and human toxicity). This occurs mainly because of electricity demand supplied by a coal-fired power plant in case of CCS, while BRY is almost self-sufficient in electricity.
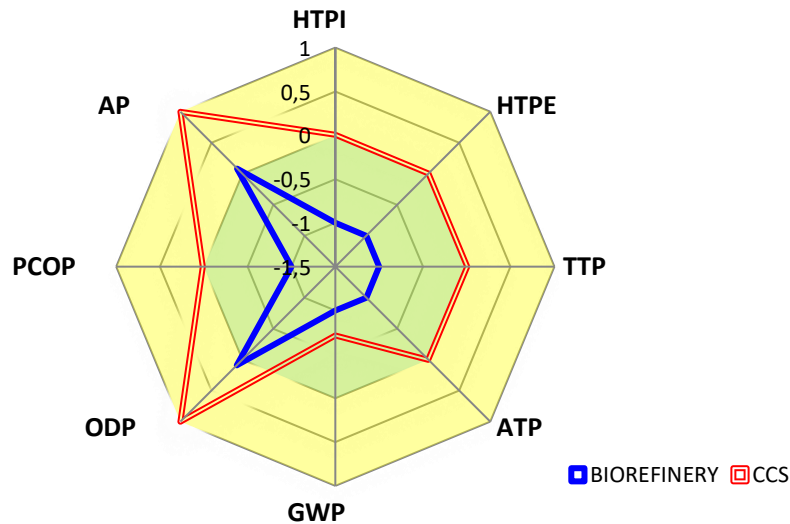
Fig. 2.8. Radar diagram for the impact categories. Scores are expressed per ton of net CO_2 and normalized by the maximum absolute value.

2.6.3. Economic analysis results

Table 2.5 presents OPEX and revenue breakdown for BRY and CCS routes. The major share in OPEX for the BRY is the production of O_2 (39%) while low pressure steam (57%) is the highest cost share in CCS. CAPEX share of the BRY first area (BRY-1) is 70% (including 15% for GSD and 20% for PBR). Hence, increase in volumetric productivity is the most impacting development for improving economic performance of BRY. For CCS, CAPEX is evenly distributed between the capture plant and the pipeline (~45% each), with both operations having considerably higher technological maturity and, hence, less perspective of significant reduction in CAPEX. Although CAPEX in BRY is much larger than in CCS (Fig. 2.9), BRY in counterpart has lower OPEX, in addition to its revenues (MeOH, oil and liquefied CO_2) (Table 2.5).
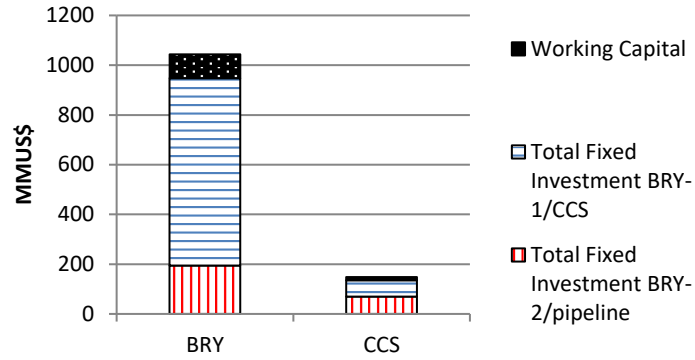
Fig. 2.9. **CAPEX breakdown for BRY and CCS.**

Table 2.5. OPEX and revenue breakdown for BRY and CCS.

Item	BRY (MMUS$)	CCS (MMUS$)
Microalga Medium + Flocculant / MEA	0.7	0.9
Steam (6.9 bar)	4.9	45.7
Electricity	1.0 (cogeneration $= -9.5$)	13.2 (pipeline $= 6.4$)
Cooling Water	3.4	5.9
Oxygen	6.3	-
Total Variable / Fixed Cost	16.3 / 20.5	65.7 / 15.1
OPEX	36.8	80.8
MeOH/Microalga oil	44.4 / 14.8	0.0
Revenue	59.2	0.0

The differences between the cash flow performing capture and the cash flow without capture, Eq. 2.6, are generated for BRY and CCS. The cumulative cash flows results are presented in Fig. 2.10, assuming that the plants are located in Brazil. BRY cash flow has periodic decays (5 years period) due to replacement of PBR. Since the cumulative cash flow differences are negative for both routes at the end of project lifetime, the target of superior economic performance in comparison to paying CO_2 taxes is not attained. Hence, at the assumed taxation level of 50$/t CO_2, none of the alternatives are recommended, being economically preferable to pay CO_2 taxes. The result, however, is strongly dependent of the assumption of a fixed tax value along the project lifetime. Environmental pressures are likely to force an increase in CO_2 taxation.
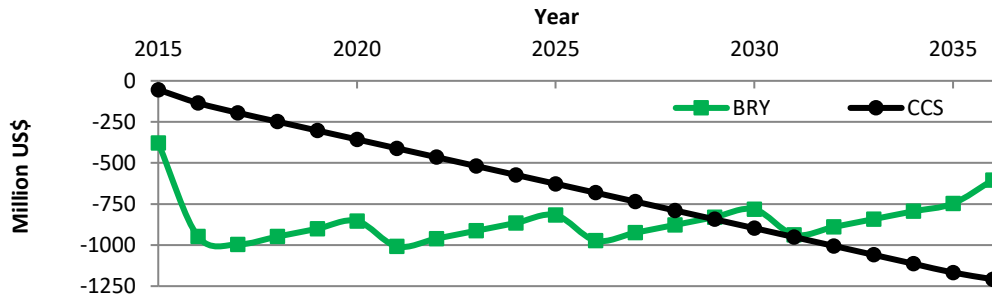
Fig. 2.10. **Estimative of cumulative cash flow differences (Eq. 6) for BRY and CCS routes located in Brazil.**

Nevertheless, the cash flow comparison presents long-term economic advantage of the microalga-based technology, with superior return compared to CCS from 2029 due to its revenues. CCS has lower economic penalty compared to microalga-based technology if considering 10 years of project lifetime, which is a commonly accepted period for investment evaluation in the chemical industry unlike the energy industry, that usually works with a horizon of 20 years. The capture cost for the BRY, considering the lifetime of 20 years, is less than half of the CCS cost because of lower NPV and higher capture efficiency, resulting in 139\$/t CO_2 for BRY against 304\$/t for CCS, as presented in Table 2.6. However, the capture cost is much higher than the considered carbon taxation (50\$/t CO_2) in both routes.

Table 2.6. Estimative capture cost for BRY and CCS routes.

	BRY	CCS
Net Present Value (NPV) (MMUS$)	-$1,341.0	-$1,945.0
CO_2 Feed (t/h)	92.21	92.21
CO_2 capture efficiency	73%	48%
Net CO_2 captured (t/h)	67.30	44.63
Net CO_2 captured cost in 20 years (US$/t)	139.17	304.39

In Fig. 2.11, the economic analysis is presented for plants located in the USA, with a scenario of low-priced natural gas at 3 \$/MMBtu (EIA, 2016a) and electricity cost of 0.072 \$/kWh (EIA, 2016b). The Nationalization Factor is set to 1.0. It can be observed that BRY only reach CCS cash flow performance in 20 years of project lifetime. Hence, improving economic environment reduces advantages of BRY faced to CCS.
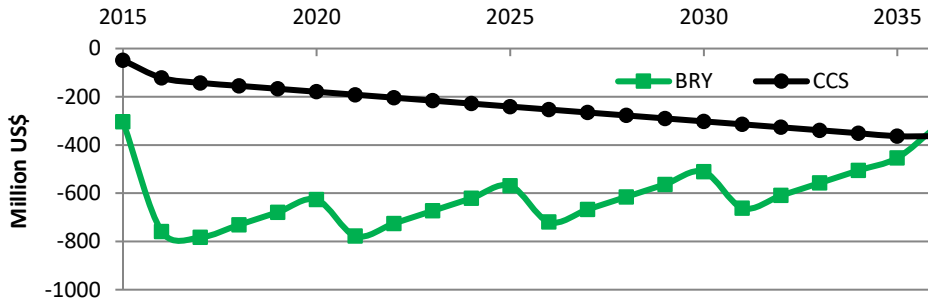
Fig. 2.11. Estimative of cumulative cash flow differences (Eq. 6) for BRY and CCS routes located in the USA.

Sensitivity analyses were performed to evaluate the direction for feasibility of the microalga-based biorefinery in the Brazilian scenario, which has been shown as more appropriate location for the BRY comparatively to CCS than the USA. The total cost of the PBR is varied, resulting from increasing the volume to surface parameter (V/S), decreasing the cost per area and/or increasing volumetric productivity. The impact of microalga oil value is also analyzed. Fig. 2.12 presents the BRY NPV surface (Eq. 6) formed by changes in these variables. Although both variables impact the process economic performance, oil price is more sensitive. BRY can be economically feasible if microalga oil price were superior to 2.50 US$/kg for high PBR cost, or even 1.50 US$/kg if PBR were <100 million US$.
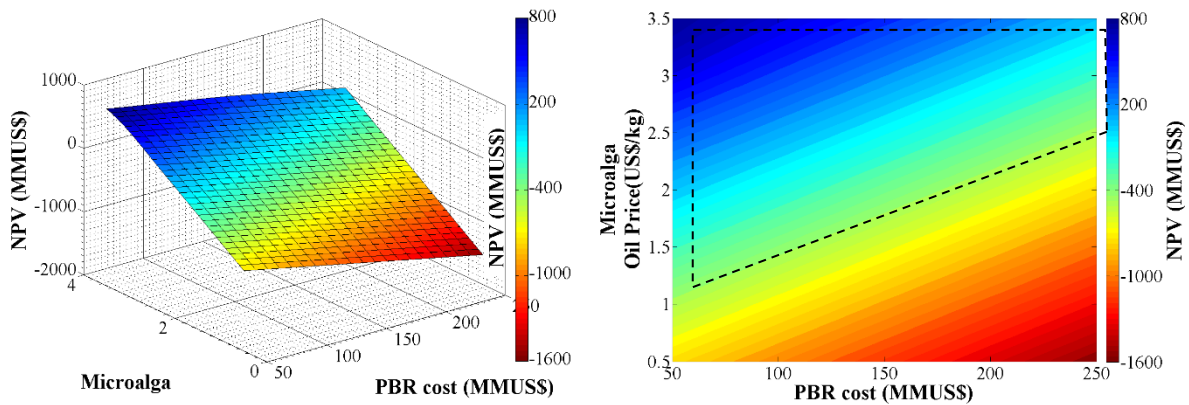
Fig. 2.12. Sensitivity analysis of PBR cost and microalga oil price in BRY NPV (MMUS$) (Eq. 2.6): 3D plot (left); contour levels (right)

Richardson et al. (2010) report minimum microalga oil price ranges from 1.87 $/kg to 8.10 $/kg for economic feasibility. The high performance is due to technology improvements considered in the microalga biofixation step (PBR).

Since microalga oil price is more impacting than PBR cost, it was selected as independent variable in a second sensitivity analysis of the NPV, which also considers varying CO_2 taxation. Fig. 2.13 shows that BRY can be economically more attractive than simply paying the CO_2 tax, as it has a positive NPV. For instance, BRY would be viable for tax values higher than 100 US\$/t CO_2 if microalga oil were 0.5 US\$/kg. The higher the microalga oil price, the lower the minimum taxation for economic feasibility. Specifically, if the oil price were raised to 2 US\$/kg, the minimum tax for feasibility would be lowered to ~40 US\$/t CO_2. Moreover, the higher the taxation, the greater the NPV difference between BRY and CCS routes, as shown in the contour levels, in the right of Fig. 2.13, because of the higher CO_2 capture efficiency in the BRY route.
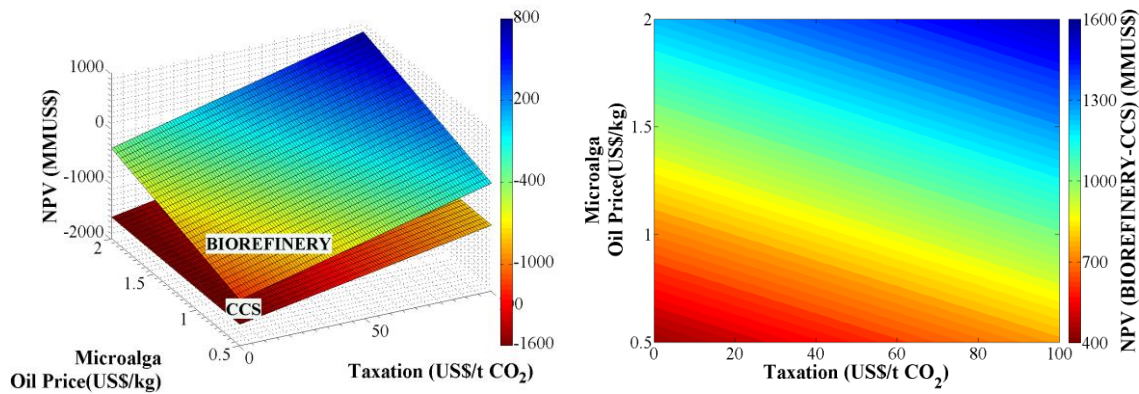
Fig. 2.13. Sensitivity analysis of Taxation and Microalga Oil in NPV (MMUS\$): 3D plot (left); contour levels of the difference (BRY − CCS) between the surfaces (right).

2.7. Conclusions for Chapter 2

A CCU process based on CO_2 biofixation with microalgae, with further production of MeOH and microalga oil in a biorefinery arrangement (BRY), is evaluated and compared to a conventional CCS route for the destination of CO_2 from power plant exhaust gases, on economic and environmental grounds. Although considering optimistic premises for the PBR, the BRY is economically unfeasible and poses technology gaps, with total land area required for operation of about 1000 ha. Biofixation and oil extraction (BRY-1) is responsible for 70% of the BRY CAPEX, as it is equivalent to about 1000 MMUS\$. Nevertheless, considering 20 years of project lifetime and net CO_2 capture efficiency of 73.0% and 48.4%, respectively for the BRY and CCS alternatives, the CO_2 capture cost in Brazil would be 139 \$/tCO_2 and 304 \$/tCO_2, exhibiting superior performance compared to CCS. At the assumed taxation level of

50\$/t CO_2, none of the alternatives are recommended, being economically preferable to pay CO_2 taxes.

Sensitivity analyses show that if the microalga oil price were higher than 2.5 US\$/kg under the incidence of CO_2 taxation (US\$50/t), CCU operation would be more advantageous than paying the taxation. The extremely high area requirement suggests that improvements must be made in the PBR volumetric productivity and in the volume/surface ratio (determinant of areal productivity). For economic feasibility, these parameters should be ~3 kg $m^{-3}d^{-1}$ and 0.8 m^3/m^2, which remains beyond the state-of-the-art of PBR.

The proposed process for MeOH production has superior avoidance of CO_2 emissions comparatively to CO_2 hydrogenation (twice higher) and bi-reforming (six times higher) processes. The BRY is also more efficient in terms of carbon capture than conventional CCS with CO_2 capture by amine: 73% versus 48%. Moreover, environmental impact categories (eight indexes calculated with the WAR Algorithm) indicate that BRY performs better than CCS, with six environmental categories with negative scores (e.g., aspects where BRY is beneficial to the environment), including GWP. These results place the CO_2 capture by microalgae as a promising technology for mitigating CO_2 emissions, although technical drawbacks must be overcome, notably the total land area required resulting from low areal productivity.

At last, sensitivity to CO_2 taxation indicates that a value of 100 US\$/t would render BRY economically viable even with low microalga oil price (0.5 US\$/kg).

2.8. References of Chapter 2

[1] Acién, F.G., Fernández, J.M., Magán, J.J., Molina, E., 2012. Production cost of a real microalgae production plant and strategies to reduce it. Biotechnol. Adv., 30, 6, 1344-1353, http://dx.doi.org/10.1016/j.biotechadv.2012.02.005.

[2] Araújo, O.Q.F., De Medeiros, J.L., Alves, R.M.B., 2014. CO_2 utilization: A process systems engineering vision, in: Morgado, C.R.V., Esteves, V.P.P. (Eds.), CO_2 Sequestration and Valorization. InTech, 35-88, http://dx.doi.org/10.5772/57560.

[3] Aresta, M., 2010. Carbon Dioxide as Chemical Feedstock, WILEY-VCH Verlag GmbH & Co.

[4] Chisti, Y., 2007. Biodiesel from microalgae. Biotechnol. Adv., 25, 3, 294-306, http://dx.doi.org/10.1016/j.biotechadv.2007.02.001.

[5] Chisti, Y., 2016. Large-Scale Production of Algal Biomass: Raceway Ponds, in Algae Biotechnology – Products and Processes. pages 21-40. Bux. F. and Chisti, Y. (Eds), Springer. ISBN: 978-3-319-12333-2.

[6] Cheah, W.Y., Ling, T.C., Juan, J.C., Lee, D.J., Chang, J.S., Show, P.L., 2016. Biorefineries of carbon dioxide: From carbon capture and storage (CCS) to bioenergies production. Bioresource Technology, 215, 346–356. http://dx.doi.org/10.1016/j.biortech.2016.04.019.

[7] Chiu, F. P., Kuo, H.I., Chen, C.C., Hsu, C.S., 2015. The energy price equivalence of carbon taxes and emissions trading—Theory and evidence. Applied Energy, 160, 164-171.

[8] Cuéllar-Franca, R.M., Azapagic, A., 2015. Carbon capture, storage and utilisation technologies: A critical analysis and comparison of their life cycle environmental impacts. Journal of CO_2 Utilization, 9, 82–102. http://dx.doi.org/10.1016/j.jcou.2014.12.001.

[9] Davis, R., Biddy, M., Jones, S., 2013. Algal lipid extraction and upgrading to hydrocarbons technology pathway. Technical Report, National Renewable Energy Laboratory (NREL).

[10] Davis, R., Kinchin, C., Markham, J., Tan, E., Laurens, L., Sexton, D., Knorr, D., Schoen, P., Lukas, J., 2014. Process design and economics for the conversion of algal biomass to biofuels: algal biomass fractionation to lipid- and carbohydrate-derived fuel products. Technical Report, National Renewable Energy Laboratory (NREL).

[11] Dillon, D.J., White, V., Allam, R.J., Wall, R.A., Gibbins, J., 2005. IEA Greenhouse Gas R&D Programme: Oxy-combustion processes for CO_2 capture from power plant. Engineering Investigation Report.

[12] Dissou, Y., Siddiqui, M.S., 2004. Can carbon taxes be progressive? Energy Economics, 42, 88–100. http://dx.doi.org/10.1016/j.eneco.2013.11.010

[13] Duan, P., Jin, B., Xu, Y., Yang, Y., Bai, X., Wang, F., 2013. Thermo-chemical conversion of *Chlorella pyrenoidosa* to liquid biofuels. Bioresource Technol., 133, 197-205, http://dx.doi.org/10.1016/j.biortech.2013.01.069.

[14] Eberhard, K., 2014. All the world's carbon pricing systems in one animated map. In sightline daily. http://www.sightline.org/2014/11/17/all-the-worlds-carbon-pricing-systems-in-one-animated-map (accessed 08/28/2016).

[15] Feron, P.H.M., 2010. Exploring the potential for improvement of the energy performance of coal fired power plants with post-combustion capture of carbon dioxide. Int J Greenh Gas Con, 4, 152–160, http://dx.doi.org/10.1016/j.ijggc.2009.10.018.

[16] García, C.A., Betancourt, R., Cardona, C.A., 2016. Stand-alone and biorefinery pathways to produce hydrogen through gasification and dark fermentation using Pinus Patula, Journal of Environmental Management, http://dx.doi.org/10.1016/j.jenvman.2016.04.001

[17] Gatti, M., Martelli, E., Marechal, F., Consonni, S., 2014. Review, modeling, heat integration, and improved schemes of Rectisol-based processes for CO_2 capture. Appl. Therm. Eng., 70, 1123-1140, http://dx.doi.org/10.1016/j.applthermaleng.2014.05.001.

[18] Goli, A., Shamiri, A., Talaiekhozani, A., Eshtiaghi, N., Aghamohammadi, N., Aroua, M. K., 2016. An overview of biological processes and their potential for CO_2 capture. Journal of Environmental Management 183, 41-58. http://dx.doi.org/10.1016/j.jenvman.2016.08.054.

[19] Gong, M. H., Yi, Q., Huang, Y., Wu, G.S., Hao, Y. H., Feng, J., Li, W. Y., 2016. Coke oven gas to methanol process integrated with CO_2 recycle for high energy efficiency, economic benefits and low emissions. Energy Conversion and Management, 133, 318–331 http://dx.doi.org/10.1016/j.enconman.2016.12.010.

[20] Gupa, P., Lee, S. M., Choi, H. J., 2015. A mini review: photobioreactors for large scale algal cultivation. World J Microbiol Biotechnol, 31(9), http://dx.doi.org/1409-1417. 10.1007/s11274-015-1892-4

[21] Higginbotham, P., White, V., Fogash, K., Guvelioglu, G., 2011. Oxygen supply for oxycoal CO_2 capture. Energy Procedia, 4, 884-891, http://dx.doi.org/10.1016/j.egypro.2011.01.133.

[22] Huntley, M.E., Redalje, D.G., 2007. CO_2 mitigation and renewable oil from photosynthetic microbes: a new appraisal. Mitig. Adapt. Strat. Glob. Change, 12, 4, 573-608, http://dx.doi.org/10.1007/s11027-006-7304-1.

[23] IEA, 2016a. Natural gas spot and futures prices (NYMEX). http://www.eia.gov/dnav/ng/ng_pri_fut_s1_m.htm (accessed12/22/2016).

[24] IEA, 2016b. Electricity Data. https://www.eia.gov/electricity/monthly/epm_table_grapher.cfm?t=epmt_5_6_a. (accessed 12/22/2016).

[25] IHS Chemical, 2014. Chemical Plant Database. Specifically compiled for the needs of the Joint Research Center (JRC).

[26] IPCC, 2011. IPCC special report on renewable energy sources and climate change mitigation. Prepared by Working Group III of the Intergovernmental Panel on Climate

Change. Edenhofer, O., Pichs-Madruga, R., Sokona, Y., Seyboth, K., Matschoss, P., Kadner, S. Zwickel, T., Eickemeier, P., Hansen, G., Schlömer, S., Von Stechow, C. (Eds). Cambridge University Press, Cambridge, United Kingdom and New York, NY, USA, 1075 pp.

[27] Kourkoumpas, S. Papadimou, E., Atsonios, K., Karellas, S., Grammelis, P., Kakaras, E., 2016. Implementation of the Power to MeOH concept by using CO_2 from lignite power plants: Techno-economic investigation. International Journal of Hydrogen Energy, 41, 16674-16687. http://dx.doi.org/10.1016/j.ijhydene.2016.07.100

[28] Kurt, M., Aksoy, A., Sanin, F., 2015. Evaluation of solar sludge drying alternatives by costs and area requirements. Water Res., 82, 47-57, http://dx.doi.org/10.1016/j.watres.2015.04.043.

[29] Kypreos, S., Turton, H, 2011. Climate change scenarios and Technology Transfer Protocols. Energy Policy, 39, 844–853, http//dx.doi.org/10.1016/j.enpol.2010.11.003.

[30] Letelier-Gordo, C., Holdt, S., De Francisci, D., Karakashev, D., Angelidaki, I., 2014. effective harvesting of the microalgae *Chlorella protothecoides* via bioflocculation with cationic starch. Bioresource Technol., 167, 214-218, http://dx.doi.org/10.1016/j.biortech.2014.06.014.

[31] Liu, A., Chen, W., Zheng, L., Song, L., 2011. Identification of high-lipid producers for biodiesel production from forty-three green algal isolates in China. Prog. Nat. Sci.-Mater., 21, 4, 269-276, http://dx.doi.org/10.1016/S1002-0071(12)60057-4.

[32] Matzen M, Alhajji M, Demirel Y., 2015. Chemical storage of wind energy by renewable MeOH production: Feasibility analysis using a multi-criteria decision matrix. Energy, 93, 343–353.

[33] Mazzetti, M.J., Nekså, P., Walnum, H.T., Hemmingsen, A.K.T., 2014. Energy-efficient technologies for reduction of offshore CO_2 emissions. Oil and Gas Facilities, February 2014, 89-96, http://dx.doi.org/10.2118/169811-PA.

[34] McCollum, D.L., Ogden, J.M., 2006. Techno-economic models for carbon dioxide compression, transport, and storage & correlations for estimating carbon dioxide density and viscosity − Section I. Institute of Transportation Studies.

[35] Molina Grima, E., Belarbi, E.-H., Acién Fernández, F.G., Robles Medina, A., Chisti, Y., 2003. Recovery of microalgal biomass and metabolites: process options and economics. Biotechnol. Adv., 20(7-8), 491-515, http://dx.doi.org/10.1016/S0734-9750(02)00050-2.

[36] Moheimani, N. R., 2016. Tetraselmis suecica culture for CO2 bioremediation of untreated flue gas from a coal-fired power station. J Appl Phycol, 28, 2139–2146. http://dx.doi.org/10.1007/s10811-015-0782-3.

[37] Olah, G.A., Goeppert, A., Prakash, G.K.S., 2009. Beyond oil and gas: the MeOH economy, 2nd updated and enlarged edition. WILEY-VCH Verlag GmbH & Co. KGaA, Weinheim.

[38] Pereira, A.M., Pereira, R.M., Rodrigues, P.G., 2016. A new carbon tax in Portugal: A missed opportunity to achieve the triple dividend? Energy Policy, 93,110–118.

[39] Pérez-Fortes, M., Schöneberger, J.C., Boulamanti, A., Tzimas, E., 2016. MeOH synthesis using captured CO_2 as raw material: techno-economic and environmental assessment. App. Energ., 161, 718−732, http://dx.doi.org/10.1016/j.apenergy.2015.07.067.

[40] Picardo, M.C., Medeiros, J.L., Monteiro, J.G.M., Chaloub, R.M., Giordano, M., Araújo, O.Q.F., 2013. A methodology for screening of microalgae as a decision making tool for energy and green chemical process applications. Clean Technol. Envir., 15, 2, 275-291, http://dx.doi.org/10.1007/s10098-012-0508-z.

[41] Richardson, J.W., Outlaw, J.L., Allison, M., 2010. The economics of microalgae oil. *AgBioForum*, 13, 2, 119-130.

[42] Skjanes, K., Lindblad, P., Muller, J., 2007. $BioCO_2$ − A multidisciplinary, biological approach using solar energy to capture CO_2 while producing H_2 and high value products. Biomol. Eng., 24, 405−413, http://dx.doi.org/10.1016/j.bioeng.2007.06.002.

[43] Tang, D., Han, W., Li, P., Miao, X., Zhong, J., 2011. CO_2 biofixation and fatty acid composition of *Scenedesmus obliquus* and *Chlorella pyrenoidosa* in response to different CO_2 levels. Bioresource Technol., 102, 3, 3071-3076, http://dx.doi.org/10.1016/j.biortech.2010.10.047.

[44] Turton, R., Bailie, R.C., Whiting, W. B., Shaeiwitz, J.A., Bhattacharyya, D. Analysis, Synthesis, and Design of Chemical Processes. Prentice Hall, 2012, 4th edition, Michigan, USA. ISBN-13: 978-0-13-261812-0.

[45] Üçtug, F. G., Agralı, S., Arıkan, Y., Avcıoglu, E., 2014. Deciding between carbon trading and carbon capture and sequestration: An optimisation-based case study for MeOH synthesis from syngas. Journal of Environmental Management 132, 1-8.

[46] Uduman, N., Qi, Y., Danquah, M.K., Forde, G.M., Hoadley, A., 2010. Dewatering of microalgal cultures: a major bottleneck to algae-based fuels. J. Renew. Sust. Energ., 2, 012701, http://dx.doi.org/10.1063/1.3294480.

[47] Vanden Bussche, K.M., Froment, G.F., 1996. A steady-state kinetic model for MeOH synthesis and the water gas shift reaction on a commercial $Cu/Zno/Al_2O_3$ catalyst. J. Catal., 161, 1-10, http://dx.doi.org/10.1006/jcat.1996.0156.

[48] Wang, W., Han, F., Li, Y., Wu, Y., Wang, J., Pan, R., 2014. Medium screening and optimization for photoautotrophic culture of *Chlorella pyrenoidosa* with high lipid productivity indoors and outdoors. Bioresource Technol., 170, 395-403, http://dx.doi.org/10.1016/j.biortech.2014.08.030.

[49] Wiesberg, I.L., de Medeiros, J.L., Alves, R.M.B., Coutinho, P.L.A., Araújo, O.Q.F., 2016. Carbon dioxide management by chemical conversion to MeOH: hydrogenation and bi-reforming. Energ. Convers. Manage., http://dx.doi.org/10.1016/j.enconman.2016.04.041.

[50] Williams, P., Laurens, L., 2010. Microalgae as biodiesel & biomass feedstocks: review & analysis of the biochemistry, energetics & economics. Energ. Environ. Sci., 3, 554-590, http://dx.doi.org/10.1039/B924978H.

[51] Wong, S., 2006. CO_2 compression & transportation to storage reservoir, in: APEC Energy Working Group (Ed.), Building Capacity for CO_2 Capture and Storage Project in the APEC Region.

[52] Xu, X., Song, C., Miller, B., Scaroni, A., 2005. Adsorption separation of carbon dioxide from flue gas of natural gas-fired boiler by a novel nanoporous "molecular basket" adsorbent. Fuel Process. Technol., 86, 14-15, 1457-1472, http://dx.doi.org/10.1016/j.fuproc.2005.01.002.

[53] Young, D.M., Cabezas, H., 1999. Designing sustainable processes with simulation: the waste reduction (WAR) algorithm. Comput. Chem. Eng., 23, 1477-1491, http://dx.doi.org/10.1016/S0098-1354(99)00306-3.

[54] Zhang, B. J., Xu, T., He, C., Chen, Q. L., Luo, X. L. 2017. Material stream network modeling, retrofit and optimization for raw natural gas refining systems. J Clean Prod, 142, Part 4, 3419–3436.

3. CARBON DIOXIDE MANAGEMENT VIA EXERGY-BASED SUSTAINABILITY ASSESSMENT: CARBON CAPTURE AND STORAGE VERSUS CONVERSION TO METHANOL

Abstract

Carbon Capture and Storage and Carbon Capture and Utilization refer to carbon dioxide management technologies for its removal from flue-gases, followed by carbon recycling or storage, aiming at limiting global warming. For large-scale deployment, geological storage is the most promising alternative but imposes an economic penalty to the emitting process, while the utilization monetizes carbon dioxide contributing to compensate for the large capture costs. The exergy concept builds a suitable framework to measure useful power according to the Second Law of Thermodynamics, such that maximizing exergy efficiency necessarily promotes sustainability. This work applies a novel framework for exergy assessment of processes with chemical reactions, which is employed to evaluate the performance of two methanol production routes from carbon dioxide from power plant flue-gas: the direct hydrogenation and the indirect conversion through natural gas bi-reforming for synthesis gas production. Exergy efficiency of the direct route is about 66.3%, against 55.8% for the indirect one, indicating the lower sustainability of the latter. Carbon capture and storage had the worst Exergy efficiency, even lower than the emission scenario, accounting for 44.8% against 53.5%. Exergy metrics pinpoint low scalability as the main drawback of the utilization technologies, despite high exergy and capture efficiency.

Keywords: Exergy Analysis; Methanol Production; CO_2 Hydrogenation; CO_2 Bi-reform; Natural Gas; CO_2 Capture.

Abbreviations

CCU Carbon Capture and Utilization; CCS Carbon Capture and Storage; DIRECT Direct methanol production route through CO_2 hydrogenation; EOR Enhanced Oil Recovery; INDIRECT Indirect methanol production route through NG bi-reforming; LCA Life Cycle

Assessment; LPS Low-pressure steam; MEA Monoethanolamine; NG Natural Gas; PFD Process Flow Diagram; RER Reference Environmental Reservoir.

Nomenclature

$\dot{\Xi}$	: Energy rate transferred between a chemical reservoir and the system (kW)
μ	: Chemical potential (kJ/mol)
$\dot{\Omega}_k, \dot{\Omega}_S$	: Creation rate of component k (mol/s) and entropy (kW/K)
$\dot{E}$	: Exergy rate (kW)
F	: Molar flowrate of inlet streams (mol/s)
H	: Enthalpy (kJ)
K	: Molar flowrate of outlet streams (mol/s)
N	: Number of moles (mol)
P	: Pressure (kPa)
$\dot{Q}$	: Heat rate (kW)
R_H, R_K	: Heat and k-specie reservoir
S	: Entropy (kJ/K)
T	: Temperature (K)
U	: Internal Energy (kJ)
V	: Volume (m³)
$\dot{W}$	: Mechanical work (kW)
Y	: Molar fraction

Superscripts/Subscripts

0	: Reference state
i, k	: Index of components i and k
j	: Index of streams
nc	: Number of components
nfs	: Number of feed streams
nps	: Number of product streams
$\overline{A}$	: Molar property of A ([A]/mol)

Exergy Indicators

η	: Efficiency
eCE	: Capture efficiency
eDR	: Destruction ratio
eIP	: Improvement potential
eRR	: Recoverability ratio
eSI	: Sustainability index
eSR	: Scalability ratio
eWR	: Waste ratio

3.1. Introduction

Carbon Capture and Utilization (CCU) technologies have potential to considerably contribute for improved sustainability of industrial and power generation activities while adding

revenues to carbon dioxide (CO_2) destination from chemical conversion to marketed products. Thus, CCU stands as an important solution to limit global warming while potentially enabling economically feasible replacement of fossil feedstocks to the chemical and energy industries. In this sense, methanol synthesis has been considered as one of the most promising routes for large-scale CCU [1], accounting for its widespread use and potential for a rapid growing demand, not only as a bulk commodity but also for its direct use as vehicle [2] and shipping fuel [3], as renewable energy carrier [4]. Moreover, methanol-to-olefins technology is of great importance because it replaces oil-derived products [5]. However, due to its chemical stability [6], CO_2 conversion requires severe reaction conditions [1], resulting in compression and heating operations. A review of Life Cycle Assessments (LCA) of various CCU routes showed that the efficiency of the carbon removal and the environmental impacts varies greatly and are not always exciting when compared to CCS [7]. Unfortunately, as far as the authors are aware, there is no LCA study in the literature comparing CCS and CCU with methanol production.

Carbon Capture and Storage (CCS) alternatives, on the other hand, have the economic obstacle of being unprofitable activities that require large capital investment [8] and may only be economically attractive if the storage site is an oil reservoir, for Enhanced Oil Recovery (EOR), or a stringent carbon taxation policy is applied [9]. Indeed, the majority of the early CCS projects are for EOR purposes [10]. However, CCS is a promising technology for CO_2 mitigation from power plants emissions in a long term [8]. In order to increase its techno-economic feasibility, Calderon et al [11] analyzed the recirculation of exhaust gases to rise the CO_2 partial pressure in the flue-gas of a NG power plant, simultaneously lowering the regeneration duty, its flow rate and its O_2 concentration. The net efficiency of the power plant with CCS increased 0.5% with the recycle.

Due to their exposed potential niches, this work evaluates the sustainability of two CCU technologies by means of exergy analysis: CO_2 hydrogenation [12] (DIRECT route) versus NG bi-reforming producing syngas for posterior conversion to methanol [13] (INDIRECT route). They have already been evaluated in terms of mass and energy balances. Pérez-Fortes et al. [14] calculated the amount of avoided CO_2 per ton of methanol produced in the DIRECT route and Wiesberg, et al. [15] compared them on technical, economic and environmental grounds, pointing best overall sustainability of the DIRECT route. Moreover, the DIRECT allows larger utilization of CO_2 than INDIRECT, which has considerable mass

percentual derived from fossil feedstock, but is challenged by large-scale hydrogen production from renewable sources, e.g., water electrolysis supplied by solar, hydro, wind or geothermal energy [16].

Santos and Park [17] claim that sustainability assessments should have a multilevel approach taking advantage of the thermodynamic perspective of processes. In this sense, the exergy concept is defined as the maximum work that it is possible to obtain from a process stream in relation to a given RER, a dead state condition that must be defined so that exergy can be evaluated [18]. Thus, the exergy of a process stream is always a positive value and is always destroyed in real (irreversible) processes, remaining constant in theoretical reversible ones. Exergy analysis can be performed to assess exergy degradation and lost work associated to chemical processes or equipment, integrated with chemical process simulators [19]. The higher the rate of exergy lost, the higher the associated environmental impacts, as exergy expresses a potential capacity for transforming the environment. The use of exergy analysis is an important tool for sustainable development and has gained great importance in the development of public policies [20]. Conceptual discussions on exergy meaning and its uses, besides the relationships between exergy and sustainability issues, are found in [18].

Environmental impacts and resources depletion are measured from a perspective that cannot be explicitly revealed by simple mass and energy balances [17], so that technology developments would benefit from exergy assessments. It should be noted that only limited improvements can be achieved, so that qualitative decisions can be necessary, e.g. opting for another energy resource. In this sense, Hepsbali [21] reviewed the theoretical background of exergy efficiency for several renewables-based systems, besides collecting exergy-derived metrics, to assess the efficiency of resources utilization in an economy.

A recurrent issue in exergy analysis relies on choosing the most adequate Reference Environment Reservoirs (RER) for a given system [22]. Rosen and Dincer [18] explained the reason for the existence of different RER approaches, indicating weaknesses of some formulations. Of major concern, however, is the contrast between classical and rigorous thermodynamic computation methods – truly referring to a specific RER – with formulation of exergy rates calculated with universally fixed (standardized) contribution of chemical species [23]. The problem with such approaches is that exergy should not be treated as an intrinsic property of matter, since its value is highly dependent on environment conditions where the system is allocated. Hence, the use of chemical exergy tables made of forming

elements has become very common in literature [24] assisting handy calculations with a lack of a critical discussion on the RER selection.

Additionally, situations exist where even non-thermodynamic characteristics – such as scarcity – play a role being unduly accounted in exergy rates. Mixing reference environments is also a recurrent error, amplifying the internal inconsistences and contradictions, eventually leading to negative values of exergy (a gross error). These and other controversial aspects of such alternative methods for exergy analysis are discussed and criticized by Gaudreau [23].

Exergy analyses have been used as a tool to assess the efficiency of methanol production and CCS technologies. Blumberg et al [25] analyzed a conventional methanol plant based on NG steam reforming and reported an exergy efficiency of 37.7%. Amrollahi et al [26] compared the exergy efficiency of several configurations of chemical absorption with monoethanolamine (MEA) from flue-gas of a NG-fueled power plant, concluding that exergy efficiency downgraded from 52.7% to 49.5% with the capture. Ibrahim et al [27] compared exergy analyses of NG combined-cycle power plants, identifying that the combustion chamber is the main source of irreversibilities due to combustion reactions. However, to perform a fair and relevant judgement of carbon managing technologies, a study must overcome the usual analysis of the CO_2 conversion stage or the analysis of only one technology (CCS or CCU).

3.1.1 The present work

Exergy Analysis is used in this work as a chemical process analysis tool, instead of the generally used economic and environmental metrics, helping the decision-making of the most sustainable one. Exergy analysis is utilized for comparing CCU and CCS, from the generation of the flue-gas until the mitigation (and not only just a single step), identifying hotspots of exergy losses, capture efficiency and scalability issues, with the support of two original exergy metrics. Two innovative technologies for methanol production from CO_2 is considered in the CCU. Moreover, instead of using standard tables for chemical exergy, RER parameters are obtained through commercial process simulators (Aspen Hysys and Aspen Plus), providing molar enthalpy and entropy of pure compounds, for a given thermodynamic package, which allows calculation of the chemical potentials for the chosen RER [22].

The analyzed routes in this work are shown in Fig. 3.1, combining three stages: the STAGE-1 is the power plant with a nominal capacity of 210 MW, the STAGE-2 is a post combustion

capture [10] to produce a pure stream of CO_2 from the flue-gas, and the STAGE-3 is the utilization (CCU) or storage (CCS) of the purified CO_2. A Business as Usual scenario of just emitting the flue-gas to the atmosphere is considered as reference scenario of CO_2 mitigation. Moreover, this work also investigates coupling the hydrogenation process to a pure CO_2 source, as in a bioethanol or ethylene oxide plant, releasing the cost of capture [28]. In addition to the flue gas recycle, it is also employed a CO_2-rich NG, a low-cost (due to its low calorific value) fuel resource, abundant in the Brazilian Pre-salt reserves, where associated gas exhibits high CO_2 content [29], requiring upgrading before use in power plants.
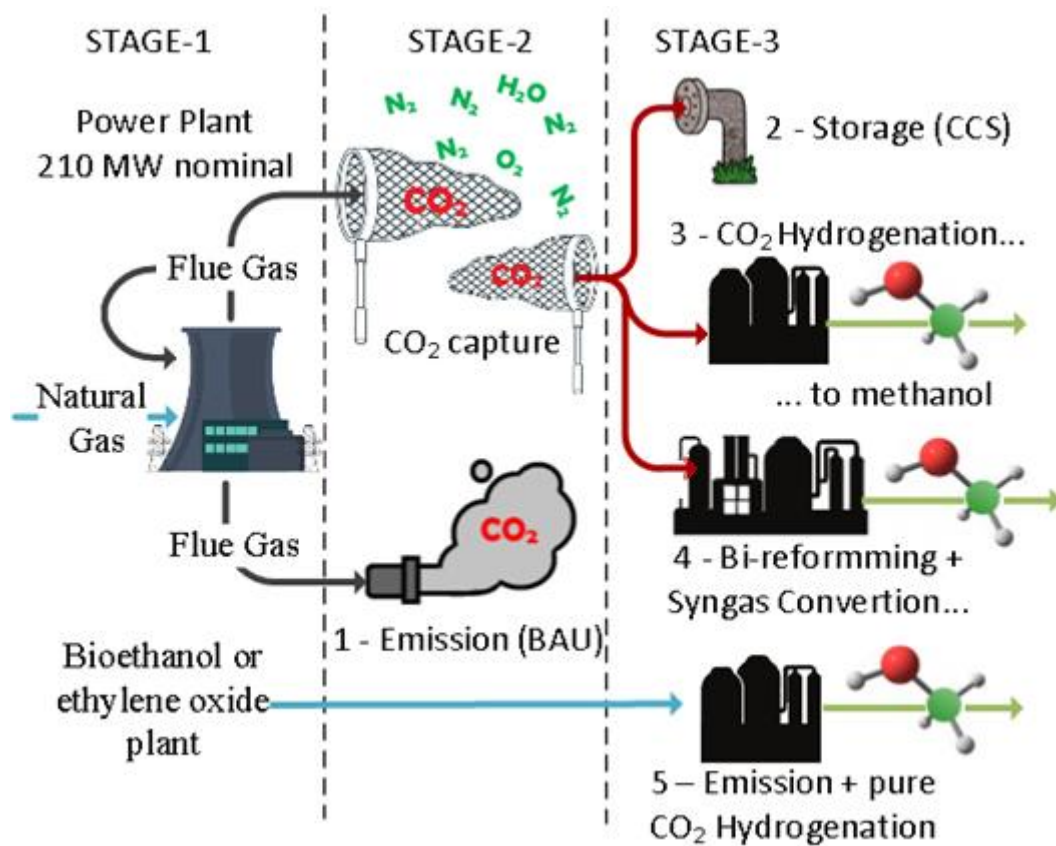
Fig. 3.1. Routes for exergy analyses: 1-Emission, 2-CCS, 3-Capture + CO_2 hydrogenation, 4-Capture + Syngas conversion, 5- Pure CO_2 hydrogenation.

3.2. Methods

Aspen-Hysys and Aspen-Plus process simulators solve mass-energy balances and stream thermodynamic variables required to evaluate the exergy flow rate of process streams, so that the exergy balance of process units can be performed. The Cubic-Plus-Association Equation-of-State (CPA-EOS) is used, except for the post-combustion CO_2 capture via aqueous-MEA absorption, in which the HYSYS Acid-Gas package is employed. Exergy assessment is

performed in spreadsheets with automatic data import from process simulators – molar enthalpy, molar entropy and component flowrates of all streams crossing a given enveloped unit/process under analysis. All calculation steps are performed, relatively to a chosen RER, in a spreadsheet – without relying upon chemical exergy tables – and all the required data is retrieved from the simulations. At last, Sankey diagrams are generated (using *sankeymatic.com*) for visualization of exergy flows and evaluation of exergy metrics, from the power plant to CO_2 storage or utilization. Economic aspects are not considered in Exergy Analysis. In Exergy Analysis, the "value" of a stream corresponds to its exergy flow rate relative to some Reference Environmental Reservoir (RER).

3.2.1. Process description

Process Flow Diagrams (PFD) are described with respective inputs to simulate the processes.

3.2.1.1. Natural Gas Power Plant

The simplified PFD for the NG power plant, STAGE-1, is presented in Fig. 3.2 and is based on Calderon [11], consisting of a NG combined-cycle (NGCC) plant with flue-gas recirculation.
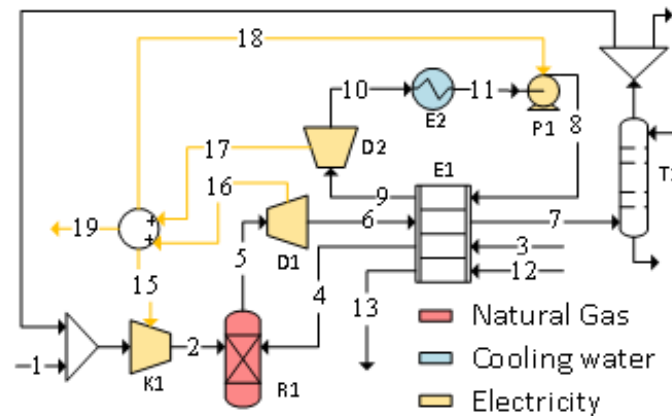
Fig. 3.2. Flow diagram of NG combined-cycle (NGCC) power plant.

In this work, compressed air (stream 2) and heated CO_2-rich NG (stream 4) are sent to the gas-turbine combustor, which is modelled as a Gibbs reactor (*R1*). The hot flue-gas at 1300ºC feeds the expander (*D1*). The turbine outlet flue-gas is sent to the heat recovery section (*E1*), for combined heat and power generation in a sub-critical Rankine cycle (Streams 8-11), with low-pressure steam (LPS) (stream 13) as heating utility for solvent regeneration (not required in CO_2-emitting scenario) and for NG preheating (stream 4). Flue-gas is cooled in a washing

tower (*T1*) and 35% is recycled for mixing with the gas-turbine inlet air to rise the CO_2 content in flue-gas. Table 3.1 presents the process premises for power plant simulation.

Table 3.1. Process premises for NGCC power plant.

Item	Simulation inputs (equipment tags)
CO_2-rich NG Feed (Stream 3)	Flowrate: 1811 kmol/h; P=20.5 bar; T=40°C; Molar composition: CO_2: 0.2013; Methane: 0.7044; Ethane: $4.918.10^{-2}$; Propane: $3.2555.10^{-2}$; Isobutane: $4.8081.10^{-3}$; n-butane: $3.2054.10^{-3}$; isopentane: $3.005.10^{-3}$; n-pentane: $1.502.10^{-3}$
Machines (Compressors, Pumps and Expanders)	*D1*: Gas-turbine expander – from 19.6 to 1.063 bar; *D2*: Steam-turbine – from 25 to 0.08353 bar; *K1*: Gas-turbine air compressor – from 1 to 20 bar; *P1*: Rankine-cycle pump: from 0.08353 to 25.5 bar
Reactor (Combustor)	Modelled as an adiabatic Gibbs reactor, with air excess (Stream 1) adjusted to target 1300°C in outlet gas (expander inlet – Stream 5).
Heat Exchanger	*E1*: Minimum approach = 15 °C; Pressure drops: 5 kPa in hot-side and 50 kPa in tube-side passages. NG preheating to 300°C (Stream 4)
Washing Tower	*T1*: 3 theoretical stages, Pressure profile: 100.3-101.3 kPa, Feed water flowrate adjusted to target 32°C in outlet gas.

3.2.1.2. Carbon Capture and Storage

The simplified PFD for carbon capture named as STAGE-2 is presented in Fig. 3.3 together with the CO_2 compression train referred as STAGE-3 (compressors K2-K4). Cooled flue-gas from the washing tower is admitted at the bottom of an absorption column (*T1*) for CO_2 removal by 30%w/w aqueous MEA. While the CO_2-lean gas is emitted to the atmosphere, the CO_2-rich solvent is sent to the regeneration column (*T2*), which produces nearly pure CO_2 sent to the compression train (not required in the CCU scenarios), basically consisting of three intercooled compression stages and a pump, allowing transportation to geological storage or EOR as supercritical dense fluid. Lean solvent from the regeneration column (*T2*) is recycled to the absorber (*T1*) after mixed with make-up. The heat in the stripper reboiler is

supplied by LPS (5 bar) obtained from a NG co-generation plant, substantially reducing the Rankine-cycle efficiency. The solvent flowrate is adjusted to target 90% of CO_2 captured from feed. Table 3.2 presents the premises for its simulation.
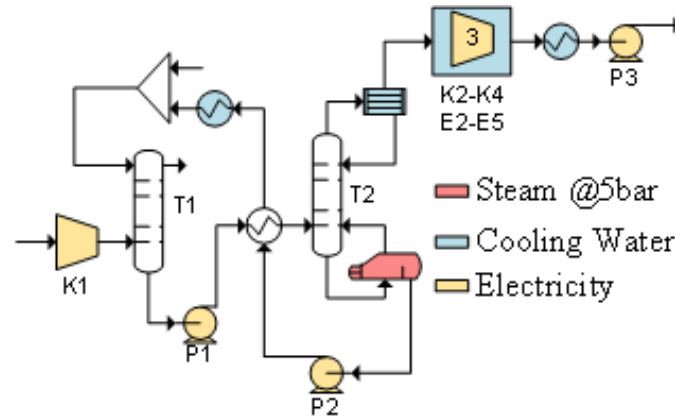
Fig. 3.3. Flow diagram of CO_2 capture with MEA.

Table 3.2. Process premises for CO_2 capture.

Item	Simulation inputs (equipment tags)
Columns	*T1: 20-Staged Absorber; P^{Top}=100 kPa; P^{Bottom}=110 kPa;* *T2: 20-Staged Regenerator; P^{Top}=170 kPa; P^{Bottom}=190 kPa;* *$T^{Condenser}$=45°C; $T^{Reboiler}$=120°C*
Machines	*K1: Flue-Gas Fan; P^{Inlet}=100.3 kPa; P^{Outlet}=110 kPa;* *K2,K3,K4: 3-Staged CO_2 Compression; P^{Inlet}=1.7 bar; P^{Outlet}=92 bar;* *P1: Rich MEA Pump: P^{Outlet}=4.0 bar;* *P2: Lean MEA Pump: P^{Outlet}=2.3 bar,* *P3: Supercritical CO_2 Pump: P^{Inlet}=92 bar; P^{Outlet}=300 bar.*

3.2.1.3. Hydrogenation of carbon dioxide to methanol (DIRECT route)

Fig. 3.4 depicts the PFD proposed for methanol production via CO_2 hydrogenation, alternative used as STAGE-3, which adopts a two-stages reaction path. The two reactors are intermediated by raw methanol withdrawal and syngas compression to >100 bar to shift chemical equilibrium towards methanol production, minimizing the flow rate of non-converted reactants, lowering H_2 consumption.

Two compressors (*K1* and *K2*) raise the pressure prior to the reactors (*R1* and *R2*), which are cooled by means of heat integration to generate steam. The first stage partially converts the reactants to methanol, which is condensed upon cooling and separated, while the remainder follows to the second stage, at higher pressure. The higher suction pressure and smaller volumetric flowrate contributes to reduce the power required in *K2*. Crude methanol follows to

the purification area, composed by two distillation columns (*T1* and *T2*). Table 3.3 describes the process streams, while Table 3.4 describes main simulation premises.

Fig. 3.4. Flow diagram of methanol production via CO₂ hydrogenation (DIRECT route).

Table 3.3. Streams for methanol production via CO₂ hydrogenation (DIRECT route).

Streams	Description
1, 2	Reactants: Pure CO_2 and Pure H_2
17, 42, 47	By-products: purge gas, light distillate and water, respectively
46	Product: commercial methanol, 99.85%w
7, 28	Boiler Feed Water

Table 3.4. Premises for methanol production via CO₂ hydrogenation (DIRECT route).

Item	Simulation inputs (equipment tags)
Feed of Reactants	H_2 and CO_2 are fed at stoichiometric ratio (3:1); *Stream 1:* Pure CO_2, 2000 kmol/h, 1.7 bar, 51.2°C; *Stream 2*: Pure H_2, 6000 kmol/h, 30 bar, 25°C.
Machines	*K1*: CO_2 compressor – 03 intercooled-stages – from 1.013 to 30.0 bar; *K2*: from 30 to 58.5 bar; *K3*: from 56 to 170 bar.
Reactors	Methanol synthesis is modelled in equilibrium reactors (*R1* and *R2*); *R1*: Isothermal reactor with steam generation, T=230°C, P=58.5 bar; *R2*: Isothermal reactor with steam generation, T=230°C, P=170 bar
Distillation Columns	*T1*: 10 theoretical stages, P≈5.0 bar, 0.9 reflux ratio *T2*: 30 theoretical stages, P≈1.5 bar, 1.2 reflux ratio, methanol purity 99.85%w

3.2.1.4. Conversion of carbon dioxide to methanol via syngas from bi-reforming (INDIRECT route)

Fig. 3.5 depicts the PFD designed for the methanol production via syngas through bi-reforming (INDIRECT route), used as alternative route in STAGE-3. Steam, CO_2 and NG feed the bi-reforming reactor (*R1*) to produce syngas, which is cooled via heat integration. The steam flowrate is varied to result in syngas with stoichiometric number *S* close to 2.0, which passes

through a 3-stage compression train (*K1*) and is mixed with the unreacted gas prior to entering reactor (*R2*). The reaction medium is cooled to condensate methanol, which is separated and sent to purification in columns *T1* and *T2* similarly as in the DIRECT route, while the unreacted gas is recycled. Table 3.5 and Table 3.6 respectively describe process streams and simulation premises.

Table 3.5. Streams for methanol production via bi-reforming (INDIRECT route).

Stream	Description
1, 2, 5	Reactants: NG, CO_2 and H_2O.
46, 12, 47, 6	Utilities: NG, boiler feed water (12, 47) and air (6)
10, 36, 47	By-products: purge gas, light distillate and water
44	Product: commercial methanol 99.85%w

Table 3.6. Premises for methanol production via bi-reforming (INDIRECT route).

Item	Simulation inputs (tags of equipment items)
Feed of Reactants	*Stream 1:* NG – 5560 kmol/h, 1.7 bar, 35ºC, molar composition: Methane: 90%, Ethane: 6% Propane: 2%, N_2: 2% *Stream 2:* CO_2 – 2000 kmol/h, 1.7 bar, 51.2°C *Stream 5:* Pure H_2O – 4700 kmol/h, 1 bar, 30°C
Machines	*K1*: Syngas compressor – 03 stages – from 5.5 to 70.5 bar, *K2*: Recycle compressor –01 stage – from 69.0 to 70.5 bar *K3*: Air blower – from 1.013 to 1.50 bar
Reactors	NG bi-reforming and methanol synthesis are modelled in equilibrium-based reactors *R1*: NG bi-reformer, P≈5.5 bar, T≈950°C, O_2 excess = 30% *R2*: Methanol synthesis reactor, P≈70bar, T≈260°C
Distillation Columns	*T1*: 05 theoretical stages, P≈5.0 bar, 0.7 reflux ratio *T2*: 25 theoretical stages, P≈1.5 bar, 0.57 reflux ratio, methanol purity 99.85%w
Tee	10% of tail gas for purge (Stream 10)
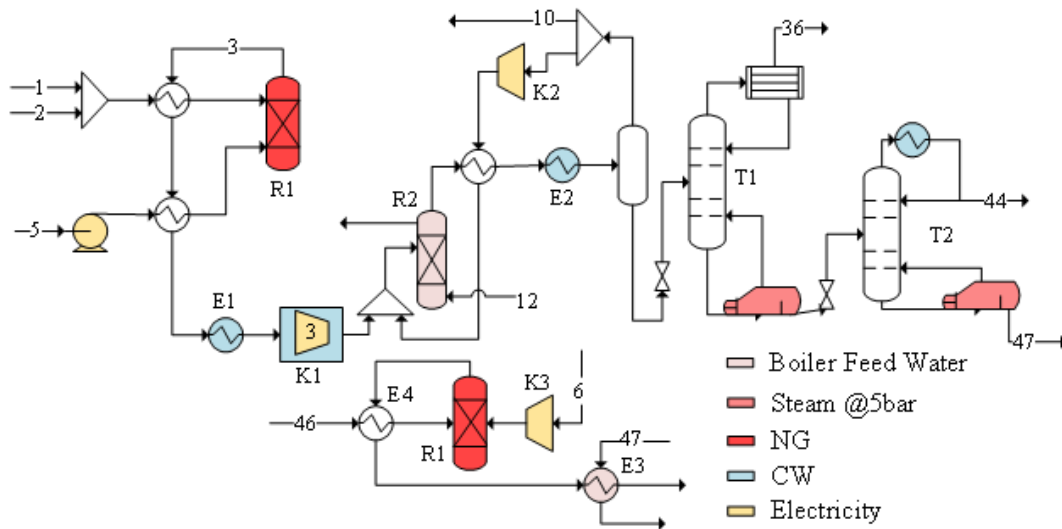
Fig. 3.5. Flow diagram of methanol production via bi-reforming (INDIRECT route).

3.2.2. Exergy

Exergy equations derive from combining the 1st and 2nd Laws of Thermodynamics, respectively ruling energy conservation and entropy creation of real processes. In the present approach, illustrated in Fig. 3.6, the process is considered as an open system of constant volume and in steady state involving several input/output energy and material streams. The reference environment reservoir (RER) is formed by uniting reservoirs for heat and chemical components. It is considered that exported work rates are positive and exported heat rates are negative. The molar flow rate of inlet streams is represented with F while for outlets K is used. $\dot{Q}$ and $\dot{W}$ refer to heat and work rates.
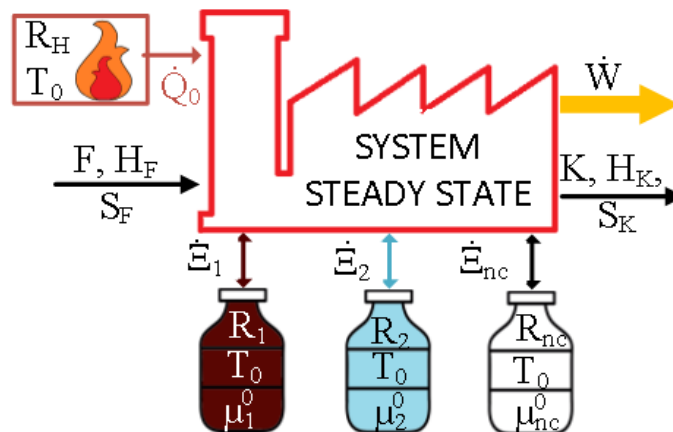
Fig. 3.6. Open-system representation and its interactions with reservoirs.

The system portrayed in Fig. 3.6 interacts with component reservoirs $(R_1, R_2, ..., R_{nc})$ in equilibrium with each other, where nc is the number of components, each at T_0 and μ_k^0. Only component k is able to be transferred across the boundaries in any direction between the system and the corresponding chemical reservoir, being accompanied by energy transfer $\dot{\Xi}_k$. Finally, the system interacts with the ambient heat reservoir R_H, which is enabled to exchange heat at a rate $\dot{Q}_0$ at constant volume and temperature (T_0). Thereby, the system only interacts with the RER, which is the union of the $nc+1$ reservoirs. Since the temperatures are not conflicting and the chemical potentials μ_k^0 are the ones in the considered RER composition, all reservoirs can be gathered to compose the RER, Eq. (3.1). Applying the 1st Law of Thermodynamics to the system in Fig. 3.6, results in Eq. (3.2). The operating equations of the reservoir, Eqs. (3.3) and (3.4), can be written with the fundamental relation of thermodynamics in the integral form and in terms of rates $\left(\dot{U} = T\dot{S} - P\dot{V} + \sum_k \mu_k \dot{N}_k \right)$:

$$RER = R_H + R_1 + R_2 + \cdots + R_{nc} \tag{3.1}$$

$$\sum_j^{nps} K_j \bar{H}_{K_j} = \sum_j^{nfs} F_j \bar{H}_{F_j} + \sum_k^{nc} \dot{\Xi}_k + \dot{Q}_0 - \dot{W} \tag{3.2}$$

$$\dot{U}^{(R_H)} = T_0 \dot{S}^{(R_H)} = -\dot{Q}_0 \quad , \dot{V}^{(R_H)} = 0 \tag{3.3}$$

$$\dot{U}^{(R_k)} = T_0 \dot{S}^{(R_k)} + \mu_k^0 \dot{N}_k^{(R_k)} = -\dot{\Xi}_k \tag{3.4}$$

Equations of entropy and component balance in the Universe are enabled for the system depicted in Fig. 3.6, reducing the degrees of freedom. The entropy balance, solved for entropy creation rate, is given by Eq. (3.5) and the component k balance, also solved for its creation rate, is given by Eq. (3.6).

$$\dot{\Omega}_S = \dot{S}^{sys} + \dot{S}^{(R_H)} + \sum_k^{nc} \dot{S}^{(R_k)} - \sum_j^{nfs} F_j \bar{S}_{F_j} + \sum_j^{nps} K_j \bar{S}_{K_j} \tag{3.5}$$

$$\dot{\Omega}_k = \dot{N}_k^{Sys} + \dot{N}_k^{(R_k)} - \sum_j^{nfs} F_j Y_{kF_j} + \sum_j^{nps} K_j Y_{kK_j} \tag{3.6}$$

Considering $\dot{S}^{(R_H)} = -Q_0/T_0$ given that this reservoir is isothermal and in equilibrium, and using the steady state system condition, Eq. (3.7) can be obtained from Eq. (3.5). Similarly, $\dot{N}_k^{Sys}$ is also zero due to steady state. Moreover, the creation rate of component k in the Universe $(\dot{\Omega}_k)$ can always be set to zero, even with the occurrence of chemical reaction in the system. When a reaction takes place, the respective species are stored or generated by the reservoir, reversibly and under chemical equilibrium, to compensate the variations that must occur because of the reaction. In that way, the component variation in the Universe (RER plus system) is null and the hypothesis is valid. With these facts, Eq. (3.8) is obtained from Eq. (3.6).

$$\dot{S}^{(R_H)} + \sum_{k}^{nc} \dot{S}^{(R_k)} = \dot{\Omega}_S + \sum_{j}^{nfs} F_j \bar{S}_{F_j} - \sum_{j}^{nps} K_j \bar{S}_{K_j} \tag{3.7}$$

$$\dot{N}_k^{(R_k)} = \sum_{j}^{nfs} F_j Y_{kF_j} - \sum_{j}^{nps} K_j Y_{kK_j} \tag{3.8}$$

Substituting Eq. (3.4), Eq. (3.3), Eq. (3.7) and Eq. (3.8) into Eq. (3.2), one can obtain Eq. (3.9), which relates the mechanical work produced with the thermodynamics properties of the process streams.

$$-\dot{W} = \sum_{j}^{nps} K_j \left(\bar{H}_{K_j} - T_0 \bar{S}_{K_j} - \sum_{k}^{nc} \mu_k^0 Y_{kK_j} \right) - \sum_{j}^{nfs} F_j \left(\bar{H}_{F_j} - T_0 \bar{S}_{F_j} - \sum_{k}^{nc} \mu_k^0 Y_{kF_j} \right) + T_0 \dot{\Omega}_S \tag{3.9}$$

Considering that the maximum work is obtainable when the process is reversible, the term $\dot{\Omega}_S$ must be set to zero, so that there is no creation of entropy in the system. The maximum rate of work is equal to the negative of the change on exergy rate, Eq. (3.10). By comparison, it is evident the mathematical definition of exergy in Eqs. (3.11) and (3.12). Eq. (3.14) is also obtained when comparing Eqs. (3.10) to (3.13).

$$\Delta \dot{E} = -\dot{W}^{MAX} \tag{3.10}$$

$$\dot{E}_{inlet} = \sum_{j}^{nfs} F_j \left(\bar{H}_{F_j} - T_0 \bar{S}_{F_j} - \sum_{k=1}^{nc} \mu_k^0 Y_{kF_j} \right) \tag{3.11}$$

$$\dot{E}_{outlet} = \sum_{j}^{nps} K_j \left(\bar{H}_{K_j} - T_0 \bar{S}_{K_j} - \sum_{k=1}^{nc} \mu_k^0 Y_{kK_j} \right) \tag{3.12}$$

$$\dot{W}^{loss} = \dot{W}^{MAX} - \dot{W} \tag{3.13}$$

$$\dot{W}^{loss} = T_0 \dot{\Omega}_S \tag{3.14}$$

The exergy balance throughout the process is represented by Eq. (3.15) [30], where $\dot{E}$ is the exergy rate (in kW) and $\dot{E}^W$ is the exergy rate from purely mechanical energy streams (in kW). Eqs. (3.11) and (3.12) are applied for each inlet and outlet stream, considering the equipment and the chemical plant as the control volume, individually, so that only the $\dot{E}_{destroyed}$ is not known in Eq. (3.15). The variables $\dot{E}_{in}$ and $\dot{E}_{out}$ are defined in Eqs. (3.16) and (3.17), and the difference between them is the destroyed exergy.

$$\dot{E}_{inlet} + \dot{E}_{inlet}^W = \dot{E}_{waste} + \dot{E}_{products} + \dot{E}_{outlet}^W + \dot{E}_{destroyed} \tag{3.15}$$

$$\dot{E}_{in}^{total} = \dot{E}_{inlet} + \dot{E}_{inlet}^W \tag{3.16}$$

$$\dot{E}_{out}^{total} = \dot{E}_{waste} + \dot{E}_{products} + \dot{E}_{outlet}^W \tag{3.17}$$

3.2.3. Reference Environmental Reservoirs

According to Eqs. (3.11) and (3.12), it is necessary to calculate the chemical potential of the components in the RER μ_k^0 before calculating the exergy of the streams. The atmosphere RER is at sea level, in internal equilibrium, with coordinates P_0 and T_0 being 1 atm and 25°C. The atmosphere is considered formed by nitrogen (N_2), oxygen (O_2), argon (Ar), CO_2 and H_2O in the standard composition admitting saturation in water, forming an infinite body of liquid pure in water. All other oxidizable species present in the process – i.e. monoxide carbon (CO), hydrogen (H_2), methanol (CH_3OH), methane (CH_4), ethane (C_2H_6), propane (C_3H_8) – are assumed in chemical equilibrium with the species of the Standard Atmosphere via combustion equations. All species are assumed in equilibrium with the respective reservoirs of components (R_k), such that the RER can be taken as the union of them. Since Aspen Hysys does not have a tool to evaluate the chemical potential, its value in the RER for each component, $\mu_i^0(P_0, T_0)$, is performed in all processes through Eq. (3.18) [22], which considers the vapor phase as ideal gas.

$$\mu_i^0(P_0, T_0) = \mu_i^{f,0}(T_0) + RT_0 \ln(P_0 Y_i^0) \tag{3.18}$$

Where $\mu_i^{f,0}(T_0)$ is the pure component chemical potential formation at standard conditions and Y_i^0 is the molar fraction of the component i in the RER. The term $\mu_i^{f,0}(T_0)$ can be calculated with Aspen Hysys by defining pure streams at P_0 and T_0, sufficient conditions to consider it an ideal gas, as assumed. Thus, since the molar Gibbs free energy is exactly equal to the chemical potential for pure substances, the term $\mu_i^{f,0}(T_0)$ can be obtained by Eq. (3.19), where index i may refer to any component present in the analysis, provided that it is in gaseous state and has a defined molar fraction in the RER. This excludes H_2O, CH_4, H_2, CO, CH_3OH, C_2H_6, C_3H_8 and MEA. Since the system is supposed to be in vapor-liquid equilibrium with water, phases have the same chemical potentials, allowing the use of Eq. (3.20) in a free-water approach of liquid phase.

$$\mu_i^{f,0}(T_0) = \bar{H}(pure\,i, T_0, P_0) - T_0 \bar{S}(pure\,i, T_0, P_0), \; i = N_2, O_2, CO_2, Ar \tag{3.19}$$

$$\mu_i^0(P_0, T_0) = \mu_i^{L,0}(P_0, T_0) = \bar{H}^L(pure\,i, T_0, P_0) - T_0 \bar{S}^L(pure\,i, T_0, P_0), \; i = H_2O \tag{3.20}$$

The chemical potential of species that are not present in the Standard Atmosphere (e.g. methanol) is calculated by chemical equilibrium in the respective combustion reactions, using the potentials of the species that are originally present. The equilibrium is obtained through complete combustion chemical reactions, forming H_2O and CO_2 that are present in the atmosphere. Using methanol as an example, the reaction represented by Eq. (3.21) is used in the calculation of $\mu_i^0(P_0, T_0)$, as shown in Eq. (3.22).

$$CH_3OH(g) + 3/2\,O_2(g) \rightleftarrows CO_2(g) + 2\,H_2O(g) \tag{3.21}$$
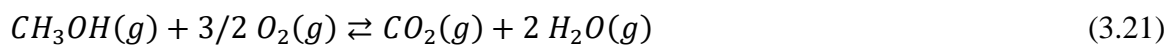
$$\mu_{CH_3OH}^0 = \mu_{CO_2}^0 + 2\,\mu_{H_2O}^0 - 3/2\,\mu_{O_2}^0 \tag{3.22}$$

Thus, methanol is introduced into RER with this chemical potential, and in equilibrium with the other species. This procedure is performed for all the oxidizable species in the standard atmosphere, they are: CH_4, H_2, CO, CH_3OH, C_2H_6 and C_3H_8. Table 3.7 shows the resulting chemical potential of this procedure in both process simulators.

Table 3.7. RER composition and chemical potentials.

Component	Molar fraction	$\mu_i^0(P_0, T_0)$ (kJ/mol)	
		Aspen Plus	Aspen Hysys
N_2	0.75610	-6.929E-1	-4.485E+1
O_2	0.20282	-3.956E+0	-4.719E+1

Component	Molar fraction	$\mu_i^0(P_0, T_0)$ (kJ/mol)	
		Aspen Plus	Aspen Hysys
CO_2	0.00038	-4.139E+2	-4.647E+2
Ar	0.00904	-1.167E+1	-4.743E+1
H_2O	0.03165	-2.372E+2	-3.022E+2
CH_4	-	-8.803E+2	-9.747E+2
H_2	-	-2.352E+2	-2.786E+2
CO	-	-4.119E+2	-4.411E+2
CH_3OH	-	-8.823E+2	-9.983E+2
C_2H_6	-	-1.525E+3	-1.671E+3
C_3H_8	-	-2.170E+3	-2.367E+3
MEA	-	-	-1.856E+3

3.2.4. Exergy performance metrics

The process performances are evaluated by means of exergy metrics. Several metrics are obtained from the literature and two new metrics are proposed in this work derived from exergy assessment: the exergy Capture Efficiency (eCE) and Scalability Ratio (eSR).

3.2.4.1. Exergetic efficiency

Different ways to define exergy efficiency (η) can be employed [30], but the rational efficiency, Eq. (3.23), is used.

$$\eta = (\dot{E}_{products} + \dot{E}_{outlet}^W)/(\dot{E}_{inlet} + \dot{E}_{inlet}^W) \qquad (3.23)$$

Methanol and sweet-gas are considered product material streams and the pure mechanical stream in the outlet is the electricity produced by the power plant. Sweet-gas must be considered a product, when the objective to capture a given percentage of CO_2 is accomplished, since it will always have exergy, even if the CO_2 removal is total. As the product and the produced electricity are maximized or the process inputs are minimized, as well as their exergies, the exergy efficiency and, consequently, the sustainability of the system increase.

3.2.4.2. Waste Exergy Ratio

The Waste Exergy Ratio (eWR) is defined as the ratio of the exergy being wasted to the inlet exergy as shown by Eq. (3.24) [31]. Waste of exergy is the lost plus the destroyed exergy, while Loss streams are the hot cooling water, water, flue-gases and light gas.

$$eWR = \dot{E}^{Waste} \big/ \dot{E}_{inlet} = (\dot{E}^{Loss} + \dot{E}^{Destroyed}) \big/ (\dot{E}_{inlet} + \dot{E}^{W}_{inlet}) \qquad (3.24)$$

3.2.4.3. Exergy Recoverability Ratio

The Exergy Recoverability Ratio (eRR) is evaluated by the ratio of the useful Exergy to the inlet of exergy as shown by Eq. (3.25) [31]. Streams considered in the $\dot{E}_{Useful}$ are the condensed steam, residual gas, produced steam and stored CO_2.

$$eRR = \dot{E}^{Useful} \big/ (\dot{E}_{inlet} + \dot{E}^{W}_{inlet}) \qquad (3.25)$$

3.2.4.4. Exergy Destruction Ratio

The Exergy Destruction Ratio (eDR) metric is evaluated by the ratio of the Destroyed Exergy to the inlet of exergy, as shown by Eq. (3.26) [31].

$$eDR = \dot{E}^{Destroyed} \big/ (\dot{E}_{inlet} + \dot{E}^{W}_{inlet}) \qquad (3.26)$$

3.2.4.5. Exergetic Sustainability Index

The Exergetic Sustainability Index (eSI) is the ratio of the efficiency to the sum of the eWR with eDR; i.e., the ratio between useful exergy flow rate and exergy losses in Eq. (3.27) [31].

$$eSI = \eta / (eWR + eDR) = (\dot{E}_{products} + \dot{E}^{W}_{outlet}) \big/ (\dot{E}^{Loss} + \dot{E}^{Destroyed}) \qquad (3.27)$$

3.2.4.6. Improvement Potential

The Improvement Potential (eIP) in Eq. (3.28), is useful to compare the amount of exergy that can be saved among completely different processes, since the destroyed exergy depends on the process scale and its efficiency [32].

$$eIP = (1 - \eta) \dot{E}^{destroyed} \qquad (3.28)$$

3.2.4.7. Capture Efficiency

This work proposes a new metric to indicate the process that uses the resources to mitigate CO_2 more efficiently. The Capture Efficiency (eCE) is evaluated as the efficiency (η) in the

CO2 capture stages (capture with MEA and CO2 destination), as shown in Eq. (3.29). In the CCS case, the CO2 stored is considered a product.

$$eCE = \dot{E}_{products}^{CO2 \ capture \ stages} \Big/ (\dot{E}_{inlet} + \dot{E}_{inlet}^{W})^{CO2 \ capture \ stages} \qquad (3.29)$$

3.2.4.8. Scalability Ratio

This work proposes a Scalability Ratio (*eSR*) to indicate how easily a process can be scaled up and is the ratio of the exergy of the flue-gas stream to the total inlet exergy in the capture stages, as shown by Eq. (3.30). It is the inverse of how much extra exergy is required to mitigate CO2 emissions, i.e. the lower its value, the higher is the amount of required exergy in the capture stages, as raw materials and utilities, and the lower is the scalability. Therefore, the higher the input of exergy (power or resource) to mitigate CO2, the harder is the process to be scaled up. In case of emitting the flue-gas to atmosphere, the *eSR* is 100%, since the inlet of exergy in the last stage would be the same as in the flue-gas.

$$eSR = \dot{E}_{flue \ gas} \Big/ \dot{E}_{inlet \ of \ the \ capture \ stages} \qquad (3.30)$$

3.3. Results and Discussion

Process simulation results are shown in Table 3.8 with literature data shown for validation purpose. The net efficiency reported by Calderon [11] is higher than in this work mainly because of the lower pressure of the CO2 to be stored, 110bar [11] against 300bar (this work), with consequent reduced electrical duties. The obtained CO2 content in the flue-gas is higher because of the fuel composition, CO2-rich fuel is herein used. The performance of CO2 capture by MEA absorption is inferior to the reported by Calderon [11], mainly because it does not operate at the same conditions, although close enough for an overall comparison of exergy performance.

The bi-reforming reactor reported by Olah [33] operates at lower temperature (910°C against 950°C) and higher pressure (7bar against 5.5bar), which partially explains the higher conversion and H2/CO ratio of this work (Le Chatelier's principle). Methanol yields are slightly higher than most common literature values [25], as an equilibrium-based model was utilized (Gibbs reactor), thus giving optimistic estimation of the reactor performance, with higher H2 conversion per reactor pass. In the case of the high-pressure synthesis at CO2 hydrogenation (*R2*), however, not only the equilibrium condition is favoured but also the

model is more accurate [34]. However, the overall reaction stoichiometry is respected and the achieved CO_2 and CH_4 intensities – respectively expressed as $t_{CO2}/t_{methanol}$ and $t_{CH4}/t_{methanol}$ – are close to literature values.

Table 3.8. Simulated process performance.

Process	Variable	Unit	This study	Literature
Power plant w/o capture	Net efficiency	%LHV	57.7	-
Power plant designed for capture	Net efficiency	%LHV	45.9	52.6 (110bar) [11]
	CO_2 in Flue-gas	mol%	7.69	6.57 [11]
MEA capture	Reboiler Duty	GJ/tCO_2	3.723	3.489[11]
	Lean Loading	molCO_2/molMEA	0.2185	0.263 [11]
	Solvent cycle	kgsolv/kgCO_2	13.32	-
Hydrogenation	$R1$ conversion	(CO + CO_2)%	29.2	22 [35]
	$R2$ conversion	(CO + CO_2)%	96.2	92.5 [34]
Bi-reforming	H_2/CO	mol/mol	2.10	1.99 [33]
	$R1$ conversion	CH_4%	95%	86% [33]
	$R2$ conversion	CO%	66.7	64% [25]
		H_2%	50	12.8% [25]
	CO_2 feed intensity	$t_{CO2}/t_{methanol}$	0.403	0.420 [25], 0.347 [36]
	Methane intensity	$t_{CH4}/t_{methanol}$	0.434	0.54 [25], 0.439 [36]
	$R2$ Recycle ratio	-	0.86	4.2 [25]
	Energy efficiency	%	38.7	35.9 [25]

3.3.1. Exergy analyses

The first exergy analysis presented adopts the plant as control volume, considering all the equipment items, calculating the rate of exergy destruction and the rate of entropy creation, and the respective deviation between these values, with results shown in Table 3.9. Differences between exergy destruction rate and entropy creation rate times T_0 are all below 0.06%, excepting for post-combustion capture aqueous-MEA unit which shows 1.96% owing to small inaccuracies typically generated by thermodynamic model transitions in process simulators (e.g., from CPA-EOS to Acid-Gas Package). Moreover, model transitions are dangerous to exergy assessment, as thermodynamic properties (e.g., $\bar{H}, \bar{S}$) can be obtained from different standard states generating conflicting results. Hence it was decided to analyze only the overall post-combustion aqueous-MEA capture unit.

The power plant designed for CO_2 capture (STAGE-1) has higher exergy destruction than the plant without capture: 44.1% against 42.4%, as seen in Table 3.9. Although MEA-based capture has the highest percentage of exergy destroyed, the absolute rate of exergy destruction is among the lowest, second only to the CO_2 storage step. At last, the methanol production in INDIRECT route (NG bi-reforming followed by methanol synthesis) destroys more exergy than in DIRECT route (CO_2 hydrogenation) – 22.7% against 7.0% – and also presents the highest sink in terms of exergy destruction rate – 507 MW against 30 MW.

Table 3.9. Exergy analyses of overall processes.

Envelope	$\dot{E}_{in}$ (kW)	$\dot{E}_{out}$ (kW)	$\dot{E}_{destroyed}$ (kW)	$T_0\dot{\Omega}_S$ (kW)	Error	%destroyed
Power plant w/o capture	399,191	229,961	169,230	169,230	0.000%	42.4%
Power plant with capture	402,937	225,075	177,861	177,855	0.004%	44.1%
Aqueous-MEA capture	41,637	22,463	19,174	18,802	1.942%	46.1%
CO_2 Storage	20,824	16,812	4,013	4,010	0.058%	19.3%
CO_2 hydrogenation (DIRECT route)	426,504	396,847	29,658	29,669	0.039%	7.0%
CO_2 bi-reforming (INDIRECT route)	2,236,419	1,729,426	506,993	507,061	0.013%	22.7%

Next, to spot main exergy destructing items within process alternatives, a second analysis is performed for separately evaluating each equipment item. From the power plant (with/without CO_2 capture) to CCU (CO_2 conversion to methanol via DIRECT and INDIRECT routes), Fig. 3.7 (A-E) shows exergy flow rates entering/leaving each unit with respective exergy destruction rates, and overall process performances. Unit tags are in accordance with PFDs in Figs. 3.2-3.5. No thermodynamic inconsistencies or negative exergy flow rates were found.
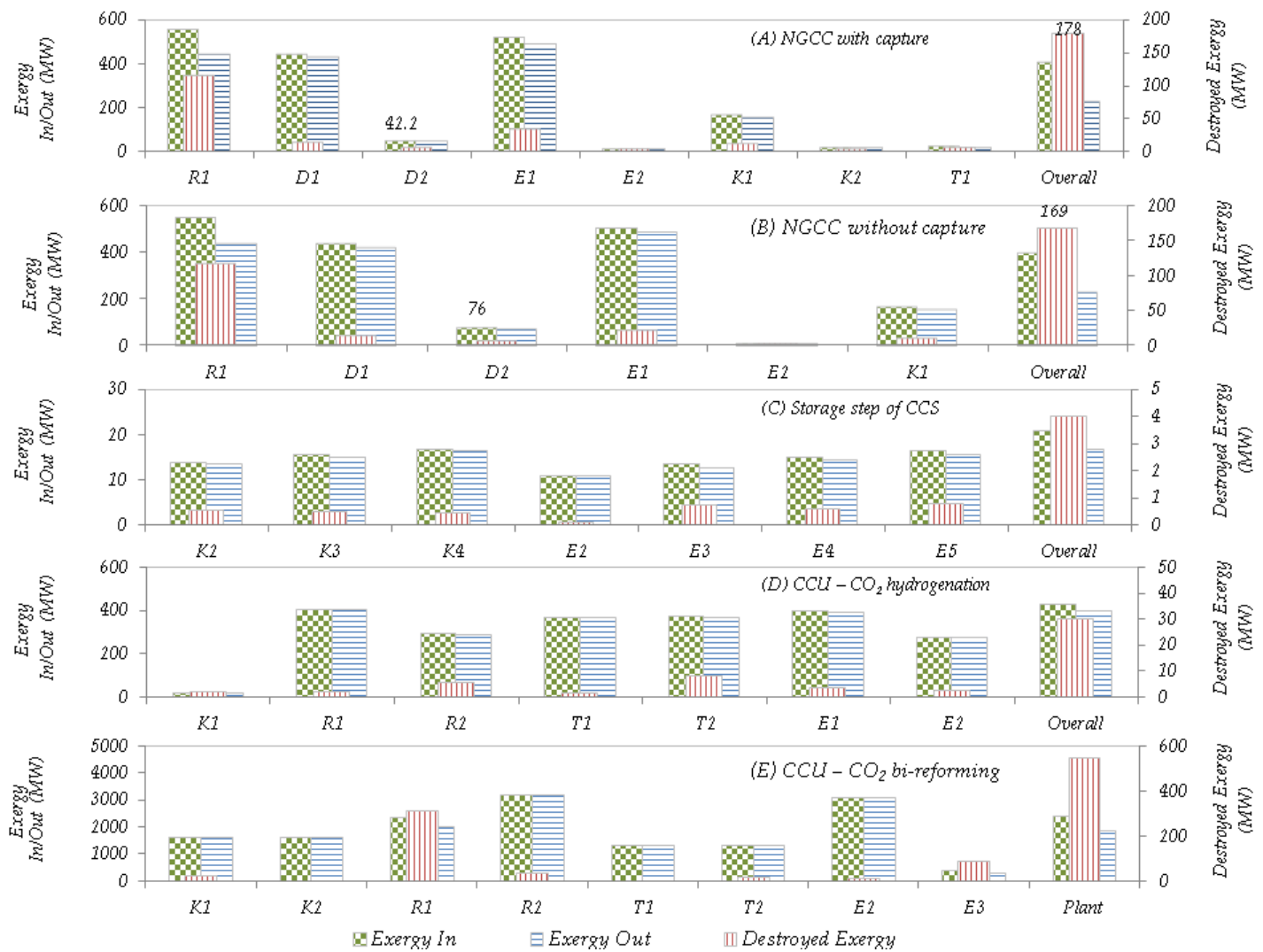
Fig. 3.7. Exergy analyses (MW) of units and overall process: (A) NGCC with CO₂ capture; (B) NGCC without capture; (C) CCS storage step; (D) Methanol production via CO₂ hydrogenation (DIRECT); and (E) By-reforming methanol production (INDIRECT).

Figs. 3.7A and 3.7B show the results of the NGCC power plant, designed and not to perform CO_2 capture, respectively, both regarded as STAGE-1 (Fig. 3.1). The biggest difference among them is the exergy inlet rate to the steam turbine (*D2*), accounting for 42MW in the capture scenario against 76MW without capture, since considerable portion of the recovered heat is deviated to supply the reboiler duty of MEA regeneration column, consisting of an energy penalty for capturing CO_2. However, the percentages of destroyed exergy in equipment items are very close in both scenarios, with the CO_2-capturing plant showing higher overall exergy destruction: 178 against 169MW. The main sink of exergy rate is the combustor (*R1*), which also has the highest rate of exergy inlet.

76

Fig. 3.7C shows the results for the CO_2 conditioning system to target specification to geological storage, STAGE-3 in Fig. 3.1. Every compression stage has similar contribution to exergy destruction, expressing simulation premise of fixed adiabatic efficiencies, being the heat exchangers (*E3-E5*) slightly more inefficient than the compressors. For STAGE-3 (Fig. 3.1), which produces methanol (CCU), Fig. 3.7D presents exergy destruction in CO_2 hydrogenation (DIRECT route), while Fig. 3.7E shows the corresponding results for CO_2 by-reforming (INDIRECT route). The second reactor (*R2*) and the second column (*T2*) are the main sink of exergy in the hydrogenation process, while the reformer reactor (*R1*) is the biggest sink in the INDIRECT route, much higher than other equipment of all STAGES depicted in Fig. 3.1, accounting for almost 60% of all the exergy lost in the process. This occurs because molecules of high chemical potential (C_1, C_2 and C_3 – fuels) are oxidized to produce species of lower chemical potential (CO_2 and H_2O). Since it is a characteristic of reforming reactors, susceptibility for exergy loss minimization is limited. Moreover, the heat exchanger *E3* is the second biggest exergy sink, as high delta temperatures are expected to be found in the convective zone of reforming furnaces, especially when considering the production of saturated steam. The second distillation column (*T2*) in the INDIRECT route is not as inefficient as the corresponding column of the DIRECT route, showing lower percent of exergy destruction (1.41% against 2.07%), since the DIRECT route is featured by raw methanol of much higher water content (≈50%mol) as CO_2 is the only source of carbon to methanol synthesis, which yields methanol and water in the same proportion accordingly to reaction stoichiometry.

3.3.2. Sankey Diagrams

Figs. 3.8 to 3.12 respectively portrait the Sankey diagrams of CCS, CCU via DIRECT route, CCU via INDIRECT route, and CO_2 hydrogenation – also as a DIRECT route, but dispensing CO_2 capture – using a readily available pure CO_2 stream. In Fig. 3.8, the "capture" bar, in the lower middle part of the Sankey diagram, is the chemical absorption with MEA, while the "storage" bar in the right is the compression of the separated CO_2; the "power plant" bar, in the upper left, is the primary source of CO_2. The plant inputs are placed in the left of each of these bars while on the right are positioned the outputs. As can be seen in Fig. 3.8, the largest part of the exergy destruction comes from the power plant, when compared to the capture and the storage (180MW against 19MW and 4MW, respectively). Moreover, the exergy required to mitigate about 3MW of CO_2 emissions (from 9MW in the "flue gas to capture" to 6MW in the "sweet gas") is about 33MW, being the major part of it represented by the required steam.

Similar representation is used in the others Sankey diagrams (Figs. 3.9 to 3.12). The width of each stream is proportional to the exergy flow rate.

Figs. 3.8 to 3.10 evidence the share of the power plant in the exergy flow throughout the production chain steeply decreasing as storage is replaced by the DIRECT CO_2 conversion to methanol and then by the INDIRECT one. In fact, CO_2 destination through NG bi-reforming (Fig. 3.10) for syngas generation is much more exergetically intensive than CO_2 hydrogenation (Fig. 3.9) and storage (Fig. 3.8): 2,236 MW against 426 and 20.8 MW, respectively. Notably, the exergy leaving the flue-gas of the bi-reformer furnace is even higher than the flue-gas from the power plant (39.4 MW against 8.9 MW), indicating that CO_2 capture is not effective in this route. Fig. 3.11 shows that product exergy in electricity form is retrieved from the capture requirements by removing this step, when carrying the DIRECT route with pure CO_2 sources (213.7 MW against 180.2 MW when the capture is required). This is also true for the emission scenario, as depicted in Fig. 3.12.
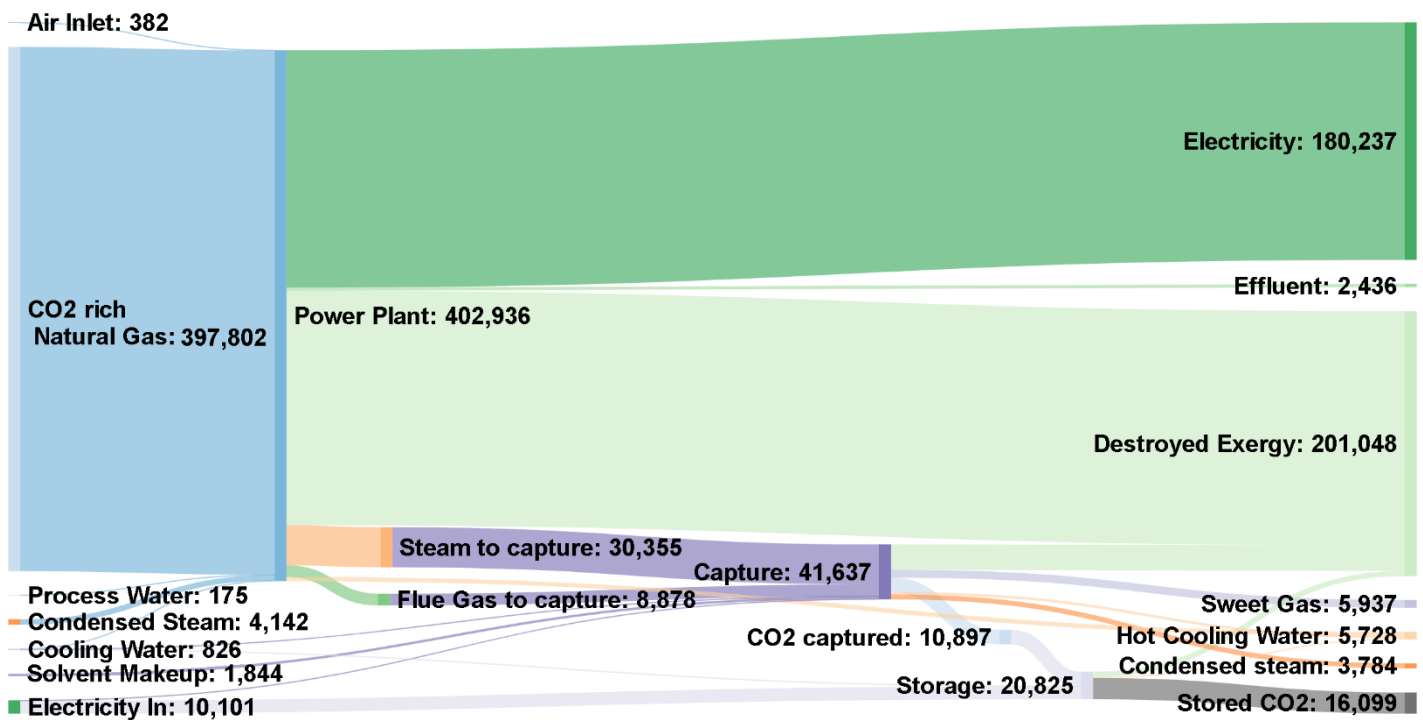
Fig. 3.8. Sankey diagram (kW): CCS route.
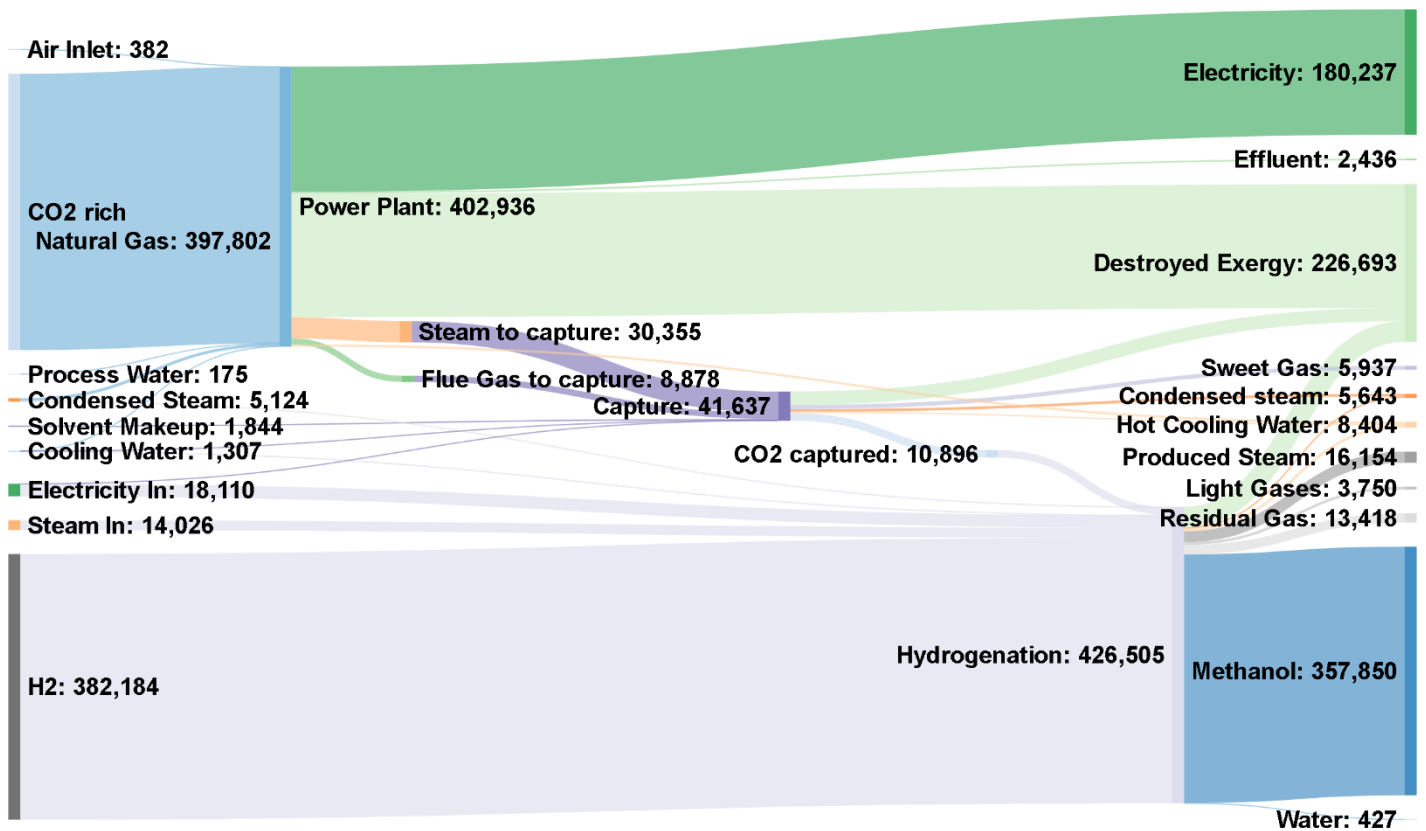
Fig. 3.9. Sankey diagram (kW): CCU DIRECT route (CO₂ hydrogenation to methanol).
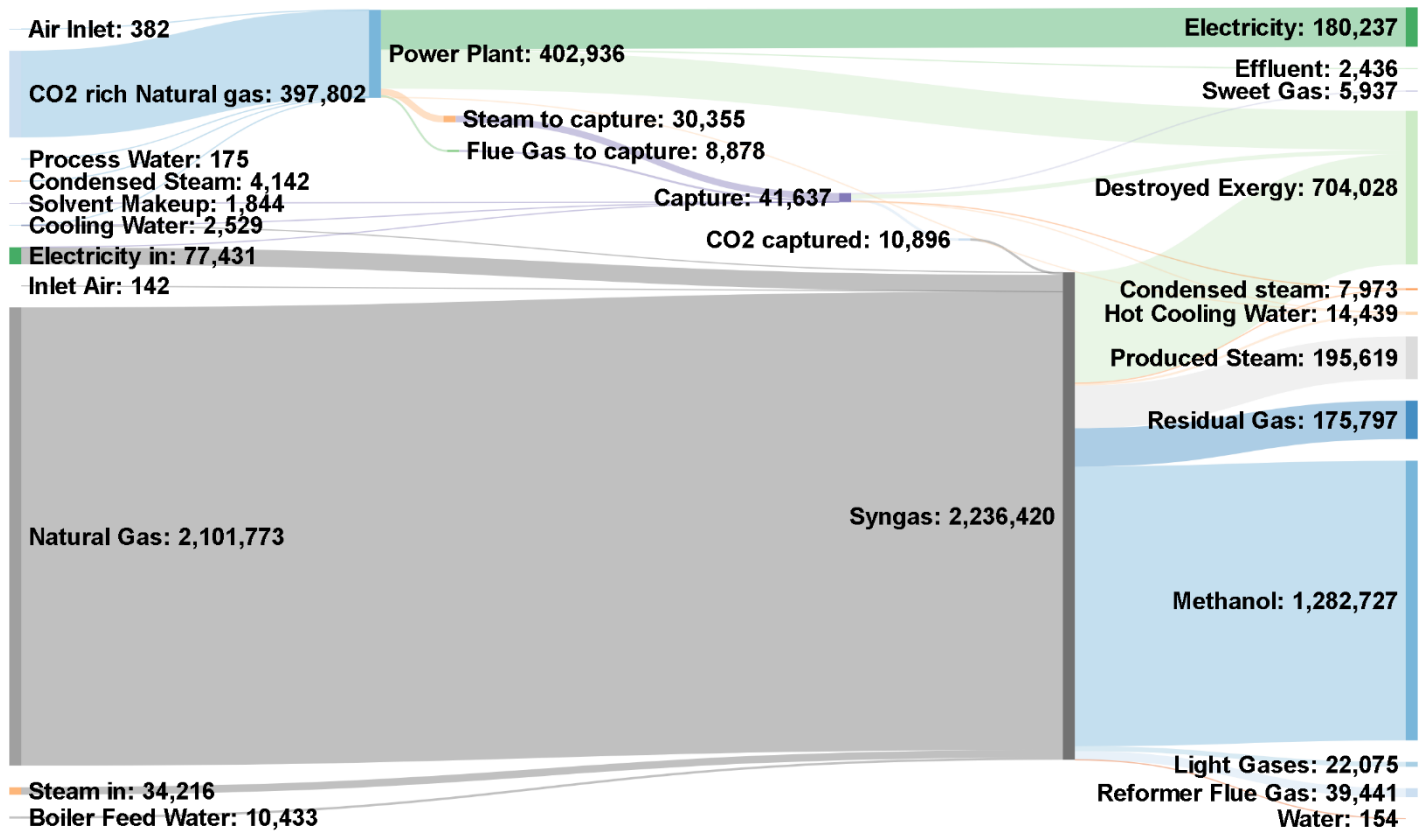
Fig. 3.10. Sankey diagram (kW): CCU INDIRECT route (methanol via bi-reforming) .
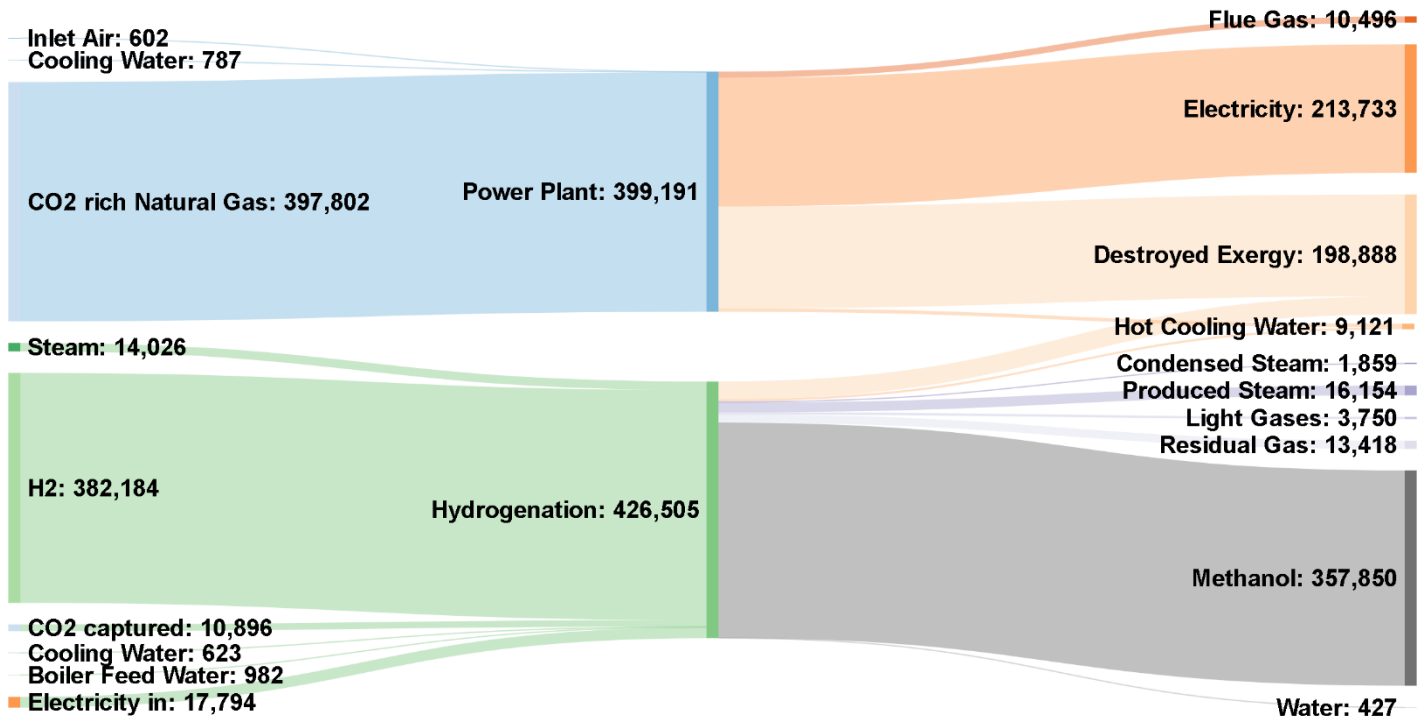
Fig. 3.11. Sankey diagram (kW): DIRECT route (pure CO₂ hydrogenation to methanol).
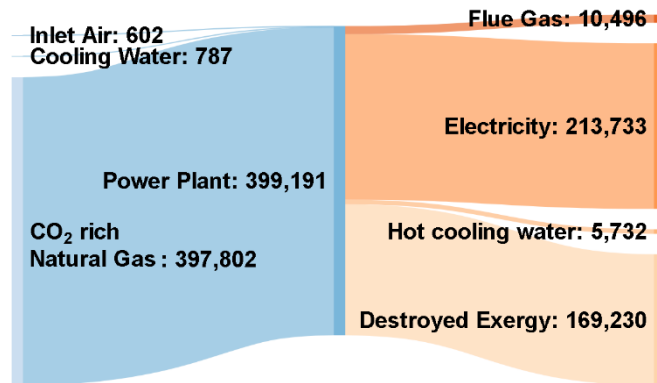
Fig. 3.12. Sankey diagram (kW): power plant emitting flue-gas to atmosphere.

3.3.3. Exergy Metrics

With Sankey diagrams, Table 3.10 presents various categories of exergy flow rates: product, destruction, waste, useful, among others, so that exergy-based metrics are calculated for process evaluation (Fig. 3.1). Calculated exergy metrics of processes are shown in Table 3.11.

Table 3.10. Categories of exergy flows (kW): processes in Fig. 3.1.

Exergy Flow (kW)	CCS	CCU Hydrogenation	CCU Syngas	Pure CO_2 hydrogenation	Emission
Products	186,174	544,024	1,468,901	571,583	213,733
Inlet	415,268	820,949	2,633,782	825,696	399,191
Loss	8,164	15,017	81,464	23,794	16,228
Destroyed	201,048	226,693	704,028	198,888	169,230
Useful	19,883	35,215	379,389	31,431	0
Products of STAGE-3	22,036	363,787	1,288,664	357,850	0
Flue-gas to STAGE-2	8,878	8,878	8,878	10,896	10,496
Inlet to STAGE-2 and 3	51,565	457,246	2,270,079	426,505	10,496

Table 3.11. Exergy metrics: processes in Fig. 3.1.

Metric	Description	CCS	CCU Hydrogenation	CCU Syngas	Pure CO_2 hydrogenation	Emission
η	Exergy Efficiency	44.8%	66.3%	55.8%	69.2%	53.5%
eWR	Exergy-Waste Ratio	50.4%	29.4%	29.7%	27.0%	46.5%
eRR	Recoverability Ratio	4.8%	4.3%	14.4%	3.8%	0.0%
eDR	Destruction Ratio	48.4%	27.6%	26.8%	24.1%	42.4%
eSI	Sustainability Index	88.9	225.1	187.7	256.7	115.2
eIP	Improvement Potential	110,914	76,469	310,945	61,209	78,621
eCE	Capture Efficiency	42.7%	79.6%	56.8%	0.0%	0.0%
eSR	Scalability Ratio	17.2%	1.94%	0.39%	2.55%	100%

CCU-Hydrogenation $(\eta = 66.3\%)$ has higher exergy efficiency than CCU with NG bi-reforming $(\eta = 55.8\%)$ and CCS $(\eta = 44.8\%)$, which makes this alternative as a promising candidate for being more sustainable for CO_2 mitigation from power plants. Hydrogenation of readily available pure CO_2 streams is evidently more efficient $(\eta = 69.2\%)$, showing that these streams should be considered in first place whenever possible before deciding on performing CO_2 capture.

Comparing the CCS scenario with the CO_2 emission alternative, the exergy efficiency is reduced from 53.5% to 44.8% because of the capture step requirements (exhaust gas recycle and steam production). It is interesting to note that the sustainability, in terms of η and eSI, is higher for the configurations that are emitting the flue-gas (pure CO_2 hydrogenation and emission scenarios) than for the CCS, reasonably expressing the fact that CCS systems

naturally increase the use of energy resources, contributing to resources depletion as well as to life-cycle environmental impacts related to upstream fuel processing.

Table 3.11 shows that CCU to methanol via the DIRECT route has the highest exergy-derived Capture Efficiency $(eCE = 79.6\%)$, followed by the INDIRECT route $(eCE = 56.8\%)$ and by CCS $(eCE = 42.7\%)$, which remarkably demonstrated the worst exergy Destruction Ratio $(eDR = 48.4\%)$. On the other hand, CCS emerged as the best option by far among proposed mitigation alternatives in terms of eSR, 17.2% compared to less than 2.6% of the others processes. To achieve the objective of environmentally friendly energy production, CCU technologies must increase its eSR by decreasing the exergy flow required to convert CO_2. On the other hand, CCS needs to increase its exergy efficiency, by lowering the exergy deviated from the power plant to the CO_2 capture step, for instance.

Fig. 3.13 shows a radar diagram with the metrics at its vertices and the processes along the axis. All metrics are normalized, so that 0 corresponds to worst performance and 1 to the best one for each indicator. Hence, to make the polygon vertices point to best alternative, eWR and eDR were replaced by $(1-eWR)$ and $(1-eDR)$. Results for η and eSI metrics are similar, together with the $(1-eWR)$ and $(1-eDR)$. They show a similar trend: readily available pure CO_2 hydrogenation presenting the best results followed by CCU-Hydrogenation, with the worst performance by CCS, followed by flue-gas emission. Moreover, eRR and eIP are another pair sharing the same results. Therefore, only η, eRR, eCE and eSR are considered as representative metrics in this case. As can be seen in Fig 3.13, the emission scenario is concentrated on the centre of the chart, showing that the emission do not perform well for the majority of the exergy metrics.
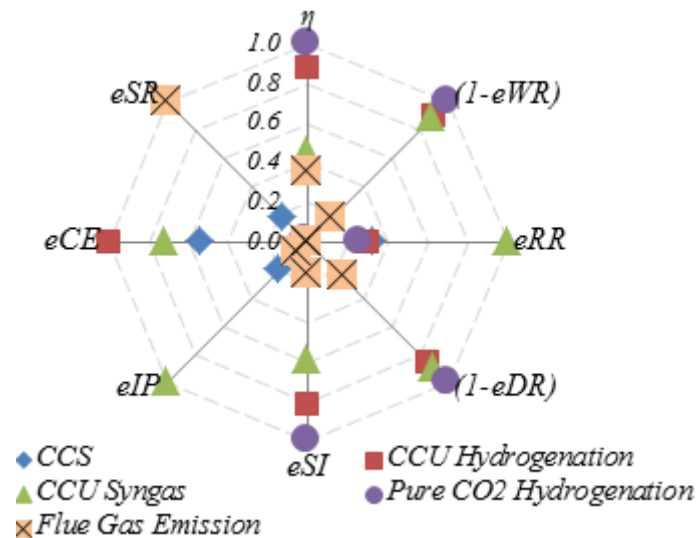
Fig. 3.13. Radar-plot of normalized exergy metrics: 0≡worst, 1≡best.

3.4. Conclusions for Chapter 3

In the present work, CCS and CCU (DIRECT and INDIRECT methanol production) routes, besides hydrogenation of readily available pure CO_2 streams, were analysed through a framework oriented by eight exergy-based indicators, applicable to reacting systems. For this set of metrics, two original indicators were developed to enlighten process specificities: the exergy Scalability Ratio (eSR) and Capture Efficiency (eCE), both calculated using exergy flow rates. Only four of the eight metrics are independent and necessary to rank the processes. Among CCU options, the DIRECT route through CO_2 hydrogenation showed the highest exergy efficiency – $\eta = 66.3\%$ versus $\eta = 55.8\%$ in the INDIRECT route – ratifying its supposed greater sustainability. The outlet exergy flow rate of flue-gas in the INDIRECT route was even higher than the power plant one, indicating its low sustainability. CCS had the worst exergy efficiency and a low capture efficiency (44.8% and 42.7%, respectively). On the other hand, scalability issues were found in the CCU options, with less than 2.6% in this metric, while CCS had the best result, 17.2%.

In the INDIRECT route, the bi-reforming reactor together with the heat recovery from the furnace flue-gas are major destructors of exergy – or hotspots of inefficiencies – impairing the competitiveness of such alternative concerning CO_2 mitigation. Also of significant relevance was the higher exergy efficiency of the CO_2-emitting power plant than a corresponding system including CCS, confirming the well-known effect of increased use of resources, generally indicated by energy penalties. The results of this work demonstrate that exergy assessments may

provide a thermodynamically sound framework to screen the sustainability of processes and can also be used as an optimization tool for CCS and CCU processes.

It can be concluded, therefore, that exergy-based metrics are able to properly identify sustainability issues within a real process. This suggests that such exergy-based framework may replace energy-oriented indicators and, to a limited extent, also some environmental indicators.

3.5. References for Chapter 3

[1] Ganesh I. Conversion of carbon dioxide into methanol – a potential liquid fuel: fundamental challenges and opportunities (a review). Renew Sustain Energy Rev 2014;31:221–57. https://doi.org/10.1016/j.rser.2013.11.045

[2] EIA. International data revisions and the short-term energy outlook forecast. US Department of Energy, Energy Information Administration, February 2017.

[3] Svanber, M, Ellis J, Lundgren J, Landälv I. Renewable methanol as a fuel for the shipping industry. Renew Sustain Energy Rev 2018;94:1217–28. https://doi.org/10.1016/j.rser.2018.06.058

[4] Olah GA, Goeppert A, Prakash GKS. Beyond oil and gas: the methanol economy. 2nd ed. Weinheim: WILEY-VCH; 2009.

[5] Wang C, Xu J, Qi G, Gong Y, Wang W, Gao Pan, Wang Q, Feng N, Liu X, Deng F, Methylbenzene hydrocarbon pool in methanol-to-olefins conversion over zeolite H-ZSM-5, J Catal 2015;332:127-37. https://doi.org/10.1016/j.jcat.2015.10.001

[6] Aresta M. Carbon dioxide as chemical feedstock. Weinheim: Wiley-VCH; 2010. https://doi.org/10.1002/9783527629916

[7] Cuéllar-Franca RM, Azapagic A. Carbon capture, storage and utilisation technologies: A critical analysis and comparison of their life cycle environmental impacts. J CO_2 Util 2015, 9:82-102. https://doi.org/10.1016/j.jcou.2014.12.001

[8] Jin SW, Li YP, Nie S, Sun J. The potential role of carbon capture and storage technology in sustainable electric-power systems under multiple uncertainties. Renew Sustain Energy Rev 2017;80:467–80. https://doi.org/10.1016/j.rser.2017.05.230

[9] Araújo OQF, de Medeiros JL. Carbon capture and storage technologies: present scenario and drivers of innovation. Curr Opin Chem Eng 2017;17:22–34. https://doi.org/10.1016/j.coche.2017.05.004

[10] Adu E, Zhang Y, Liu D. Current Situation of Carbon Dioxide Capture, Storage, and Enhanced Oil Recovery in the Oil and Gas Industry. Can J Chem Eng 2018;97(5):1048-76. https://doi.org/10.1002/cjce.23393

[11] Calderon AMA, Díaz MOG, Mendez A, Santaló JMG, Díaz AG. Natural gas combined cycle with exhaust gas recirculation and CO2 capture at off-design operation. J Energy Inst 2017;92:370–81. https://doi.org/10.1016/j.joei.2017.12.007

[12] Andika R, Nandiyanto ABD, Putra ZA, Bilad MR, Kim Y, Yun CM, Lee M. Co-electrolysis for power-to-methanol applications. Renew Sustain Energy Rev 2018;95:227–41. https://doi.org/10.1016/j.rser.2018.07.030

[13] Liu WC, Baek J, Somorjai GA. The methanol economy: methane and carbon dioxide conversion. Top Catal 2018: 61(7-8):530–41. https://doi.org/10.1007/s11244-018-0907-4

[14] Pérez-Fortes M, Schöneberger JC, Boulamanti A, Tzimas E. Methanol synthesis using captured CO_2 as raw material: Techno-economic and environmental assessment. Appl Energ 2016;161:718–32. https://doi.org/10.1016/j.apenergy.2015.07.067

[15] Wiesberg IL, de Medeiros JL, Alves RMB, Coutinho PLA, Araújo OQF. Carbon dioxide management by chemical conversion to methanol: hydrogenation and bi-reforming. Energy Convers Manage 2016;125:320–35. https://doi.org/10.1016/j.enconman.2016.04.041

[16] Szima S, Cormos CC, Improving methanol synthesis from carbon-free H2 and captured CO2: A techno-economic and environmental evaluation. *J CO2 Util* 2018; 24:555-63. https://doi.org/10.1016/j.jcou.2018.02.007

[17] Santos MT, Park SW. Sustainability and biophysics basis of technical and economic processes: a survey of the reconciliation by thermodynamics. Renew Sustain Energy Rev 2013;23:261–71. https://doi.org/10.1016/j.rser.2013.03.006

[18] Rosen MA, Dincer I. On exergy and environmental impact. Int J Energy Res 1997;21:643–54. https://doi.org/10.1002/(SICI)1099-114X(19970610)21:7<643::AID-ER284>3.0.CO;2-I

[19] Hinderink AP, Kerkhof FPJM, Lie ABK, Arons JS, van der Kooi HJ. Exergy analysis with a flowsheeting simulator — I. Theory; calculating exergies of material streams. Chem Eng Sci 1996; 51(20):4693-700. https://doi.org/10.1016/0009-2509(96)00220-5

[20] Bilgen S, Sarikaya I. Exergy for environment, ecology and sustainable development. Renew Sustain Energy Rev 2015;51:1115–31. https://doi.org/10.1016/j.rser.2015.07.015

[21] Hepsbali A. A key review on exergetic analysis and assessment of renewable energy resources for a sustainable future. Renew Sustain Energy Rev 2008;12:593–661. https://doi.org/10.1016/j.rser.2006.10.001

[22] Teixeira AM, Arinelli LO, de Medeiros JL, Araújo OQF. Exergy analysis of monoethylene glycol recovery processes for hydrate inhibition in offshore natural gas fields. J Nat Gas Sci Eng 2016;35:798–813. https://doi.org/10.1016/j.jngse.2016.09.017

[23] Gaudreau K, Fraser RA, Murphy S. The characteristics of the exergy reference environment and its implications for sustainability-based decision-making. Energies 2012;5(7):2197–213. https://doi.org/10.3390/en5072197

[24] Szargut J. Chemical exergies of the elements, Appl Energy 1989;32(4):269–86. https://doi.org/10.1016/0306-2619(89)90016-0

[25] Blumberg T, Morosuk T, Tsatsaronis G. Exergy-based evaluation of methanol production from natural gas with CO_2 utilization. Energy 2017;141:2528–39. https://doi.org/10.1016/j.energy.2017.06.140

[26] Amrollahi, A, Ertesvåg IS, Bolland O. Optimized process configurations of post-combustion CO2 capture for natural-gas-fired power plant—Exergy analysis. Int J Greenh Gas Com 2011;5:1393–405. https://doi.org/10.1016/j.ijggc.2011.09.004

[27] Ibrahim TK, Mohammed MK, Awad OI, Abdalla NA, Basrawi F, Mohammed MN, Najafi G, Mamat R. A comprehensive review on the exergy analysis of combined cycle power plants. Renew Sustain Energy Rev 2018;90:835–50. https://doi.org/10.1016/j.rser.2018.03.072

[28] IEAGHG. Potential for Biomass and Carbon Dioxide Capture and Storage, 2011. https://www.eenews.net/assets/2011/08/04/document_cw_01.pdf . Last accessed: April 9, 2019.

[29] Gaffney, Cline, Associates, 2010. Review and evaluation of ten selected discoveries and prospects in the pre-salt play of the deepwater Santos basin, Brazil. CG/JW/ RLG/C1820.00/ GCABA.1914, ANP, September 15th.

[30] Ghannadzadeh A, Thery-Hetreux R, Baudouin O, Baudet P, Floquet P, Joulia X. General methodology for exergy balance in ProSimPlus process simulator. Energy 2012;44:38–59. https://doi.org/10.1016/j.energy.2012.02.017

[31] Midilli A, Inac S, Ozsaban M. Exergetic sustainability indicators for a high pressure hydrogen production and storage system, Int J Hydrogen Energ 2017;42(33):21379–91. https://doi.org/10.1016/j.ijhydene.2017.04.299

[32] Van Gool W. Exergy analysis of industrial processes. Energy 1992;17:791–803. https://doi.org/10.1016/0360-5442(92)90123-H

[33] Olah GA, Goeppert A, Czaun M, Prakash GKS. Bi-reforming of methane from any source with steam and carbon dioxide exclusively to metgas (CO-$2H_2$) for methanol and hydrocarbon synthesis. J Am Chem Soc 2013;135(2):648–50. https://doi.org/10.1021/ja311796n

[34] Bennekom JG, Venderbosch RH, Winkelman JGM, Wilbers E, Assink D, Lemmens KPJ, Heeres HJ. Methanol synthesis beyond chemical equilibrium. Chem Eng Sci 2013;87:204–8, https://doi.org/10.1016/j.ces.2012.10.013

[35] Matsushita, T. Process for Producing Methanol. US 2013/0237618 A1.

[36] Milani D, Khalilpour R, Zahedi G, Abbas A. A model-based analysis of CO_2 utilization in methanol synthesis plant, J CO2 Util 2015;10:12–22. http://dx.doi.org/10.1016/j.jcou.2015.02.003

4. BIOENERGY PRODUCTION FROM SUGARCANE BAGASSE WITH CARBON CAPTURE AND STORAGE: SURROGATE MODELS FOR TECHNO-ECONOMIC DECISIONS

Abstract

The use of biomass in cogeneration is a sustainable alternative of energy production, allowing replacing fossil fuels and reduction of greenhouse gas emissions. This work discloses an integrated process analyzer framework comprising surrogate models for estimation of fixed capital investment, revenues, costs of manufacturing as well as several performance responses of cogeneration units of sugarcane-biorefineries burning bagasse, with/without post-combustion carbon capture and storage. A restricted number of inputs are required, namely bagasse availability and heat requirements of the sugarcane-biorefinery. To develop the investment models, a 3^3 factorial computational-experimental design was performed, where AspenOne Portfolio was used in each run to simulate the process allowing estimating the fixed capital investment. Surrogate models were adjusted to fit capital estimates, resulting in 1.9% and 1.3% mean errors for the cogeneration and the post-combustion capture steps, respectively. Capture costs were estimated by analytical equations using the investment values and other estimates from the process analyzer framework, reaching 262 USD/t, but can be as low as 17.2 USD/t if limitations from the agricultural sector are disregarded; namely seasonality, operating time and capacity. The developed framework can assist in sugarcane-biorefinery investment decision making regarding bioenergy with carbon capture and storage or to develop carbon mitigation policies.

Keywords

Abbreviations

APEA ASPEN Process Economics Analyzer; BECCS Bioenergy with Carbon Capture and Storage; BRL BR Real; BST Biomass Steam-Turbine; CCS Carbon Capture and Storage; CW Cooling-Water; CHP Combined Heat-and-Power; EOR Enhanced Oil Recovery; GTCC Gas-Turbine Combined-Cycle; LPS Low-Pressure Steam; MEA Monoethanolamine; MMUSD Million US Dollar; MPS Medium-Pressure Steam; NGCC Natural Gas Combined-Cycle; SBAF Sugarcane-Biorefinery Analyzer Framework; SHPS Super High-Pressure Steam.

Nomenclature

bb	: Boiler blowdown (%)
C_i	: Component i cost (MMUSD/t)
CC	: Capture cost (USD/tCO2)
COL, COM, CUT	: Labor, manufacturing and utility costs (MMUSD/a)
FCI	: Fixed capital investment (MMUSD)
dh	: Fraction of MPS and LPS for heating (%)
$\hat{H}_i$	: Specific enthalpy of stream i (GJ/t)
$\Delta \hat{H}_{S2-S1} = \hat{H}_{S2} - \hat{H}_{S1}$	: Difference of specific enthalpies S2 and S1 (GJ/t)
LF	: Dimensionless location factor
LHV	: Lower heating value (MJ/kg)
$\dot{m}$	: Flowrate (t/h)
$MARR$	: Minimal acceptable rate of return (%)
MSP	: Minimum steam selling-price (USD/t)
mu	: Make-up water (%)
NPV	: Net present value (MMUSD)
OT	: Operating time per annum (h/a)
P	: Pressure (bar)
T	: Temperature (°C)
W	: Power (MW)
X	: Bagasse flowrate (t/h)
Y	: Percentage of SHPS for MPS+LPS production (%)
Z	: MPS percentage in LPS plus MPS (%)

4.1. Introduction

Recently environment concerns have become a major issue on political agendas, directing efforts towards using renewable sources to supply the increasing energy demand. Forecasts show that by 2050 renewable fuels should displace petroleum as primary energy source [1], indicating the relevance of biomass-based Combined Heat and Power (CHP) systems. Biomass-based CHP, or cogeneration, produces steam and electricity with optimum efficiency [2] from the same source of bioenergy. Biomass-based CHP can fulfill two

objectives: supply energy efficiently in many forms with economic benefits while mitigating greenhouse gas emission [3]. It also entails the benefit of energy security; i.e., the uninterrupted electricity availability during shortages of the main tributary of the energy matrix, e.g., hydroelectric plants in drought periods [4]. That is, biomass-based CHP becomes a sustainable and reliable alternative for energy production, allowing replacing fossil fuels.

Interest in biomass-based CHP has increased due to increasing fossil fuel costs and environmental concerns. Not only biomass, but a variety of renewable fuels can be used in CHP, including biogas, landfill-gas, solar energy, fuel-cells and waste-heat [5]. Natural gas can also be used in CHP, but it has environmental issues and gives inferior economic response than biogas in some configurations [5]. In the present study, bioethanol production from sugarcane takes advantage of the bagasse availability to feed CHP.

Brazil is one of the biggest bioethanol producers globally, accounting for ≈26% of global production, second only to the USA which responds for ≈58% [6]. In the past, low-pressure boilers were used in Brazilian sugarcane-biorefineries because they were cheaper and sufficient for energy needs. However, the integrated sugarcane-biorefinery producing bioethanol, sugar and electricity surplus from bagasse burnt in high-pressure boilers was the most common configuration in the new 2007 Brazilian bioenergy projects [7]. This configuration became competitive with the 2004 reform of the Brazilian electricity sector that created conditions for commercialization of surplus electricity to the grid [8].

The two main configurations of biomass-fired CHP are: (i) biomass gasification integrated to Gas-Turbine-Combined-Cycle (GTCC); and (ii) Biomass-to-Steam-Turbine (BST). The former converts the biomass into fuel gas to the GTCC, while the latter, a mature technology, converts the biomass heating value into super high-pressure steam (SHPS) for steam-turbine expansion in Rankine Cycles. One can, for example, prescribe BST sugarcane-biorefineries producing first and second-generation bioethanol and still generating power surpluses when SHPS boilers are employed [9]. Dantas et al. [8] found that BST has greater viability after comparing three bagasse utilizations in sugarcane-biorefineries: (i) BST; (ii) biomass gasification with GTCC; and (iii) second-generation ethanol production.

The higher the boiler pressure, the higher the fixed capital investment (*FCI*, *MMUSD*) but the increase in electricity production is even higher. Therefore, high-pressure boilers are worthwhile [9], but it is not always possible to sell the electricity surplus if facilities are

located far from demand sites [10]. This high *FCI* together with the feedstock supply assurance are the biggest barriers to new projects [11]. Moreover, the high number of uncertain variables seems to repel investors [12]. Papadimitriou et al. [13] analyzed eight Greek CHP operating plants showing that only half achieved the break-even point and five were oversized, i.e., operate far below design capacities.

Using fuzzy logic Ngan et al. [14] analyzed actions to mitigate risks in CHP palm-oil pyrolysis plants for bio-oil production in Malaysia, wherein risks were classified into regulatory, financial, technological, supply-chain, business and social-environmental. Financial incentives to reduce interest rate were found the most impactful actions for risk reduction, followed by revision of the feed-in tariff. The least important factor to risk management was the increase in bio-oil demand by replacing fossil fuel utilization. Moreover, supply-chain improvements were found more important than technology and process improvements.

Regarding carbon management of a CHP plant, the carbon dioxide (CO_2) content in dry flue-gas of bagasse-fired boilers is $\approx$12%mol [15], while in a natural gas combined-cycle power plants (NGCC) it is only $\approx$4.2%mol increasing to 6.6%mol if flue-gas recirculation is adopted [16]. The advantage of flue-gas recirculation is a higher %mol CO_2 in exhaust-gas, increasing by 0.5% the efficiency of Carbon Capture and Storage (CCS) [16]. Even so, the exergy efficiency of power generation decreases from 53.5% to 44.8% with CCS [17], indicating the economic impact of CCS in NGCC's. Thus, the high CO_2 content in bagasse-fired flue-gas is beneficial to CCS.

Massive implementation of bioenergy with CCS (BECCS) technologies is considered the best strategy to limit the increase in the average planetary temperature by a maximum of 1.5 °C by 2100, since BECCS technologies are the only carbon-negative processes available [18]. Gibon et al. [19] performed Life-Cycle Assessment of various electricity production technologies, using renewable sources or not, with/without BECCS/CCS. BECCS solutions achieved negative net emissions in all scenarios, but had a high increase in resource utilization as a trade-off. The BECCS potential of sugarcane-biorefineries at 1000 t/h of sugarcane corresponds to 659.6 tCO_2/h in the CHP and only 39.7 t/h in the bioethanol fermentation step [20], where the CO_2 emission rate is estimated as 700 $kgCO_2$/MWh for the bagasse-fired cogeneration, while for a NGCC it reaches 400 $kgCO_2$/MWh. However, the Life-Cycle Assessment estimated a Global Warming Potential of only 8.6-10 $kgCO_2$/MWh

for district heat and 32-38 $kgCO_2$/MWh for CHP electricity production [21], vis-à-vis 460 $kgCO_2$/MWh when the CHP is a natural gas GTCC [22].

There are five major operational bioethanol BECCS plants in the world, located in the USA and Canada [23]. The biggest one stores geologically 1 Mtpa of CO_2 from corn-to-ethanol fermentation, while the other projects inject CO_2 for enhanced oil recovery (EOR) purposes. CO_2 from bioethanol fermentation is the only CO_2 source in all projects. A UK project in early development breaks this pattern: the Drax BECCS Project plans to capture 4.3 Mtpa of CO_2 from the flue-gas of a biomass-fired boiler, with geological storage as destination.

Fuss et al. [24] performed a literature review on BECCS costs for bioethanol production considering different CO_2 sources, finding that it is cheaper for the fermentation CO_2 (40-120 USD/tCO_2) than for both fermentation CO_2 and CHP CO_2 (180-200 USD/tCO_2). The reason is because the fermentation CO_2 is almost pure and trivially captured [25], though it is just released into the atmosphere in practically all current plants. When BECCS is performed only in the flue-gas from a biomass-fired power plant, capture costs of 88-288 USD/tCO_2 were reported, but various capture technologies and power plant configurations were considered in this range. Assuming geological storage as destination, Laude et al. [26] evaluated the BECCS potential for the fermentation CO_2 only and coupled to the CHP CO_2 finding CCS costs of 86 USD/tCO_2 and 143 USD/tCO_2 respectively, considering a 2050 carbon price of 200 EUR/tCO_2 for the base-case. The authors claim that the 60,000 m^3/a capacity of the bioethanol biorefinery is the reason behind this poor performance.

The work of de Souza et al. [27] evaluated the integration of CHP with a sugarcane-biorefinery, finding that the electricity cost is competitive compared to small systems. Carminati et al. [6] estimated the Net Present Value (*NPV*) of a sugarcane-biorefinery with/without BECCS. The economic performance of the BECCS biorefinery is even better than the non-BECCS counterpart, considering some stringent carbon-market scenarios reacting to a high climate-change severity and oil dependence. Guandalini et al. [28] studied the CCS of a biomass-based power plant disclosing a cost estimation model that can be used to foresee if a new technology performs better than the benchmark post-combustion capture via chemical-absorption with aqueous-monoethanolamine (aqueous-MEA). It also estimates the breakeven *FCI* and Cost of Manufacturing (*COM*) of a potential new technology attaining same capture cost of the benchmark aqueous-MEA absorption. Authors claim that capture

technologies requiring mainly heat should be considered first when heat is available, as in the CHP case, due to a lower *COM*.

4.1.1. The Present Work

Following our previous studies [6], [20] and [25] on onuses and bonuses related to BECCS implementation in sugarcane-biorefineries, this work develops and demonstrates quantitative tools to estimate *FCI* and *COM* changes, as well as the carbon capture cost, related to BECCS implementation in sugarcane-biorefineries. Since, for comparison purposes, the non-BECCS biorefinery has to be modeled beforehand, this work discloses surrogate models created by adjusting response surfaces over computer-experiments to estimate *FCI* and *COM* for installation of a new CHP plant coupled to sugarcane-biorefinery. The CHP uses BST technology with/without BECCS. The proposed generic-location model is applied to the South-East Brazilian scenario as one should realize that *FCI* and *COM* from other regions may substantially differ. The only required inputs are the energy requirements of the sugarcane-biorefinery – i.e., mass flowrates of low-pressure steam (LPS) and medium-pressure steam (MPS) – and bagasse availability. The sugarcane-biorefinery can be, for example, a sugar mill or a bioethanol fermentation-distillation plant. Considering typical steam consumption for sugarcane-biorefinery with distillery, the *FCI* curve against produced power is presented and compared to the literature and to power auctions in Brazil. The developed models are used to evaluate the Minimum Steam Selling-Price (*MSP*), BECCS costs and carbon capture cost under different scenarios of capacity and market prices. The scope of this work and the inputs/outputs of the developed models are highlighted in Fig. 4.1. It is adopted a distinct owner scenario, wherein bagasse is bought from a sugarcane-biorefinery and steam/electricity are sold to it. The price of exported electricity, sold to the sugarcane-biorefinery or to the grid as surplus, is obtained from national auctions. Thus, BECCS costs are allocated to the CHP plant, allowing comparisons with/without BECCS. Moreover, this is the first sugarcane-biorefinery work analyzing *FCI* against the capacity of the bagasse-fired CHP plant with and without BECCS. It is also reported a robust mass/energy balance model for estimating material/power streams of the bagasse-fired CHP, besides bleed-steam and net/total power given bagasse mass flowrate and energy requirements.
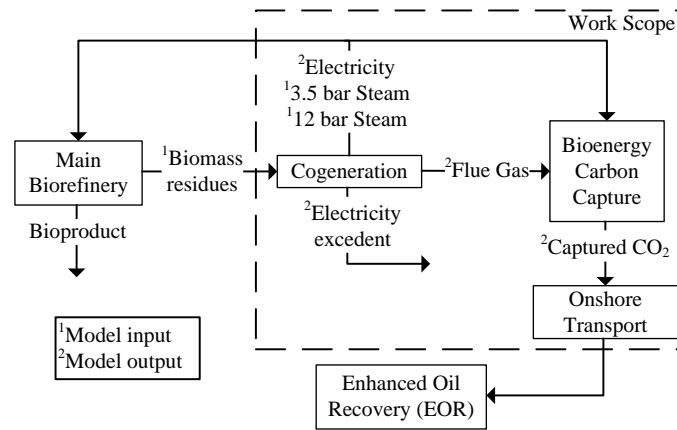
Fig. 4.1. Work scope diagram.

The main advantages of the *FCI* surrogate model are its accuracy, compactness and simplicity, besides the possibility to participate in plant optimizations, where the optimum capacity of each area is sought. The sugarcane-biorefinery feasibility for sugar/bioethanol productions [29] can be surrogated based on sugarcane intake and on the desired sugar/ethanol allocation. Conceivable novel technological extensions of the sugarcane-biorefinery operating in BECCS mode – such as production of ethylene/H_2 from bioethanol [30] or CO_2-to-methanol [17] to substitute the geological storage – can also be surrogated and included in the predictive framework developed here to optimize such extended sugarcane-biorefineries. Analogously, other complex bioenergy processes that have BECCS potential – e.g., anaerobic digestion, 2nd generation ethanol fermentation, syngas-to-ethanol anaerobic fermentation, biomass pyrolysis – can be efficiently modeled and optimized with such strategy of surrogate modeling.

4.2. Methods

The developed method consists of four steps: (i) process flowsheet development; (ii) flowsheet simulation in Aspentech portfolio; (iii) factorial 3^3 design of computational-experiments, leading to 27 flowsheet simulations for the CHP and three for the CCS configuration, allowing estimating *FCI* of flowsheets (base-year 2018) with Aspen Process Economic Analyzer (APEA) V11; and (iv) generation of surrogate models for *FCI* and *COM* based on the sugarcane-biorefinery energy requirements and bagasse availability. A surface response for *FCI* prediction is proposed, while *COM* is evaluated based on Turton et al. [31], for the estimated *FCI*. The *FCI* model is used in all conducted analyses, including sensitivity analyses and *FCI* curves of the CHP plant for typical Brazilian sugarcane-biorefineries.

94

4.2.1. Process Flowsheet

The CHP-CCS flowsheet comprehends three areas: biomass-fired boiler (A10), power-house (A20) and CCS plant (A30, if present). The boiler burns bagasse from the sugarcane milling producing SHPS. The power-house exports heating utilities (LPS/MPS) and electricity from SHPS. The CCS plant captures and processes CO_2 abating biorefinery emissions.

In the boiler area in Fig. 4.2, it is considered the Bubbling Fluidized Bed type which offers an efficient, fuel-flexible and cost-effective burner for low-grade biomass with modest heating value and high humidity/ash contents [32]. The lignocellulosic bagasse stream (1) feeds the boiler furnaces (H-11). The boiler is also fed with demineralized-water (12), which is pre-heated with flue-gas, vaporized and superheated as SHPS in the radiation zone. The boiler exports SHPS (13) to the power-house (A20) steam-turbines; flue-gas (10) to the CCS plant (or to atmosphere) and ashes to the plantation fields (11). The boiler also receives primary (4), secondary (5) and tertiary (6) pre-heated air streams after pre-heating atmospheric air (2) via heat-recovery (E-11) from hot flue-gas (8). Cooled flue-gas is sent to the electrostatic precipitator (S-11), where particulates (soot) are removed as ashes (11), normally used as fertilizer. The final flue-gas with low particulate content (10) is liberated in the atmosphere or sent to the CCS unit (A30).
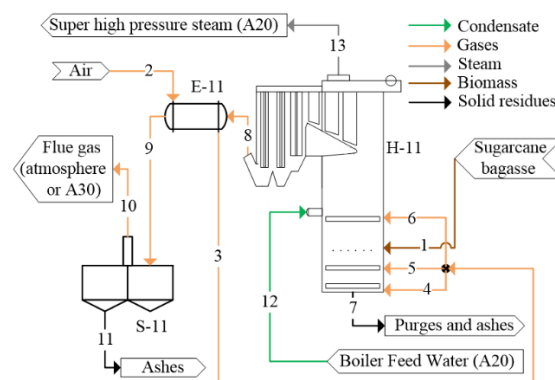
Fig. 4.2. Boiler flowsheet (A10).

The considered power-house (A20) in Fig. 4.3 is the topping cycle, which consists in electricity generation prior to LPS/MPS generation to fulfill biorefinery demand [23]. SHPS (13) feeds a counter-pressure turbine (M-21) with MPS extraction (14). A fraction of the expanded steam from the backpressure-turbine (17) becomes the LPS (18) for process heating purposes, while the remainder goes to the condensing turbine (M-22). The low-pressure

turbine outlet stream (20) is condensed (E-21) and pumped (P-21) to the pressurized deaerator (V-21), which also receives process condensates (23) and aerated water make-up (24). V-21 is injected with part of the MPS extracted from the counter-pressure turbine (16) – so-called bleed-stream – to adjust V-21 temperature providing the separation of purged air (25). The boiler feed water (26) is pumped by P-22.
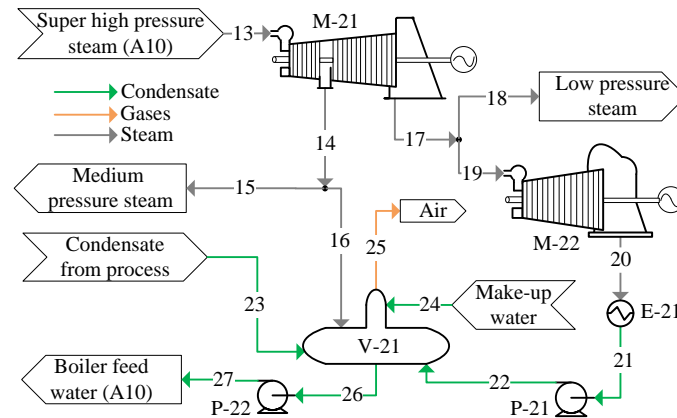
Fig. 4.3. Power-house flowsheet (A20).

4.2.2. Simulation of Process Flowsheets

The flowsheets of CHP and CCS plants are respectively installed in two process simulators, namely, ASPEN-Plus® v11 and ASPEN-HYSYS® v11. A10 and A20 are simulated using the ASPEN NRTL-RK thermodynamic package, whereas the CCS plant uses the HYSYS Acid-Gas Amine Package. Bagasse is modeled as cellulose during combustion, where 99.9% undergoes complete combustion Eq. (4.1a) and 0.1% follows incomplete combustion in Eq. (4.1b). Enthalpy data of cellulose is adjusted to match its lower heating value (LHV) of 7.5 MJ/kg (50%w/w moisture). Table 4.1 shows the general simulation assumptions and Table 4.2 lists Base-Case assumptions.

$$C_6H_{10}O_5\left(bagasse\right) + 6\ O_2 \rightarrow 6\ CO_2 + 5\ H_2O \tag{4.1a}$$

$$C_6H_{10}O_5\left(bagasse\right) + 3\ O_2 \rightarrow 6\ CO + 5\ H_2O \tag{4.1b}$$
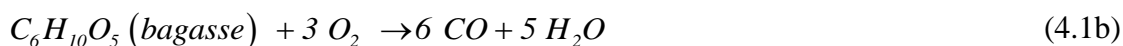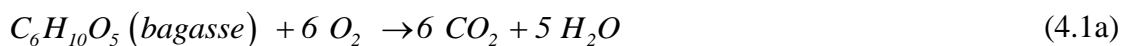
Table 4.1. Process simulation assumptions.

Item	Description	Area	Assumptions
1	*Bagasse*	A10	*Dry-bagasse=47.8%w/w; Moisture=50%w/w; Ash=2.2%w/w; LHV=7.5 MJ/kg.*
2	*Combustion Air*	A10	*Excess air: 50%.*
E-11	*Combustion Air Heater*	A10	*T_{out}=120 ºC; ΔP=0 bar.*

96

Item	Description	Area	Assumptions
H-11	Biomass-Fired Boiler	A10	P=90 bar; T_{SHPS}=520 ºC; Purged-Ashes=90%; T_{Bed}=1000 ºC; P_{Bed}=1 atm.
S-11	Electrostatic Precipitator	A10	Isobaric-Adiabatic Flash.
12	Boiler Feed-Water	A10	P_{inlet}=109 bar; Steam:Bagasse Mass-Ratio=2.093; Flowrate(kg/h)=Bagasse(kg/h)*2.093/0.99.
M-21	Extraction Backpressure-Turbine	A20	Type Isentropic; Adiabatic Efficiency: η=85%; Mechanical Efficiency: η_{mech}^{M} =96%; $P_{Extraction}$=12 bar; $P_{Discharge}$=3.5 bar;
M-22	Condensing-Turbine	A20	Type Isentropic; Adiabatic Efficiency η=85%; Mechanical Efficiency: η_{mech}^{M} =96%; $P_{Discharge}$=0.1 bar;
E-22	M-22 Condenser	A20	ΔP=0 bar; Vapor-Fraction=0.
P-21	Condenser Pump	A20	P_{outlet}=3.55 bar.
23	Condensate	A20	P_{inlet}=3.5 bar; Vapor-Fraction=0.
24	Demineralized-Water	A20	Air=0.1%w/w; Water=99.9%w/w; P_{inlet}=3.5 bar; T_{inlet}=25 ºC.
V-21	Deaerator V-21	A20	P=3.5 bar; T=100 ºC; Recovery: Water=98%, Air=100%.
P-22	Boiler Pump	A20	P^{outlet}=109 bar. Mechanical Efficiency η_{mech}^{P} =96%;
15+18	Total Steam	A20	50% Direct-Heating; 50% Shell-and-Tube Exchangers
All	CCS Plant	A30	Aqueous-MEA Chemical-Absorption [9]; Solvent: MEA=30%w/w; Water=70%w/w; CO_2 Capture Efficiency: 90%.

Table 4.2. Base-Case Assumptions.

Variable	Value	Reference
Sugarcane (t/h)	500	[33]
Bagasse:Sugarcane Ratio ($t^{Bagasse}/t^{Sugarcane}$)	0.276	[29]
Biorefinery Steam Requirements (kg/$t^{Sugarcane}$)	LPS=429; MPS=36.9	[29]
Biorefinery Power Requirement (kWh/$t^{Sugarcane}$)	28.0	[29]
Power Surplus (kWh/$t^{Sugarcane}$)	83.4	[29]

4.2.3. Design of Computational-Experiments

A factorial 3^3 computational-experimental design is created with the following factors: bagasse capacity as X (t/h); LPS plus MPS productions as percentage of SHPS production $Y(\%)$; MPS as percentage of LPS plus MPS production $Z(\%)$. Eq. (4.2) defines the factors, where $\dot{m}_i$ is the mass flowrate of stream i (t/h).

$$X(t/h)=\dot{m}_1; \ Y(\%)=100(\dot{m}_{15}+\dot{m}_{18})/\dot{m}_{13}; \ Z(\%)=100\dot{m}_{15}/(\dot{m}_{15}+\dot{m}_{18}) \qquad (4.2)$$

Only X affects flue-gas (10) flowrate, and consequently, the CCS plant (A30). Therefore, A30 has only three simulation runs instead of 27. The X levels are 33.75 (-1), 67.50 (0) and 135.0 (+1); while Y and Z levels are 25% (-1), 50% (0) and 75% (+1). Table 4.3 shows the planning of computational runs.

Table 4.3. Three-level, three-factor experimental planning (*X,Y,Z*).

Run 1	Run 2	Run 3	Run 4	Run 5	Run 6	Run 7	Run 8	Run 9
-1,-1,-1	-1,-1,0	-1,-1,1	-1,0,-1	-1,0,0	-1,0,1	-1,1,-1	-1,1,0	-1,1,1
Run 10	**Run 11**	**Run 12**	**Run 13**	**Run 14**	**Run 15**	**Run 16**	**Run 17**	**Run 18**
0,-1,-1	0,-1,0	0,-1,1	0,0,-1	0,0,0	0,0,1	0,1,-1	0,1,0	0,1,1
Run 19	**Run 20**	**Run 21**	**Run 22**	**Run 23**	**Run 24**	**Run 25**	**Run 26**	**Run 27**
1,-1,-1	1,-1,0	1,-1,1	1,0,-1	1,0,0	1,0,1	1,1,-1	1,1,0	1,1,1

The response variables of each run comprise the FCI^{CHP} and FCI^{CCS} (2018 Brazil conditions). FCI is estimated via APEA, after equipment sizing via mass/energy balance results from simulations. In APEA, the boiler H-11 is evaluated as an oil-fired erected boiler. APEA is configured with 32% contingency for FCI^{CCS} [34], and 15% contingency for FCI^{CHP} since CHP is a mature technology. The resulting FCI is multiplied by the process plant location factor $LF=1.18$ from Intratec [35] to convert 2018 USA FCI to 2018 Brazil conditions. FCI results from the computational-experimental simulations are used via minimization of the sum of residue squares for estimation of parameters a, b, c, d, $a^{\#}$, $b^{\#}$ in Eq. (4.3) and Eq. (4.4) for predicting FCI^{CHP} and FCI^{CCS}, respectively. In the right hand side of Eq. (4.3), the first term is a cost-to-capacity function to evaluate FCI at different capacities (X); the second term reflects the fact that larger net SHPS flowrate (i.e., discounting LPS+MPS) entails larger FCI of steam-turbines resulting in the $(1-Y/100)$ exponent; and the last term translates the fact that high X and Y increase Z relevance. As these models were formulated following typical FCI behaviors, they have a prediction capacity outside the analyzed range of factors.

$$FCI^{CHP} = 1.15LF\left(aX^{b} + cX^{1-Y/100} - dX(Y/100)(Z/100) \right) \tag{4.3}$$

$$FCI^{CCS} = 150 + 1.32LF\left(a^{\#}X^{b^{\#}} \right) \tag{4.4}$$

COM^{CHP} and COM^{CCS} are estimated via Eq. (4.5) according to Turton et al. [31], where COL (MMUSD/a) is the annual cost of labor; CRM (MMUSD/a) and CUT (MMUSD/a) represent annual costs of raw-materials and utilities. COL is independent of capacity, as the number of

operators typically depends on the number of equipment items and not on their capacities. $(CRM+CUT)^{CHP}$ and $(CRM+CUT)^{CCS}$ are respectively calculated by Eq. (4.6) and Eq. (4.10), where C_{CW} (USD/t), C_{DW} (USD/t), C_X (USD/t), and OT (h/a) respectively represent cooling-water (CW) cost, demineralized-water cost, bagasse cost and annual operation time. Moreover, $\left(\dfrac{\dot{m}_{CW}}{\dot{m}_{20}}\right)^*$, $\left(\dfrac{\dot{m}_{13}}{X}\right)^*$ and $\left(\dfrac{\dot{m}_{CO2}}{X}\right)^*$ are constant ratios obtained from the Base-Case simulation. Eq. (4.7) estimates the CO_2 mass flowrate in the flue-gas. Only FCI has parameters to be estimated since COM^{CHP} and COM^{CCS} are available via Eq. (4.5) once FCI^{CHP} and FCI^{CCS} are estimated.

$$COM = 0.18FCI + 3.969COL + 1.235(CRM + CUT) \tag{4.5}$$

$$(CRM + CUT)^{CHP} = \left(X\left(\frac{\dot{m}_{13}}{X}\right)^* (1 - Y/100)\left(\frac{\dot{m}_{CW}}{\dot{m}_{20}}\right)^* C_{CW} + XC_X + \dot{m}_{24}C_{DW} \right) OT * 10^{-6} \tag{4.6}$$

$$\dot{m}_{CO2} = X\left(\frac{\dot{m}_{CO2}}{X}\right)^* \tag{4.7}$$

When a CCS plant exists, the biorefinery energy requirements supplied by the CHP must be increased, since LPS is required in the aqueous-MEA reboiler and electricity (W) is required to drive CO_2 compressors for pipeline transportation. LPS consumption and W are estimated via Eqs. (4.8) and (4.9) respectively, where $\left(\dfrac{\dot{m}_{LPS}^{CCS}}{X}\right)^*$ and $\left(\dfrac{W^{CCS}}{X}\right)^*$ are constant ratios from the Base-Case simulation with CCS. FCI^{CCS} and COM^{CCS} are obtained via Eq. (4.4) and Eq. (4.5), where $(CRM+CUT)^{CCS}$ comprehends only CW consumption via Eq. (4.10), where $\left(\dfrac{\dot{m}_{CW}^{CCS}}{X}\right)^*$ is another constant ratio from the Base-Case simulation with CCS.

$$\dot{m}_{LPS}^{CCS} = X\left(\frac{\dot{m}_{LPS}^{CCS}}{X}\right)^* \tag{4.8}$$

$$W^{CCS} = X\left(\frac{W^{CCS}}{X}\right)^* \tag{4.9}$$

$$(CRM + CUT)^{CCS} = XC_{CW} \left(\frac{\dot{m}_{CW}^{CCS}}{X} \right)^{*} OT * 10^{-6} \tag{4.10}$$

LPS, MPS and electricity are CHP products leading to revenues. Moreover, the captured CO_2 is monetized considering EOR activity and cap-and-trade regulations (similar to the EU Emissions Trading System) [36]. The BECCS biorefinery considers CO_2 sold to oil operators as EOR fluid (e.g., as in the offshore Brazilian Pre-Salt basin). Indeed, in the Pre-Salt oil recovery can be as low as 24% (e.g., offshore Campos basin [37]), creating a market for the captured CO_2. The price of CO_2-to-EOR derives from oil price, since up to 4.35 bbl of oil can be recovered with 1 tCO_2.

4.2.4. Sugarcane-Biorefinery Analyzer Framework

The sugarcane-biorefinery analyzer framework (SBAF) starts with Eqs. (4.3) and (4.4), and comprehends all forthcoming equations in Secs. 4.2.3/4.2.4/4.2.5. SBAF calculates all *FCI* and cost terms, revenues, power effects and all critical streams from inputs *X*, *Y*, *Z*. To do this, the first step is to obtain *Y* and *Z* from *X* and LPS/MPS biorefinery requirements. For example, with Eq. (4.2), *Y* is given via Eq. (4.11a); and consequently, since its maximum value is 100%, the minimum feasible *X* is obtained via Eq. (4.11b). Performing an energy balance around steam-turbines M-21 and M-22 (Fig. 4.3), one can show that the gross power W^M of M-21 and M-22 is obtained via Eq. (4.12), where $\Delta \hat{H}_{S2-S1} \equiv \hat{H}_{S2} - \hat{H}_{S1}$ represents the difference of specific enthalpies S2 and S1, and η_{mech}^M is the mechanical efficiency of steam-turbines (Table 4.1). Therefore, knowing bagasse availability (X) and the biorefinery MPS/LPS requirements, one can obtain *Z* via Eq. (4.2) and *Y* via Eq. (4.11a). Terms $\Delta \hat{H}_{S2-S1}$ are also constants from the Base-Case simulation, because the involved temperatures, pressures and compositions are invariant. The powers of pumps P-22 and P-21 (Fig. 4.3) are obtained via Eq. (4.13a) and Eq. (4.13b) respectively. The net CHP power W^{CHP} is obtained subtracting P-22 and P-21 powers from W^M in Eq. (4.14).

$$Y = 100(\dot{m}_{LPS} + \dot{m}_{MPS}) \left(X \left(\frac{\dot{m}_{13}}{X} \right)^{*} \right)^{-1} \tag{4.11a}$$

$$X_{min} = (\dot{m}_{LPS} + \dot{m}_{MPS}) \left(\left(\frac{\dot{m}_{13}}{X} \right)^{*} \right)^{-1} \tag{4.11b}$$

$$\frac{W^M}{\eta^M_{mech}} = \dot{m}_{MPS}\left(\frac{\Delta\hat{H}_{13-14}+\Delta\hat{H}_{13-17}+\Delta\hat{H}_{19-20}}{(Y/100)(Z/100)}-\Delta\hat{H}_{13-17}-\frac{\Delta\hat{H}_{19-20}}{Z/100}\right)-\dot{m}_{16}\left(\Delta\hat{H}_{13-17}+\Delta\hat{H}_{19-20}\right)\quad(4.12)$$

$$\frac{W^{P22}}{\eta^{P22}_{mech}} = X\left(\frac{\dot{m}_{13}}{X}\right)^{*}\Delta\hat{H}_{27-26}\tag{4.13a}$$

$$\frac{W^{P21}}{\eta^{P21}_{mech}} = \left(X\left(\frac{\dot{m}_{13}}{X}\right)^{*}-\frac{\dot{m}_{MPS}}{Z/100}-\dot{m}_{16}\right)\Delta\hat{H}_{22-21}\tag{4.13b}$$

$$W^{CHP} = W^M - W^{P22} - W^{P21}\tag{4.14}$$

Performing mass and energy balances for the deaerator V-21 and using previous definitions, several streams related to V-21 are calculated: $\dot{m}_{26}$ via Eq. (4.15); $\dot{m}_{23}$ via Eq. (4.16); $\dot{m}_{24}$ via Eq. (4.17); $\dot{m}_{25}$ via Eq. (4.18); and finally the bleed-steam $\dot{m}_{16}$ via Eq. (4.19), where *mu*, *bb* and *dh* represent, respectively, make-up percentage (2%), boiler blowdown percentage (1%) and percentage of MPS+LPS used as direct heat (50%).

$$\dot{m}_{26} = \frac{X}{(1-bb/100)}\left(\frac{\dot{m}_{13}}{X}\right)^{*}\tag{4.15}$$

$$\dot{m}_{23} = (dh/100)\left(\dot{m}_{MPS}+\dot{m}_{LPS}\right)\tag{4.16}$$

$$\dot{m}_{24} = -\frac{X\left(\dfrac{\dot{m}_{13}}{X}\right)^{*}\left(1-\dfrac{1}{1-bb/100}-mu/100\right)+(\dot{m}_{MPS}+\dot{m}_{LPS})(-1+dh/100)}{1-bb/100}\tag{4.17}$$

$$\dot{m}_{25} = X\left(\frac{\dot{m}_{13}}{X}\right)^{*}(mu/100)+\dot{m}_{24}(bb/100)\tag{4.18}$$

$$\dot{m}_{16} = \frac{\left(X\left(\dfrac{\dot{m}_{13}}{X}\right)^{*}-\dot{m}_{MPS}-\dot{m}_{LPS}\right)\hat{H}_{22}+\dot{m}_{24}\hat{H}_{24}+\dot{m}_{23}\hat{H}_{23}-\dot{m}_{25}\hat{H}_{25}-\dot{m}_{26}\hat{H}_{26}}{\hat{H}_{22}-\hat{H}_{16}}\tag{4.19}$$

4.2.5. Application of the Sugarcane-Biorefinery Analyzer Framework

SBAF starts with the calibrated *FCI* predictor model, Eq. (4.3), which estimates FCI^{CHP} for a typical sugarcane biorefinery exporting electricity surplus for a given X and LPS/MPS

consumptions, which are converted in terms of Y and Z. SBAF – Eqs. (4.3) to (4.19) – then estimates W^{CHP}, COM^{CHP} and all critical streams.

The Minimum Steam Selling-Price (MSP) of the produced steam of the Base-Case is evaluated with/without the CCS plant. For this purpose, a NPV analysis is performed using SBAF estimates for FCI, COM and revenues. NPV is evaluated via Eq. (4.20), given the total steam price and the annual interest (%) rate j, where t is the project lifetime plus construction time and CF is the cash flow, which depends on the steam price. As a simplification, the steam produced is the sum of the mass flowrates of LPS and MPS, and is referenced hereinafter as Total-Steam, with only one price. The MSP is the Total-Steam price giving $NPV = 0$ and using the minimal acceptable rate of return ($MARR$) as interest rate in Eq. (4.21). The Total-Steam MSP is evaluated instead of the electricity price due to its higher uncertainty, since the Brazilian electricity auctions define electricity contracts price.

$$NPV\left(j, Total - Steam\ Price\right) = \sum_{i=1}^{t} \frac{CF_i\left(Total - Steam\ Price\right)}{\left(1 + j/100\right)^i} \tag{4.20}$$

$$NPV\left(j = MARR, Total - Steam\ MSP\right) = \sum_{i=1}^{t} \frac{CF_i\left(Total - Steam\ MSP\right)}{\left(1 + MARR/100\right)^i} = 0 \tag{4.21}$$

To evaluate the BECCS cost, the CO_2 avoidance cost [38] is used. For sake of simplicity, it is here called Capture Cost (CC). CC is readily compared to CO_2 emissions tax and represents its minimum value that incentives carbon capture, when the taxation is applied to both BECCS and non-BECCS biorefinery [38]. A minor modification in the original equation is required to use it in the proposed scenario. The MSP (USD/t) is used instead of the electricity price, in Eq. (4.22), where "Reference" refers to the CHP plant without CCS and $CO_2\ Emissions$ is the ratio ($tCO2/t^{Total\text{-}Steam}$) of CO_2 emitted per Total-Steam produced.

$$CC = \frac{\left(MSP^{CCS} - MSP^{Reference}\right)}{CO_2\ Emissions^{Reference} - CO_2\ Emissions^{CCS}} \tag{4.22}$$

Table 4.4 shows the required information for NPV and MSP analyses, also used for sensitivity analyses. Sensitivity analyses are performed for some parameters to evaluate possible feasible scenarios.

Table 4.4. Base-Case assumptions for economic analysis.

Parameter	Value	Reference
Engineering & Construction	*1 year*	*APEA*
Project Lifetime	*20 years*	*Assumption*
MARR	*8%*	*Assumption*
Reference Year	*2018*	*Assumption*
Bagasse Cost (BRL/t)	*59.22*	*[39]*
Operator/Supervisor Wage (USD/month/worker)	*2710.4/5789.4*	*Assumption*
2018 BRL/USD	*3.6542*	*Assumption*
FCI of 150 km CO_2 Pipeline	*150 MMUSD*	*[6]*
CW & Demineralized-Water costs (C_{CW}, C_{DW})	*4.29e-8 MMUSD/t*	*Assumption*
Electricity Price (average of 2018 Brazilian auctions)	*188 BRL/MWh*	*[40]*
OT	*5856 h/a (8 months)*	*[41]*
Salvage Value	*0%*	*Assumption*
CO_2-to-EOR	*25 USD/t*	*[36]*
Cap-and-trade	*40 USD/t*	*[36]*

The Brazil Process Plant Cost Index from Intratec is used to update the publicly available 2018 Brazilian CHP costs. The values are 323.34 and 165.48 for 2018 and 2010, respectively [42]. The publicly costs are initially converted to Brazil currency BRL, then are multiplied by the ratio of the Index of the desired year by the Index of the original year, and finally, are converted back to USD in 2018. Moreover, USA BECCS costs are also updated to 2018 and compared to the results without considering the location-factor.

4.3. Results

The Base-Case ($X = 138t / h, Y = 80.565\%, Z = 7.929\%$) simulation results are shown in Table 4.5 and compared to literature values for validation. Boiler and CHP efficiencies and Power-to-Heat ratio are within the reported range, while %mol CO_2 in the dry-basis flue-gas is higher than the theoretical 13.07% [15]. This is due to the difference in carbon content considered for sugarcane bagasse, since it is represented as cellulose in this work. The total power W^{CHP} predicted by SBAF is close to similar literature simulation results, with divergences of $\approx 1\%$. Regarding the CCS plant, although the same method from a previous work for coal-fired plants [17] was used, a lower value for the reboiler duty was achieved, due to the higher %mol CO_2 in the sugarcane-biorefinery flue-gas (14%mol versus 7.69%mol), increasing CO_2 fugacity. The CO_2 loading and the solvent capture-ratio also have better results than the conventional coal-plant CCS for the same reason.

Table 4.5. Base-Case simulation results.

Process	Variable	Unit	This study	Literature
CHP	Boiler Efficiency	%	88.9%	69-88% [43]
	CHP Efficiency	%	64.9%	61-73% [43]
	Power-to-Heat Ratio	-	0.35	0.3-0.5 [43]
	Flue-Gas CO_2	%mol (dry-basis)	14.98%	13.07% [15]
	Total Power Generated	kWh	56.33	55.7 [29]
CCS with Aqueous-MEA	Reboiler Heat-Ratio	GJ/tCO_2	3.612	3.723 [17]
	Lean Loading	mol^{CO2}/mol^{MEA}	0.2230	0.2185 [17]
	Solvent Capture-Ratio	$kg^{Solvent}/kg^{CO2}$	12.89	13.32 [17]

The parameters obtained from simulation are shown in Table 4.6, while the adjusted parameters for the *FCI* predictor are shown in Table 4.7. The parameters for the FCI^{CHP} predictor Eq. (4.3) are kept constant whether CCS is performed or not. The small average errors of 1.9% and 0.139% respectively for FCI^{CHP} and FCI^{CCS}, together with the respective correlation coefficients (0.9960 and 0.9911), indicate a good fit of the *FCI* predictor models over the computational-experimental data. The scale-factor exponents for FCI^{CHP} and FCI^{CCS} are 0.5891 and 0.6808 respectively, meaning that the former is more benefited from higher capacities.

Table 4.6. SBAF coefficients from Base-Case simulation.

Area	Coefficient	Value	Unit
CHP (A10 + A20)	$\Delta \hat{H}_{13-14}$	0.4694	GJ/t
	$\Delta \hat{H}_{13-17}$	0.2171	GJ/t
	$\Delta \hat{H}_{19-20}$	0.4583	GJ/t
	$\Delta \hat{H}_{27-26}$	0.01786	GJ/t
	$(\dot{m}_{13}/X)^*$	2.093	t/t
	$(\dot{m}_{CW}/\dot{m}_{20})^*$	63.03	t/t
	$\hat{H}_{16}, \hat{H}_{22}, \hat{H}_{23}$ $\hat{H}_{24}, \hat{H}_{25}, \hat{H}_{26}$	-13.00, -15.78, -15.31 -15.71, -14.37, -15.54	GJ/t
	$(\dot{m}_{CO2}/X)^*$	0.7777	t/t
CCS (A30)	$(m_{LPS}^{CCS}/X)^*$	1.072	t/t
	$(W^{CCS}/X)^*$	90.50	kWh/t
	$(m_{CW}^{CCS}/X)^*$	23.11	t/t

Table 4.7. Estimated parameters for *FCI* predictors.

	FCI^{CHP} (A10+A20)				*FCI^{CCS}* (A30)	
	a	*b*	*c*	*d*	*a^#*	*b^#*
Estimated value	2.368	0.5891	0.1670	0.03545	3.051	0.6808
Average absolute error	1.91%				1.31%	
Error range	[-4.09%, 3.55%]				[-1.7%, 1.8%]	
Correlation coefficient	0.9960				0.9911	

Fig. 4.4 shows observed (computational-experiments) and predicted *FCI^{CHP}* via Eq. (4.3), already considering the contingencies but without CCS. One can see that *X* is the most impacting factor on *FCI^{CHP}*, which is the same in the 1-9, 10-18 and 19-27 runs. Furthermore, factor *Y* is more important than *Z* since there is a greater displacement for each triad of runs than inside each one. Factor *Z* only plays an important role when high *X* and *Y* are present. The estimated *FCI^{CHP}* is within 25-30 MMUSD for *X=33.75 t/h* of bagasse, within 35-45 MMUSD for *X=67.5 t/h* and within 55-65 MMUSD for *X=135 t/h*. The confidence limits indicate the range wherein values of *FCI^{CHP}* with 15% maximum error (Class 4 project) are located with 95% of probability. If more accurate data is provided, the 95% confidence band would shrink.
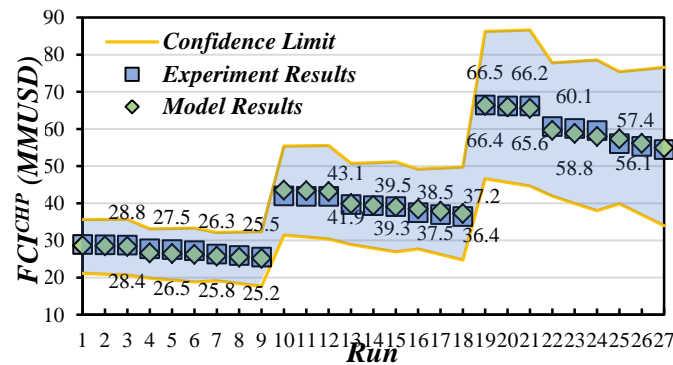
Fig. 4.4. Observed and predicted *FCI^{CHP}* results (no CCS).

Fig. 4.5 depicts predicted versus observed *FCI^{CHP}* for all runs, together with 15% error bars and without CCS. Points are close to the diagonal, translating a good performance of the *FCI^{CHP}* predictor.
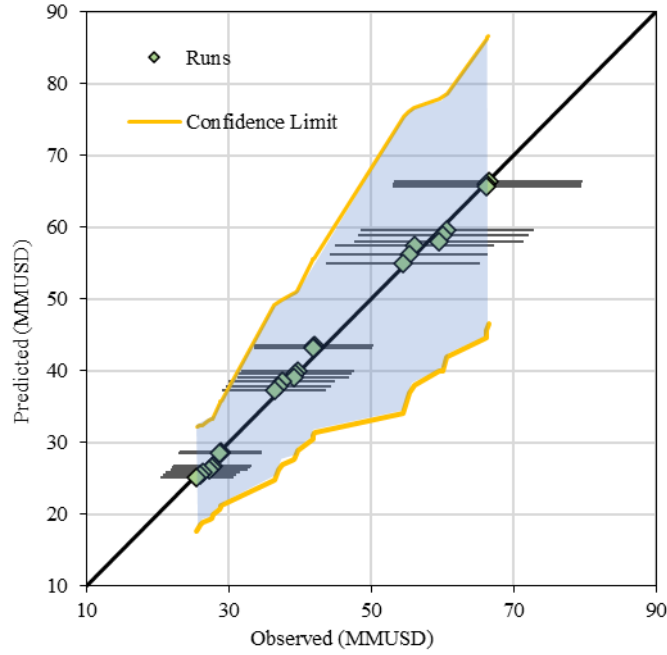
Fig. 4.5. Observed versus predicted FCI^{CHP} (A10+A20, no CCS).

Fig. 4.6 depicts FCI^{CCS} versus X, including the investment of a 150 km CO_2 pipeline. It is notorious that FCI^{CCS} is considerably higher than FCI^{CHP}. For example, at $X=67.5$ *t/h* of bagasse, FCI^{CCS} is 200-300 MMUSD, while FCI^{CHP} is within 30-60 MMUSD (Fig. 4.4) without CCS. The pipeline FCI accounts for a good portion of FCI^{CCS}, ranging from 50% to 75%; but the higher the capacity, the lower the unitary (i.e., per tCO2) pipeline contribution.
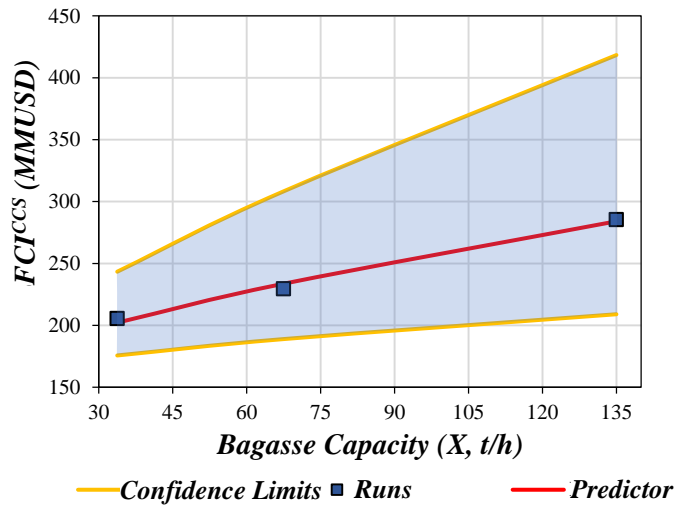
Fig. 4.6. Observed and predicted FCI^{CCS} (A30) versus bagasse capacity.

Table 4.8 compares sugarcane-biorefinery FCI^{CCS} per capture capacity (MMUSD/tCO2[Captured]/h) with 2018 USA plants. The comparison only considers the FCI of

the CO_2 capture and compression unit. The FCI^{CCS} predictor of this work is close to the results of [34], showing divergences of 15% and 10% for capacities of 118 and 379 tCO2^{Captured}/h, respectively. However, specific values from [34] are lower than the counterparts of [38]: 1.08 MMUSD/tCO2^{Captured}/h against 1.3 MMUSD/tCO2^{Captured}/h, even at high capture capacities of 378.8 tCO2^{Captured} /h and 500.4 tCO2^{Captured} /h, respectively. Fig. 4.7 shows COM^{CHP} with/without CCS and COM^{CCS} versus simulation runs. FCI^{CHP} increases considerably with CCS up to 34% in the analyzed scenarios, for the same power output. The numbers of operators/supervisors are 2/1 for the CHP and 5/1 for the CCS plant, resulting in COL values of 0.67 MMUSD/a and 1.16 MMUSD/a, respectively. It can be seen that the trend of COM^{CHP} is similar to the FCI^{CHP} analogue; i.e., X impacts more than Y, which impacts more than Z. The underlying reason is the fact that FCI is a relevant factor in COM with a minimum contribution of 86%; on the other hand, a minor (but not insignificant) tributary to COM is COL, the cost of labor.

Table 4.8. FCI^{CCS} predictor results versus literature results.

Case	Flue-Gas %mol CO$_2$	Capacity tCO2^{Captured}/h	$FCI^{CCS\,(a)}$ MMUSD / tCO2^{Captured}/h	Source
550 MW Subcritical Pulverized Coal	12.88%	500.4	1.30	[38]
550 MW Supercritical Pulverized Coal	12.88%	480.4	1.32	[38]
559 MW NGCC	3.91%	202.1	1.87	[38]
430 MW Subcritical Pulverized Coal	12.80%	378.8	1.08$^{(b)}$	[34]
430 MW Subcritical Pulverized Coal	12.80%	118.0	1.63$^{(b)}$	[34]
Base-Case 56.3 MW CHP, X=138 t/h	13.98%	96.60	1.51	This work
69 MW CHP, X=169 t/h	13.98%	118.0	1.42	This work
118 MW CHP, X=118 t/h		202.1	1.20	
221 MW CHP, X=541 t/h		378.7	0.98	

(a) Only CO$_2$ capture and compression unit: USA values updated to 2018 via Intratec Process Plant Cost Indexes; (b) Flue-gas desulfurization unit removed from FCI^{CHP}; Let-down turbine/generator included but not required in sugarcane-biorefinery CHP.
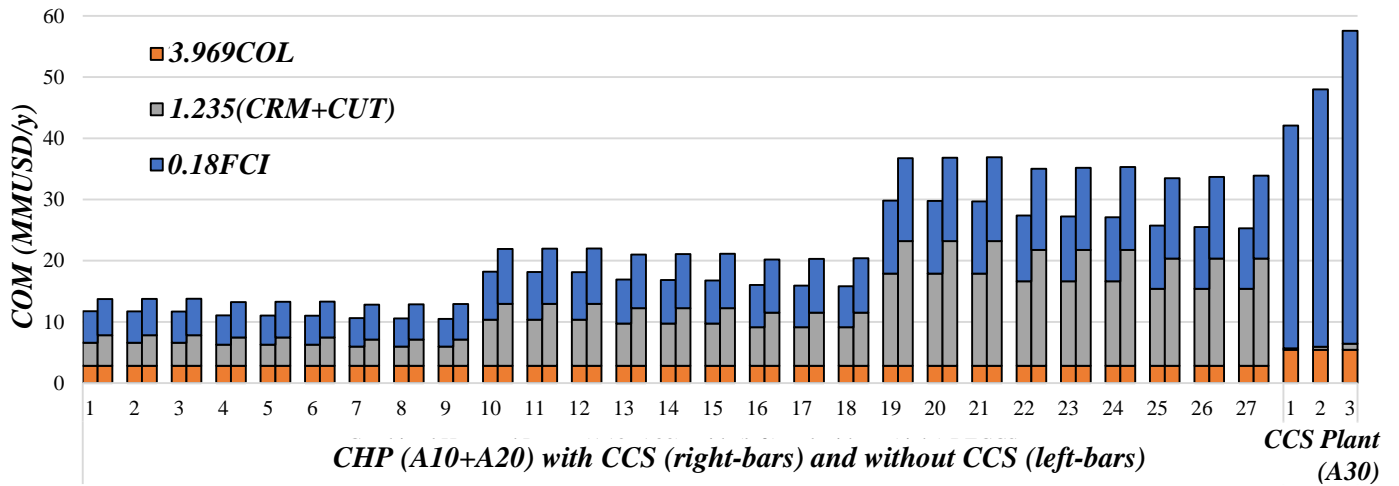
Fig. 4.7. COM^{CHP} **with/without CCS and** COM^{CCS} **vs simulated runs.**

Fig. 4.8 shows the FCI^{CHP} behavior (no CCS included) against power exported for a typical sugar-bioethanol sugarcane-biorefinery, and its comparison with the literature. The specific FCI^{CHP} (USD/kW) is also shown in the right axis. This time, the fitted FCI^{CHP} equation does not depend on (Y,Z) because FCI^{CHP} was handled to match a typical biorefinery configuration requirements; i.e., the change in X does not change the other factor values of the Base-Case $(Y = 80.5653\%,\ Z = 7.9287\%)$. The FCI^{CHP} in Brazil for 500 t/h sugarcane using an 82 bar boiler was estimated at 126 MMBRL in 2010 [33], or a 2018 updated value of 65.6 MMUSD. Brazilian 2018 electricity auctions gave an average specific FCI^{CHP} of 4000 BRL/kW with 50 MW of power average [41]. The SBAF model agrees with the available public data since they are within the considered error margin for a preliminary study. However, the specific FCI^{CHP} from electricity auctions in Brazil vary significantly from 1000 BRL/kW to 8000 BRL/kW, even considering only the new ventures, because sometimes they are installed next to a pre-existing plant sharing infrastructure and reducing costs [41]. Even so, the average 2008 specific FCI^{CHP} of 4000 BRL/kW for 50 MW of power average [41] shows that SBAF reasonably represents the Brazilian scenario.
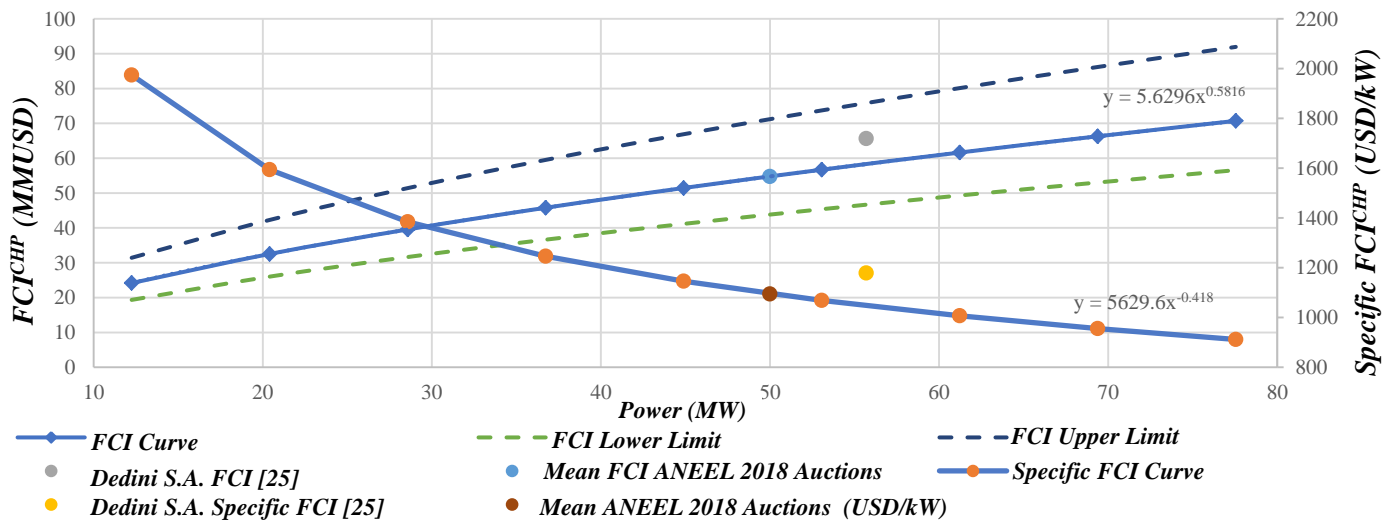
Fig. 4.8. Absolute FCI^{CHP} (MMUSD) and specific FCI^{CHP} (USD/kW) of typical sugar/ethanol biorefineries (Brazil, 2018) and comparison with literature.

The *MSP* of the Base-Case (no CCS) Total-Steam was found at 11.3 USD/t. Fig. 4.9 shows the composition of the destination of total revenue for the Base-Case without CCS considering a Total-Steam price of 23.7 USD/t. Fig. 4.9 shows that 18.1% of revenues is destinated to the Return of Investment (*ROI*) in order to achieve the investment *MARR*, which is obviously the most important revenue destination after raw-materials (basically sugarcane) compromising 27.5% of revenues. The smallest revenue destination is *COL*, accounting only for 2.6% of revenues.
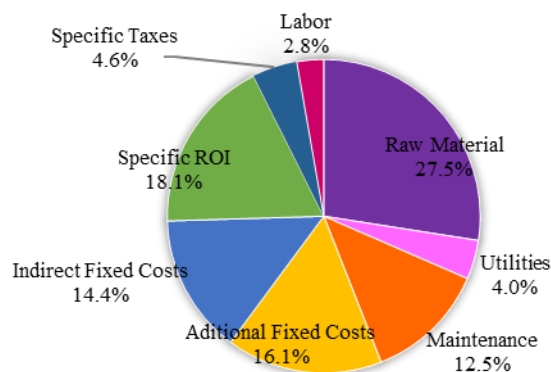
Fig. 4.9. Revenue destination: Base-Case (no CCS).

Fig. 4.10 shows one-dimensional *MSP* sensitivity analyses regarding changes in parameters and factors (i.e, considering one parameter at a time). Bagasse cost (*Base-Case=11 USD/t*), electricity price (*Base-Case=51.45 USD/MWh*), bagasse capacity (*Base-Case=138 t/h*), Capacity Factor (*Base-Case=100%*), OT (*Base-Case=5856 h/a*) and FCI^{CHP} (*Base-*

109

Case=58.72 MMUSD) were varied by ±50%, except for the Capacity factor, which was varied from -50% to 0%. One can see that an increase in electricity price has a higher effect on *MSP* than a decrease in bagasse cost, 5.1 USD/t against 7.3 USD/t for a 50% change. An increase in CHP capacity is only recommended when there is a real demand for the extra power generated, since *MSP* sensitivity to the Capacity Factor is the greatest among the analyzed parameters. For example, a capacity increase from the Base-Case to 207 t/h bagasse capacity decreases the *MSP* from 11.1 to 8.8 USD/t; but if the Capacity Factor is 40% lower, it can double the *MSP*. The decrease in FCI^{CHP} – e.g., CHP sharing some infrastructure or revamping an existing plant – can have a greater *MSP* impact. For each MMUSD saved in FCI^{CHP}, a *MSP* decrease of 0.22 USD/t is achieved. Moreover, some plants burn alternative biomass fuels in the off-season to increase its yearly *OT*, reducing *MSP* to 6.5 USD/t for CHP plants available all over the year.
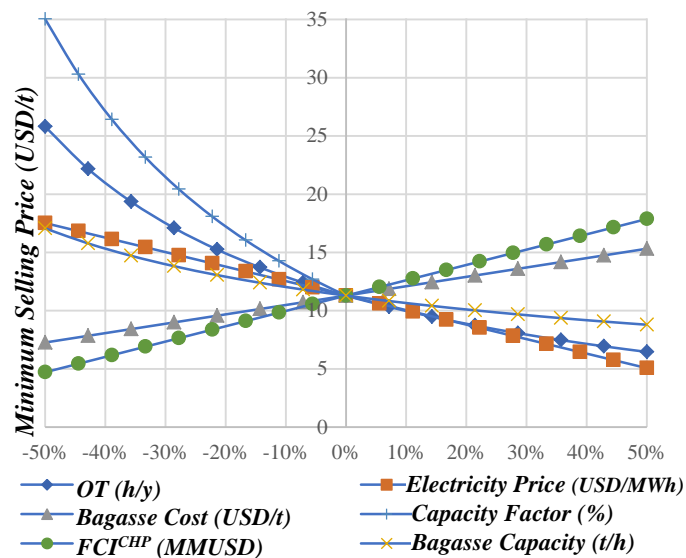
Fig. 4.10. Base-Case (no CCS): Total-Steam *MSP* sensitivity to changes in electricity price, bagasse price, bagasse capacity, capacity factor, *OT* and FCI^{CHP}.

For the Base-Case with CCS, the increase of LPS requirement due to the stripping heat-ratio in the post-combustion aqueous-MEA plant is estimated as 157.4 t/h. Thus, the bagasse requirement increases 57.7 t/h to keep the same power output (56.3 *MW*). The new requirement values of bagasse, LPS, and MPS (respectively 195.7 t/h, 371.7 t/h and 18.45 t/h) result in $X = 195.7\,t\,/\,h, Y = 95.2\%, Z = 4.7\%$.

The captured CO_2 of 96.6 t/h represents 90% of the original CO_2 emitted and 63.5% of the actual CO_2 produced, since there is an increase in the bagasse requirement and, consequently,

110

in the CO_2 produced (152.2 t/h). The CO_2 exportation revenue is 36.8 MMUSD/a, wherein 38.5% is for EOR purposes and the remainder for Cap-and-Trade market. The gross CHP produced power is 75.9 MW, with a net value of 56.28 MW, discounting the power of CO_2 pump and compressors. This CHP net power with CCS is practically equal to the CHP net power without CCS (56.33 MW). The new FCI^{CHP} with CCS is 71.8 MMUSD, a 22.3% increase over the Base-Case without CCS, while FCI^{CCS} reaches 256 MMUSD, wherein the CO_2 pipeline accounts for $\approx 60\%$ of FCI^{CCS}. Table 4.9 compares both scenarios in terms of technical and economic metrics.

Table 4.9. Comparison of CHP performances with/without CCS.

Variable	No CCS	With CCS
Inputs (LPS(t/h); MPS(t/h); X(t/h))	214.3; 18.45; 138.0	371.7; 18.45; 195.71
Y (%); Z(%)	80.6%; 7.93%	95.2%; 4.73%
$FCI^{CHP}+FCI^{CCS}$ (MMUSD)	58.7+0	71.8+256
COM^{CHP} (MMUSD/y)	25.0	95.4
$CO_2^{Flue\text{-}Gas}$ (t/h)	107.3	152.2
$CO_2^{Captured}$ (t/h)	0	96.6
CCS Efficiency (%)	0%	63.5%
W^{CHP}(MW)	56.3	56.3

In the Base-Case with CCS, considering the CO_2 revenue, the CC is 262 USD/tCO_2, perfectly within the literature range 88-288 USD/tCO_2, while the MSP is 69.5 USD/t. The CC proximity to the upper limit has probably to do with the technology chosen; namely, post-combustion capture with 30%w/w aqueous-MEA, while the lower limit is normally associated to oxy-fuel technologies [24]. This is also the increase of total revenue that must be fulfilled to pay for CCS operations while keeping the same NPV of the Base-Case without CCS; otherwise, the NPV would become negative in 647 MMUSD, considering the steam value of 11.3 USD/t. Fig. 4.11 shows the composition of the total revenue destination for the Base-Case with CCS. The main difference from the Base-Case without CCS (Fig. 4.10) is the increase in the Specific ROI composition (18.1% to 28.3%) to achieve the $MARR$, due to a higher FCI ($FCI^{CHP}+FCI^{CCS}$), resulting in higher COM as well.
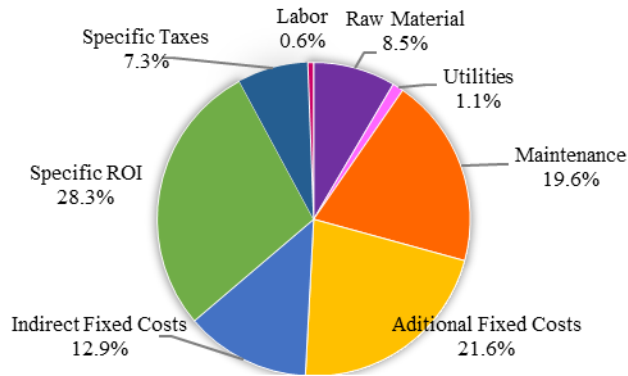
Fig. 4.11. Revenue destination: Base-Case with CCS.

Sensitivity analyses were performed for the CC of the Base-Case with CCS by means of $\pm50\%$ variations on the following items: FCI^{CHP}, CO_2 revenues (cap-and-trade and CO_2-to-EOR), OT, electricity price and bagasse capacity without CCS – 138 t/h in the Base-Case without CCS, even if extra bagasse is required to perform CCS, since this is an input to SBAF model and the total bagasse is adjusted to give the same power output. To perform the sensitivity analysis, the following procedure is used: (i) run SBAF without CCS at the new perturbed condition (ignoring changes in FCI^{CHP} or in CO_2 revenue, if they are the perturbed factors); (ii) evaluate and record the Total-Steam MSP; (iii) run SBAF for the new perturbed condition with CCS and adjust X to achieve the same power output; (iv) estimate the new MSP; (v) evaluate CC; (vi) repeat for all perturbed conditions.

Results of sensitivity analyses are shown in Fig. 4.12. CHP with CCS is only economically advantageous in the event of carbon taxation (40-80 USD/tCO$_2$ [6]) under extreme conditions (as in a total FCI lower than 240 MMUSD) resulting in $CC=50\ USD/tCO_2$. CC has a low sensitivity to CO_2 revenues of 3.3 USD/tCO$_2$ for each MMUSD/a increased; i.e., for a 100% increase of CO_2 revenues, other factors unchanged, CC would still be 141 USD/tCO$_2$. OT and bagasse capacity can also contribute to feasibility: a 50% increase in bagasse capacity reduces CC to 179.4 USD/tCO$_2$, while reaching 139.7 USD/t for 50% OT increase. CC is insensitive to electricity price because Total-Steam MSP changes to counterbalance electricity price changes, maintaining total revenue constant.
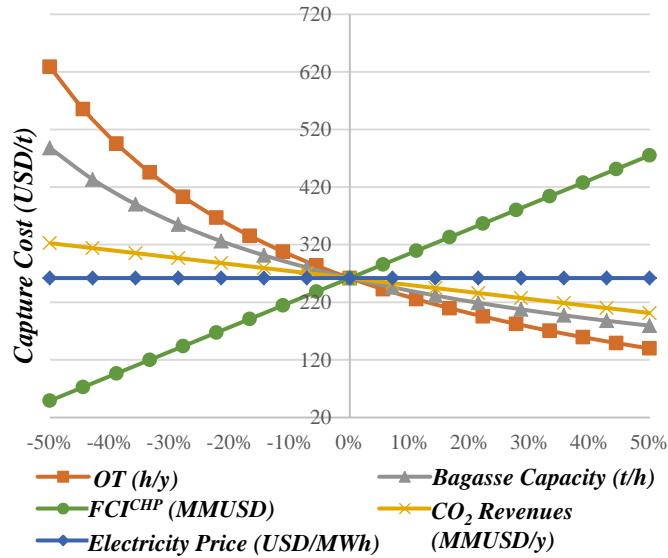
Fig. 4.12. Base-Case with CCCS: Capture Cost sensitivity to changes in FCI^{CHP}, CO_2 revenues, bagasse capacity without CCS, electricity price and OT.

A combination of changes of -20% in FCI^{CHP}, +25% in CO_2 revenue, +20% in OT and +50% in bagasse capacity – all of them plausible changes in the short-term – result in $CC = 78.5 USD/tCO_2$ starting to be more advantageous than a taxation of 80 USD/tCO₂. However, the actual case is far from feasible and capturing only CO_2 from the fermentation step should be considered first as a BECCS option. Moreover, considering 378.8 t/h of CO_2 capture and $OT=8000$ h/a (i.e., like any conventional power plant), CC becomes only 17.2 USD/tCO₂. This shows that the main drawback of the sugarcane-biorefinery enterprise is its low agricultural-based capacity and the consequent low OT, resulting in a high downtime of an expensive BECCS plant.

4.4. Conclusions for Capter 4

This work analyzed investments in CHP units to supply heat and power to typical Brazilian sugarcane-biorefineries with/without CCS. A robust Sugarcane-Biorefinery Analyzer Framework (SBAF) was developed to assist in sugarcane-biorefinery BECCS decision making. SBAF solves CHP/CCS mass-energy balances, simultaneously estimating net electricity exportation, CO_2 emissions, CO_2 revenues, besides COM^{CHP} and COM^{CCS} together with surface response models for FCI^{CHP} and FCI^{CCS}. With SBAF it is possible to predict FCI^{CHP}, FCI^{CCS}, COM^{CHP} and COM^{CCS} of both scenarios (with or without CCS) in a simple way, regarding only bagasse availability and LPS/MPS requirements. The average errors of FCI^{CHP} and FCI^{CCS} models against the observed values were 1.9% and 1.3% with correlation coefficients of 0.996 and 0.991, respectively. When SBAF is used to calculate the

requirements of a typical ethanol/sugar sugarcane-biorefinery with electricity surplus, its results are compatible with the Brazilian auctions and with literature data.

The CHP capacity in terms of bagasse consumption is the most important input factor in FCI^{CHP}, followed by the SHPS percentage (Y) converted into MPS/LPS, while the less important factor is the SHPS percentage converted into MPS and bleed-steam. The decision to invest in a BECCS sugarcane-biorefinery, under constant electricity exportation, can increase FCI^{CHP} as high as 34%, while also similarly increasing COM^{CHP} fueled by its dependency on FCI^{CHP}, which responds for more than 40% of COM^{CHP}. The FCI^{CCS}, by its turn, has the pipeline investment as its biggest burden, which accounts for more than 50% of FCI^{CCS}, while FCI^{CCS} is, at least, 4 times higher than FCI^{CHP} without CCS. These values evince a certain lack of viability, due to a considerable increase in investment and costs, but deprived of a proper revenue increase from the captured CO_2 due to its low commercial value of at most 100 USD/tCO_2. Therefore, BECCS is not yet feasible.

The CC of the Base-Case with CCS is estimated as 262 USD/tCO_2, within the literature range 88-288 USD/tCO_2. Sensitivity analyses were performed and almost all perturbed scenarios resulted in CC within the literature range. Such analyses show that CC can drop to 50 USD/tCO_2 if $FCI^{CH}+FCI^{CCS}$ reduce by 50%, the most sensible factor. A further combination of factor changes can reduce CC to less than 80 USD/tCO_2. Moreover, assuming OT and capture capacity typical of conventional power plants leads to CC of only 17.2 USD/tCO_2, showing that they represent the biggest challenges for BECCS sugarcane-biorefineries.

4.5. References for Chapter 4

[1]   Capuano DL. International Energy Outlook 2020 (IEO2020) 2019:7.
[2]   Raj NT, Iniyan S, Goic R. A review of renewable energy based cogeneration technologies. Renew Sustain Energy Rev 2011;15:3640–8. https://doi.org/10.1016/j.rser.2011.06.003.
[3]   Eksi G, Karaosmanoglu F. Combined bioheat and biopower: A technology review and an assessment for Turkey. Renew Sustain Energy Rev 2017;73:1313–32. https://doi.org/10.1016/j.rser.2017.01.093.
[4]   Veiga JPS, Malik A, Lenzen M, Ferreira Filho JB de S, Romanelli TL. Triple-bottom-line assessment of São Paulo state's sugarcane production based on a Brazilian multi-regional input-output matrix. Renew Sustain Energy Rev 2018;82:666–80. https://doi.org/10.1016/j.rser.2017.09.075.
[5]   Brizi F, Silveira JL, Desideri U, Reis JA dos, Tuna CE, Lamas W de Q. Energetic and economic analysis of a Brazilian compact cogeneration system: Comparison between natural gas and biogas. Renew Sustain Energy Rev 2014;38:193–211. https://doi.org/10.1016/j.rser.2014.05.088.

[6]   Carminati HB, Milão R de FD, de Medeiros JL, Araújo O de QF. Bioenergy and full carbon dioxide sinking in sugarcane-biorefinery with post-combustion capture and storage: Techno-economic feasibility. Appl Energy 2019;254:113633. https://doi.org/10.1016/j.apenergy.2019.113633.

[7]   Riveras I. Brazil ethanol production could be more efficient. Reuters 2007.

[8]   Dantas GA, Legey LFL, Mazzone A. Energy from sugarcane bagasse in Brazil: An assessment of the productivity and cost of different technological routes. Renew Sustain Energy Rev 2013;21:356–64. https://doi.org/10.1016/j.rser.2012.11.080.

[9]   Dias MOS, Junqueira TL, Jesus CDF, Rossell CEV, Maciel Filho R, Bonomi A. Improving second generation ethanol production through optimization of first generation production process from sugarcane. Energy 2012;43:246–52. https://doi.org/10.1016/j.energy.2012.04.034.

[10]   Arshad M, Ahmed S. Cogeneration through bagasse: A renewable strategy to meet the future energy needs. Renew Sustain Energy Rev 2016;54:732–7. https://doi.org/10.1016/j.rser.2015.10.145.

[11]   Malico I, Nepomuceno Pereira R, Gonçalves AC, Sousa AMO. Current status and future perspectives for energy production from solid biomass in the European industry. Renew Sustain Energy Rev 2019;112:960–77. https://doi.org/10.1016/j.rser.2019.06.022.

[12]   Tataraki KG, Kavvadias KC, Maroulis ZB. A systematic approach to evaluate the economic viability of Combined Cooling Heating and Power systems over conventional technologies. Energy 2018;148:283–95. https://doi.org/10.1016/j.energy.2018.01.107.

[13]   Papadimitriou A, Vassiliou V, Tataraki K, Giannini E, Maroulis Z. Economic Assessment of Cogeneration Systems in Operation. Energies 2020;13:2206. https://doi.org/10.3390/en13092206.

[14]   Ngan SL, How BS, Teng SY, Leong WD, Loy ACM, Yatim P, et al. A hybrid approach to prioritize risk mitigation strategies for biomass polygeneration systems. Renew Sustain Energy Rev 2020;121:109679. https://doi.org/10.1016/j.rser.2019.109679.

[15]   Hugot E. Handbook of Cane Sugar Engineering. Elsevier; 2014.

[16]   Alcaráz-Calderon AM, González-Díaz MO, Mendez Á, González-Santaló JM, González-Díaz A. Natural gas combined cycle with exhaust gas recirculation and CO_2 capture at part-load operation. J Energy Inst 2019;92:370–81. https://doi.org/10.1016/j.joei.2017.12.007.

[17]   Wiesberg IL, Brigagão GV, Araújo O de QF, de Medeiros JL. Carbon dioxide management via exergy-based sustainability assessment: Carbon Capture and Storage versus conversion to methanol. Renew Sustain Energy Rev 2019;112:720–32. https://doi.org/10.1016/j.rser.2019.06.032.

[18]   Vinca A, Rottoli M, Marangoni G, Tavoni M. The role of carbon capture and storage electricity in attaining 1.5 and 2 °C. Int J Greenh Gas Control 2018;78:148–59. https://doi.org/10.1016/j.ijggc.2018.07.020.

[19]   Gibon T, Arvesen A, Hertwich EG. Life cycle assessment demonstrates environmental co-benefits and trade-offs of low-carbon electricity supply options. Renew Sustain Energy Rev 2017;76:1283–90. https://doi.org/10.1016/j.rser.2017.03.078.

[20]   Milão R de FD, Araújo O de QF, de Medeiros JL. Second Law analysis of large-scale sugarcane-ethanol biorefineries with alternative distillation schemes: Bioenergy carbon capture scenario. Renew Sustain Energy Rev 2021;135:110181. https://doi.org/10.1016/j.rser.2020.110181.

[21]   Guest G, Bright RM, Cherubini F, Michelsen O, Strømman AH. Life Cycle Assessment of Biomass-based Combined Heat and Power Plants. J Ind Ecol 2011;15:908–21. https://doi.org/10.1111/j.1530-9290.2011.00375.x.

[22] Morales-Mora MA, Pretelìn-Vergara CF, Martínez-Delgadillo SA, Iuga C, Nolasco-Hipolito C. Environmental assessment of a combined heat and power plant configuration proposal with post-combustion CO_2 capture for the Mexican oil and gas industry. Clean Technol Environ Policy 2019;21:213–26. https://doi.org/10.1007/s10098-018-1630-3.

[23] Facilities - Global CCS Institute 2020. https://co2re.co/FacilityData (accessed December 15, 2020).

[24] Fuss S, Lamb WF, Callaghan MW, Hilaire J, Creutzig F, Amann T, et al. Negative emissions—Part 2: Costs, potentials and side effects. Environ Res Lett 2018;13:063002. https://doi.org/10.1088/1748-9326/aabf9f.

[25] Milão R de FD, Carminati HB, Araújo O de QF, de Medeiros JL. Thermodynamic, financial and resource assessments of a large-scale sugarcane-biorefinery: Prelude of full bioenergy carbon capture and storage scenario. Renew Sustain Energy Rev 2019;113:109251. https://doi.org/10.1016/j.rser.2019.109251.

[26] Laude A, Ricci O, Bureau G, Royer-Adnot J, Fabbri A. CO_2 capture and storage from a bioethanol plant: Carbon and energy footprint and economic assessment. Int J Greenh Gas Control 2011;5:1220–31. https://doi.org/10.1016/j.ijggc.2011.06.004.

[27] de Souza CC, Leandro JP, dos Reis Neto JF, Frainer DM, Castelão RA. Cogeneration of electricity in sugar-alcohol plant: Perspectives and viability. Renew Sustain Energy Rev 2018;91:832–7. https://doi.org/10.1016/j.rser.2018.04.047.

[28] Guandalini G, Romano MC, Ho M, Wiley D, Rubin ES, Abanades JC. A sequential approach for the economic evaluation of new CO_2 capture technologies for power plants. Int J Greenh Gas Control 2019;84:219–31. https://doi.org/10.1016/j.ijggc.2019.03.006.

[29] Pina EA, Palacios-Bereche R, Chavez-Rodriguez MF, Ensinas AV, Modesto M, Nebra SA. Reduction of process steam demand and water-usage through heat integration in sugar and ethanol production from sugarcane – Evaluation of different plant configurations. Energy 2017;138:1263–80. https://doi.org/10.1016/j.energy.2015.06.054.

[30] Rossetti I, Tripodi A, Ramis G. Hydrogen, ethylene and power production from bioethanol: Ready for the renewable market? Int J Hydrog Energy 2020;45:10292–303. https://doi.org/10.1016/j.ijhydene.2019.07.201.

[31] Turton R. Analysis, Synthesis, and Design of Chemical Processes. Prentice Hall; 2003.

[32] Saidur R, Abdelaziz EA, Demirbas A, Hossain MS, Mekhilef S. A review on biomass as a fuel for boilers. Renew Sustain Energy Rev 2011;15:2262–89. https://doi.org/10.1016/j.rser.2011.02.015.

[33] Dias MOS, Junqueira TL, Cavalett O, Cunha MP, Jesus CDF, Mantelatto PE, et al. Cogeneration in integrated first and second generation ethanol from sugarcane. Chem Eng Res Des 2013;91:1411–7. https://doi.org/10.1016/j.cherd.2013.05.009.

[34] Ciferno J. Carbon dioxide capture from existing coal-fired power plants 2020. https://www.sciencebase.gov/catalog/item/5140ac5ae4b089809dbf53bb (accessed December 13, 2020).

[35] Process Plant Location Factors, Intratec Solutions, https://www.intratec.us/user/products/process-plant-location-factors (accessed December 10, 2020).

[36] Brigagão GV, Wiesberg IL, Pinto JL, Araújo O de QF, de Medeiros JL. Upstream and downstream processing of microalgal biogas: Emissions, energy and economic performances under carbon taxation. Renew Sustain Energy Rev 2019;112:508–20. https://doi.org/10.1016/j.rser.2019.06.009.

[37] Brazil laying foundations for exploration revival. Offshore 2018. https://www.offshore-mag.com/regional-reports/article/16762057/brazil-laying-foundations-for-exploration-revival (accessed December 1, 2020).

[38] Zoelle A, Keairns D, Pinkerton LL, Turner MJ, Woods M, Kuehn N, et al. Cost and Performance Baseline for Fossil Energy Plants Volume 1a: Bituminous Coal (PC) and Natural Gas to Electricity Revision 3. NETL; 2015. https://doi.org/10.2172/1480987.

[39] Quanto custa o bagaço? Confira aqui [Portuguese]. JornalCana 2019. https://jornalcana.com.br/quanto-custa-o-bagaco-confira-aqui/ (accessed December 3, 2020).

[40] Resultado de Leilões - ANEEL 2020. https://www.aneel.gov.br/resultados-de-leiloes (accessed December 3, 2020).

[41] Albuquerque B, Pereira MFD, Barros R, Isfer RB, de Oliveira AV, Ferreira TVB, et al. Governo Federal Ministério de Minas e Energia MME/SPE n.d.:39.

[42] Process Cost Plant Indexes, Intratec Solutions, https://www.intratec.us/user/products/process-plant-cost-indexes (accessed December 10, 2020).

[43] Birru E, Erlich C, Martin A. Energy performance comparisons and enhancements in the sugar cane industry. Biomass Convers Biorefinery 2019;9:267–82. https://doi.org/10.1007/s13399-018-0349-z.

5. UPGRADING EXERGY UTILIZATION AND SUSTAINABILITY VIA SUPERSONIC SEPARATORS: OFFSHORE PROCESSING OF CARBONATED NATURAL GAS

This chapter is published as an article in Journal of Cleaner Production

Abstract

Offshore processing of natural gas with 44%mol carbon dioxide at remote deep-water oil-and-gas fields is invariably characterized by low-efficiency power generation via gas-fired turbines releasing hot flue-gas and entailing high degradation of resources, high carbon emissions and low sustainability. This work demonstrates how to upgrade exergy utilization and consequently process sustainability by using supersonic separators in some gas processing steps; namely: (i) water dew-point adjustment; (ii) hydrocarbon dew-point adjustment; and (iii) carbon dioxide abatement to 20%mol. To accomplish this, the exergy performance of two supersonic separator gas processing alternatives are compared with conventional gas processing comprising triethylene-glycol absorption for water dew-point adjustment, Joule-Thomson expansion hydrocarbon dew-point adjustment and membrane-permeation carbon dioxide removal. Since exergy is measured relatively to a reference environmental reservoir, two such reference reservoirs are used: RER-1: standard atmosphere with 2%mol water containing hydrocarbons at combustion chemical equilibrium with air species; and RER-2: 1atm water-saturated raw natural gas in equilibrium with liquid water. Aspen-HYSYS simulations are used to solve mass/energy balances and thermodynamic property calculations. With RER-2 the conventional gas processing conserves 63.3% of the inlet exergy, while the two alternative supersonic separator processes attain 66.5% and 72.4% of exergy conservation, proving the associate gains of exergy efficiency and sustainability.

Keywords

Exergy Analysis; Natural Gas Conditioning; Supersonic Separator; CO2-rich Natural Gas; Exergy Sustainability.

Abbreviations

CO$_2$ Carbon Dioxide; C3+ Propane and Heavier Hydrocarbons; CW Cooling-Water; EOR Enhanced Oil Recovery; GT Gas-Turbine; HCDPA Hydrocarbon Dew-Point Adjustment; JT Joule-Thomson; LTX Low-Temperature Separator; MP Membrane-Permeation; NG Natural Gas; NGL Natural Gas Liquids; PHW Pressurized-Hot-Water; RER Reference Environment Reservoir; SS Supersonic Separator; TEG Triethylene–glycol; WDPA Water Dew-Point Adjustment.

Nomenclature

$\dot{B}$	*Exergy flowrate (MW)*
F_j	*j^{th} feed flowrate (kmol/s)*
D	*Diameter (m)*
$\bar{H}$	*Molar enthalpy (MJ/kmol)*
K_j	*j^{th} product flowrate (kmol/s)*
nc, nfs, nps	*Numbers of components/feeds/products*
nwi, nwe	*Numbers of imported/exported powers*
Ma	*Mach Number*
P	*Pressure (bar)*
R	*Ideal gas constant R=8.314*10^{-5}bar.m^3/mol.K*
$\bar{S}$	*Molar entropy (MJ/kmol.K)*
T	*Temperature (K)*
$\dot{W}$	*Shaft-Power (MW)*
y	*Molar fraction*

Greek Symbols

α,β	*SS converging and diverging wall angles (degrees)*
μ$_k$	*Chemical potential of kth species (MJ/kmol)*
η, ϵ	*Exergy and adiabatic efficiencies*
$\dot{\Omega}_S$	*Entropy creation rate (MW/K)*

Superscripts, Subscripts

0	*Reference state*
EXP, CMP	*Expansion, Compression*
in, in.total	*Inlet, Total Inlet*
out, out.total	*Outlet, Total Outlet*
$\dot{M}$	*Rate of property M (M/s)*
Shock	*Just-before-normal-shock-and-condensate-withdrawal*

5.1. Introduction

Natural Gas (NG) is the fossil fuel that is expected to have the highest rise until 2050 of 1.1% per year, while the share of petroleum-based liquid fuels, the most used source of energy, should fall (EIA, 2019). The high competitiveness of NG is supported by its abundant resources and increasing production (EIA, 2017), some still in the early stage of development and production, as NG hydrate (Chong et al., 2016) and associated gas in Brazilian Pre-Salt deep-water fields. Moreover, the advantage of the NG expansion is that it has the lowest ratio of carbon dioxide (CO_2) emission per generated energy among the fossil fuels (EIA, 2016), resulting in the cleanest combustion. Since NG will still play a significant role in this century, it is of central importance to increase the efficiency of its exploration and production, especially at new remote offshore fields which are invariably characterized by low-efficiency power generation via gas-fired turbines releasing hot flue-gas and entailing high degradation of resources, high carbon emissions and low sustainability. This is crucial because oil-and-gas offshore rigs operate with significant environmental impact, emitting CO_2 and CH_4 from on-site power generation, flare systems and processing facilities. Besides, these effects are even more impacting at platform end-life conditions (Nguyen et al., 2014). Thus, new offshore processing configurations must be developed for better utilization of resources in order to satisfy the growing NG demand and global sustainability needs.

5.1.1. Offshore Conditioning of CO_2-Rich Natural Gas

Besides the global NG expansion, the exploration and production of offshore oil-and-gas fields with high gas-to-oil ratio and high CO_2 content is increasing substantially, in spite of its lower methane content that imposes several technical issues for its utilization and conditioning. This is the case of Brazilian Pre-Salt deep-water oil-and-gas fields, characterized by CO_2 contents as high as 79%mol and gas-to-oil ratios around 20,000 scf/bbl (Gaffney et al., 2010). Besides the harder exploitation of deep-water fields, the treatment of this type of raw NG is also complex due to the high number of required units for its conditioning, together with the limitations of area and weight in deep-water offshore rigs (Pinto et al., 2014). A typical offshore platform in Gulf of Mexico or North Sea fields requires only Water Dew-Point Adjustment (WDPA) because of the high-quality NG, and the rest of the conditioning process can be performed onshore (Botham, 2005). WDPA is mandatory to prevent corrosion and hydrates formation, which makes water the most undesirable NG contaminant (Santos et al., 2017). In a highly carbonated NG, however, the

WDPA is even more crucial due to higher corrosion issues and CO_2 hydrates (Gandhidasan et al., 2001).

The biggest challenge for offshore processing of highly carbonated NG, however, is to proper allocate the CO_2, avoiding emission to atmosphere. This is a recent issue; not long ago, the gas would be fully burned in giant flares emitting indescribable amounts of CO_2 to the atmosphere, since there was total prioritization to oil production in offshore oil-and-gas enterprises (Araújo et al., 2017).

Treating highly carbonated NG at offshore rigs requires huge CO_2 removal units, but has the advantage of maintaining the reservoir pressure if the captured CO_2 is reinjected, a destination known as Enhanced Oil Recovery (EOR). Performing EOR in the early stage of the exploitation has significant economic benefits, including more economically viable oil recovery and accelerated opportunities for CO_2 storage (Malone et al., 2014). In the Pre-Salt fields, CO_2-rich NG conditioning comprises WDPA, seconded by HCDPA for propane and heavier alkanes ($C3^+$) removal and finally CO_2 removal (de Melo et al., 2019). Henceforth, offshore CO_2-rich NG conditioning is structured as WDPA+HCDPA+CO_2 removal, and the denomination of the process at hand results from replacing each processing step by the name of the technology performing it (e.g., TEG+JT+MP, wherein the abbreviations stand for triethylene-glycol absorption WDPA, Joule-Thomson expansion HCDPA and membrane-permeation CO_2 removal), except when a single unit can perform both WDPA and HCDPA.

5.1.2. Supersonic Separator and Energy Efficiency of Offshore Gas-and-Oil Rigs

Diverse ways to increase the efficiency of oil-and-gas offshore platforms are analyzed in the literature, including deep-water utilization as primary cooling (Cruz et al., 2018) and electric integration of the platform to the onshore grid (Nguyen et al., 2016). The power production from hot flue-gas in the gas-turbine area, with a Waste Heat Recovery Unit, can be also optimized via multi-objective formulations considering air bottoming cycle (Pierobon and Haglind, 2014), organic cycle (Pierobon et al., 2013) and steam bottoming cycle (Nguyen et al., 2014) configurations. The optimization of the gas-turbine area results in fuel-gas savings, consequently, increasing NG exportation.

The supersonic separator (SS) is a novel technology for removal of heavy species from a gas stream via condensation and swirling promoted within a supersonic flow. SS consists of a converging-diverging Laval nozzle, a liquid collector and an ending-diffuser. Its advantages

over the Joule-Thomson expansion valve comprise its nearly isentropic Laval expansion and the pressure-recovery promoted by the normal shock and the subsequent ending-diffuser reducing the head-loss and lowering the power demand; i.e., pressure drop is the driving-force for the separation (Yang et al., 2014). The Laval expansion generates a deep temperature drop, condensing heavy species as a mist that is directed to the walls by the centrifugal field and caught in the liquid collector. Brigagão et al. (2020) performed exergy analysis of a new air pre-purification unit with a low-pressure SS and found that SS utilization cuts 70% of the exergy destruction of the conventional process.

SS for NG processing including CO_2 removal and/or simultaneous WDPA/HCDPA is well documented in the literature. Alfyorov et al. (2005) affirms that SS NG processing requires 10%-20% less compressor power and gives better $C3^+$ recovery than the JT valve counterpart. Moreover, the investment return benefits of a SS performing WDPA/HCDPA were already demonstrated for ordinary NG (Machado et al., 2012) and for CO_2-rich NG (Arinelli et al., 2017). Arinelli et al. (2017) also successfully reported CO_2 removal performed by SS wherein the CO_2 content of a CO_2-rich NG was reduced from 44%mol to 21.85%mol, entailing lower compression power when compared to Membrane-Permeation (MP) units executing the same service. This occurs due to the replacement of CO_2 compressors by CO_2 pump for the SS liquid condensate, and to the pressure-recovery of the treated gas in the SS.

In the conventional offshore processing of CO_2-rich NG, CO_2 is removed via MP and the WDPA and HCDPA are performed via Triethylene-glycol (TEG) absorption and Joule-Thomson (JT) expansion, respectively – the so-called TEG+JT+MP route. The use of a SS unit for simultaneous WDPA/HCDPA creates the so-called SS+MP route; and the use of another SS for CO_2 removal – the so-called SS+SS route – have also been studied for CO_2-rich NG conditioning (Arinelli et al., 2019). Arinelli et al. (2019) claim that the SS+SS process has better technical, environmental and economic performances for CO_2-rich NG conditioning when compared to TEG+JT+MP and to SS+MP analogous configurations. Moreover, Melo et al. (2019) analyzed the SS+SS alternative against a conventional route prescribing molecular sieve (MS) for WDPA – the so-called MS+JT+MP configuration – for ultra-rich CO_2 NG. It was found that the SS+SS route has a net present value 33% higher with a 10% lower fixed capital investment. Araújo et al. (2017) compared the sustainability of NG conditioning alternatives of a CO_2-rich NG by means of energy, economic and

footprint metrics. The authors support that CO_2 removal using Chemical-Absorption with methyl-diethanolamine and piperazine has the best performance on technical, economic, environmental and footprint grounds, but did not analyze any SS-based configuration.

5.1.3. Exergy Analysis of Offshore Gas-and-Oil Rigs

The literature has studies on Exergy Analysis of offshore oil-and-gas platforms aiming at performance investigation and optimization. The exergy flowrate is a thermodynamic property that represents the maximum power obtainable by a stream, when it reaches the equilibrium with a given reference environment reservoir (RER). In this context, there is the perception that compressors represent the lion share of all exergy destroyed in offshore gas conditioning (Voldsund et al., 2014). When the entire offshore rig is considered, combustors in the power generation area and the production manifold are also important exergy sinks (Nguyen et al., 2013). Exergy analysis of a typical offshore platform was also performed throughout the project-life time, with the conclusion that the compression system efficiency is even lower at the final stages of the campaign, due to recirculation of compressed gas as anti-surge strategy (Gallo et al., 2017).

Given that the RER for exergy analysis is arbitrarily chosen, a bad selection can mask the inefficiency of unit operations by inflating the exergy flowrate of inlet/outlet streams (Teixeira et al., 2016). Therefore, it is of good practice to use at least two different RERs in exergy analyses to avoid blind spots (Brigagão et al., 2020). Exergy analysis of a North Sea platform executing WDPA unveiled that only 0.5-1.5% of the exergy flowrate was destructed (Nguyen et al., 2013), probably evincing a bad RER selection. Consequently, it is a common practice to define variations of the exergy efficiency (η) to overcome this inflation. Baccanelli et al. (2016) used the functional efficiency in dual-pressure distillation columns for CO_2 removal from a CO_2-rich NG and found an efficiency of 56.52%, against 99.04% for η. Ghannadzadeh et al. (2012) used the rational exergy efficiency in NG treatment to uncover equipment irreversibility, while η attained values above 99.44% in most units. Furthermore, it is usual to perform exergy analysis with reference tables of pure substances to emulate the RER (Szargut, 1989). This approach should be avoided due to inconsistences in its formulation that could even give negative exergy flowrates (Gaudreau et al., 2012).

5.1.4. The Present Work

Besides techno-economic and environmental analyses of offshore CO_2-rich NG processing, exergy analysis is necessary to evaluate efficiency gains promoted by the SS+SS alternative compared to the SS-MP and conventional routes. This is a subject still unexplored in the SS and NG literatures. To the authors knowledge, this work is the first to perform complete exergy analysis of offshore conditioning of CO_2-rich NG ($\approx 45\%$ mol CO_2) to compare the conventional and the SS-based processing configurations. The efficiency impacts of NG processing in the gas-turbines for power production are also analyzed. Moreover, counterpointing the tendency of stipulating ad hoc empirical exergy efficiency metrics, this work adopts the original and thermodynamically ballasted strategy of selecting the appropriate RER that best discriminates unit inefficiencies. The exergy results allow constructing Sankey diagrams of exergy flows throughout the system in order to prove that SS+SS gas processing has the best exergy conservation and highest exergy efficiency. Fig. 5.1 sketches the analyzed configurations – TEG+JT+MP, SS+MP, SS+SS. In SS+SS the 1st SS unit (SS-1) performs WDPA/HCDPA, replacing TEG+JT units of a conventional rig, while the 2nd SS unit (SS-2) removes CO_2 from NG, replacing the MP unit.
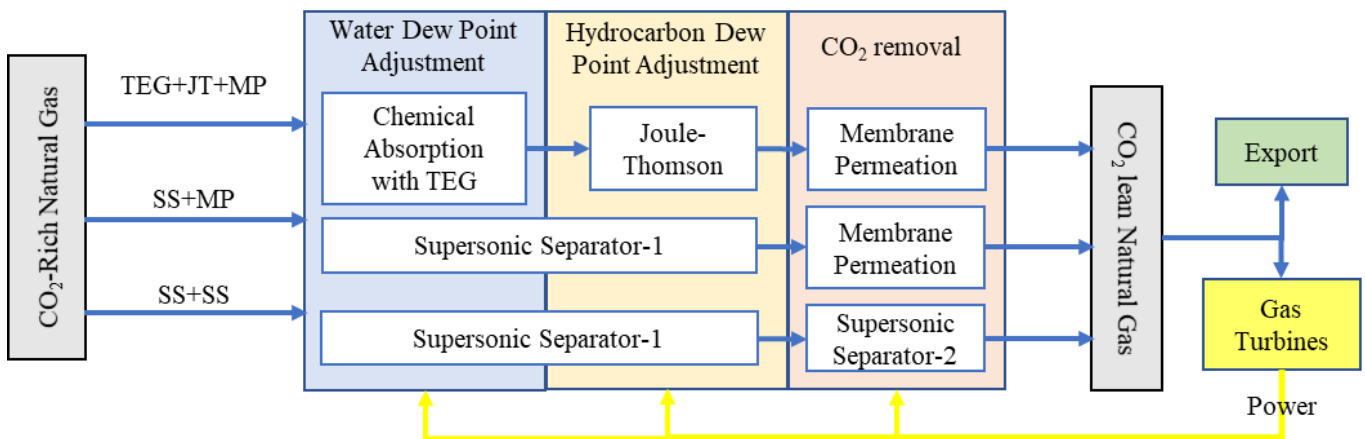
Fig. 5.1. Offshore processing routes for CO_2-rich NG: TEG+JT+MP, SS+MP, SS+SS.

5.2. Methods

Aspen-HYSYS® process simulation solves mass/energy balances providing the thermodynamic properties to evaluate exergy flows allowing performing exergy analysis of units and the overall process. HYSYS implementation of the Peng-Robinson Equation-of-State (PR-EOS) is used in the whole process, excepting in the TEG dehydration unit, which uses the HYSYS glycol-package as thermodynamic model.

Since MP and SS are not present in HYSYS as operation units, the respective simulations and designs are performed with MP-UOE and SS-UOE unit operation extensions previously developed (Arinelli et al., 2017). SS-UOE uses rigorous multiphase sound speed via multiphase-equilibrium provided by another HYSYS unit operation extension PEC-UOE (de Medeiros et al., 2017). The inputs for SS-UOE are the maximum Mach number attained at the Laval end (Ma^{Shock}) and SS parameters: inlet and outlet diameters (D_I, D_O), converging and diverging wall angles (α, β), and the adiabatic efficiencies of SS expansion and compression steps ($\eta_{EXP}\%, \eta_{CMP}\%$). The SS feed stream must be defined at equilibrium stagnated conditions in the simulation. The MP-UOE inputs are the retentate and permeate outlet pressures, MP area and feed temperature, pressure and composition. MP permeances for CO_2-rich NG were calibrated using real MP operation data (Arinelli et al., 2017). The differences of fugacities between retentate and permeate are the MP driving forces for all components.

Data manipulation for exergy analysis is performed with Microsoft Excel and only basic data of the streams – i.e., molar enthalpy, entropy and component flows – are required. There is no need for third-party software or reference exergy tables.

5.2.1. Process description

The offshore processing produces NG with WDP<-45ºC (1.01 bar), HCDP<0ºC (45bar) and $CO_2 \approx 20\%$mol, sufficient to be used as fuel in the Gas-Turbine (GT) area (Arinelli et al., 2017) and for exportation to land facilities. The CO_2 in the raw NG is $\approx 44\%$mol and the removed CO_2 is injected in the reservoir for EOR. Fig. 5.2 depicts the gas processing flowsheets for all three configurations (TEG+JT+MP, SS+SS and SS+MP).

In TEG+JT+MP 11.3MMSm³/d of water-saturated NG (Stream 1) at 40°C is compressed from 25 to 65 bar prior to WDPA with TEG absorption (Tower **T1**). The raw gas composition (%mol) is: CH_4=49.82%, C_2H_6=2.989%, C_3H_8=1.993%, iC_4H_{10}=0.2989%, C_4H_{10}=0.1993%, iC_5H_{10}=0.1993%, nC_5H_{12}=0.09964%, C_6H_{14}=0.09964%, C_7H_{16}=0.04982%, C_8H_{18}=0.02989%, C_9H_{20}=0.009964%, $C_{10}H_{22}$=0.009964%, H_2O=0.36%, CO_2=43.84%. TEG is regenerated (T2) and recirculated to the absorber after make-up (stream 8), while the dry-gas (stream 7) is sent to HCDPA through JT expansion, condensing C3+ and producing NG liquids NGL (stream 22). NG conditioning is completed via MP CO_2 removal to 20%mol in the final NG. The captured CO_2 and the decarbonated NG are

compressed in 4-staged and in 2-staged compression trains (K2 and K3) to 450bar and 200bar, respectively, generating product streams 25 and 26.
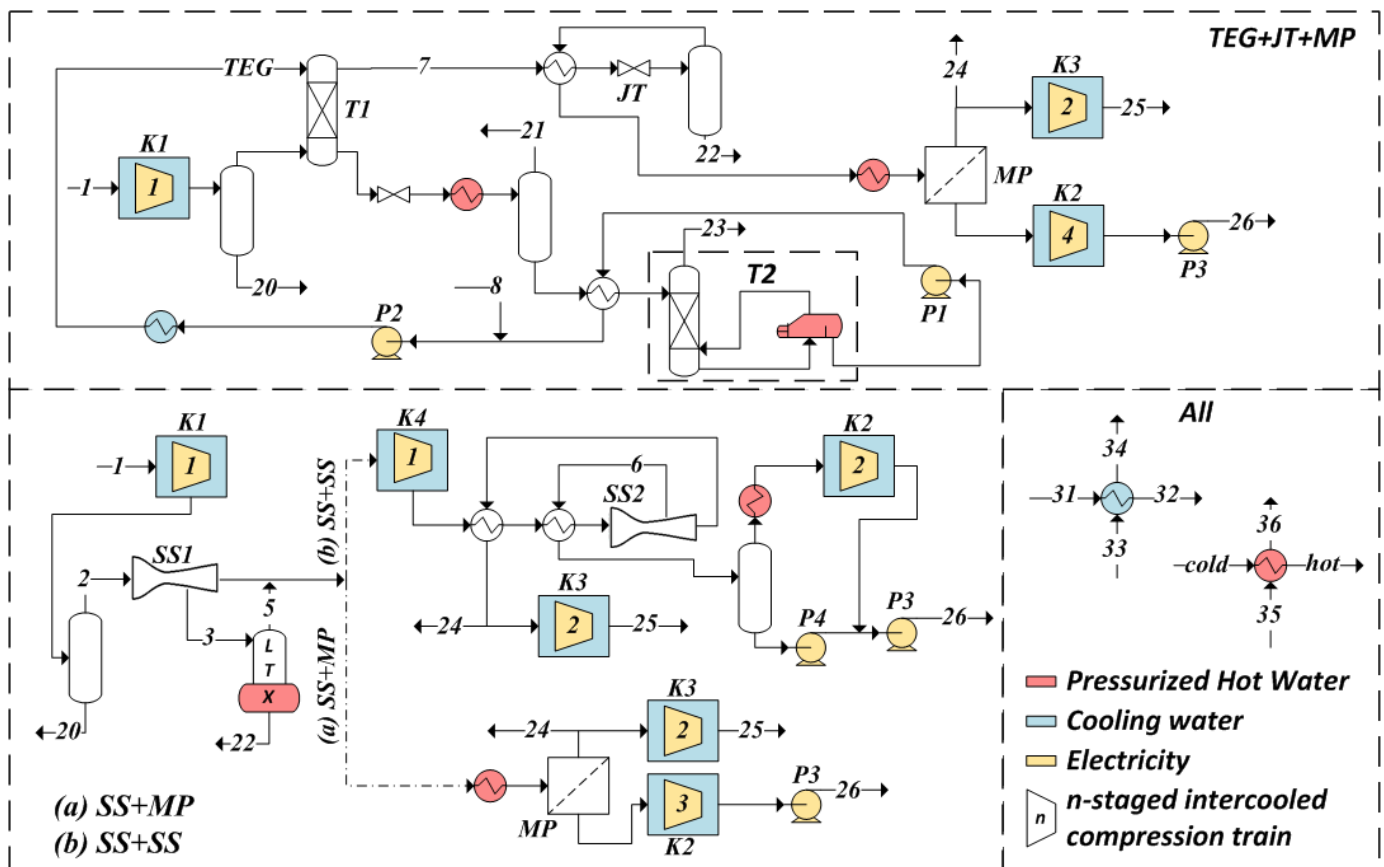
Fig. 5.2. TEG+JT+MP, SS+MP and SS+SS flowsheets for offshore processing of CO$_2$-rich NG.

The first step of SS+MP and SS+SS is the same compression of raw NG to 50 bar (stream 2) prior to performing WDPA/HCDPA in 6 paralleled SS units (SS1), producing a two-phase condensate (stream 3) with water and C3+ hydrocarbons. A heated Low-Temperature Separator (LTX) receives the ejected condensate at 1°C to prevent gas-hydrate formation. The LTX produces water and NGL as bottoms at 20°C and a top slip-gas which is added to the SS1 lean gas. The second half of SS+MP is identical to the MP part of TEG+JT+MP.

In SS+SS the treated gas from SS1 is compressed to 85bar and feeds a second battery of 6 paralleled SS units (SS2) wherein CO$_2$ is removed as condensate (stream 6). CO$_2$ removal in SS+SS is limited by the minimum temperature to avoid CO$_2$ freeze-out inside SS2, which is defined by the chosen Ma^{Shock}. The exported CO$_2$ stream and the treated NG are compressed in two separated 2-staged compression trains (K3 and K4).

126

The cooling-water (CW) circuit in all configurations uses seawater at 25ºC (stream 33) to cool down the hot CW (stream 31) from 45°C to 30°C (stream 32), producing a seawater effluent at 35ºC (stream 34). Pressurized-Hot-Water (PHW, stream 35) is generated in the gas-turbine area at 210°C with GT hot flue-gas and used as heating utility, cooling down to 150°C in the process (stream 36) and returning to the GT area.

A fraction of the treated NG (stream 24) becomes fuel-gas (FG) to the GT area to power the platform in all configurations, as shown in Fig. 5.3. Atmospheric air (stream 41) is compressed and feeds the combustor (R1) with fuel-gas (stream 24). Hot combustion gases pass through the GT expander generating shaft-power to drive the electric generator. The expanded gas is the low-pressure hot flue-gas (stream 42) that heats the required PHW flowrate (stream 36). The resulting, still hot, flue-gas is emitted into the atmosphere (stream 43). Table 5.1 presents definitions and assumptions of the units that compose the gas processing and power producing areas of a typical oil-and-gas offshore rig.
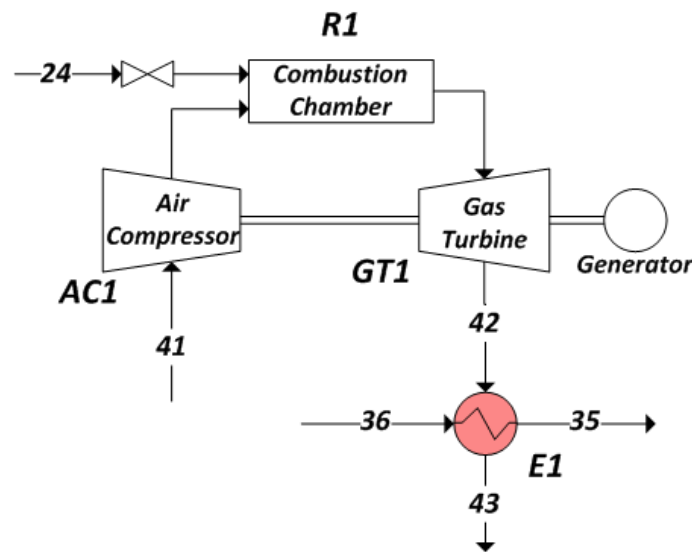
Fig. 5.3. Flowsheet of a GT element in the gas-turbine area.

Table 5.1. Definitions for simulation.

Equipment	Definitions
Towers[#]	T1: P=65bar, 10-staged; T2: P=1bar, 5-staged, $T^{Reboiler}$=200°C.
MPUnits	Countercurrent Spiral-Wound Single-Stage;
	Retentate: P^{Inlet}=47bar; P^{Outlet}=46bar; Permeate: P^{Outlet}=1bar.
JT Unit	P^{Inlet}=64bar; P^{Outlet}=48bar.
SS Units	SS1: 6 SS, Ma^{Shock}=1.5, η_{EXP}%= η_{CMP}%=100%, D_I=76.2mm, D_O=48mm, α=15°, β=2.75°.
	SS2: 6 SS, Ma^{Shock}=1.6, η_{EXP}%= η_{CMP}%=100%, D_I=76.2mm, D_O=48mm, α=15°, β=2.75°.
Compressors	Adiabatic Efficiency: 75%; Intercoolers: T^{Outlet}=35°C; ΔP=0.5 bar.
GT Area	GT Model: Siemens SGT-A35; GT Unit Maximum Shaft Power: 35MW;

Equipment	Definitions
	GT Expander Adiabatic Efficiency: 90%;
	GT Air Compressor Adiabatic Efficiency: 84%
	Number of GTs: TEG+JT+MP=3; SS+MP=3; SS+SS=2;
	Expanded Flue-Gas: $T^{Flue\text{-}Gas}$=500°C (defining air flowrate);
	Combustion Air: Table 5.2.
Background Consumption	$Power^{Background}$=15MW

#*Theoretical stages.*

5.2.2. Exergy Flows

Eq. (5.1a) and Eq. (5.1b) evaluate the total inlet/outlet exergy flows ($\dot{B}_{in,total}$, $\dot{B}_{out,total}$) of a steady-state system (Cruz et al., 2020) where $\dot{B}_{in}$, $\dot{B}_{out}$ stand for inlet/outlet exergy flowrates of material-streams; $\dot{B}_{in}^{W}$, $\dot{B}_{out}^{W}$ represent inlet/outlet total powers, evaluated by the summation of terms $\dot{W}_{j}^{imported}$, $\dot{W}_{j}^{exported}$ on the right-hand side; nfs/nps are the numbers of feed/product streams; nwi/nwe are the numbers of pure-work streams imported/exported, and Fj/Kj are the molar flowrates of the imported/exported stream j. The molar Enthalpy, molar Entropy and molar fraction of the component k of the stream i, $\bar{H}_i$, $\bar{S}_i$, $y_{k,i}$, are imported from HYSYS, while the chemical potentials of species in the considered RER (μ_k^0) and T_0 come from RER calculations in the next section.

$$\dot{B}_{in,total} = \dot{B}_{in} + \dot{B}_{in}^{W} = \sum_{j=1}^{nfs} F_j \left(\bar{H}_{Fj} - T_0 \bar{S}_{Fj} - \sum_{k=1}^{nc} \mu_k^0 y_{k,Fj} \right) + \sum_{j=1}^{nwi} \left| \dot{W}_j^{imported} \right| \tag{5.1a}$$

$$\dot{B}_{out,total} = \dot{B}_{out} + \dot{B}_{out}^{W} = \sum_{j=1}^{nps} K_j \left(\bar{H}_{Kj} - T_0 \bar{S}_{Kj} - \sum_{k=1}^{nc} \mu_k^0 y_{k,Kj} \right) + \sum_{j=1}^{nwe} \left| \dot{W}_j^{exported} \right| \tag{5.1b}$$

Eq. (5.2) calculates the exergy destruction rate (MW) of a system ($\Delta\dot{B}$) as the difference of inlet and outlet exergy flows. $\Delta\dot{B}$ should be equal to the rate of lost work, $\dot{W}^{LOST}$, in Eq. (5.3), where $\dot{\Omega}_S$ is the rate of entropy creation in the Universe due to system operation. The exergy efficiency $\eta(\%)$ is defined as $100 * \dot{B}_{out,total} / \dot{B}_{in,total}$. This is the exergy framework used by Wiesberg et al. (2019), Brigagão et al. (2020) and Cruz et al. (2020) to perform exergy analyses of, respectively, methanol production from CO_2, air pre-purification SS route, and exergy comparison of compressor systems in offshore rigs.

$$\Delta\dot{B} = (\dot{B}_{out} + \dot{B}_{out}^{W}) - (\dot{B}_{in} + \dot{B}_{in}^{W}) \tag{5.2}$$

$$\dot{W}^{LOST} = T_0 . \dot{\Omega}_S \qquad\qquad (5.3)$$

Exergy analysis is performed for each unit independently. In a second stage, the overall gas processing plant (i.e., separations, exchangers, pumps and compressors) is considered as the analyzed system; and in a third stage, the self-sufficient plant comprising the gas processing plant and the power production GT area is the analyzed system. Each analysis consists of evaluating $\dot{B}_{in,total}$, $\dot{B}_{out,total}$, $\Delta \dot{B}$ and then comparing $\Delta \dot{B}$ with $\dot{W}^{LOST}$ to check consistency.

5.2.3. Reference Environmental Reservoir (RER)

According to Eq. (5.1a) and Eq. (5.1b) μ_k^0 – the chemical potentials of species in the RER at hand – are necessary to determine the exergy flows of streams. Two RERs – with perfect internal equilibrium at T_0=298.15 K, P_0=1atm – are considered. RER-1 consists of the standard atmosphere with hydrocarbons and TEG in combustion chemical equilibrium with CO_2, O_2 and H_2O; while RER-2 corresponds to the raw, water-saturated CO_2-rich NG in equilibrium with liquid water containing TEG at infinite-dilution. RER-2 is appropriate for exergy analysis of physical processes (e.g., separators, compressors, exchangers and pumps), while RER-1 is appropriate for chemical processes (e.g., combustion in GT area). Using RER-1 to physical processes with NG streams would entail extra-large inlet/outlet exergy flows and, consequently, all exergy efficiencies near to 100% precluding the discrimination of exergy performances of units. Therefore, only RER-1 is considered in the GT area, while both are considered in the conditioning process.

RER-1 corresponds to the Standard Atmosphere with N_2, O_2, Ar, CO_2 and H_2O in the standard composition without water saturation (*2%mol*) at $P_0 = 1.013\,bar, T_0 = 298.15\,K$. All hydrocarbon species in raw NG and TEG are in chemical equilibrium with the Standard Atmosphere via combustion equations. On the other hand, RER-2 comprises an infinite amount of the raw CO_2-rich NG in equilibrium with an infinite body of liquid water also at $P_0 = 1.013\,bar, T_0 = 298.15\,K$. To account for the presence of TEG in the physical processes (e.g., TEG+JT+MP), the liquid phase of RER-2 contains TEG approximately at infinite-dilution, and thanks to its very low vapor-pressure, there is practically no TEG in the vapor (raw NG) phase. Since RER-2 is made of hydrocarbons, CO_2 and H_2O in internal equilibrium, it obviously cannot have O_2 (neither Ar and N_2, which are absent in the raw NG

feed), but this is not a problem since RER-2 is only used with physical processes of the gas processing plant which do not have presence of O_2 in the streams. RER-2 is not conventional, but it is consistent with the performed analyses because the chemical potentials (μ^0) of the RER-2 species have the same magnitude of the counterparts throughout the physical operations of the gas processing; i.e., they are not too low, allowing discriminating exergy destructions and exergy efficiencies of physical units.

For consistency reasons, the chemical potentials in RER-1 and RER-2 (μ_k^0) should be calculated with the same enthalpy and entropy references that HYSYS uses for calculating thermodynamic properties of streams. But creating HYSYS streams with RER-1 and RER-2 compositions is of no avail, because chemical potentials are not exported by HYSYS. In other words, some stratagem must be used to obtain μ_k^0 with HYSYS. Thus, only pure component streams are created at $P_0 = 1.013\,bar,\ T_0 = 298.15\,K$ (state f) in HYSYS because the respective chemical potential is obtained via exportable molar enthalpy and entropy (i.e, $\mu^f = \bar{H}^f - T_0.\bar{S}^f$). Then, it is considered that the vapor phases of RER-1 and RER-2 are ideal gases, which is reasonable given that $P_0 = 1.013\,bar,\ T_0 = 298.15\,K$. Thus, the calculation of μ_k^0 in RER-1 and RER-2 for a component that exists as a pure gas at $P_0 = 1.013\,bar,\ T_0 = 298.15\,K$ and appears in the RER with a molar fraction y_k^0 is conducted through Eq. (5.4).

$$\mu_k^0 = \mu_k^f\left(T_0, P_0\right) + RT_0\ ln\left(\frac{P_0\, y_k^0}{P_0}\right) \tag{5.4}$$

In Eq. (5.4) y_k^0 is the mole fraction of component k in the RER vapor phase, and $\mu_k^f\left(T_0, P_0\right)$ is the chemical potential of pure species k in a HYSYS stream of pure k at (P_0, T_0) which is calculated via Eq. (5.5) with the values of molar enthalpy and entropy exported by HYSYS. Eq. (5.5) excludes water, TEG, iso-pentane and heavier hydrocarbons (C5+), since they are in liquid state as pure component streams at $P_0 = 1.013\,bar,\ T_0 = 298.15\,K$. To circumvent this problem for H_2O and C5+ species, pure component streams are created at a sufficiently low-pressure for the gas state to exist; i.e., at $P=0.01bar$ and $T_0 = 298.15K$. Extracting the molar enthalpy and entropy for these low-pressure streams, $\mu_i^f\left(T_0, P_0\right)$ of H_2O and C5+ species are given by Eq. (5.6). The case of TEG is analyzed ahead.

130

$$\mu_k^f\left(T_0,P_0\right)=\bar{H}\left(pure\ k,\ T_0,P_0\right)-T_0\bar{S}\left(pure\ k,\ T_0,P_0\right),\ \ k\neq H_2O,TEG,C5^+ \tag{5.5}$$

$$\mu_k^f\left(T_0,P_0\right)=\bar{H}\left(pure\ k,\ T_0,0.01\ atm\right)-T_0\bar{S}\left(pure\ k,\ T_0,0.01\ atm\right)+$$
$$+RT_0\ ln\left(\frac{1bar}{0.01bar}\right)\ ,\ \ k=H_2O,C5^+ \tag{5.6}$$

5.2.3.1. RER-1 Chemical Potentials

Table 5.2 shows the composition of the vapor phase of RER-1 and the respective chemical potentials μ_k^0 considering only the species of the standard atmosphere.

Table 5.2. RER-1 composition and μ_k^0 of species in the Standard Atmosphere (2%mol H₂O).

Component	RER-1 Mol Fraction	μ_k^0 (kJ/mol)
N_2	0.765194	-44.816
O_2	0.205264	-47.165
CO_2	0.000389	-464.694
Ar	0.009153	-47.406
H_2O	0.020000	-303.296

To complete RER-1, the μ_k^0 of hydrocarbon species and TEG are calculated via combustion chemical equilibrium with O_2, H_2O and CO_2. The equilibrium is obtained through complete combustion chemical reactions, forming H_2O and CO_2 that exist in the atmosphere. Using CH_4 as an example, the combustion reaction in Eq. (5.7) is used to calculate μ_k^0 in Eq. (5.8). This procedure is performed for all hydrocarbon and TEG species as shown in Table 5.3.

$$CH_4\left(g\right)+2O_2\left(g\right)=CO_2\left(g\right)+2H_2O\left(g\right) \tag{5.7}$$

$$\mu_{CH4}^0=\mu_{CO_2}^0+2\ \mu_{H_2O}^0-2\ \mu_{O_2}^0 \tag{5.8}$$

Table 5.3. RER-1 μ_k^0 of combustible species.

Component k	μ_k^0 Equation	μ_k^0 (kJ/mol)
CH_4	$\mu_{CO_2}^0+2\ \mu_{H_2O}^0-2\ \mu_{O_2}^0$	-976.96
C_2H_6	$2\mu_{CO_2}^0+3\ \mu_{H_2O}^0-3.5\ \mu_{O_2}^0$	-1674.19
C_3H_8	$3\mu_{CO_2}^0+4\ \mu_{H_2O}^0-5\ \mu_{O_2}^0$	-2371.44
$C_4H_{10}=iC_4H_{10}$	$4\mu_{CO_2}^0+5\ \mu_{H_2O}^0-6.5\ \mu_{O_2}^0$	-3068.68
$C_5H_{12}=iC_5H_{12}$	$5\mu_{CO_2}^0+6\ \mu_{H_2O}^0-8\ \mu_{O_2}^0$	-3765.93
C_6H_{14}	$6\mu_{CO_2}^0+7\ \mu_{H_2O}^0-9.5\ \mu_{O_2}^0$	-4463.17

Component k	μ_k^0 Equation	μ_k^0 (kJ/mol)
C_7H_{16}	$7\mu_{CO_2}^0 + 8\ \mu_{H_2O}^0 - 11\ \mu_{O_2}^0$	-5160.41
C_8H_{18}	$8\mu_{CO_2}^0 + 9\ \mu_{H_2O}^0 - 12.5\ \mu_{O_2}^0$	-5857.65
C_9H_{20}	$9\mu_{CO_2}^0 + 10\ \mu_{H_2O}^0 - 14\ \mu_{O_2}^0$	-6554.90
$C_{10}H_{22}$	$10\mu_{CO_2}^0 + 11\ \mu_{H_2O}^0 - 15.5\ \mu_{O_2}^0$	-7252.14
TEG $C_6H_{14}O_4$	$6\mu_{CO_2}^0 + 7\ \mu_{H_2O}^0 - 7.5\ \mu_{O_2}^0$	-4557.49

5.2.3.2. RER-2 Chemical Potentials

RER-2 is a two-phase system and TEG is only present infinitely diluted in the aqueous phase, while the molar fractions of the remaining components in the vapor phase correspond to the water-saturated CO_2-rich raw NG at $P_0 = 1.013\,bar, T_0 = 298.15\,K$. The μ_k^0 of the species in the vapor phase of RER-2 are calculated via Eqs. (5.4) to (5.6), where the RER-2 fractions y_k^0 are obtained for the vapor phase solving the VLE with water via the saturate HYSYS unit-operation at $P_0 = 1.013\,bar, T_0 = 298.15\,K$. The exception is the μ_k^0 of TEG which does not exist in the raw NG feed. It is represented as $\mu_{TEG}^{0,\infty}$ and is evaluated via a graphical tangent construction with $\bar{G}(T_0, P_0, x_{TEG})$ for TEG-water liquid mixtures at $P_0 = 1.013\,bar, T_0 = 298.15\,K$. The derivative of $\bar{G}(T_0, P_0, x_{TEG})$ at pure liquid water ($x_{TEG} = 0$) is evaluated numerically in Eq. (5.9) (where $\sigma = 1E-6$) with extracted values of molar enthalpy and entropy at $x_{TEG} = 0$. Table 5.4 shows the composition of RER-2 and the μ_k^0 of components. The graphical construction for $\mu_{TEG}^{0,\infty}$ is shown in Fig. 5.4.

$$\mu_{TEG}^{0,\infty} = \left(\bar{H} - T_0 * \bar{S}\right)\Big|_{x=0} + \frac{\left(\bar{H} - T_0 * \bar{S}\right)\Big|_{X=0+\sigma} - \left(\bar{H} - T_0 * \bar{S}\right)\Big|_{x=0}}{\sigma} \qquad (5.9)$$

Table 5.4. RER-2 composition and μ_k^0 of species.

Component	RER-2 Vapor Molar Fraction	μ_k^0 (kJ/mol)
H_2O	0.0310	-302.23
CO_2	0.4263	-447.34
C1	0.4845	-131.41
C2	0.0291	-151.77
C3	0.0194	-161.98
C4	0.0019	-179.87
iC4	0.0029	-197.14
C5	0.0010	-211.66

Component	RER-2 Vapor Molar Fraction	μ_k^0 (kJ/mol)
iC5	0.0019	-205.77
C6	0.0010	-233.55
C7	0.0005	-265.58
C8	0.0003	-271.93
C9	0.0001	-337.32
C10	0.0001	-372.86
TEG	-	-868.62
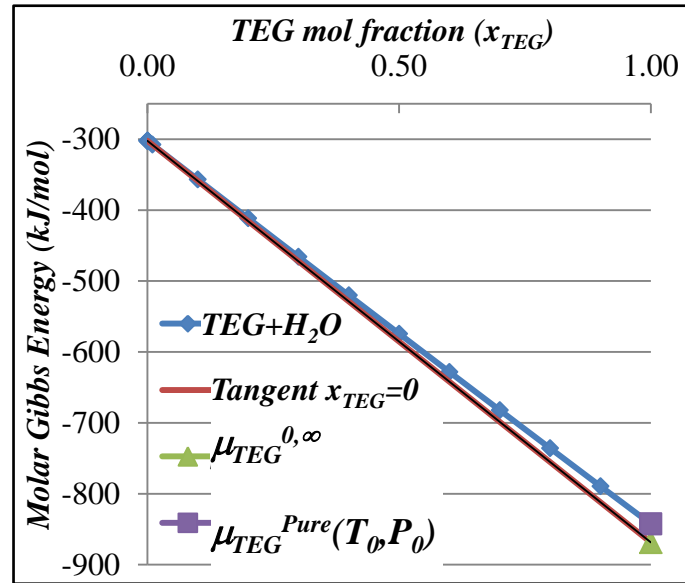
Fig. 5.4. Tangent framework: nearly infinite-dilution TEG chemical potential at T_0, P_0.

5.3. Results and Discussion

Fig. 5.5 shows the destination of the inlet species CO_2, CH_4, C_2H_6, C_{3+}, H_2O and TEG among the product streams NGL (stream 22), CO_2-Rich (stream 26) and total NG (streams 24 plus stream 25) for the processes TEG+JT+MP, SS+MP and SS+SS. H_2O and TEG are plotted in the axis at the right. The recoveries are relative to the material inlet, the inlet gas (1) and TEG makeup (8). For example, from the total CO_2 inlet in TEG+JT+MP, about 70% goes to CO_2-rich stream to EOR and 30% remains in NG Exported. Regarding WDPA and HCDPA, SS+SS produces a cleaner NG since it has additional water and C_{3+} condensation in SS-2. This can be seen by analyzing the NG Exported, which has the lowest recovery of C_{3+} of about 10% in the SS+SS process, against more than 80% for the other configurations. The majority of C_{3+} goes to the CO_2-rich stream to EOR from SS+SS, i.e., the condensate stream of SS-2 accounting for 70.9%, while more than 80% remains in the NG Exported from TEG+JT+MP and SS+MP. In the H_2O case, none of it is present in the NG Exported for

SS+SS, while more than 0.3% is present in the NG Exported of TEG+JT+MP and SS+MP. Moreover, CH_4 has the highest recovery in the SS+SS configuration, accounting for ≈89% against ≈85% for TEG+JT+MP and SS+MP. The only negative result for the SS+SS is the worst CO_2 removal, with the NG Exported still containing 29.6% of the inlet CO_2, against 27.6% and 27.1% for TEG+JT+MP and SS+MP, respectively.
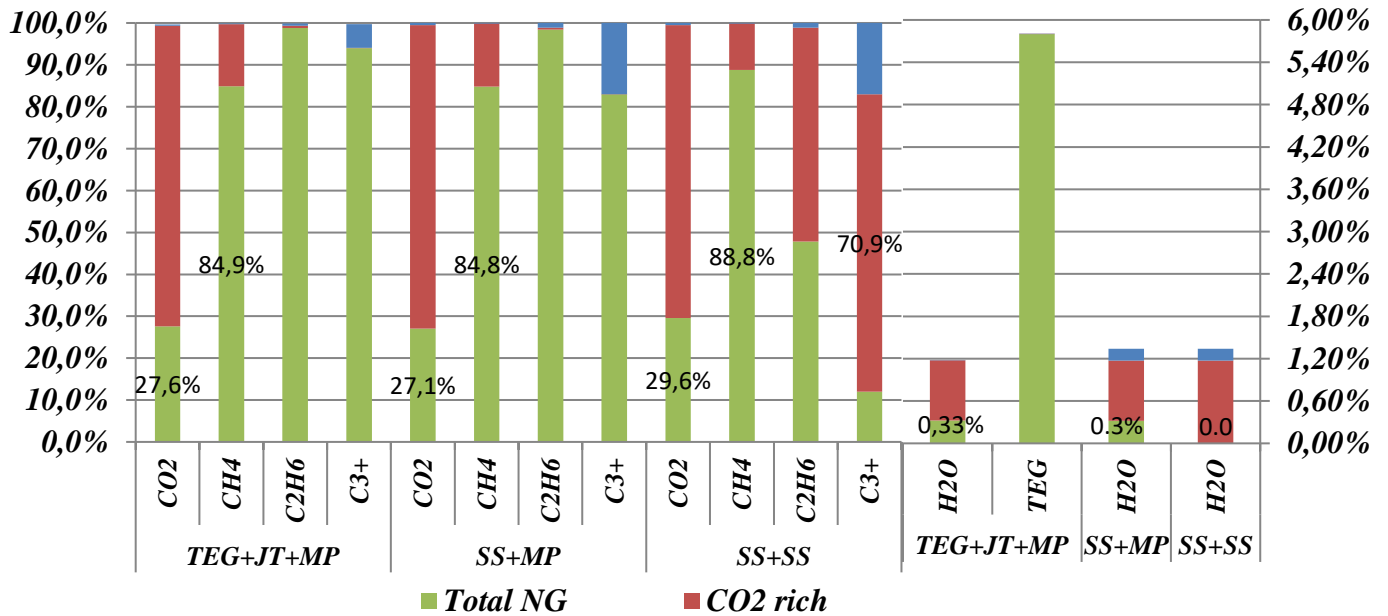
Fig. 5.5. Destination of inlet components through the gas processing thread to NGL, CO₂-rich and total NG (fuel-gas + NG exported) streams.

The μ_k^0 of hydrocarbons and TEG, differs widely between the RERs, influencing the exergy analyses. Values of μ_k^0 of hydrocarbons for RER-1 are strongly negative, resulting in streams with very high exergy flowrate. On the other hand, RER-2 exergy flowrates of the same streams exhibit much lower positive values, due to the higher reference chemical potentials. Table 5.5 shows exergy flowrates of boundary-crossing streams; i.e., streams that are inlets/outlets of the overall gas processing plants. It can be observed that RER-2 exergy flowrates are two orders of magnitude shorter, resulting in values with similar magnitude of the exergy destruction rates, which, by the way, are independent of the chosen RER.

Table 5.5. Exergy flowrates (kW) of inlet/outlet streams of the gas processing plants according to RER-1 and RER-2.

Stream Name (Inlet/outlet)	Tag	TEG+JT+MP		SS+MP		SS+SS	
		RER-1	RER-2	RER-1	RER-2	RER-1	RER-2
Feed Raw-Gas(in)	1	3.25E+06	4.52E+04	3.25E+06	4.52E+04	3.25E+06	4.52E+04
TEG makeup(in)	8	2.18E+02	1.41E+00	N/A	N/A	N/A	N/A

Stream Name (Inlet/outlet)	Tag	TEG+JT+MP		SS+MP		SS+SS	
		RER-1	RER-2	RER-1	RER-2	RER-1	RER-2
Condensate(out)	20	1.65E+01	2.41E+00	1.43E+01	1.73E+00	1.43E+01	1.73E+00
CO_2 emission(out)	21	1.07E+03	2.63E+01	0.00E+00	0.00E+00	0.00E+00	0.00E+00
NGL(out)	22	4.50E+04	1.92E+02	1.14E+05	4.38E+02	1.14E+05	4.38E+02
Fuel-Gas(out)	24	2.89E+05	3.43E+03	2.85E+05	3.44E+03	1.94E+05	2.52E+03
NG Exported(out)	25	2.51E+06	3.80E+04	2.45E+06	3.77E+04	2.20E+06	3.90E+04
EOR(out)	26	4.25E+05	2.99E+04	4.32E+05	3.02E+04	7.68E+05	3.01E+04
SW^{in} (in)	33	1.44E+05	1.14E+03	1.29E+05	1.02E+03	1.14E+05	9.02E+02
SW^{out} (out)	34	1.46E+05	2.85E+03	1.30E+05	2.55E+03	1.16E+05	2.26E+03
PHW(in)	35	8.33E+03	6.35E+03	3.10E+03	2.37E+03	2.08E+03	1.59E+03
PHW^{out}(out)	36	5.10E+03	3.12E+03	1.89E+03	1.16E+03	1.27E+03	7.78E+02
Power(in)	P1+P2	4.79E+01	4.79E+01	N/A	N/A	N/A	N/A
Power(in)	P3	5.94E+03	5.94E+03	6.01E+03	6.01E+03	6.78E+03	6.78E+03
Power(in)	P4	N/A	N/A	N/A	N/A	1.73E+02	1.73E+02
Power(in)	K1	1.98E+04	1.98E+04	1.40E+04	1.40E+04	1.40E+04	1.40E+04
Power(in)	K2	3.04E+04	3.04E+04	3.07E+04	3.07E+04	7.11E+03	7.11E+03
Power(in)	K3	1.44E+04	1.44E+04	1.43E+04	1.43E+04	1.74E+04	1.74E+04
Power(in)	K4	N/A	N/A	N/A	N/A	1.06E+04	1.06E+04

Fig. 5.6 shows exergy analysis results of main units and for the three overall gas processing plants. The first parts of SS+MP and SS+SS plants (i.e., the SS-1 unit) are exactly the same and its equipment items belong to the scenario "SS+…". The second parts of SS+MP and SS+SS plants are different; i.e., respectively the MP unit and the SS-2 unit, whose equipment items respectively belong to the scenarios "…+MP " and "…+SS". The results show the importance the RER selection, since the efficiency is almost 100% with RER-1 for most units, similarly to the results found by Ghannadzadeh et al. (2012). RER-2 has a better discernment of the exergy destruction and can pinpoint the units whose design optimization should be prioritized and can affect more intensely the exergy efficiency. The consistency of the present exergy analysis is attested via the cross-check of $\Delta \dot{B}$ and $\dot{W}^{LOST}$ values. The highest divergence found between $\Delta \dot{B}$ and $\dot{W}^{LOST}$ belongs to unit T2 reaching only −0.18%.

The overall exergy efficiencies of the gas processing plants (involving only physical operations) reached 72.4%, 66.5% and 63.3% respectively for SS+SS, SS+MP and TEG+JT+MP via RER-2. That is, RER-2 could perfectly pinpoint the better utilization of resources promoted by SS+SS. On the other hand, using RER-1 for exergy analysis of the same physical gas processing plants, values of 99.2%, 98.9% and 98.7% are respectively obtained for SS+SS, SS+MP and TEG+JT+MP. That is, using RER-1, the exergy

performances of SS+SS, SS+MP and TEG+JT+MP seem very similar and practically equally efficient; but the reality is different. In other words, RER-1 is totally inappropriate for discriminating exergy performances of physical processes.

The biggest exergy sink of TEG+JT+MP is the CO_2 compression train K2, with 12.26MW of exergy destruction, seconded by MP with a destruction of 10.25MW and efficiency of 80.5% according to RER-2. Together, K2 and MP represent 49.5% of the overall exergy destruction of TEG+JT+MP. Surprisingly, JT expansion has a RER-2 efficiency of 94.7%. Similar results are obtained for SS+MP, while in SS+SS the most impactful unit is the NG compression train K3, accounting for 5.89MW of exergy destruction, followed by SS2 with 4.28MW, representing together 35.6% of overall exergy destruction. SS2 is more exergy efficient than MP as CO_2 removal unit attaining 93%, while SS-1 is even more efficient with 99.1%, both values for RER-2. The lower value of SS2 is explained by the lower pressure-recovery of SS2 relatively to SS1, a consequence of a higher Ma^{Shock} in SS2 necessary for great condensation of CO_2 (Table 5.1). Similar exergy efficiencies of SS units (91.1% and 99.2%) were found by Brigagão et al. (2020).
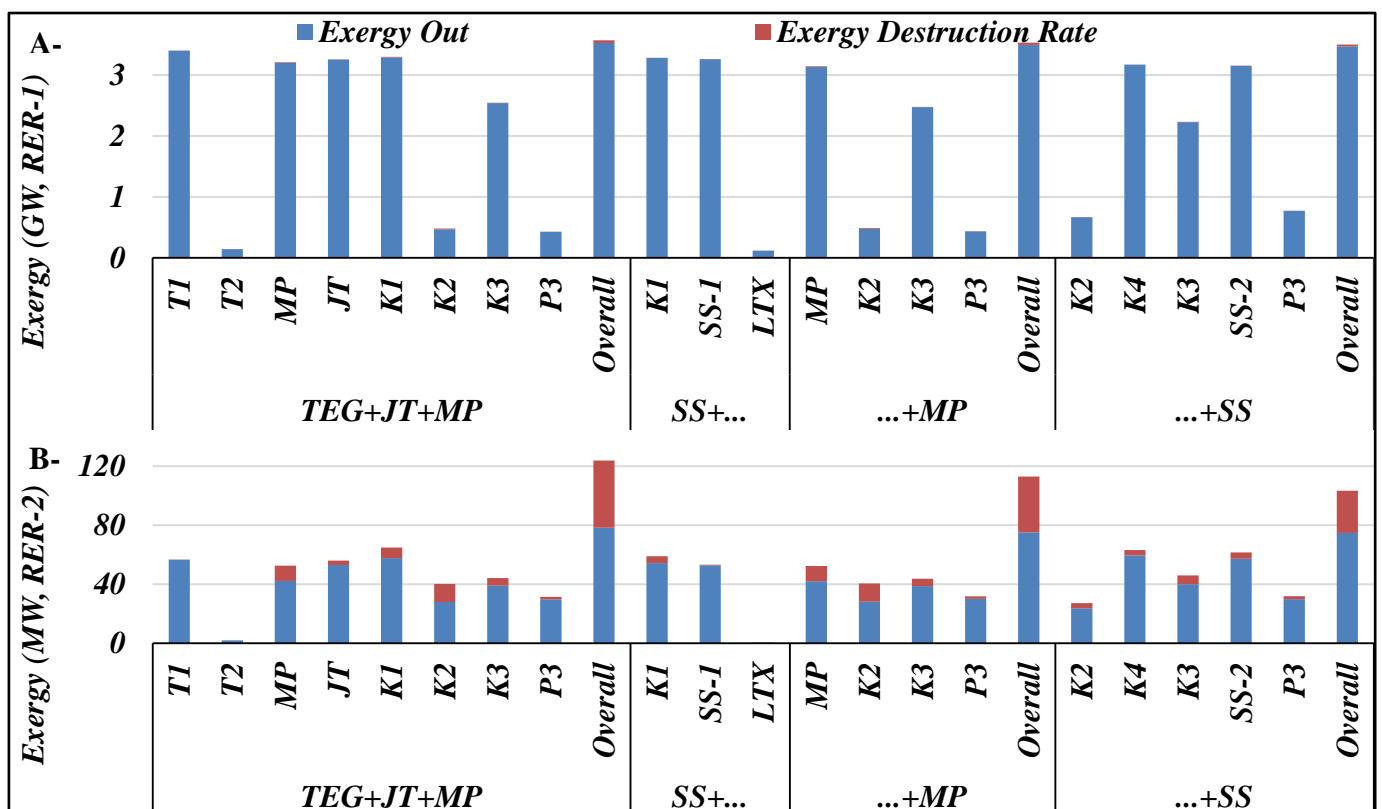
Fig. 5.6. Exergy analyses of TEG+JT+MP, SS+MP and SS+SS gas processing plants for units and overall process: (A) RER-1 (GW); (B) RER-2 (MW).

Fig. 5.7 shows the breakdown of exergy destruction rates (do not depend on the used RER) per equipment type for the three conditioning plants. Compressors are the main source of exergy destruction, totaling 12MW, 11MW and 10MW for TEG+JT+MP, SS+MP and SS+SS, respectively. When the intercoolers are also considered in the compression trains, these values are increased by 9MW, 9MW and 5MW, respectively, resulting in a share of 46.3%, 53.2% and 50.8% of the respective total exergy destructions of TEG+JT+MP, SS+MP and SS+SS.
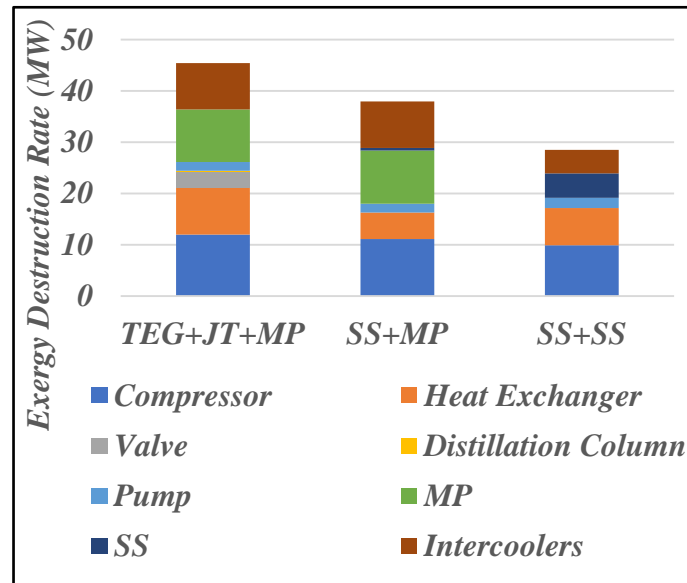
Fig. 5.7. Breakdown of exergy destruction rates (MW) per equipment type for TEG+JT+MP, SS+MP and SS+SS gas processing plants.

Fig. 5.8 shows RER-1 exergy analyses of the respective GT areas of TEG-JT-MP, SS+MP and SS+SS considering equipment items and the overall GT areas. The results are similar for the three GT areas, where the SS+SS has the highest exergy efficiency of 75.3%, against 75.2% and 75.1% for TEG+JT+MP and SS+MP, respectively. The exergy destruction rates attained 75.1MW, 110.9MW and 114.1MW for SS+SS, TEG+JT+MP and SS+MP. The main reduction of exergy destruction of SS+SS occurs in the heat exchanger E1, with ≈0.6 MW of savings, when compared to the TEG+JT+MP counterpart. This can be explained by the lower E1 duty of 1.2MW in SS+SS against 3.1MW for TEG+JT+MP due to a lower PHW flowrate demanded in SS+SS (1238 kmol/h against 467.3 kmol/h). However, the main difference regarding the three GT areas is the lower power requirement of SS+SS, to be shown later, but can already be inferred from its lower exergy flowrate.
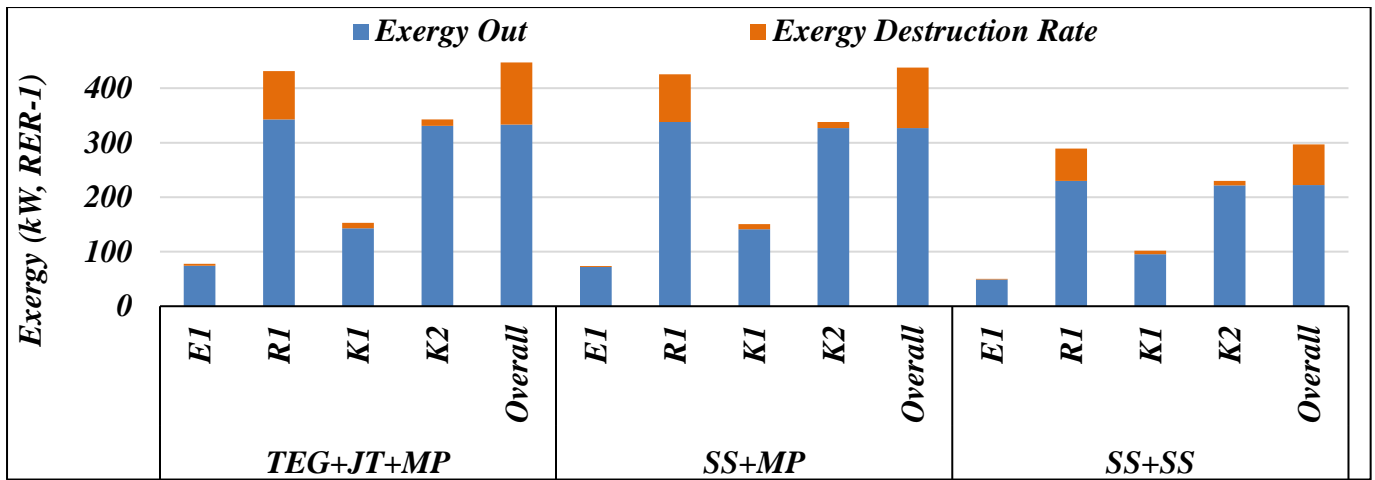
Fig. 5.8. RER-1 exergy analyses (MW) of the respective GT areas of TEG+JT+MP, SS+MP and SS+SS gas processing plants per equipment and overall.

Fig. 5.9 depicts six Sankey diagrams of overall exergy flows for TEG+JT+MP, SS+MP and SS+SS according to RER-1 and RER-2. Only exergy flows associated to inlet/outlet streams of the overall gas processing plants are taken into account. For example, the flows associated to CW are not seen because the CW loops are perfectly within the respective plants; but the seawater streams cross the plants boundaries and the respective exergy flows are taken into account. It can be appreciated how the exergy flows of the inlet raw CO_2-rich NG, fuel-gas and NG exported change dramatically according to the used RER.

The relative differences of exergy destructions and power consumptions regarding the inlet exergy flow are significant whether RER-1 or RER-2 are used. RER-1 shows negligible exergy destructions and power demand relatively to the total inlet flow of exergy in the CO_2-rich NG. In opposition to this, more meaningful proportions of exergy destruction and power demand relatively to the inlet exergy flow are obtained with RER-2. In TEG+JT+MP, for example, 71MW of power is required against 3252MW of CO_2-rich NG inlet exergy with RER-1, while there is the same 71MW of power against 45MW of CO_2-rich NG inlet exergy with RER-2. This means that RER-2 lets explicit that the main input of exergy for gas processing is the power to drive the compressors, which is correct since JT, MP and SS use pressure as driving force for separation. On the other hand, RER-1 entails similar magnitude of flows for power and seawater exergy flow, a not meaningful result. Considering RER-2, the total exergy inlet in TEG+JT+MP is 123MW, while it is 113MW in SS+MP and 104MW in SS+SS. Thus, a reduction of ≈8% in the inlet exergy is obtained when SS1 is used to perform WDPA/HCDPA and about 15% when SS2 is used for CO_2 removal. Another

138

advantage of using SS1 is the lower PHW requirement (2MW in SS+MP and SS+SS against 6MW for TEG+JT+MP with RER-2). Thus, more exergy is left available in SS+MP and SS+SS for a possible waste-heat recovery unit for combined-cycle power generation.
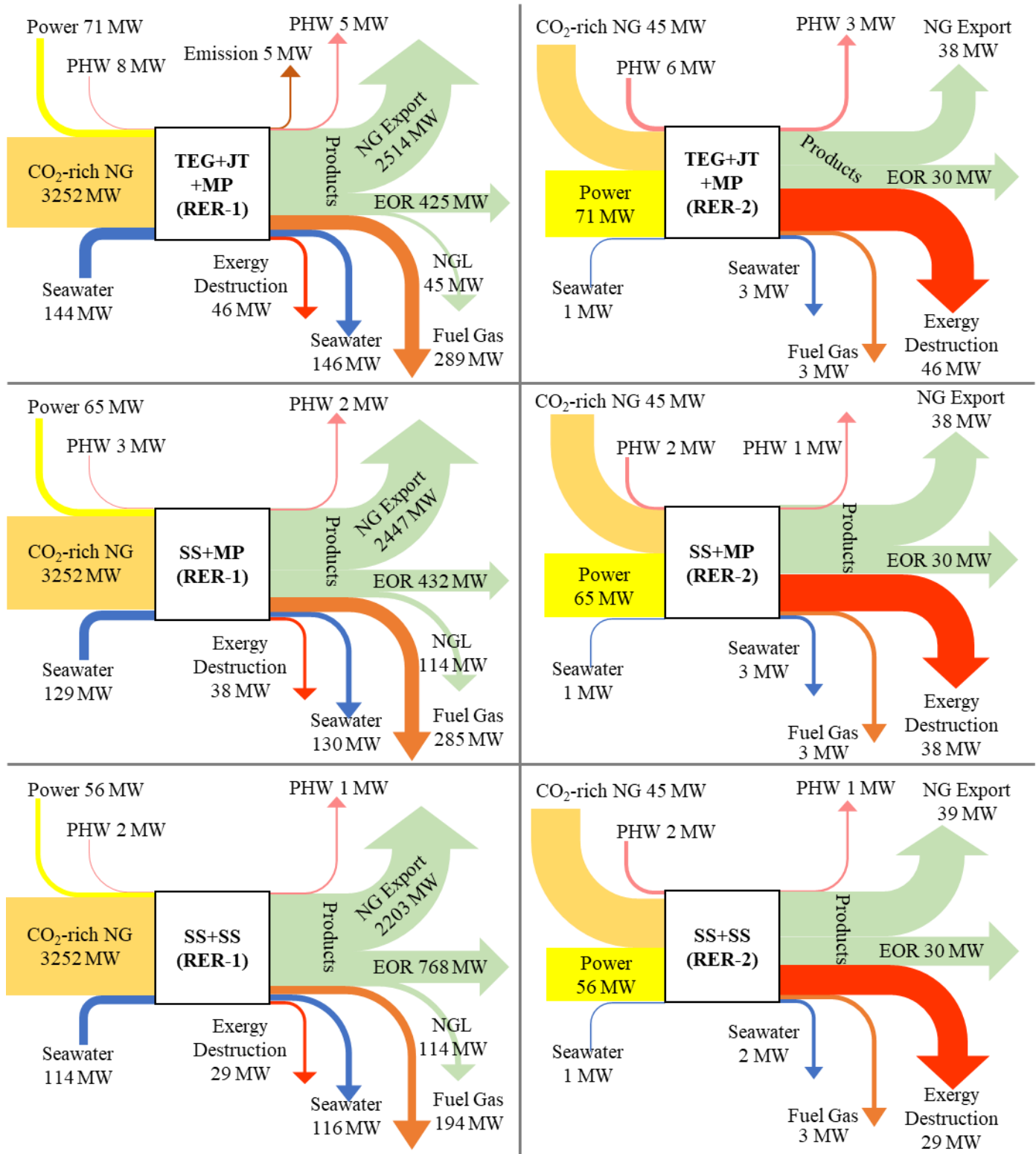
Fig. 5.9. Sankey Diagrams of exergy flows (MW) for the gas processing plants: RER-1 (left); RER-2 (right); TEG+JT+MP (top); SS+MP (middle); and SS+SS (bottom).

Figs. 5.10 to 5.12 respectively depict the exergy analyses for TEG-JT-MP, SS+MP and SS+SS coupled to the respective GT areas. The exergy flowrates of air inlets to the GTs are zero since they are in the same state as RER-1. CW and PHW streams are also absent since CW and PHW loops are 100% within the enlarged plants. RER-1 is the only available option, since RER-2 is not suitable for GT areas due to the combustion reactions. The power output of the GT area supplies the requirements in the gas processing plants plus a "backpower" consumption of 15MW (Table 5.1) to sustain peripheral facilities (e.g., lights and secondary machines). Since an integer number of active GTs Siemens SGT-A35 (shaft power of 35MW) should be used (2 for SS+SS and 3 for TEG+JT+MP and SS+MP), in TEG+JT+MP and SS+MP cases a power surplus results so that a fair comparison can be made despite of the different numbers of GTs. Exergy destruction reduces from 159MW in TEG-JT-MP to 149MW in SS+MP (i.e., using SS1 in place of TEG+JT), and further reduces to 104MW when SS2 replaces MP in SS+SS; a 35% reduction. Moreover, the exergy flows of products increase from 2984MW to 2993MW when using SS1 in place of TEG+JT, and to 3084MW when SS2 replaces MP, a ≈5% increase. Exergy efficiencies of the coupled processes are 95.3%, 95.6% and 96.9% for TEG+JT+MP, SS+MP and SS+SS respectively.
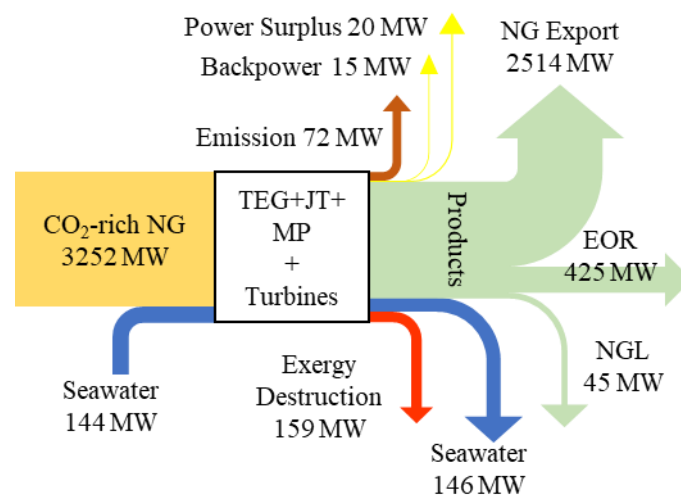
Fig. 5.10. RER-1 Sankey diagram of exergy flows (MW) for TEG+JT+MP coupled to its GT area (TG inlet air has zero exergy flowrate since it is equal to RER-1).
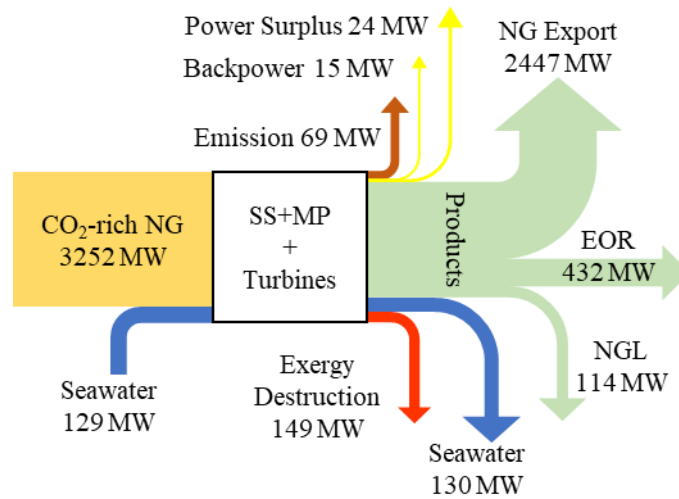
Fig. 5.11. RER-1 Sankey diagram of exergy flows (MW) for SS+MP coupled to its GT area (TG inlet air has zero exergy flowrate since it is equal to RER-1).
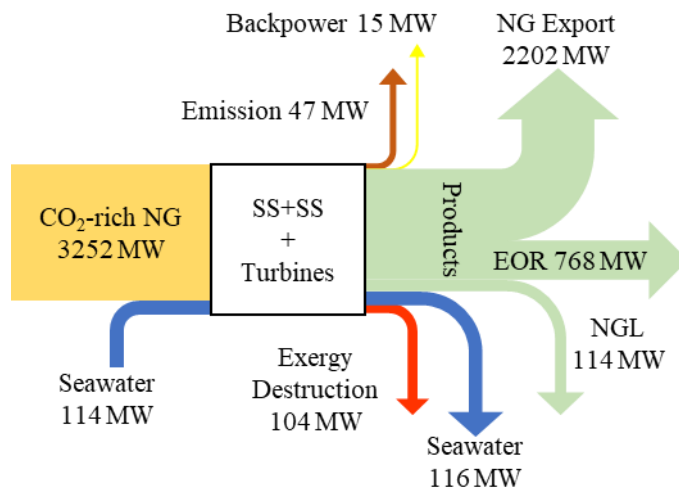
Fig. 5.12. RER-1 Sankey diagram of exergy flows (MW) for SS+SS coupled to its GT area. (TG inlet air has zero exergy flowrate since it is equal to RER-1).

5.4. Conclusions for Chapter 5

A trustful model for exergy analyses of CO_2-rich NG processing in offshore rigs was developed and three offshore gas processing plants was compared in terms of exergy destruction and efficiency. Two of them use the new SS technology, namely SS+MP and SS+SS, and are innovative, while the third one is a conventional TEG+JT+MP plant. All exergy destructions, using both RER-1 and RER-2, diverge from the lost work formula via the 2nd Law of Thermodynamics by less than 0.18%, an acceptable value given that hundreds round-off errors and dozens HYSYS convergence tolerances are affecting the results, which validates the method.

It is shown that only RER-1 is appropriate to perform exergy analysis of chemically reactive processes like the GT areas, while RER-2 is appropriate for physical processes – i.e., deprived of chemical reactions – like the NG processing plants and their units. The magnitude of exergy destructions in RER-2 is of the same order as the respective total inlet exergy flows, turning exergy efficiencies meaningful and allowing the correct identification of exergy sinks for future improvement of process performance, while using RER-1 for the physical units entails efficiencies near to 100% making hard to discriminate their exergy performances. Thus, the non-conventional RER-2 is recommended for exergy analysis of the physical units for raw NG conditioning (i.e., envelopes without chemical reactions). At the same time, only RER-1 is adequate for exergy analysis of the envelopes wherein chemical reactions take place like the GT areas and the whole rig comprehending the GT area and the NG processing plant.

Technical results show that SS+SS and SS+MP gas processing plants perform WDPA/HCDPA with better efficiency than the conventional TEG+JT+MP. Only 10% of the C3+ from the inlet raw NG appears in the NG Exported from SS+SS, against more than 80% for TEG+JT+MP and SS+MP, while 0% of the inlet water remains in the NG Exported of SS+SS, against more than 0.3% for the other two. Besides its better technical performance, SS attained also high exergy efficiencies of 99.1% for SS1 and 93.0% for SS2, against 94.7% for JT and 80.5% for MP, considering RER-2.

Lastly, it is proved that SS+SS is more exergy efficient for CO_2-rich NG conditioning than TEG+JT+MP: 72.4% versus 63.3% exergy efficiency for RER-2, with SS+MP in an intermediary position at 66.5%. These results show the improvement of sustainability brought by using SS units in place of conventional separations. Moreover, considering RER-1 and the enlarged plants comprising the gas processing coupled to the respective GT areas, the utilization of SS units allows increasing the exergy output by 5% relatively to the conventional TEG+JT+MP coupled to its GT area.

5.5. References for Chapter 5

Alfyorov, V., Bagirov, L.A., Dmitriev, L.M., Feygin, V.I., Imayev, S., Lacey, J.R., 2005. Supersonic nozzle efficiently separates natural gas components. Oil Gas J 2005; 103:53–58.

Araújo, O. de Q.F., Reis, A. de C., de Medeiros, J.L., Nascimento, J.F. do, Grava, W.M., Musse, A.P.S., 2017. Comparative analysis of separation technologies for processing carbon dioxide rich natural gas in ultra-deepwater oil fields. J. Clean. Prod., Sustainable Development of Energy, Water and Environmental Systems 155, 12–22. https://doi.org/10.1016/j.jclepro.2016.06.073

Arinelli, L. de O., Trotta, T.A.F., Teixeira, A.M., de Medeiros, J.L., Araújo, O. de Q.F., 2017. Offshore processing of CO2 rich natural gas with supersonic separator versus conventional routes. J. Nat. Gas Sci. Eng. 46, 199–221. https://doi.org/10.1016/j.jngse.2017.07.010

Arinelli, L. de O., Teixeira, A.M., de Medeiros, J.L., Araújo, O. de Q.F., 2019. Supersonic separator for cleaner offshore processing of natural gas with high carbon dioxide content: Environmental and economic assessments. J. Clean. Prod. 233, 510–521. https://doi.org/10.1016/j.jclepro.2019.06.115

Baccanelli, M., Langé, S., Rocco, M.V., Pellegrini, L.A., Colombo, E., 2016. Low temperature techniques for natural gas purification and LNG production: An energy and exergy analysis. Appl. Energy 180, 546–559. https://doi.org/10.1016/j.apenergy.2016.07.119

Brigagão, G.V., Arinelli, L. de O., de Medeiros, J.L., Araújo, O. de Q.F., 2020. Low-pressure supersonic separator with finishing adsorption: Higher exergy efficiency in air pre-purification for cryogenic fractionation. Sep. Purif. Technol. 248, 116969. https://doi.org/10.1016/j.seppur.2020.116969

Chong, Z.R., Yang, S.H.B., Babu, P., Linga, P., Li, X.-S., 2016. Review of natural gas hydrates as an energy resource: Prospects and challenges. Appl. Energy 162, 1633–1652. https://doi.org/10.1016/j.apenergy.2014.12.061

Cruz, M. de A., de Queiroz Fernandes Araújo, O., de Medeiros, J.L., 2018. Deep seawater intake for primary cooling in tropical offshore processing of natural gas with high carbon dioxide content: Energy, emissions and economic assessments. J. Nat. Gas Sci. Eng. 56, 193–211. https://doi.org/10.1016/j.jngse.2018.06.011

Cruz, M. de A., Araújo, O. de Q.F., de Medeiros, J.L., 2020. Exergy comparison of single-shaft and multiple-paralleled compressor schemes in offshore processing of CO2-Rich natural gas. J. Nat. Gas Sci. Eng. 81, 103390. https://doi.org/10.1016/j.jngse.2020.103390

de Medeiros, J.L., Arinelli, L. de O., Araújo, O. de Q.F., 2017. Speed of sound of multiphase and multi-reactive equilibrium streams: A numerical approach for natural gas applications. J. Nat. Gas Sci. Eng. 46, 222–241. https://doi.org/10.1016/j.jngse.2017.08.006

de Melo, D.C., Arinelli, L. de O., de Medeiros, J.L., Teixeira, A.M., Brigagão, G.V., Passarelli, F.M., Grava, W.M., Araujo, O. de Q.F., 2019. Supersonic separator for cleaner offshore processing of supercritical fluid with ultra-high carbon dioxide content: Economic and environmental evaluation. J. Clean. Prod. 234, 1385–1398. https://doi.org/10.1016/j.jclepro.2019.06.304

EIA. Carbon dioxide emissions coefficients. U.S. Department of Energy; 2016

EIA. World Energy Outlook 2017, U.S. Department of Energy, 2017.

EIA. World Energy Outlook 2019, U.S. Department of Energy, 2019.

Gaffney, Cline & Associates: Review and Evaluation of Ten Selected Discoveries and Prospects in the Pre-salt Play of the Deepwater Santos Basin, Brazil, 2015, CG/JW/RLG/C1820.00/ GCABA.1914, ANP, September 15th, 2010. Viewed 20 December 2015. www.anp.gov.br/?dw=39137

Gallo, W.L.R., Gallego, A.G., Acevedo, V.L., Dias, R., Ortiz, H.Y., Valente, B.A., 2017. Exergy analysis of the compression systems and its prime movers for a FPSO unit. J. Nat. Gas Sci. Eng. 44, 287–298. https://doi.org/10.1016/j.jngse.2017.04.023

Gandhidasan, P., Al-Farayedhi, A.A., Al-Mubarak, A.A., 2001. Dehydration of natural gas using solid desiccants. Energy 26, 855–868. https://doi.org/10.1016/S0360-5442(01)00034-2

Gaudreau, K., Fraser, R.A., Murphy, S., 2012. The Characteristics of the Exergy Reference Environment and Its Implications for Sustainability-Based Decision-Making. Energies 5, 2197–2213. https://doi.org/10.3390/en5072197

Ghannadzadeh, A., Thery-Hetreux, R., Baudouin, O., Baudet, P., Floquet, P., Joulia, X., 2012. General methodology for exergy balance in ProSimPlus® process simulator. Energy, Integration and Energy System Engineering, European Symposium on Computer-Aided Process Engineering 2011 44, 38–59. https://doi.org/10.1016/j.energy.2012.02.017

Machado, P.B., Monteiro, J.G.M., Medeiros, J.L., Epsom, H.D., Araujo, O.Q.F., 2012. Supersonic separation in onshore natural gas dew point plant. J. Nat. Gas Sci. Eng. 6, 43–49. https://doi.org/10.1016/j.jngse.2012.03.001

Malone, T., Kuuskraa, V., DiPietro, P., 2014. CO2-EOR Offshore Resource Assessment (No. NETL/DOE-2014/1631). National Energy Technology Laboratory (NETL), Pittsburgh, PA, Morgantown, WV, and Albany, OR (United States). https://doi.org/10.2172/1523638

Nguyen, T.-V., Pierobon, L., Elmegaard, B., Haglind, F., Breuhaus, P., Voldsund, M., 2013. Exergetic assessment of energy systems on North Sea oil and gas platforms. Energy 62, 23–36. https://doi.org/10.1016/j.energy.2013.03.011

Nguyen, T.-V., Tock, L., Breuhaus, P., Maréchal, F., Elmegaard, B., 2014. Oil and gas platforms with steam bottoming cycles: System integration and thermoenvironomic evaluation. Appl. Energy 131, 222–237. https://doi.org/10.1016/j.apenergy.2014.06.034

Nguyen, T.-V., Tock, L., Breuhaus, P., Maréchal, F., Elmegaard, B., 2016. CO2-mitigation options for the offshore oil and gas sector. Appl. Energy 161, 673–694. https://doi.org/10.1016/j.apenergy.2015.09.088

Pierobon, L., Nguyen, T.-V., Larsen, U., Haglind, F., Elmegaard, B., 2013. Multi-objective optimization of organic Rankine cycles for waste heat recovery: Application in an offshore platform. Energy 58, 538–549. https://doi.org/10.1016/j.energy.2013.05.039

Pierobon, L., Haglind, F., 2014. Design and optimization of air bottoming cycles for waste heat recovery in off-shore platforms. Appl. Energy 118, 156–165. https://doi.org/10.1016/j.apenergy.2013.12.026

Pinto, A.C.C., Martins Vaz, C.E., Moreira Branco, C.C., Ribeiro, J., 2014. An Evaluation of Large Capacity Processing Units for Ultra Deep Water and High GOR Oil Fields. Presented at the Offshore Technology Conference, OnePetro. https://doi.org/10.4043/25274-MS

Santos, M.G.R.S., Correia, L.M.S., de Medeiros, J.L., Araújo, O. de Q.F., 2017. Natural gas dehydration by molecular sieve in offshore plants: Impact of increasing carbon dioxide content. Energy Convers. Manag. 149, 760–773. https://doi.org/10.1016/j.enconman.2017.03.005

Szargut, J., 1989. Chemical exergies of the elements. Appl. Energy 32, 269–286. https://doi.org/10.1016/0306-2619(89)90016-0

Teixeira, A.M., Arinelli, L. de O., Medeiros, J.L. de, Araújo, O. de Q.F., 2016. Exergy Analysis of Monoethylene glycol recovery processes for hydrate inhibition in offshore natural gas fields. J. Nat. Gas Sci. Eng. 35, 798–813. https://doi.org/10.1016/j.jngse.2016.09.017

Voldsund, M., Nguyen, T.-V., Elmegaard, B., Ertesvåg, I.S., Røsjorde, A., Jøssang, K., Kjelstrup, S., 2014. Exergy destruction and losses on four North Sea offshore platforms: A comparative study of the oil and gas processing plants. Energy 74, 45–58. https://doi.org/10.1016/j.energy.2014.02.080

Wiesberg, I.L., Brigagão, G.V., Araújo, O. de Q.F., de Medeiros, J.L., 2019. Carbon dioxide management via exergy-based sustainability assessment: Carbon Capture and Storage versus conversion to methanol. Renew. Sustain. Energy Rev. 112, 720–732. https://doi.org/10.1016/j.rser.2019.06.032

Yang, Y., Wen, C., Wang, S., Feng, Y., 2014. Theoretical and numerical analysis on pressure recovery of supersonic separators for natural gas dehydration. Appl. Energy 132, 248–253. https://doi.org/10.1016/j.apenergy.2014.07.018

6. CONCLUDING REMARKS

This Thesis evaluates novel technologies to mitigate carbon emissions for the chemical and energy sector, contributing to its sustainable development. Emphasis was given to carbon mitigation of flue gas from the electricity generation sector through powerplants fueled by coal (Chapter 2), NG (Chapter 3) and biomass (Chapter 4). It also evaluates a possible increase in the sustainability of the NG exploitation industry (Chapter 5). The avoidance of CO_2 was also investigated for the methanol industry by the substitution of NG hydrocarbons by CO_2 (Chapter 2 and Chapter 3). Companies in the aforementioned sectors can take advantage of this work to increase the sustainability of its operations. In this sense, this Thesis contributes, to certain extent, to some of the goals of the UN's Agenda 2030, including "7 – Affordable and Clean energy production", "9 – Industry, Innovation and Infrastructure", "12 – Responsible consumption and production" and "13 – Climate Action".

Therefore, four Research Lines are addressed, all related to the main objective of pursuing the sustainable development. Line#1 evaluates CCU technologies for methanol production via microalgae culture using flue-gas from coal-fired power plant and compares it to the CCS technology. Line#2 evaluates the carbon mitigation by CCU technologies for methanol production from flue-gas of CO_2-rich NG power plants and compares it to CCS technology. Line#3 evaluates the sustainability of applying CCS to bioenergy production from sugarcane in a combined heat and power (cogeneration) facility. Line #4 evaluates the sustainability of novel technologies for offshore CO_2-rich natural gas conditioning system with Supersonic Separators with EOR destination for the captured carbon. The technologies are analyzed in terms of technical, economic, environmental and exergy aspects, highlighting aspects as sustainability and feasibility of the alternatives.

Line#1 evinces that the biorefinery consisting of microalgae cultivation for CO_2 fixation, with biomass gasification for methanol production as well as the extraction of its lipids for commercialization, as microalgae oil, has a poor technical performance.

Line#2 claims that the attachment of a CO_2 capture unit to treat flue-gas from a CO_2-rich NG power plant prior to its utilization for methanol production can be a feasible solution for carbon mitigation. This is particularly true for the direct CO_2 hydrogenation route with superior exergy efficiency, while the bi-reforming of CO_2-rich NG is not as sustainable, when compared through the exergy efficiency prism. The exergy efficiency of the CCU by direct

hydrogenation is 66.3%, while the Syngas route is 55.8%, and the CCS is only 44.8%. It's interesting to highlight that CCS had lower exergy efficiency than the business as usual (BAU) scenario of flue-gas emission (44.8% against 53.5%) because of the capture step requirements. An even more interesting point is that the BAU scenario of flue-gas emission together with the conversion to methanol of pure CO_2, from bioethanol or ethylene oxide plant, has an even higher exergy efficiency of 69.2%. Therefore, avoiding the capture step is a good strategy to increase the sustainability of CO_2 mitigation. Moreover, the developed Exergy Analysis for CCU with methanol production is consistent, as it results in positive values for exergy of each stream and the final error for each equipment is negligible.

In Line#1, the case of the biorefinery route for CCU, the carbon balance analysis points its superiority over competing CCU alternatives for methanol production. However, the results of the economic analysis show that it is only economic feasible with a severe carbon taxation, higher than 100USD/t. Moreover, technical bottlenecks must be solved prior to its implementation, notably concerning the microalgae cultivation and harvesting units. Although considering optimistic premises for the photobioreactor, the biorefinery would hardly be technical viable as total area needed accounts for ≈1000 ha for a ≈100 MW coal power plant, suggesting that technological improvements, mainly in the photobioreactor, are required. The results of the surrogate model developed are compatible with the Brazilian auctions and with literature data, with errors in the Fixed Capital Investments (FCI) of the CHP and the CCS of 1.9% and 1.3%, respectively, when compared with the observed values, with correlation coefficients of 0.996 and 0.991. The capacity of the Combined Heat and Power (CHP) unit, in terms of bagasse consumption, is the variable with more weight in its FCI, while it is the pipelines in the CCS unit, which accounts for more than 50% of it.

Line#3 claims that performing CCS in bioenergy generation (BECCS) has a certain lack of viability, due to a considerable increase in investment and operational costs, of almost 4 times of a Combined Heat and Power (CHP) without CCS but deprived of a proper revenue increase from the captured CO_2 due to its low commercial value of at most 100 USD/tCO_2. The capture cost of the Base-Case with CCS is estimated at 262 USD/tCO_2, within the literature range of 88-288 USD/tCO_2. All perturbed scenarios of the sensitivity analyses resulted in capture costs within the literature range. However, assuming operational time and capture capacity typical of conventional NG fueled power plants, instead of biomass industry, leads to capture cost of only 17.2 USD/tCO_2, showing that the low capacity together with the high idle time represent the biggest challenges for BECCS in sugarcane-biorefineries.

Line#4 claims that the selection of the Reference Environmental Reservoir (RER) is important to proper identify exergy sinks for future improvement of process performance. Therefore, two distinct RERs are considered for the CO_2-rich NG processing in offshore rigs: RER-1 corresponds to the Standard Atmosphere in the standard composition without water saturation, while RER-2 comprises an infinite amount of the raw CO_2-rich NG in equilibrium with an infinite body of liquid water. Despite having a better discernment of the exergy destruction and being recommended its use, RER-2 is appropriate only for physical processes, like the NG processing plants. On the other hand, RER-1 is appropriated whenever chemical reactions takes place, like in the gas turbines area.

Line#4 also claims that, besides better technical results than the conventional route (TEG+JT+MP), the configuration using two SS units (SS+SS) attained the highest exergy efficiencies: 72.4% against 63.3%, having the SS+MP an intermediary value of 66.5% (RER-1 values). Moreover, considering RER-2, exergy efficiency of the battery of SS-1 attained 99.1% against 94.7% of the JT and SS-2 reached 93.0% against 80.5% for the MP.

The following guidelines can be recommended for carbon reduction of flue-gas based in the findings of this work:

- CO_2 hydrogenation might be considered as a potential route for carbon mitigation together with methanol production. However, a joint venture with a company operating a bioethanol plant is more advantageous. In this scenario, the flue-gas would be emitted and a similar amount of the pure CO_2 stream from the fermentation would be converted to methanol.
- Biorefineries with microalgae for CO_2 capturing requires a lot of technological improvements before investments can be performed;
- Performing CCS in a flue-gas from combined heat and power (CHP) plant should be performed only if the operating time is optimized for a large capacity. In this sense, it is possible that the capture cost given by the Sugarcane-Biorefinery Analyzer Framework is lower than a potential taxation for CO_2 emission.

The main findings of this work for carbon reduction of CO_2-rich natural gas are:

- The use of two batteries of SS, the first for WDPA+HCDPA and the second for CO_2 removal, for processing in a Deepwater offshore FPSO, is the most sustainable process for conditioning it.

In connection to recommended future works, the sustainability of the analyzed technologies should be compared with the oxyfuel technologies for energy generation with CO_2 mitigation, whether in technical-economic and environmental or in exergetic efficiency perspectives, to pursuit better sustainability processes in Line#2.

In relation to Line#3, flex plants operating with sugarcane and corn as raw material, depending on the period of the year, could be analyzed for improvements in the idle time of the capturing process. This is one big issue of traditional bioethanol plants found in this Thesis.

Lastly, the Gas-to-Wire concept can be explored, consisting in the generation of offshore electricity from CO_2-rich NG and then transmitted onshore with subsea cables. The exergetic efficiency of this system can be compared with the traditional onshore power generation of the conditioned NG.

APPENDIX A. Bibliographic production resulted from this Thesis research

Table A.1 presents the publications resulted from this thesis research. Each publication is associated to the respective appendix, publishing place, type, corresponding chapters of this thesis and to a first authorship indicator.

Table A.1. Summary of bibliographic production derived from the present research.

Research Line	Appendix/ Front Page	Product Type	Thesis Chapter	First Author
(Line#1 and Line#2) CCU for methanol production versus CCS	A-1	Conference paper	–	Yes
	A-2	Scientific article	02	Yes
	A-3	Patent application	–	–
	A-4	Conference paper	–	No
	A-5	Scientific article	–	No
	A-6	Conference paper	–	Yes
	A-7	Conference paper	–	Yes
	A-8	Scientific article	03	Yes
	A-9	Conference paper	–	Yes
	A-10	Scientific article	–	Yes
(Line#3) Bioenergy production with CCS	A-14	Conference paper	–	Yes
	A-15	Scientific article	04	Yes
(Line#4) Offshore CO_2-rich NG processing	A-11	Register of software	–	–
	A-12	Conference paper	05	Yes
	A-13	Scientific article	–	Yes

APPENDIX A.1. Conference paper on CO_2 utilization in microalga-based biorefinery producing methanol – Proceedings of SDEWES2016

WIESBERG, I. L.; BRIGAGÃO, G. V.; DE MEDEIROS, J. L.; ARAÚJO, O. Q. F. Economic and environmental analysis of a microalgae-based biorefinery utilizing CO_2 emitted from coal fired power plant. 11th Conference on Sustainable Development of Energy, Water and Environment Systems (SDEWES), Lisbon, 2016.

Economic and environmental analysis of a microalgae-based biorefinery utilizing CO_2 emitted from coal fired power plant

Igor L. Wiesberg, George V. Brigagão, Jose Luiz de Medeiros, Ofélia Q. F. Araújo[1]
School of Chemistry
Federal University of Rio de Janeiro, Rio de Janeiro, Brazil
e-mail: ofelia@eq.ufrj.br

ABSTRACT

Coal fired power plants are major stationary sources of CO_2 and environmental constraints demand technologies for abatement. Carbon Capture and Storage is the most mature route for this purpose but it imposes severe economic penalty for power generation. Chemical or biochemical conversion of CO_2 to valuable products, which is known as Carbon Capture and Utilization, monetizes CO_2, potentially mitigating the penalty associated to emissions reduction. This work evaluates the economic feasibility of CO_2 bio-capture by *Chlorella pyrenoidosa* and use of the resulting biomass as a feedstock to a biorefinery. The proposed mainstream arrangement is composed by: CO_2 biocapture at photobioreactor, microalgae oil extraction with part of the obtained biomass and gasification with the rest for biosyngas production, and finally methanol synthesis via biosyngas and purification. The photobioreactor is responsible for nearly one fifth of the total CAPEX and occupies an area of 986 ha, posing the most significant barrier to the implementation and economic feasibility of the biorefinery. Considering the net CO_2 capture, microalgae has a cost of 162 \$/t while CCS has 225\$/t.

KEYWORDS

Carbon capture and storage; carbon capture and utilization; microalgae; biorefinery; biomass gasification; methanol synthesis.

INTRODUCTION

The world economy is heavily dependent on fossil fuels, generating emissions with high concentrations of CO_2. [1] investigates the post-combustion capture of CO_2 exhaust gases and its utilization in approaches that employ different technological routes. There are few applications on a commercial scale for CO_2, both in the energy sector and in other industrial activities, resulting in emissions to the atmosphere due to lack of competitive technology to capture and allocate it.

Coal fired power plants are intensive stationary sources of carbon dioxide emissions. The atmospheric concentration of CO_2 has increased in the last decades due to the growth of industrial activity, which has impacted the natural balance of CO_2 in the atmosphere. Thus, environmental concerns promote a global research to develop technologies to reduce emissions and stabilize its concentration. One important way to reduce the global emission of greenhouse gases (GHG) is the practice of Carbon Capture, Utilization, and Storage (CCUS), which represents a group of technologies to capture CO_2 from industrial sources, e.g., flue gas, and then utilizing it physically (e.g., EOR), chemically (e.g., as a feedstock to the

APPENDIX A.2. Scientific article on CO2 utilization in microalga-based biorefinery producing methanol – Journal of Environmental Management

WIESBERG, I. L.; BRIGAGÃO, G. V.; DE MEDEIROS, J. L.; ARAÚJO, O. Q. F. Carbon dioxide utilization in a microalga-based biorefinery: efficiency of carbon removal and economic performance under carbon taxation. Journal of Environmental Management, 203, p. 988-988, 2017.

Research article

Carbon dioxide utilization in a microalga-based biorefinery: Efficiency of carbon removal and economic performance under carbon taxation

CrossMark

Igor Lapenda Wiesberg, George Victor Brigagão, José Luiz de Medeiros, Ofélia de Queiroz Fernandes Araújo[*]

Federal University of Rio de Janeiro, Rio de Janeiro, Brazil

ABSTRACT

Coal-fired power plants are major stationary sources of carbon dioxide and environmental constraints demand technologies for abatement. Although Carbon Capture and Storage is the most mature route, it poses severe economic penalty to power generation. Alternatively, this penalty is potentially reduced by Carbon Capture and Utilization, which converts carbon dioxide to valuable products, monetizing it. This work evaluates a route consisting of carbon dioxide bio-capture by *Chlorella pyrenoidosa* and use of the resulting biomass as feedstock to a microalgae-based biorefinery; Carbon Capture and Storage route is evaluated as a reference technology. The integrated arrangement comprises: (a) carbon dioxide bio-capture in a photobioreactor, (b) oil extraction from part of the produced biomass, (b) gasification of remaining biomass to obtain bio-syngas, and (c) conversion of bio-syngas to methanol. Calculation of capital and operational expenditures are estimated based on mass and energy balances obtained by process simulation for both routes (Carbon Capture and Storage and the biorefinery). Capital expenditure for the biorefinery is higher by a factor of 6.7, while operational expenditure is lower by a factor of 0.45 and revenues occur only for this route, with a ratio revenue/operational expenditure of 1.6. The photobioreactor is responsible for one fifth of the biorefinery capital expenditure, with footprint of about 1000 ha, posing the most significant barrier for technical and economic feasibility of the proposed biorefinery. The Biorefinery and Carbon Capture and Storage routes show carbon dioxide capture efficiency of 73% and 48%, respectively, with capture cost of 139$/t and 304$/t. Additionally, the biorefinery has superior performance in all evaluated metrics of environmental impacts.

© 2017 Elsevier Ltd. All rights reserved.

1. Introduction

The world economy is heavily dependent on fossil fuels, generating massive emissions of carbon dioxide (CO_2). Coal fired power plants are among the major stationary sources of CO_2 emissions, where Carbon Capture and Storage (CCS) is the leading technology for CO_2 management. Besides recognized technical barriers − e.g., existence of geological sites (Cuéllar-Franca and Azapagic, 2015), CO_2 monitoring for leakage (Cheah et al., 2016) − the absence of revenues imposes relevant economic penalty to the CO_2 source processes due to the significant capital investment required.

Alternatively, utilization of CO_2 aims to add value to the captured CO_2 (Carbon Capture and Utilization, CCU), through its chemical conversion (Aresta, 2010). The ensemble of technologies for CO_2 management is referred to CCUS (i.e., CCS + CCU), spanning from storage to physical, chemical and biochemical utilization (e.g., Enhanced Oil Recovery − EOR, methanol production). It is worth noting that a few chemical syntheses employ CO_2 as feedstock at a commercial scale (e.g., urea) (Aresta, 2010), where most alternatives are at the earlier stages of technology readiness level (most of them are still at laboratory or bench scale). Conversion of CO_2 to methanol (MeOH) outstands as a promising alternative, accordingly to technical and economic studies evaluating capital and operational expenditures, and environmental performance. Kourkoumpas et al. (2016) investigated the methanol production based on CO_2 capture from lignite power plants, estimating MeOH production cost of 421€/t in case of a power plant owner investment. Pérez-Fortes et al. (2016) investigated the direct CO_2

* Corresponding author.
 E-mail addresses: igorwg@ufrj.br (I.L. Wiesberg), george.victor@poli.ufrj.br (G.V. Brigagão), jlm@eq.ufrj.br (J.L. de Medeiros), ofelia@eq.ufrj.br (O. de Queiroz Fernandes Araújo).

APPENDIX A.3. Patent application on methanol production

BRIGAGÃO, G. V. WIESBERG, I.L., DE MEDEIROS, J. L., ARINELLI, L. O., ARAÚJO, O. Q. F., inventors; Universidade Federal do Rio de Janeiro, applicant. Processo intensificado com separador supersônico para produção de metanol a partir de gás carbônico e hidrogênio ou de gás de síntese. BR Patent Application BR1020200195689. Filed on September 25th, 2020.

Processo intensificado com separador supersônico para produção de metanol a partir de gás carbônico e hidrogênio ou de gás de síntese

RESUMO: Processo para produzir metanol intensificado por separadores supersônicos com injeção de água elevando a produção de metanol sem elevar carga, pressão reacional ou gás de reciclo. Separadores supersônicos injetando água são instalados na saída de gás do separador de metanol após o reator e no vent de topo da coluna de leves, elevando a produção de metanol ao elevar a conversão no reator deslocando o equilíbrio, e reduzindo metanol no gás de reciclo/purga e no vent da coluna de remoção de leves.

DESAFIOS E OBJETIVO: a) Elevar a conversão por passe no reator de síntese de metanol sem alterar demais condições; b) Reduzir perdas de metanol no gás de purga do loop do reator; c) Reduzir circulação de metanol no gás de reciclo do reator elevando conversão de equilíbrio; d) Reduzir perdas de metanol no vent de topo da coluna de remoção de leves de metanol bruto, ao mesmo tempo permitindo reduzir a pressão desta coluna o que favorece a separação de leves.

SOLUÇÃO: Consiste em instalar separadores supersônicos com injeção de água líquida em dois pontos do processo de produção de metanol: no loop de reação de síntese de metanol na saída de gás do separador de metanol; e no gás de vent do condensador de topo da coluna de remoção de leves do metanol. Assim eleva-se a produção de metanol ao: elevar a conversão no reator deslocando o equilíbrio; reduzir metanol no gás de reciclo, no gás de purga e no vent da coluna de remoção de leves.

TITULAR:
Universidade Federal do Rio de Janeiro (UFRJ)

INVENTORES:
George Victor Brigagão
Igor Lapenda Wiesberg
José Luiz de Medeiros
Lara de Oliveira Arinelli
Ofélia de Queiroz Fernandes Araújo

NÚMERO DO PEDIDO:
BR1020200195689

AGÊNCIA UFRJ DE INOVAÇÃO
Rua Hélio de Almeida, s/n - Incubadora de Empresas - Prédio 2 (salas 25 a 29)
Cidade Universitária | Ilha do Fundão | Rio de Janeiro - RJ | 21941614
www.inovacao.ufrj.br

Agência UFRJ de **Inovação**

APPENDIX A.4. Conference paper on sustainability analysis of biogas production from microalgae – Proceedings of LA-SDEWES2018

SDEWES.LA2018.0046

Sustainability Analysis of Biomethane from Thermo-Mechanically Pretreated Microalgae

G. Brigagão*[1], I. Lapenda Wiesberg[2], I. Barboza Boa Morte[3], J. Pinto[3], O. Araujo[1], J.L. De Medeiros[1]

[1]Federal University of Rio de Janeiro, Brazil; [2]Federal University of Rio de Janeiro, Escola de Química/ Escola Politécnica, Brazil; [3]Federal University of Rio de Janeiro, Escola de Química, Brazil (*george.victor@poli.ufrj.br)

Abstract

Biodigestion of microalgae is a potentially sustainable strategy to recycling carbon dioxide via biofixation, substituting fossil fuels. This study compares technical and economic performance of three alternative microalgae-based biorefinery arrangements, consisting of a photobioreactor growing Nannochloropsis salina, alternative preheating strategies, biodigestion of the biomass and biogas processing to produce biomethane. The alternatives differ in the biomass pretreatment stage: (i) no pretreatment; (ii) thermal pretreatment (75 °C); and (iii) thermo-mechanical pretreatment (20 bar). Flue gas waste heat is used to supply heating demand. Process simulation is employed to support technical and economic analyses. Biogas production from thermo-mechanically pretreated microalgae is twice larger than biogas obtaining with thermal pretreatment. Assuming a carbon tax of 75 US\$ per ton of emitted CO_2, the thermo-mechanical pretreatment is the only configuration among the investigated alternatives that shows Net Present Value more attractive than merely paying the tax.

APPENDIX A.5. Scientific article on techno-economic analysis of biogas production from microalgae – Renewable and Sustainable Energy Reviews

BRIGAGÃO, G. V.; WIESBERG, I. L.; PINTO, J. L.; ARAÚJO, O. Q. F.; DE MEDEIROS, J. L. Upstream and downstream processing of microalgal biogas: emissions, energy and economic performances under carbon taxation. Renewable and Sustainable Energy Reviews, 112, p. 508-520, 2019.

Upstream and downstream processing of microalgal biogas: Emissions, energy and economic performances under carbon taxation

George Victor Brigagão, Igor Lapenda Wiesberg, Juliana Leite Pinto, Ofélia de Queiroz Fernandes Araújo*, José Luiz de Medeiros

Escola de Química, Federal University of Rio de Janeiro, CT, E, Ilha do Fundão, Rio de Janeiro, RJ, 21941-909, Brazil

ABSTRACT

The study evaluates alternative and innovative arrangements for processing a microalgae biomass by anaerobic digestion to produce biogas. Cell wall limits bio-accessibility of microalgal intracellular compounds, demanding pretreatment to improve methane yield. Two pretreatments are evaluated at 75 °C using residual heat: thermal (1 bar) and thermomechanical (20 bar),which increased biogas production in 40% and 159%, respectively. Thermomechanical pretreatment is coupled to the following downstream processing cases: (i) biomethane; (ii) bioelectricity; (iii) biomethane with enhanced oil recovery; (iv) bioelectricity with enhanced oil recovery and (v) pressurized anaerobic digestion (6 bar) for biomethane with enhanced oil recovery. Processes are compared in three dimensions: energy, economic and carbon footprint. Such a framework including upstream and downstream processes, besides comparison of atmospheric and pressurized anaerobic digestion, with in-depth economic analysis, configures the main novelties of this work. Resource utilization efficiency metrics point advantage of pressurized anaerobic digestion case, while indicate biomethane production as less efficient than bioelectricity. When carbon dioxide post-combustion capture and enhanced oil recovery are applied to abate bioelectricity emissions, bioelectricity loses competitiveness to biomethane due to high energy penalties. Sensitivity of Net Present Value to varying carbon taxation (increasing costs), Capture & Trade mechanism and enhanced oil recovery (adding revenues) show superior resilience of biomethane with enhanced oil recovery. In base scenario conditions, where 30US$/GJ electricity is applied, maximum biomass costs to economic feasibility for cases (i) to (v) are 50, 21, 100, 5 and 83US$/t (dry-basis), respectively. Priced at 50US$/GJ, the bioelectricity production frontier to feasibility starts at biomass costs ≈150US$/t.

1. Introduction

Bio-based energy is shifting from intensive use of energy crops to diversified substrates, and progressively developing processes using a wide range of raw biomass [1]. Anaerobic digestion (AD) monetizes waste treatment producing a gaseous fuel, being the preferred technology for treating wastes of high moisture contents [2], e.g. microalgae suspensions and food wastes with 74–90%w water [3].

AD produces biogas with reduced Lower Heating Value (LHV) due to its high carbon dioxide (CO_2) content (30–40%) [4], with methane (CH_4) ranging 50–65% [2]. To attain high LHV without additional upgrading equipment, Li et al. [2] proposed an *in situ* biogas upgrading consisting of a conventional continuously stirred tank digester (as acidogenesis reactor) followed by a pressurized biofilm AD, evaluated at four pressure levels showing beneficial effects of increasing AD operating pressures. Despite the promising results, the technology is at proof of concept stage.

Besides its low LHV, biogas is generally produced at low pressure, and has other impurities than CO_2 – e.g. ammonia (NH_3), water (H_2O) and, depending on substrate composition, hydrogen sulfide (H_2S) [5]; being off-specified for injection in natural gas distribution grids. Hence, development of biogas upgrading techniques is required [6],

APPENDIX A.6. Conference paper on solvent screening for CO2 capture from powerplants – Proceedings of LA-SDEWES2018

WIESBERG, I. L.; CRUZ, M.A.; ARAÚJO, O.Q.F.; DE MEDEIROS, J. L; WINTER, K.P.; MENEZES, L.N.; MUSSE, A.P.S. Reducing energy penalty in chemical absorption of CO2 from fuel fired power generation: guidelines and metrics for developing new solvents. 1st Latin-American Conference on Sustainable Development of Energy Water and Environment Systems (LA-SDEWES), Rio de Janeiro, 2018.

Reducing energy penalty in chemical absorption of CO_2 from fuel fired power generation: guidelines and metrics for developing new solvents

Igor Lapenda Wiesberg[1], Matheus de Andrade Cruz[1], Ofélia de Queiroz Fernandes Araújo[2], José Luiz de Medeiros[2], Klinsmann Pereira Winter*[2], Larissa Nátali Menezes Costa[2], Ana Paula Santana Musse[3]

[1] Federal University of Rio de Janeiro, Escola de Química/Escola Politécnica
[2] Federal University of Rio de Janeiro, Escola de Química
[3] Petrobras S.A.
e-mail: klinwinter1994@ufrj.br

ABSTRACT

Fuel-fired power plants face the challenge of energy supply under increasing carbon emissions regulations, demanding progresses in carbon capture and storage (CCS) technologies. Chemical absorption of CO_2 is considered the most mature technology for carbon capture. However, it poses severe energy penalty (15-30%) to the power plant, which can be minimized through new formulations of solvents and process flowsheet modifications. The work contributes to the progress of CO_2 chemical absorption through the proposition of a reduced set of guidelines and metrics to support the development of new solvents, which is applied to the most promising solvents technology: ionic-liquids and biphasic amines. The solvents are scored based on CO_2 loading capacity, physicochemical properties, toxicity, thermal and oxidative stability and price characteristics. Among screened solvents, phase-changing solvents are pointed to possess competitive advantages, mainly due to reduced energy duty for solvent regeneration, and potential to receive such duty from waste heat streams.

KEYWORDS

Post combustion CO_2 capture; solvent screening; amine based solvents; ionic liquid solvents; solvent sustainability analysis; solvent formulation.

◢ INTRODUCTION

The demand of energy in the world is increasing as well as the concentration of CO_2 in the atmosphere. To change this scenario, environmental regulations restricting CO_2 emissions are expanding, penalizing power supply by fuel-fired power plants. Given the energy demand growth and the low maturity level of newer and greener technologies [1, 2], energy supply is still predominantly based on fossil sources [3].

Technologies for CO_2 removal from flue gases is an alternative to reduce emissions. Techniques for carbon capture from exhaust gases include post-combustion, pre-combustion and oxycombustion [4]. Post combustion capture of the CO_2 with amine-based solvents, such as monoethanolamine (MEA) and diethanolamine (DEA), is the most mature route. This technology consists in selective absorption CO_2 by the solvent, its regeneration in a stripper, releasing CO_2, and its recirculation to the absorber. However, the heat required in regeneration poses a significant energy penalty to the power plant [5] (15-30%) [6],[7].

---
* Corresponding author

APPENDIX A.7. Conference paper on exergy-based sustainability analysis of Methanol production – Proceedings of-SDEWES2018

WIESBERG, I. L.; ARAÚJO, O. Q. F.; DE MEDEIROS, J. L. Methanol production from CO2 hydrogenation and CO2 rich Natural Gas: Assessment of Environmental Performance through Exergy Analysis. 13th Conference on Sustainable Development of Energy Water and Environment Systems (SDEWES), Palermo, 2018.

Methanol Production from CO_2 Hydrogenation and CO_2 Rich Natural Gas: Assessment of Environmental Performance through Exergy Analysis.

Igor L. Wiesberg[*]
Escola de Química, Federal University of Rio de Janeiro, Rio de Janeiro, Brazil
e—mail: igorwg@ufrj.br

Ofélia de Q. F. Araújo
Escola de Química, Federal University of Rio de Janeiro, Rio de Janeiro, Brazil
e—mail: ofelia@eq.ufrj.br

José L. de Medeiros
Escola de Química, Federal University of Rio de Janeiro, Rio de Janeiro, Brazil
e—mail: jlm@eq.ufrj.br

ABSTRACT

The exergy efficiency among two methanol production routes with CO_2 mitigation is analysed, namely CO_2 hydrogenation and synthesis gas conversion generated through bi-reforming. Exergy is a thermodynamic property that links this knowledge area to the sustainability and environmental costs of a process. A novel framework is proposed for exergy assessment of processes with chemical reactions. Since exergy is a property whose meaning is relative to some datum, a Reference Environmental Reservoir (RER) must be considered. The RER is chosen to be the 25°C Standard Atmosphere at sea level with composition in chemical equilibrium with air species and unsaturated in water with 2% mol and it is shown to be thermodynamically consistent. Methanol produced by CO_2 hydrogenation retains about 76% of the exergy entering the process, while this amount is only 46% for the synthesis gas route, indicating a lower sustainability for the latter process.

KEYWORDS

Exergy analysis, CO_2 hydrogenation, natural gas, CO_2 capture, methanol production, sustainability comparison

INTRODUCTION

Carbon Capture and Utilization (CCU) of carbon dioxide (CO_2) to methanol has the potential to address relevant sustainability issues. This technology can mitigate greenhouse gas emissions and can be an economically feasible replacement of fossil raw materials for downstream products. For example, methanol can replace crude oil through Methanol-To-Olefins (MTO) route [Wang, 2015], through its use as vehicle fuel or in power production. It can even shift Natural Gas (NG) demand, the most common raw material for its production. On the other hand, Carbon Capture and Storage (CCS) does not have any products or income and, therefore, should be avoided.

In this sense, two technologies that have potential for CO_2 mitigation and methanol production are investigated by means of exergy efficiency: the CO_2 hydrogenation (DIRECT route) and the bi-reforming of NG with posterior conversion to methanol (INDIRECT route)

---

[*] Corresponding author

APPENDIX A.8. Scientific article on exergy-based sustainability analysis of CO2 capture and storage or utilization to methanol production – Renewable and Sustainable Energy Reviews

WIESBERG, I. L.; BRIGAGÃO, G. V.; DE MEDEIROS, J. L.; ARAÚJO, O. Q. F. Carbon dioxide management via exergy-based sustainability assessment: carbon capture and storage versus conversion to methanol. Renewable and Sustainable Energy Reviews, 112, p. 720-732, 2019.

Check for updates

Carbon dioxide management via exergy-based sustainability assessment: Carbon Capture and Storage versus conversion to methanol

Igor Lapenda Wiesberg, George Victor Brigagão, Ofélia de Queiroz F. Araújo, José Luiz de Medeiros*

Escola de Química, Federal University of Rio de Janeiro, CT, E, Ilha do Fundão, Rio de Janeiro, RJ, 21941-909, Brazil

A B S T R A C T

Carbon Capture and Storage and Carbon Capture and Utilization refer to carbon dioxide management technologies for its removal from flue-gases, followed by carbon recycling or storage, aiming at limiting global warming. For large-scale deployment, geological storage is the most promising alternative but imposes an economic penalty to the emitting process, while the utilization monetizes carbon dioxide contributing to compensate for the large capture costs. The exergy concept builds a suitable framework to measure useful power according to the Second Law of Thermodynamics, such that maximizing exergy efficiency necessarily promotes sustainability. This work applies a novel framework for exergy assessment of processes with chemical reactions, which is employed to evaluate the performance of two methanol production routes from carbon dioxide from power plant flue-gas: the direct hydrogenation and the indirect conversion through natural gas bi-reforming for synthesis gas production. Exergy efficiency of the direct route is about 66.3%, against 55.8% for the indirect one, indicating the lower sustainability of the latter. Carbon capture and storage had the worst Exergy efficiency, even lower than the emission scenario, accounting for 44.8% against 53.5%. Exergy metrics pinpoint low scalability as the main drawback of the utilization technologies, despite high exergy and capture efficiency.

1. Introduction

Carbon Capture and Utilization (CCU) technologies have potential to considerably contribute for improved sustainability of industrial and power generation activities while adding revenues to carbon dioxide (CO_2) destination from chemical conversion to marketed products. Thus, CCU stands as an important solution to limit global warming while potentially enabling economically feasible replacement of fossil feedstocks to the chemical and energy industries. In this sense, methanol synthesis has been considered as one of the most promising routes for large-scale CCU [1], accounting for its widespread use and potential for a rapid growing demand, not only as a bulk commodity but also for its direct use as vehicle [2] and shipping fuel [3], as renewable energy carrier [4]. Moreover, methanol-to-olefins technology is of great importance because it replaces oil-derived products [5]. However, due to its chemical stability [6], CO_2 conversion requires severe reaction conditions [1], resulting in compression and heating

operations. A review of Life Cycle Assessments (LCA) of various CCU routes showed that the efficiency of the carbon removal and the environmental impacts varies greatly and are not always exciting when compared to CCS [7]. Unfortunately, as far as the authors are aware, there is no LCA study in the literature comparing CCS and CCU with methanol production.

Carbon Capture and Storage (CCS) alternatives, on the other hand, have the economic obstacle of being unprofitable activities that require large capital investment [8] and may only be economically attractive if the storage site is an oil reservoir, for Enhanced Oil Recovery (EOR), or a stringent carbon taxation policy is applied [9]. Indeed, the majority of the early CCS projects are for EOR purposes [10]. However, CCS is a promising technology for CO_2 mitigation from power plants emissions in a long term [8]. In order to increase its techno-economic feasibility, Calderon et al. [11] analyzed the recirculation of exhaust gases to rise the CO_2 partial pressure in the flue-gas of a NG power plant, simultaneously lowering the regeneration duty, its flow rate and its O_2

APPENDIX A.9. Conference paper on feasibility analysis of CO2-utilization to methanol production – Proceedings of 4º Congresso Brasileiro de CO2 na indústria do Petróleo, Gás e Biocombustíveis

WIESBERG, I. L.; DE MEDEIROS, J.L.; ARAÚJO, O. Q. F. Feasibility study of CO2 mitigation with methanol production through hydrogenation and bi-reforming of natural gas. 4° Congresso Brasileiro de CO2 na indústria do Petróleo, Gás e Biocombustíveis, Rio de Janeiro, 2018.

IBP0095_2018
FEASIBILITY STUDY OF CO2 MITIGATION WITH METHANOL PRODUCTION THROUGH HYDROGENATION AND BI-REFORMING OF NATURAL GAS
Igor Lapenda Wiesberg[1], José Luiz de Medeiros[2], Ofélia de Queiroz Fernandes Araújo[3]

Abstract

Chemical conversion of carbon dioxide (CO_2) to methanol has the potential to address two relevant sustainability issues: economically feasible replacement of fossil raw materials and avoidance of greenhouse gas emissions. However, the high chemical stability of CO_2 is a challenging impediment to conversion, requiring harsh reaction conditions at the expense of increased energy input, adding capital, operational and environmental costs. This work evaluates two innovative chemical routes for conversion of CO_2 to methanol: the indirect conversion, which uses synthesis gas produced by bi-reforming as intermediate, and the direct conversion, via CO_2 hydrogenation. Process simulations are used to obtain mass and energy balances, needed to support economic and sensitivity analyses. Due to the uncertainties in the raw material prices, including CO_2 and hydrogen (H_2), limits for economic viability are estimated and sensitivity analysis is carried in terms of predetermined prices (base cases). It is considered the scenario of zero-cost CO_2 available at atmospheric pressure, as occurs in bioethanol from fermentation, but the sensitivity analysis of CO_2 conditioning shows results for other scenarios, as in a CO_2 rich natural gas, in which the cost of CO_2 separation is zero because it is not necessary. Economic analysis show that hydrogenation can be feasible in Brazil if hydrogen prices are lower than 1000 US$/t, while the indirect route is viable only for cheap natural gas below 3.7 US$/MMBtu. The costs of CO_2 pre-treatment are not as sensitive as in the case of other raw materials.

1. Introduction

Mitigation of carbon dioxide (CO_2) emissions has worried the world for being an important greenhouse gas. Efficient physical and chemical alternatives to address the problem have been researched, which could penalize emission processes. In this context, a potential solution is the conversion of CO_2 into products of commercial value such as chemical commodities, polymers and methanol (Aresta, 2010), thus adding an economic objective simultaneously to the environmental objective of reducing emissions.

Among the chemical alternatives to convert CO2 to methanol, two routes have a recognized potential (Bansode et al., 2014): Indirect CO_2 conversion in methanol through synthesis gas (SYNGAS ROUTE) and direct hydrogenation of CO_2 in methanol (HYDROGENATION ROUTE). The SYGNAS ROUTE consists of the coupling of dry reforming reactions together with the steam reforming of natural gas (NG) for the production of SYNGAS. SYNGAS is a mixture containing basically CO, H_2 and a small amount of CO_2) in varying proportions, which has different applications, each requiring a certain optimum relation between the components. It can be produced from almost any carbon source, including biomass. However, natural gas is the most widely used raw material (OLAH et al., 2013). Dry reform is a still immature and pilot scale technology, while steam reforming is the main form of SYNGAS production for conversion to methanol (Offermann et al., 2014). The conversion of SYNGAS to methanol is a step with mature technology (Offermanns et al., 2014). Due to the chemical stability of CO2, the proposed routes require severe reactive conditions (ARESTA, 2010), which demand energy for compression and heating, adding capital, operational and environmental costs. The degree of energy demand depends heavily on the processing route adopted.

[1] MSc, Chemical Engineer – Escola de Química, Federal University of Rio de Janeiro
[2] DSc, Professor – Escola de Química, Federal University of Rio de Janeiro
[3] PhD, Professor – Escola de Química, Federal University of Rio de Janeiro

APPENDIX A.10. Scientific article on feasibility analysis of CO2 utilization to methanol production – Materials Science Forum

WIESBERG, I. L.;DE MEDEIROS, J. L.; ARAÚJO, O. Q. F. Feasibility Study of CO2 mitigation with Methanol Production through Hydrogenation and Bi-reforming of Natural Gas. Materials Science Forum, 965, p. 117-123, 2019.

Feasibility Study of CO$_2$ Mitigation with Methanol Production through Hydrogenation and Bi-Reforming of Natural Gas

IGOR Lapenda Wiesberg[1,a*], JOSÉ Luiz de Medeiros[1,b]
and OFÉLIA de Queiroz Fernandes Araújo[1,c]

[1]Escola de Química, Federal University of Rio de Janeiro, Rio de Janeiro, Brazil

[a]igorwg@ufrj.br, [b]jlm@eq.ufrj.br, [c]ofelia@eq.ufrj.br

Abstract. Chemical conversion of carbon dioxide (CO$_2$) to methanol has the potential to address two relevant sustainability issues: economically feasible replacement of fossil raw materials and avoidance of greenhouse gas emissions. However, chemical stability of CO$_2$ is a challenging impediment to conversion, requiring harsh reaction conditions at the expense of increased energy input, adding capital, operational and environmental costs. This work evaluates two innovative chemical conversion of CO$_2$ to methanol: the indirect conversion, which uses synthesis gas produced by bi-reforming as intermediate, and the direct conversion, via hydrogenation. Process simulations are used to obtain mass and energy balances, needed to support economic analyses. Due to the uncertainties in the raw material prices, including CO$_2$ and hydrogen (H$_2$), its limits for economic viability are estimated and sensitivity analysis is carried in predetermined prices. It is considered the scenario of free CO$_2$ available in atmospheric conditions, as in a bioethanol industry, but the sensitivity analyses show the results for other scenarios, as in a CO$_2$ rich natural gas, in which the cost of processing CO$_2$ is zero. The economic analyses show that hydrogenation can be feasible if hydrogen prices are lower than 1000 US$/t, while the indirect route is viable only for cheap sources of natural gas below 4.0 US$/MMBtu. The CO$_2$ pre-treatment costs are not as sensible as the others raw materials.

Introduction

A Mitigation of carbon dioxide (CO$_2$) emissions has worried the world for being an important greenhouse gas. Efficient physical and chemical alternatives to address the problem have been researched, which could penalize emission processes. In this context, a potential solution is the conversion of CO$_2$ into products of commercial value such as chemical commodities, polymers and methanol [1], thus adding an economic objective simultaneously to the environmental objective of reducing emissions.

Among the chemical alternatives to convert CO$_2$ to methanol, two routes have a recognized potential [2]: Indirect CO$_2$ conversion in methanol through synthesis gas (SYNGAS ROUTE) and direct hydrogenation of CO$_2$ in methanol (HYDROGENATION ROUTE). The SYGNAS ROUTE consists of the coupling of dry reforming reactions together with the steam reforming of natural gas (NG) for the production of SYNGAS. SYNGAS is a mixture containing basically CO, H$_2$ and a small amount of CO$_2$) in varying proportions, which has different applications, each requiring a certain optimum relation between the components. It can be produced from almost any carbon source, including biomass. However, natural gas is the most widely used raw material [3]. Dry reform is a still immature and pilot scale technology, while steam reforming is the main form of SYNGAS production for conversion to methanol and the conversion of SYNGAS to methanol is a step with mature technology [4]. Due to the chemical stability of CO$_2$, the proposed routes require severe reactive conditions [1], which demand energy for compression and heating, adding capital, operational and environmental costs. The degree of energy demand depends heavily on the processing route adopted.

The driving force for the development of sustainable methanol synthesis lies in its use as a raw material for the chemical industry (eg, raw material for the production of olefins, formaldehyde, acetic

APPENDIX A.11. Conference paper on bioenergy production from sugarcane bagasse – Proceedings of SDEWES2020

WIESBERG, I. L.; MELLO, R.V.P.; MAIA, J.G.S.S.; BASTOS, J.B.V.; DE MEDEIROS, J.L.; ARAÚJO, O. Q. F. Bioenergy Production from sugarcan bagasse with and without carbon capture and storage: a model to assist in the investment decision making of a cogeneration plant. 15th Conference on Sustainable Development of Energy Water and Environment Systems(SDEWES), Cologne, 2020.

Bioenergy Production from Sugarcane Bagasse with and without Carbon Capture and Storage: A Model to Assist in the Investment Decision Making of a Cogeneration Plant

Igor L. Wiesberg*, Raphael V. P. de Mello, Jeiveison G. S. S. Maia, João B. V. Bastos
Engenharia de Processos e Síntese Química
Instituto SENAI de Inovação em Biossintéticos e Fibras, Rio de Janeiro, RJ, Brazil
e-mail: ilwiesberg@@cetiqt.senai.br

José L. de Medeiros, Ofélia de Q. F. Araújo
Escola de Química, Federal University of Rio de Janeiro, Rio de Janeiro, RJ, Brazil

ABSTRACT

This work discloses user-friendly models to evaluate the expenditures of a cogeneration system from sugarcane bagasse, with or without carbon capture and storage from bioenergy, to assist in the investment decision making. A restricted number of inputs are required, namely the steam and electricity requirements of the main biorefinery unit. For each run of a 3^3 full factorial, AspenOne Portfolio is used to simulate and to estimate the expenditures of the unit. A response surface model is adjusted to fit the estimated capital expenditures, resulting in a mean error of 1.9%, while the operational ones are estimated by well-known empirical equations. Considering a 390kta monoethylene glycol biorefinery with carbon capture, the capital expenditure and the operational expenditure of the cogeneration plant are estimated to be 87.3 MMUSD and 21.9 MMUSD per year, respectively. Considering the capture, these values increases to 394.1 MMUSD and 72.5 MMUSD per year, respectively.

KEYWORDS

Cogeneration unit, Technical-Economic assessment, Bioenergy with Carbon Capture and Storage, Sugarcane Bagasse, CO_2 capture, Sustainability Analysis

INTRODUCTION

In recent years, concerns about the environment and energy security have become a major issue on political agendas, directing efforts toward the production of biofuels and renewable energy sources. Forecasts indicates that by 2050 renewable fuel should displace petroleum as the most used primary energy source [1], indicating the relevance of cogeneration systems. Cogeneration is a process that produces different forms of energy simultaneously, usually steam and electricity, with optimum efficiency. The cogeneration can fulfill two objectives: supply energy in many forms for a given biorefinery, with surplus sale as well as the mitigation of greenhouse gas emission, when renewable fuel is employed. The use of biomass in cogeneration systems contributes to a sustainable alternative of energy production, with replacement of fossil fuels.

The interest in cogeneration units using alternative fuels have increased because of the rise of fuel costs and, more recently, because of the environmental concern. A variety of renewable fuels can be used in cogeneration, including biomass, biogas, landfill gas from organic wastes, solar energy, fuel cell and waste heat [2]. Natural gas can also be used as raw material, but it

---

* Corresponding author

APPENDIX A.12. Scientific article on Bioenergy production from sugarcane bagasse – Renewable and Sustainable Energy Reviews

Bioenergy production from sugarcane bagasse with carbon capture and storage: Surrogate models for techno-economic decisions

Igor Lapenda Wiesberg [a,b], José Luiz de Medeiros [a,*], Raphael V. Paes de Mello [b], Jeiveison G. S. Santos Maia [b], João Bruno V. Bastos [b], Ofélia de Queiroz F. Araújo [a]

[a] Escola de Química, Federal University of Rio de Janeiro, CT, E, Ilha do Fundão, Rio de Janeiro, RJ, 21941-909, Brasil
[b] Engenharia de Processos e Síntese Química, Instituto SENAI de Inovação em Biossintéticos e Fibras, Rio de Janeiro, RJ, 21941-857, Brasil

ARTICLE INFO

ABSTRACT

The use of biomass in cogeneration is a sustainable alternative of energy production, allowing replacing fossil fuels and reduction of greenhouse gas emissions. This work discloses an integrated process analyzer framework comprising surrogate models for estimation of fixed capital investment, revenues, costs of manufacturing as well as several performance responses of cogeneration units of sugarcane-biorefineries burning bagasse, with/without post-combustion carbon capture and storage. A restricted number of inputs are required, namely bagasse availability and heat requirements of the sugarcane-biorefinery. To develop the investment models, a 3^3 factorial computational-experimental design was performed, where AspenOne Portfolio was used in each run to simulate the process allowing estimating the fixed capital investment. Surrogate models were adjusted to fit capital estimates, resulting in 1.9% and 1.3% mean errors for the cogeneration and the post-combustion capture steps, respectively. Capture costs were estimated by analytical equations using the investment values and other estimates from the process analyzer framework, reaching 262 USD/t, but can be as low as 17.2 USD/t if limitations from the agricultural sector are disregarded; namely seasonality, operating time and capacity. The developed framework can assist in sugarcane-biorefinery investment decision making regarding bioenergy with carbon capture and storage or to develop carbon mitigation policies.

1. Introduction

Recently environment concerns have become a major issue on political agendas, directing efforts towards using renewable sources to supply the increasing energy demand. Forecasts indicates that by 2050 renewable fuels should displace petroleum as primary energy source [1], indicating the relevance of biomass-based Combined Heat and Power (CHP) systems. Biomass-based CHP, or cogeneration, produces steam and electricity with optimum efficiency [2] from the same source of bioenergy. Biomass-based CHP can fulfill two objectives: supply energy efficiently in many forms with economic benefits while mitigating greenhouse gas emission [3]. It also entails the benefit of energy security; i.e., the uninterrupted electricity availability during shortages of the main tributary of the energy matrix, e.g., hydroelectric plants in drought periods [4]. That is, biomass-based CHP becomes a sustainable and reliable alternative for energy production, allowing replacing fossil fuels.

Interest in biomass-based CHP has increased due to increasing fossil fuel costs and environmental concerns. Not only biomass, but a variety of renewable fuels can be used in CHP, including biogas, landfill-gas, solar energy, fuel-cells and waste-heat [5]. Natural gas can also be used in CHP, but it has environmental issues and gives inferior economic response than biogas in some configurations [5]. In the present study, bioethanol production from sugarcane takes advantage of the bagasse availability to feed CHP.

Brazil is one of the biggest bioethanol world producers, accounting for ≈26% of world production, second only to the USA which responds for ≈58% [6]. In the past, low-pressure boilers were used in Brazilian sugarcane-biorefineries because they were cheaper and sufficient for

APPENDIX A.13. Register of softwares for calculation of multiphase and reactive equilibrium sound speed and simulation of supersonic separators

K1. Aspen Model of Phase Equilibrium Sound Speed

ARINELLI, L. O., WIESBERG, I. L., DE MEDEIROS, J. L., BRIGAGÃO, G. V., TEIXEIRA, A. M., ARAÚJO, O. Q. F., authors; UNIVERSIDADE FEDERAL DO RIO DE JANEIRO, applicant. AMPEC (Aspen Model of Phase Equilibrium Sound Speed (C)). Registered software BR512018001031-8. Brazilian Patent and Trademark Office. Filed in June 26th, 2018.

K2. Aspen Model of Supersonic Separator Operation

ARINELLI, L. O., WIESBERG, I. L., DE MEDEIROS, J. L., BRIGAGÃO, G. V., TEIXEIRA, A. M., ARAÚJO, O. Q. F., authors; UNIVERSIDADE FEDERAL DO RIO DE JANEIRO, applicant. AMSSO (Aspen Model of Supersonic Separator Operation). Registered software BR512018001032-6. Brazilian Patent and Trademark Office. Filed in June 26th, 2018.

K3. Aspen Model of Supersonic Separator Operation 2020

ARINELLI, L. O., WIESBERG, I. L., DE MEDEIROS, J. L., BRIGAGÃO, G. V., TEIXEIRA, A. M., ARAÚJO, O. Q. F., authors; UNIVERSIDADE FEDERAL DO RIO DE JANEIRO, applicant. AMSSO (Aspen Model of Supersonic Separator Operation). Registered software BR512021001749-8. Brazilian Patent and Trademark Office. Filed in July 19th, 2021.

K4. Hysys Extension Supersonic Separator Operation 2020

ARINELLI, L. O., DE MEDEIROS, J. L., TEIXEIRA, A. M., BRIGAGÃO, G. V., ARAÚJO, O. Q. F., authors; UNIVERSIDADE FEDERAL DO RIO DE JANEIRO, applicant. HESSO (Hysys Extension Supersonic Separator Operation). Registered software BR512021001748-0. Brazilian Patent and Trademark Office. Filed in July 19th, 2021.

APPENDIX A.14. Conference paper on exergy analysis of CO2-Rich Natural Gas conditining– Proceedings of SDEWES2020

WIESBERG, ARINELLI, L.O.; DE MEDEIROS, J.L.; ARAÚJO, O. Q. F. Exergy Analysis of Offshore CO2 Rich Natural Gas Conditioing Using Supersonic Separator. 15th Conference on Sustainable Development of Energy Water and Environment Systems (SDEWES), Cologne, 2020.

Exergy Analysis of Offshore CO2 Rich Natural Gas Conditioning Using Supersonic Separator

Igor L. Wiesberg[*]
Engenharia de Processos e Síntese Química
Instituto SENAI de Inovação em Biossintéticos e Fibras, Rio de Janeiro, RJ, Brazil
e-mail: ilwiesberg@@cetiqt.senai.br

Lara de O. Arinelli, José L. de Medeiros, Ofélia de Q. F. Araújo
Escola de Química, Federal University of Rio de Janeiro, Rio de Janeiro, RJ, Brazil

ABSTRACT

The sustainability of Natural Gas (NG) treatment with Supersonic Separators (SS) in an ultra-deepwater platform is analyzed using Exergy Analysis, a method that connects thermodynamics to the sustainability of a process. The designed conditioning system goal is to process a CO_2 rich associated NG, with 45%mol, to satisfy market specifications of water and hydrocarbon dew points (HDP/WDP) and CO_2 content of 20%mol, with a CO_2 stream as by-product for Enhanced Oil Recovery. A process simulation in Aspen Hysys is used to obtain mass and energy balances, which, together with Excel spreadsheet, generates the necessary tool for exergy compilation. The configuration using two SS, one for HDP/WDP and another for CO_2 removal, has higher exergy efficiency than an intermediate (with SS only for the HDP/WDP adjustment) and a conventional technology without SS (93.7% against 92.9% and 91.7%, respectively). Thus, configurations with SS can be considered more sustainable than conventional ones.

KEYWORDS

Exergy analysis, Natural gas conditioning, Supersonic separators, CO2 rich natural gas, Floating Production Storage and Offloading, Sustainability Analysis

INTRODUCTION

Natural Gas (NG) is the fossil fuel that is expected to have the higher rise until 2040 of 1.1% per year, while the share of petroleum based liquid fuels, the most used source of energy, should fall [1]. The high competitiveness of the NG is supported by its abundant resources and increasing production [1], some still in the early stage of development and production, as the NG hydrate [2] and the associated gas in pre-salt ultra-deepwater fields. Moreover, the advantage of the NG expansion is that it has the lowest ratio of CO_2 emission per generated energy among the fossil fuels [3], resulting in the cleanest combustion. Since NG will still play a significant role in this century, it is of central importance to increase the efficiency of its exploitation, which results in environmental benefits, since less waste and more energy are produced with the same input of materials. This is crucial because oil and gas platforms are associated with significant environmental impact, with CO_2 and CH_4 emissions for on-site power generation and flare system, being even higher in the platform end-life conditions [4].

---

[*] Corresponding author

APPENDIX A.15. Scientific article on exergy analysis of CO2-Rich Natural Gas conditining – Journal of Cleaner Production

Upgrading exergy utilization and sustainability via supersonic separators: Offshore processing of carbonated natural gas

Igor Lapenda Wiesberg, Lara de Oliveira Arinelli, Ofélia de Queiroz F. Araújo, José Luiz de Medeiros *

Escola de Química, Federal University of Rio de Janeiro, CT, E, Ilha Do Fundão, Rio de Janeiro, RJ, 21941-909, Brazil

ARTICLE INFO

ABSTRACT

Offshore processing of natural gas with 44%mol carbon dioxide at remote deep-water oil-and-gas fields is invariably characterized by low-efficiency power generation via gas-fired turbines releasing hot flue-gas and entailing high degradation of resources, high carbon emissions and low sustainability. This work demonstrates how to upgrade exergy utilization and consequently process sustainability by using supersonic separators in some gas processing steps; namely: (i) water dew-point adjustment; (ii) hydrocarbon dew-point adjustment; and (iii) carbon dioxide abatement to 20%mol. To accomplish this, the exergy performance of two supersonic separator gas processing alternatives are compared with conventional gas processing comprising triethylene-glycol absorption for water dew-point adjustment, Joule-Thomson expansion hydrocarbon dew-point adjustment and membrane-permeation carbon dioxide removal. Since exergy is measured relatively to a reference environmental reservoir, two such reference reservoirs are used: RER-1: standard atmosphere with 2%mol water containing hydrocarbons at combustion chemical equilibrium with air species; and RER-2: 1atm water-saturated raw natural gas in equilibrium with liquid water. Aspen-HYSYS simulations are used to solve mass/energy balances and thermodynamic property calculations. With RER-2 the conventional gas processing conserves 63.3% of the inlet exergy, while the two alternative supersonic separator processes attain 66.5% and 72.4% of exergy conservation, proving the associate gains of exergy efficiency and sustainability.

1. Introduction

Natural Gas (NG) is the fossil fuel that is expected to have the highest rise until 2050 of 1.1% per year, while the share of petroleum-based liquid fuels, the most used source of energy, should fall (EIA, 2019). The high competitiveness of NG is supported by its abundant resources and increasing production (EIA, 2017), some still in the early stage of development and production, as NG hydrate (Chong et al., 2016) and associated gas in Brazilian Pre-Salt deep-water fields. Moreover, the advantage of the NG expansion is that it has the lowest ratio of carbon dioxide (CO_2) emission per generated energy among the fossil fuels (EIA, 2016), resulting in the cleanest combustion. Since NG will still play a significant role in this century, it is of central importance to increase the efficiency of its exploration and production, especially at new remote offshore fields which are invariably characterized by low-efficiency power generation via gas-fired turbines releasing hot flue-gas and entailing high degradation of resources, high carbon emissions and low

sustainability. This is crucial because oil-and-gas offshore rigs operate with significant environmental impact, emitting CO_2 and CH_4 from on-site power generation, flare systems and processing facilities. Besides, these effects are even more impacting at platform end-life conditions (Nguyen et al., 2014). Thus, new offshore processing configurations must be developed for better utilization of resources in order to satisfy the growing NG demand and global sustainability needs.

1.1. Offshore conditioning of CO2-Rich natural gas

Parallelly to global NG expansion, the exploration and production of offshore oil-and-gas fields with high gas-to-oil ratio and high CO_2 content is increasing substantially, in spite of its lower methane content that imposes several technical issues for its utilization and conditioning. This is the case of Brazilian Pre-Salt deep-water oil-and-gas fields, characterized by CO_2 contents as high as 79%mol and gas-to-oil ratios around 20,000 scf/bbl (Gaffney et al., 2010). Besides the harder exploitation of deep-water fields, the treatment of this type of raw NG is also complex

* Corresponding author.
E-mail address: jlm@eq.ufrj.br (J.L. de Medeiros).

APPENDIX B. Supplementary Material for Chapter 2

B.1 Detailed process description of Biorefinery (BRY)

Figs. B.1 and B.2 depict simplified Process Flow Diagrams of Areas 01 and 02 (BRY-1, BRY-2) of the proposed biorefinery. BRY-1 comprises microalgae cultivation+harvesting and lipids extraction (BRY-1), while BRY-2 comprises biomass gasification, CO_2 separation, and methanol production. BRY process simulation assumptions are presented in Table B.1.
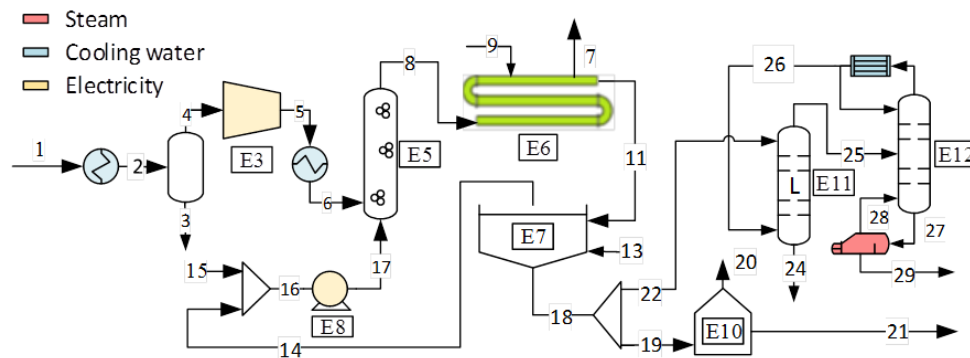
Fig. B.1. Process Flow Diagram of biomass production and oil extraction (BRY-1).
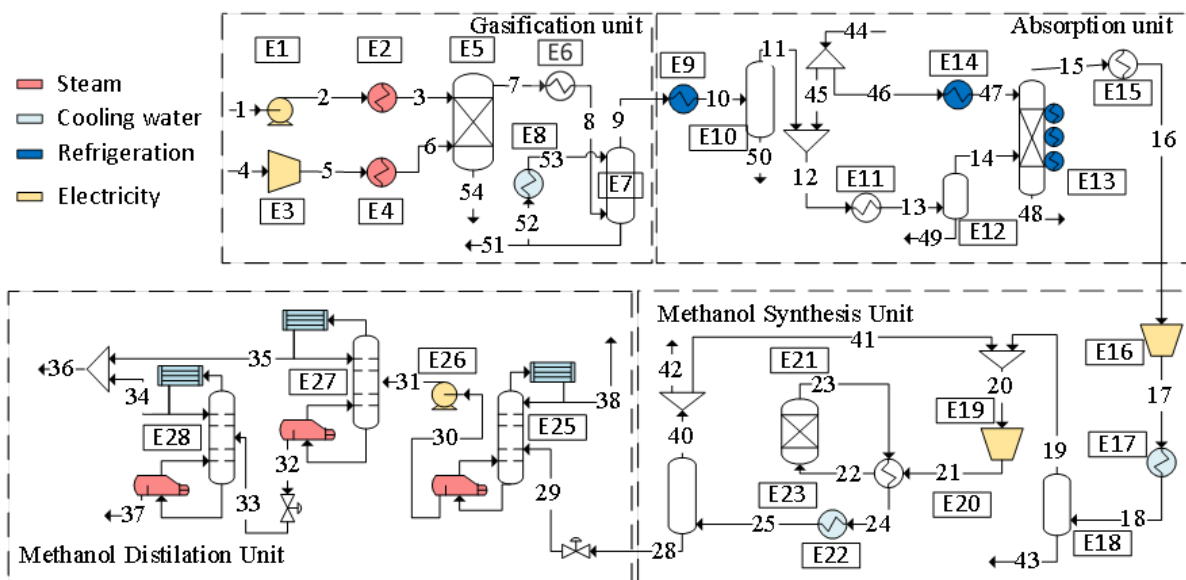
Fig. B.2. Process flow diagram for biomass gasification and methanol production (BRY-2). Solvent regeneration, CO_2 liquefaction and cogeneration are omitted, although considered in the simulation and related analyses.

At BRY-1 (Fig. B.1), CO_2 in flue gas is absorbed into water in an air lift arrangement. Carbonated water is fed to the PBR, consisting of horizontal transparent tubes in a vertical arrangement. The bioreactor product (microalga suspension at ≈ 4 g/L) is sent to dewatering, which accounts for 20-30% of the overall biomass production cost (Molina-Grima et al., 2003). Dewatering operations are: flocculation+settling (E7) and, for the biomass fraction sent to BRY-2, evaporation in Greenhouse Solar Dryer (GSD) (E10), producing biomass with 60%w water content (Kurt et al., 2015). At BRY-2 (Fig. B.2), the gasifier is fed with preheated biomass and gaseous oxygen (GOX) at high-pressure of 32 bar. The formation of tars and residual coke/char is neglected as chemical reactions are modeled via thermodynamic equilibrium approach (Gibbs reactor), minimizing Gibbs free energy for the given system of compounds: H_2, CO, CO_2, CH_4, H_2O, O_2, Ar, N_2, NH_3 and biomass model constituents, with minor S-containing components being not simulated. GOX 95%mol – supplied by a state-of-the-art low-pressure Air Separation Unit (ASU) consuming 158 kWh/t O_2 (Higginbotham et al., 2011) – is compressed to 32 bar at BRY-2. Raw syngas temperature at gasifier outlet is maintained at $\approx 900°C$ controlling GOX flow rate, which corresponds to the of GOX/Biomass (humid) mass feed ratio of 0.334. Hot CO_2-rich syngas flows through a heat recovery steam generation section, supplying the combined heat and power generation system, where it is cooled down to $\approx 100°C$. The majority of this heat is availed by a Rankine cycle that is equipped with supplemental fire driven by purge (fuel) gas from the upcoming methanol (MeOH) synthesis and distillation unit. Syngas low-grade heat is dissipated by direct contact with cooling water achieving $\approx 40°C$. HYSYS process flow diagram of Biorefinery Area 02 (BRY-2) simulation is unveiled in Fig. B.3.

The CO_2-rich syngas is then directed to a Rectisol unit (Physical-Absorption with refrigerated MeOH) for CO_2 removal, adjusting the proportion of H/C elements to achieve a syngas stoichiometric number $S = ([H_2] - [CO_2])/([CO] + [CO_2])$ of 2.15, being slightly above 2.00 as recommended for MeOH synthesis. After entering the absorption unit, the CO_2-rich syngas is cooled down to $\approx 10°C$. Raw syngas is then mixed with cold MeOH and the mixture is cooled by heat exchange with product streams. The resulting gas is sent to the absorber – which is equipped with three intermediary coolers – operating at sub-ambient temperatures of $-50 \leq T(°C) \leq -20$. Treated syngas leaving the top of the absorber has $\approx 2\%$ CO_2. The CO_2-rich solvent obtained at column bottoms is expanded in three stages to release most of the absorbed light gases, and is sent to the main stripping column, where pure MeOH is recovered at the bottom. Pure MeOH is then chilled to $-50°C$ and recycled to the top of the

main absorber as lean solvent. The HYSYS subflowsheet of CO_2 absorption unit simulation is portrayed in Fig. B.4.

The CO_2 liquefaction unit processes CO_2 captured by absorption, basically consisting of multistage intercooled compression to ≈*80 bar* followed by total condensation by cooling to ≈*30°C* and final dispatch by pumping to *100 bar* (no revenues are applied).

The considered MeOH synthesis unit is based on the Lurgi MeOH reactor and process scheme. It consists of a fixed bed reactor operated at 65 bar where the reaction temperature is maintained in the range of 240-260°C by heat recovery for steam generation. The unreacted gas – the gas phase obtained after raw MeOH condensation – is partially recycled and mixed with syngas feed in order to increase the H_2 content of reactant mixture, favoring the conversion of CO and CO_2 into MeOH. The carbon efficiency of this plant – i.e. the conversion of CO+CO_2 – is ≈*87%*. The remaining part of the H_2-rich gas (MeOH synthesis purge gas) is utilized as fuel gas for supplemental firing at the steam-cycle. The raw MeOH stream is expanded to near atmospheric pressure, mixed with impure MeOH from the absorption unit, and sent to the distillation section, consisting of a 3-column process scheme. The first column removes light contaminants, e.g. dissolved gases and dimethyl-ether, and the following two columns perform methanol/water fractionation in a heat integrated process scheme, with pure MeOH 99.9%w being recovered at the top of both columns. A small portion of this MeOH is taken for solvent make-up at the absorption unit. Released light gas of raw MeOH expansion and the top vapor of the first distillation column are mixed with the purge gas of synthesis loop and utilized as fuel gas in a boiler for supplemental fire. The HYSYS subflowsheet of methanol plant simulation is portrayed in Fig. B.5.

The cogeneration unit is based on a Rankine steam-cycle without reheat adopting two pressure levels of superheated steam. The largest part of heat supply is obtained at raw syngas cooling. Significant portion of low-pressure steam is extracted from the power-cycle in order to supply BRY heating demands (e.g. reboilers). The vacuum condenser operates at *0.11 bar* processing inlet stream with ≈*0.88* of vapor fraction.

Table B.1. Assumptions for biorefinery simulation (BRY).

Process unit	Item	Specification
(Any)	Adiabatic efficiency for compressors	85%
	Adiabatic efficiency for pumps	75%
	Electric drivers efficiency (pumps / compressors)	98%
	Thermal approach at steam generation	15 °C
	Thermal approach for shell and tube heat exchangers	10 °C
	Thermal approach for plate heat exchangers	5.0 °C
ASU	Thermodynamic model	Peng-Robinson
	GOX pressure	1.013 bar
	GOX mass fractions	N_2: 0.0173
		Ar: 0.0377
		O_2: 0.9451
		(Dillon et al., 2005)
Gasification unit	Thermodynamic model	Peng-Robinson
	Gasifier pressure	32.0 bar
	Gasifier outlet temperature	900 °C
	Reaction model	Gibbs reactor
Absorption unit	Thermodynamic model	PC-SAFT with parameters from Gatti et al. (2014)
	Solvent	Pure MeOH
	Solvent load	3.30 molMeOH/ molCO_2
	Syngas stoichiometric number	2.15
Methanol unit	Thermodynamic model	SRK for MeOH synthesis and UNIQUAC / SRK for MeOH distillation
	Reactor type	Fixed bed tubular reactor, cooled by steam generation
	Reactor pressure	64.7 bar
	Reactor temperature	240-260 °C
	Reaction modeling	Kinetic model of Vanden Bussche and Froment (1996)
CO_2 liquefaction	Thermodynamic model	Peng-Robinson
	Compressor suction/discharge pressure	6.30 / 76.0 bar
	Liquid CO_2 export pressure	100 bar
Cogeneration	Thermodynamic model for combustion	Peng-Robinson
	Thermodynamic model for the steam cycle	NBS Steam
	Steam turbine inlet pressure	98.5 / 4.10 bar
	Steam turbine outlet pressure	4.10 / 0.11 bar
	Steam turbine inlet temperature	570 / 173 °C
	Steam turbine adiabatic efficiency	90%
	Condensate content at turbine outlet (vacuum)	12%
	Generator electrical efficiency	98%

Table B.2 summarizes the main streams of BRY-1, while Table B.3 shows specific premises for its simulation.

Table B.2. Description of streams from biorefinery first area (BRY-1) – Fig. B.1.

Stream (BRY-1)	Description (PFD of Fig. B.2)
1	Mass flow: 706.5 t/h (CO_2=92.2 t/h); P =1 atm; T =70 °C; Mass fractions: N_2=0.7631, CO_2=0.1305, O_2=0.0442, H_2O=0.0622.
7	Nitrogen, oxygen and non-converted CO_2

Stream (BRY-1)	Description (PFD of Fig. B.2)
9	Microalga growth medium: $NaNO_3$=500 mg/L; $NaH_2PO_4.2H_2O$=7.7 mg/L; $FeCl_3.6H_2O$=6.3 mg/L (Wang et al., 2014).
11	Biomass of pure *Chlorella pyrenoidosa*. Mass composition (ash-free basis): Carbohydrates=21.94%; Proteins=48.85%; Lipids=29.2 % (Duan et al., 2013) Fatty acids profile (%w/w): 16:0=27.94%, 16:3=20.85%, 17:0=3.35%, 18:1=2.46%, 18:2=6.49%, 18:3=38.91% (based on Tang et al., 2011). Empirical formula: $CO_{0.473} H_{1.934} N_{0.230} P_{0.017}S_{0.005}$ (Picardo et al., 2013).
13	Cationic starch as bioflocculation agent (Letelier-Gordo et al., 2014).
15	Water makeup to PBR
20	Evaporated water at Greenhouse Solar Dryer (GSD).
21	Biomass to gasification (organic matter ≈40%w)
22	Biomass to oil extraction (organic matter ≈7%w)
24	Residual biomass from extraction
29	Microalga oil (product)

Table B.3. Operational data for simulation of biorefinery first area (BRY-1).

Item (BRY-1)	Simulation inputs
Compressor (E3)	Discharge pressure: 2 bar
Chemical-Pretreatment	H_2SO_4: mass flow is 1% of the water in feed (Davis et al., 2014).
PBR (E6)	Biomass concentration: 3.974 g/L (Chisti, 2007);
	Biomass productivity: 1.535 g/L/d (Chisti, 2007);
	Volume/surface: 0.07 m³/m² (Acién et al., 2012);
	Efficiency of CO_2 utilization: 74.5% (Acién et al., 2012);
	Daily uptime 24 h (daily average productivity);
Settler (E7)	Flocculant concentration: 0.040 g/L (Letelier-Gordo et al., 2014);
	Flocculant efficiency: 95 % (Letelier-Gordo et al., 2014);
	Organic matter in the product: 7.0 %w (Williams and Laurens, 2010)
GSD (E10)	Solar irradiation: 215 W/m²;
	Organic matter content of product: 40 % (Kurt et al., 2015).
Oil Extraction (E11)	Chemical pretreatment with H_2SO_4: 1% of water in liquor;
	Hexane load: 5 kg hexane: 1 kg dry biomass (Davis et al., 2014);

Table B.4 summarizes the main streams of BRY-2, while Table B.5 shows specific premises for its simulation.

Table B.4. Description of streams from biorefinery second area (BRY-2) – Fig. B.2.

Stream (BRY-2)	Description (PFD of Fig. B.2)
1	Biomass for gasification. Stream #21 in BRY-1 (Fig. B.1)
4	Gaseous oxygen 95%mol produced by the Air Separation Unit: 26.7 t/h, 30°C, 1 atm, 94.5%O_2, 3.77%Ar, 1.73%N_2 (%w/w).
7	Hot raw syngas – heat supply for cogeneration (steam generation at E6)

Stream (BRY-2)	Description (PFD of Fig. B.2)
9	Raw syngas – feed stream for absorption unit: 56.4 t/h; 39°C; 30 bar; Composition: 4.00% H_2, 23.35% CO, 67.20% CO_2, 3.47% N_2, 1.54% Ar (%w/w).
16	Adjusted syngas for MeOH synthesis. 19.6 t/h, 20°C, 28 bar, 11.4% H_2, 65.5% CO, 8.65% CO_2, 9.69% N_2, 4.20% Ar (%w/w)
36	Pure MeOH product stream. 13.9 t/h, 40°C, 1 atm, 99.90%w MeOH.
37	Wastewater from MeOH distillation: 0.27 t/h, 40°C, 1 atm, 100%w/w H_2O, less than 1 ppm MeOH (w/w)
38	Light contaminants in methanol+water mixture (e.g. dissolved gases).
42	Purge gas from MeOH synthesis – fuel for cogeneration; Composition: 8.17% H_2, 19.6% CO, 17.7% CO_2, 35.4% N_2, 15.4% Ar (%w/w).
54	Ashes

Table B.5. Equipment input of biorefinery second area (BRY-2).

Item (BRY-2)	Simulation inputs
Air Separation Unit	Three-column process demanding 158 kWh/t O_2 (Higginbotham et al., 2011).
Gasification unit	Thermodynamic model: Peng-Robinson; Gasifier conditions: 900°C / 32 bar. Gibbs reactor is utilized for reaction modelling. Formation of tars and residual coke/char is neglected.
Absorption unit	Thermodynamic model: PC-SAFT, with model parameters from Gatti et al. (2014); Solvent: MeOH at -50°C; load: 3.30 molMeOH/molCO_2; The absorber has three intermediate coolers (-30°C); Syngas H/C target ratio: 2.15.
MeOH unit	Thermodynamic model: SRK for MeOH synthesis section and UNIQUAC / SRK for distillation section; Reactor conditions: 240-260°C / 64.7 bar; Kinetic model from Vanden Bussche and Froment (1996).
CO_2 liquefaction	Thermodynamic model: Peng-Robinson; Compressor suction/discharge pressure: 6.30 / 76.0 bar; Liquefaction at 30°C; CO_2 exportation at 100 bar.
Cogeneration unit	Thermodynamic model: NBS Steam for the steam cycle and Peng-Robinson for the other process streams; Steam turbine inlet conditions: 570°C / 98.5 bar and 173°C / 4.10 bar (intermediate inlet stream); Steam turbine outlet conditions: 0.11 bar / 0.88 vapor fraction.
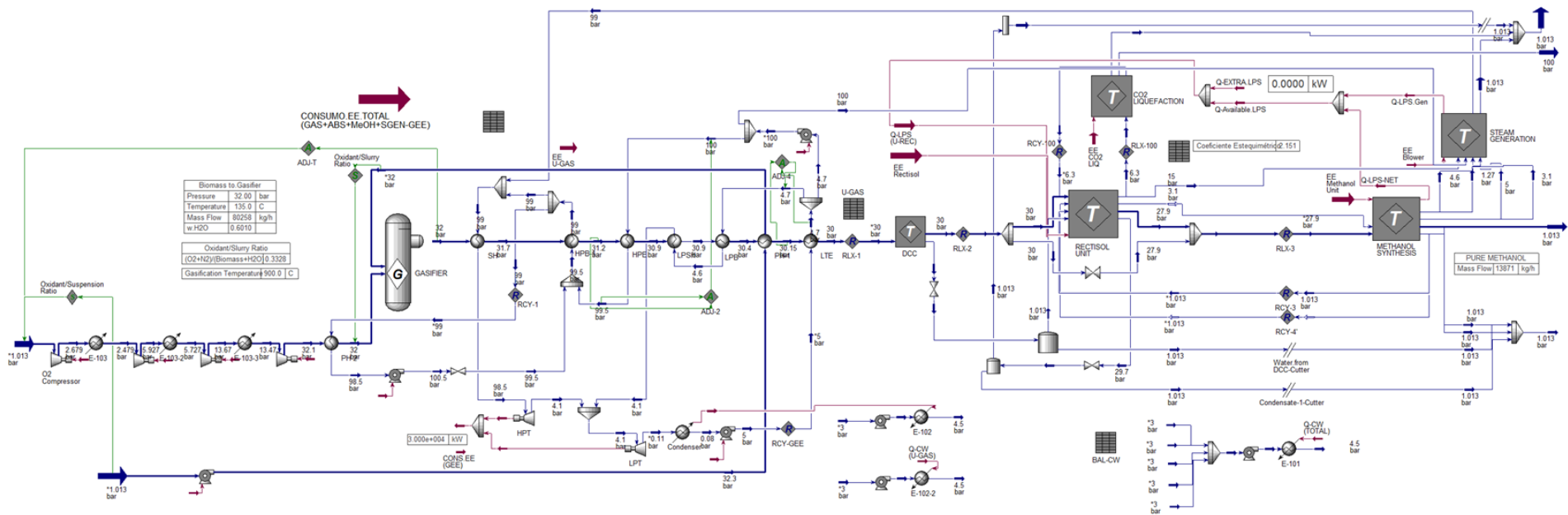
Fig. B.3. HYSYS PFD of BRY-2 simulation: overview of microalgal biomass termochemical processing for conversion to methanol.
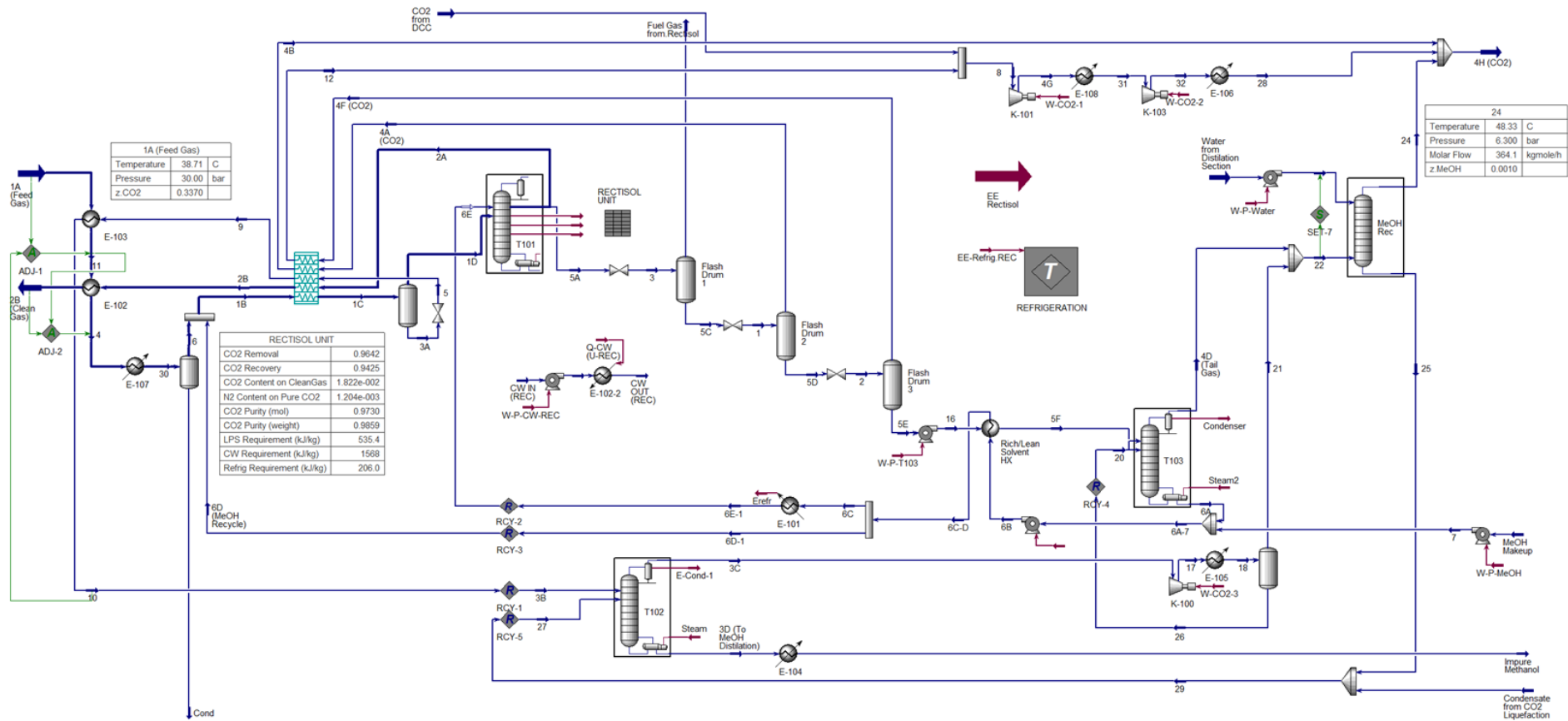
Fig. B.4. HYSYS PFD of BRY-2 simulation: subflowsheet of CO_2 physical absorption unit.
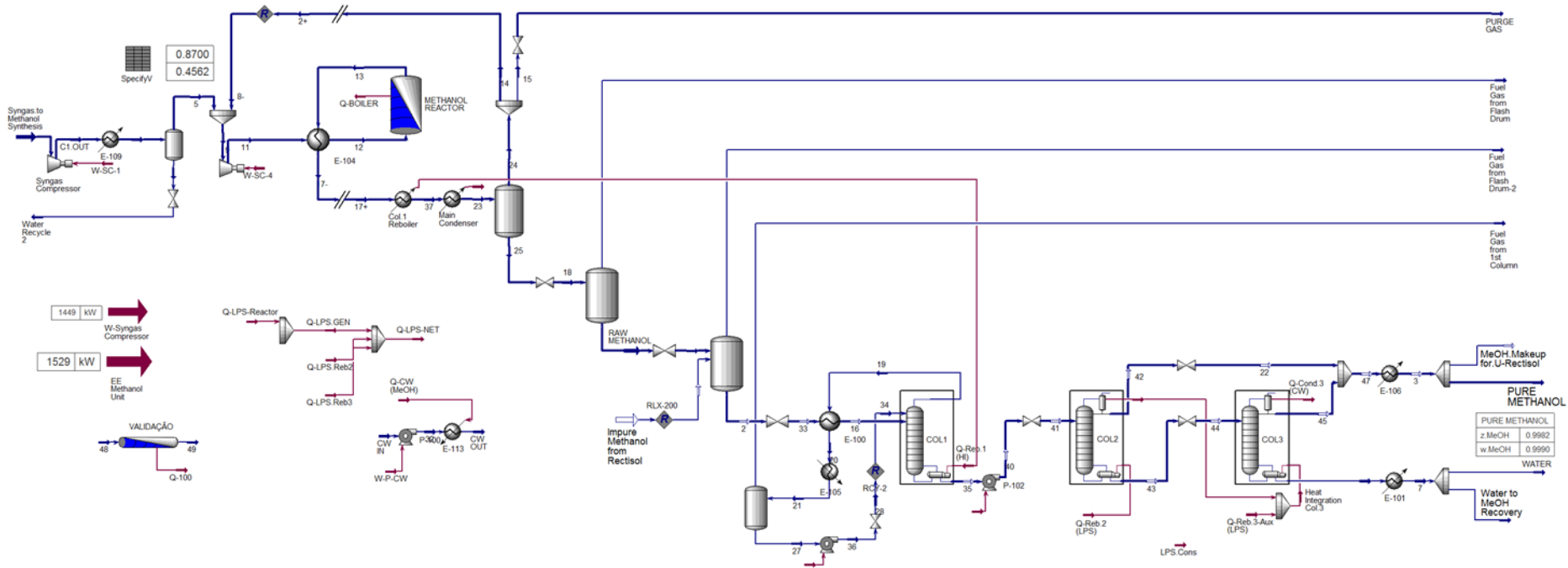
Fig. B.5. HYSYS PFD of BRY-2 simulation: subflowsheet of methanol synthesis and distillation.

Y2. References for Appendix B

Acién, F.G., Fernández, J.M., Magán, J.J., Molina, E., 2012. Production cost of a real microalgae production plant and strategies to reduce it. Biotechnol. Adv. 30 (6), 1344–1353. https://doi.org/10.1016/j.biotechadv.2012.02.005

Chisti, Y., 2007. Biodiesel from microalgae. Biotechnol. Adv. 25 (3), 294e306. https://doi.org/10.1016/j.biotechadv.2007.02.001

Davis, R., Kinchin, C., Markham, J., Tan, E., Laurens, L., Sexton, D., Knorr, D., Schoen, P., Lukas, J., 2014. Process design and economics for the conversion of algal biomass to biofuels: algal biomass fractionation to lipid- and carbohydrate-derived fuel products. Technical Report. National Renewable Energy Laboratory (NREL).

Dillon, D.J., White, V., Allam, R.J., Wall, R.A., Gibbins, J., 2005. IEA Greenhouse Gas R&D Programme: Oxy-combustion processes for CO_2 capture from power plant. Engineering Investigation Report.

Duan, P., Jin, B., Xu, Y., Yang, Y., Bai, X., Wang, F., 2013. Thermo-chemical conversion of Chlorella pyrenoidosa to liquid biofuels. Bioresour. Technol. 133, 197–205. https://doi.org/10.1016/j.biortech.2013.01.069

Gatti, M., Martelli, E., Marechal, F, Consonni, S., 2014. Review, modeling, Heat Integration, and improved schemes of Rectisol®-based processes for CO_2 capture. Appl. Therm. Eng. 70, 1123–1140. https://doi.org/10.1016/j.applthermaleng.2014.05.001

Higginbotham, P., White, V., Fogash, K., Guvelioglu, G., 2011. Oxygen supply for oxycoal CO_2 capture. Energy Proced. 4, 884–891. https://doi.org/10.1016/j.egypro.2011.01.133.

Kurt, M., Aksoy, A., Sanin, F., 2015. Evaluation of solar sludge drying alternatives by costs and area requirements. Water Res., 82, 47-57. https://doi.org/10.1016/j.watres.2015.04.043

Letelier-Gordo, C., Holdt, S., De Francisci, D., Karakashev, D., Angelidaki, I., 2014. Effective harvesting of the microalgae *Chlorella protothecoides* via bioflocculation with cationic starch. Bioresour. Technol. 167, 214–218. https://doi.org/10.1016/j.biortech.2014.06.014

Molina Grima, E., Belarbi, E.-H., Acién Fernández, F.G., Robles Medina, A., Chisti, Y., 2003. Recovery of microalgal biomass and metabolites: process options and economics. Biotechnol. Adv. 20 (7-8), 491–515. https://doi.org/10.1016/S0734-9750(02)00050-2

Picardo, M.C., de Medeiros, J.L., Monteiro, J.G.M., Chaloub, R.M., Giordano, M., Araújo, O.Q.F., 2013. A methodology for screening of microalgae as a decision making tool for energy and green chemical process applications. Clean Technol. Environ. Policy 15, 275–291. https://doi.org/10.1007/s10098-012-0508-z

Tang, D., Han, W., Li, P., Miao, X., Zhong, J., 2011. CO_2 biofixation and fatty acid composition of *Scenedesmus obliquus* and *Chlorella pyrenoidosa* in response to different CO_2 levels. Bioresour. Technol. 102(3), 3071–3076. https://doi.org/10.1016/j.biortech.2010.10.047

Uduman, N., Qi, Y., Danquah, M. K., Forde, G. M., Hoadley, A., 2010. Dewatering of microalgal cultures: a major bottleneck to algae-based fuels. J. Renew. Sust. Energy 2, 012701. https://doi.org/10.1063/1.3294480

Vanden Bussche, K.M., Froment, G.F., 1996. A steady-state kinetic model for methanol synthesis and the water gas shift reaction on a commercial $Cu/ZnO/Al_2O_3$ catalyst. J. Catal., 161(1), 1–10. https://doi.org/10.1006/jcat.1996.0156

Wang, W., Han, F., Li, Y., Wu, Y., Wang, J., Pan, R., 2014. Medium screening and optimization for photoautotrophic culture of *Chlorella pyrenoidosa* with high lipid productivity indoors and outdoors, Bioresour. Technol. 170, 395-403. https://doi.org/10.1016/j.biortech.2014.08.030

Williams, P., Laurens, L., 2010. Microalgae as biodiesel & biomass feedstocks: review & analysis of the biochemistry, energetics & economics. Energy Environ. Sci. 3, 554–590. https://doi.org/10.1039/B924978H